The copyright of this thesis vests in the author. No quotation from it or information derived from it is to be published without full acknowledgement of the source. The thesis is to be used for private study or non-commercial research purposes only.

Published by the University of Cape Town (UCT) in terms of the non-exclusive license granted to UCT by the author.

University of Cape Town

Stratigraphic and Structural Interpretation of Seismic Reflection Data Across Selected Sections of the Kaapvaal Craton

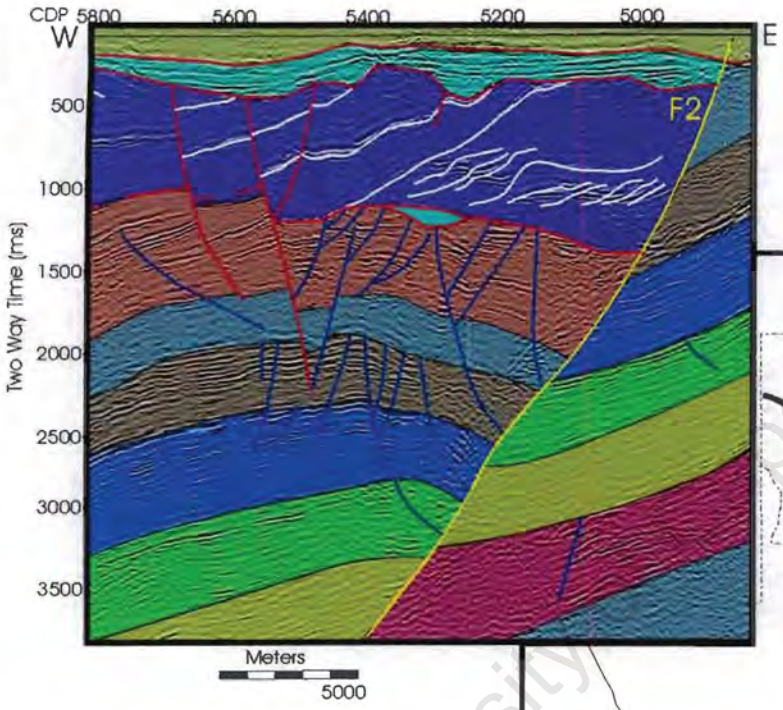

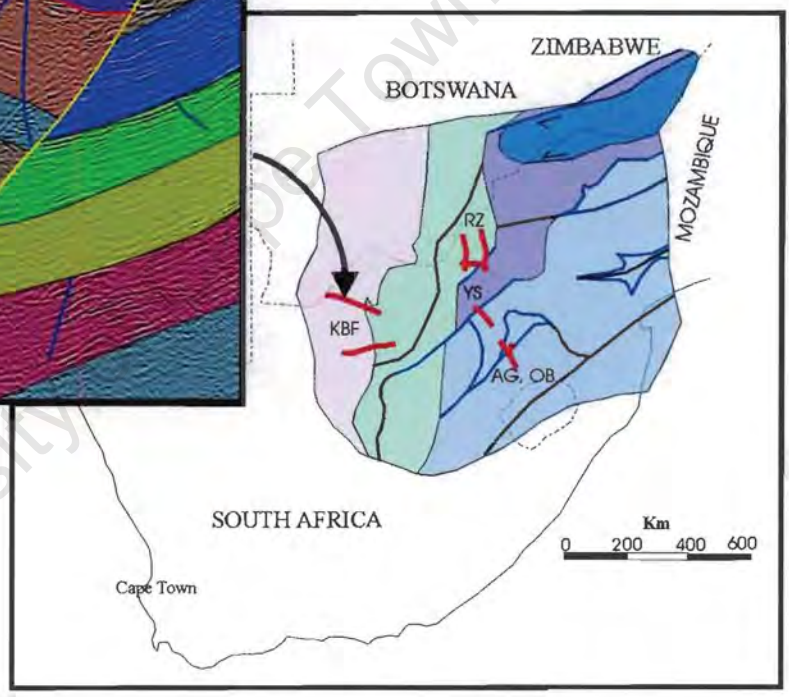

Justine Tinker
2001

Thesis presented for the degree of Master of Science
Department of Geological Sciences,
University of Cape Town

University of Cape Town

Abstract

The Kaapvaal Craton is one of the best preserved of all Archean cratons. It is partially covered by the supracrustal sequences of the Witwatersrand, Ventersdorp and Transvaal Basin (and correlated Griqualand West Basin), which span almost a billion years (~3.1 to 2.2 Ga). This thesis describes and interprets eight newly available seismic reflection profiles, acquired by the vibroseis method to 6 seconds TWT, and totaling ~720 km in length. New stratigraphic and structural features are identified across three main regions: the Kaapvaal Craton's western margin, the northern margin or Bushveld lines (flanking the Thabazimbi-Murchison Lineament and across the western extremity of the Bushveld Igneous Complex) and the Kaapvaal Craton interior. The seismic data was interpreted using Charisma seismic interpretation software, Geoframe version 3.6 (developed by Geoquest, Schlumberger) on a UNIX, SUN workstation.

In the first section, the sedimentary succession across the western margin of the craton is shown to thicken towards its edge from 0 km to > 17 km over 150 km. A normal fault with > 6 km displacement and possible strike-slip movement has been recognized. Three prominent unconformities are identified, as well as ~300 % tectonic thickening of the Hartley Formation in response to east-verging thrusting across the craton. Folding and thrusting of Griqualand West and Olifantshoek Supergroups across the craton are also apparent. The Ventersdorp Supergroup underlies the Transvaal Sequence right to the western edge of the craton.

In the second section, seismic profiles traverse a syncline which trends east/ west over several hundred kilometers and involves mainly Transvaal-aged rocks and sporadic Bushveld outcrop. Evident from these profiles are discrete Ventersdorp half grabens, up to 3 km in depth, with bounding listric normal faults that trend east/ west, subparallel to the Thabazimbi-Murchison Lineament and dip (and thus downthrow predominately to the north). These faults are truncated by the well-imaged Black Reef unconformity.

University of Cape Town

Horst and graben structures, involving the Witwatersrand and lower Ventersdorp Formations, dominate the craton interior lines (third section). Bounding listric normal faults with minimum throw of 9.5 km, trend east/ west and dip (and thus downthrow) to the north and south. The Black Reef unconformity is again distinctive, as is a Paleozoic unconformity (the Beaufort unconformity).

Archean sediment accumulation rates across the western margin average approximately two times less than those calculated for the same stratigraphic groups by previous authors and an order of magnitude lower than most modern carbonate depositional environments. This difference may be due to differing mechanisms for carbonate formation and deposition in the Archean (c.f. Grotzinger, 1989).

The extension directions during Ventersdorp times are different along the western edge (~ E-W) than the craton interior (~N-S). A tectonic model for the evolution of the craton's western margin involves initial extension and rifting, followed by thermal subsidence and then compression involving folding and thrusting eastward across the margin. The thrusting, at 1.9 to 1.7 Ga, caused lithospheric flexure. This tectono-stratigraphic sequence (lower Olifantshoek) allows the calculation of the elastic response of the lithosphere during sedimentation and tectonic loading. A lithospheric elastic thickness of 7 to 10 km is calculated for this region, at this time. This is 7 to 10 times less than the present day estimate of the lithospheric elastic thickness for the same region (60-70 km), indicating that there has been an increase or perhaps recovery of lithospheric strength. The low value for elastic thickness most likely reflects location near an Archean/ Paleoproterozoic passive cratonic margin. Similarly high plate-strength gradients have been calculated in extensional terrains such as the Norwegian, Antarctic and Andean continental margins.

The calculation of sediment accumulation rates, the analysis of lithospheric elastic thickness, coupled with the proposed model of the structural history of the western margin provides new insight into the epeiorogenic movement of the craton and aging of its lithosphere.

University of Cape Town

Table of Contents

University of Cape Town

University of Cape Town

University of Cape Town

University of Cape Town

University of Cape Town

University of Cape Town

Table of Figures

University of Cape Town

University of Cape Town

University of Cape Town

University of Cape Town

University of Cape Town

List of Tables

Acronyms

Ka	10^3 years
Ma	10^6 years
Ga	10^9 years
TWT	Two way time (in milliseconds)
CDP	Common Depth Point

University of Cape Town

Acknowledgements

Work on this project has allowed me to meet many interesting people and travel to fascinating places. It all could not have been possible without the support, enthusiasm and guidance of Maarten de Wit, my supervisor. He always managed to remind me of the big picture, but helped me keep track of the details too.

During my two visits to MIT, I had the fortune of meeting and working with an amazing group of people:
Firstly, John Grotzinger is thanked for his endless enthusiasm, support and for getting me thinking in an entirely new way about sedimentology and stratigraphy. He is also thanked for the financial support that allowed me to study at MIT, and for inviting me to take part in a fantastic and very memorable field trip to New Mexico.
Wiki Royden is thanked for sharing her expertise with patience.
Thank you, Roberta for making me so welcome in the USA, and for being so hospitable and kind.
Thank you to my friends on the 8th floor, for the wonderful experience of being at MIT.

I thank Nick Beukes at RAU for giving up his time to share his comprehensive knowledge of the Transvaal stratigraphy. Thank you to AngloGold for allowing me access to the seismic and well data. Without their generosity there would be no project. Thanks also to the Upstream Training Trust and the NRF for funding this project.

Finally, a huge thank you must go to my father and family, Dave and friends for their love and support.

University of Cape Town

Chapter 1 : Introduction

The Kaapvaal craton is one of the best preserved of all Archean cratons. It is partially covered by well-preserved remnants of the Archean to Paleoproterozoic, Witwatersrand, Ventersdorp and Transvaal- Griqualand West basins. The latter span an area of up to 500 000 km^2 across the Kaapvaal Craton, and an age of 400 million years (2.6 to 2.2 Ga).

The Transvaal and Griqualand West basins host economically important deposits of iron, manganese, lead, zinc and gold. Even with the economic exploratory interest, there are still many unknowns regarding the basins' origin and tectonic and sedimentary history. This is in part due to the obscuring cover of the Quaternary Kalahari sands in the north and west, and the Paleozoic- Mesozoic Karoo sediments and lavas in the south. Geophysical methods have, however, allowed researches to penetrate cover and gather information. In their exploration for gold, AngloGold has acquired several hundred thousand kilometers of seismic reflection data across the Kaapvaal Craton. Of this data, eight seismic profiles are described and interpreted in this project.

This project is a small part of a greater, multinational and multidisciplinary effort, called the Kaapvaal Craton Project. The goal of Kaapvaal Craton Project is to uncover the origins of the Kaapvaal Craton as well as explore how surface processes may reflect deep mantle processes (Carlson *et al.*, 1996). Initially it was hoped that the seismic data interpreted here, may allow detailed sequence stratigraphic work on the Transvaal sediments in order to establish the epeiorogenic history of the craton during Transvaal Basin formation. This aim of the project has evolved as new information from the interpretation of the seismic profiles emerged. Unfortunately, the location of the released lines, some of which traverse Ventersdorp material alone, together with their coarse vertical resolution and lack of well data, made detailed sequence stratigraphic work impossible. Thus the aim of this project changed in scope to include a broader range of topics from the tectonic history and lithospheric thickness of the western margin of the Kaapvaal Craton, through to examination of the discrete Ventersdorp listric fault-bounded basins of the craton interior.

University of Cape Town

1.1. Geological Setting

The seismic profiles transect strata ranging in age from Archean to Jurassic, including the Dominion, Witwatersrand, Ventersdorp, Transvaal, Olifantshoek and Karoo Groups and Supergroups. These strata have been subject to various deformational episodes, and, predominately on geophysical evidence, have been arranged into a number of tectonic provinces. This chapter provides a rough outline of:

1) The position of the seismic profiles relative to tectonic subdomains of the Kaapvaal Craton.
2) The litho-and chronostratigraphy of the Dominion, Witwatersrand, Ventersdorp, Transvaal, Olifantshoek and Karoo Groups and Supergroups, all successive volcano-sedimentary cover sequences of the Kaapvaal granite-greenstone basement.

1.2. Tectonic overview

Southern Africa is composed of a variety of tectonic provinces shown in figure 1.1. Bordering the Kaapvaal Craton to the north is the Limpopo Belt, to the east is the Lebombo Monocline, to the south is the Namaqua-Natal Mobile belt and to the west is a thin skinned fold and thrust Belt (part of which is named the Kheis Belt). The seismic lines have all been shot on the Kaapvaal Craton, though the KBF lines extend to the Craton/ Kheis boundary.

1.2.1. The Kaapvaal Craton

The Kaapvaal Craton, which stabilised between 3.7 and 2.7 Ga, consists of a mosaic of subdomains joined by processes that are similar to today's plate tectonics (De Wit *et al.*, 1992, Carlson *et al.*, 1996). The margins of the craton are delineated using magnetic data (figure 1.2). Figure 1.3 shows the location of the seismic profiles relative to the suggested outline of the subdomains, or terrains of the Kaapvaal Craton. The Rz, Karoo and Ys lines are located in the Amalia, Southern, Vredefort and Witwatersrand Terrains (figure 1.3).

University of Cape Town

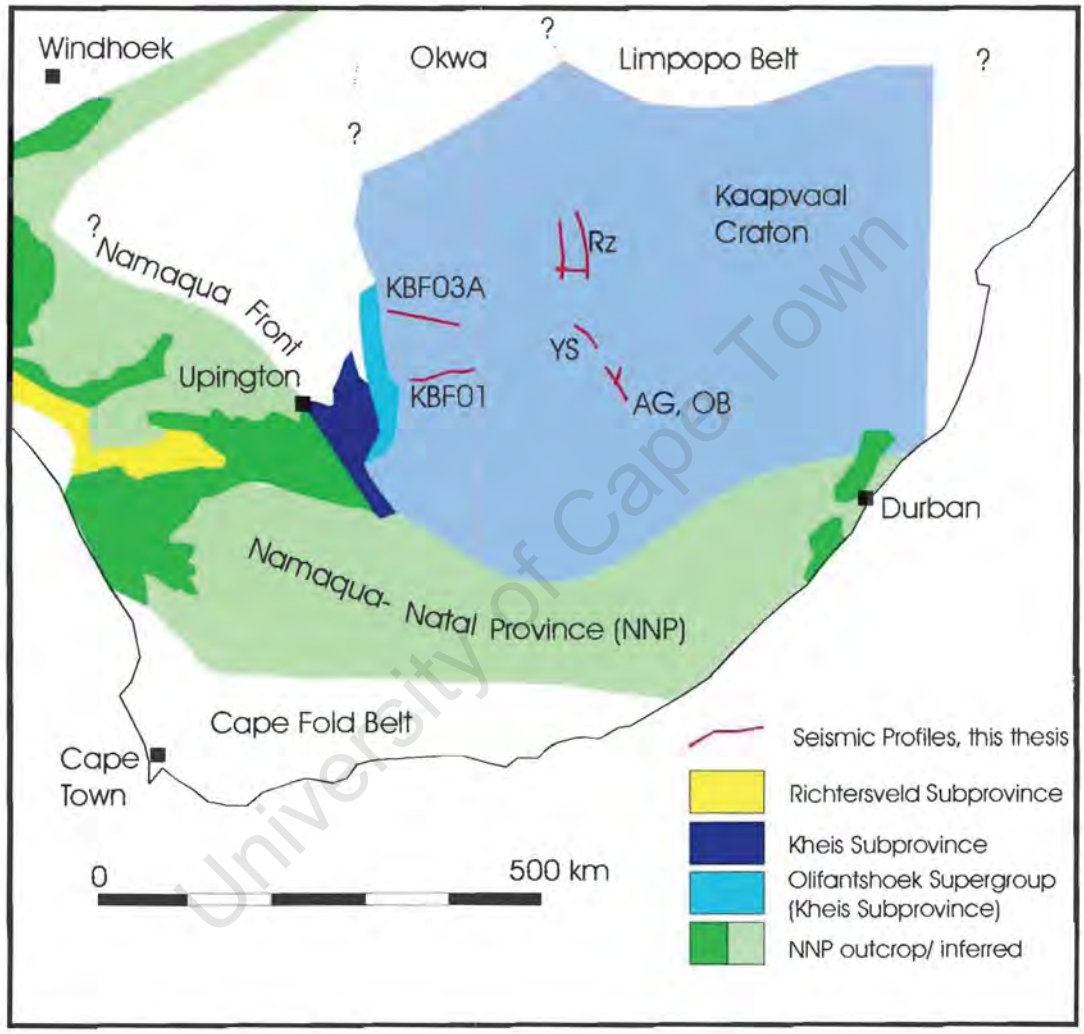

University of Cape Town

Figure 1.1: Location of the seismic reflection profiles relative to the tectonic provinces of southern Africa (modified after Thomas et al., 1993).

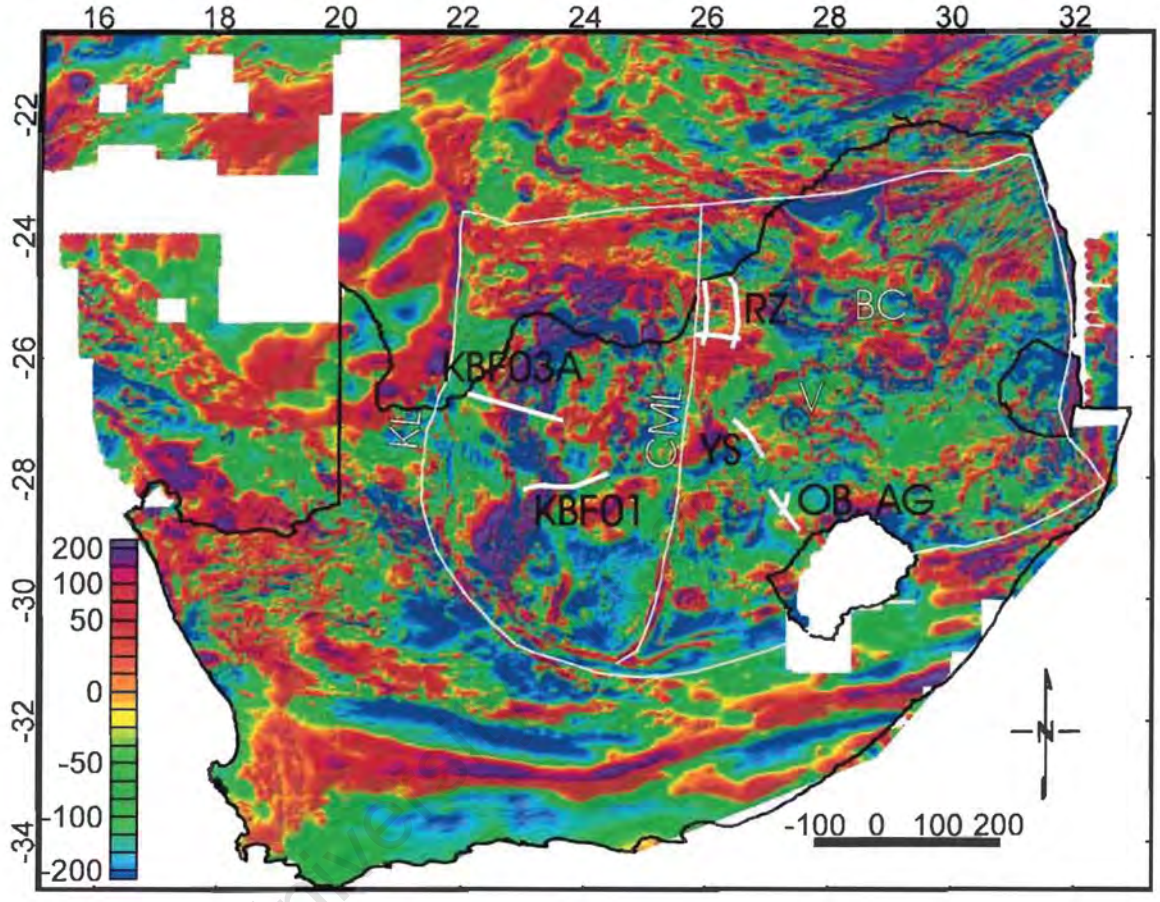

Figure 1.2: Southern Africa magnetic data. Boundaries of the Kaapvaal Craton have been delineated at magnetic anomaly trends. KL = Kalahari Line, CML = Colesberg Magnetic Lineament, BC = Bushveld Complex, V = Vredefort Dome (Doucouré and de Wit, 2001).

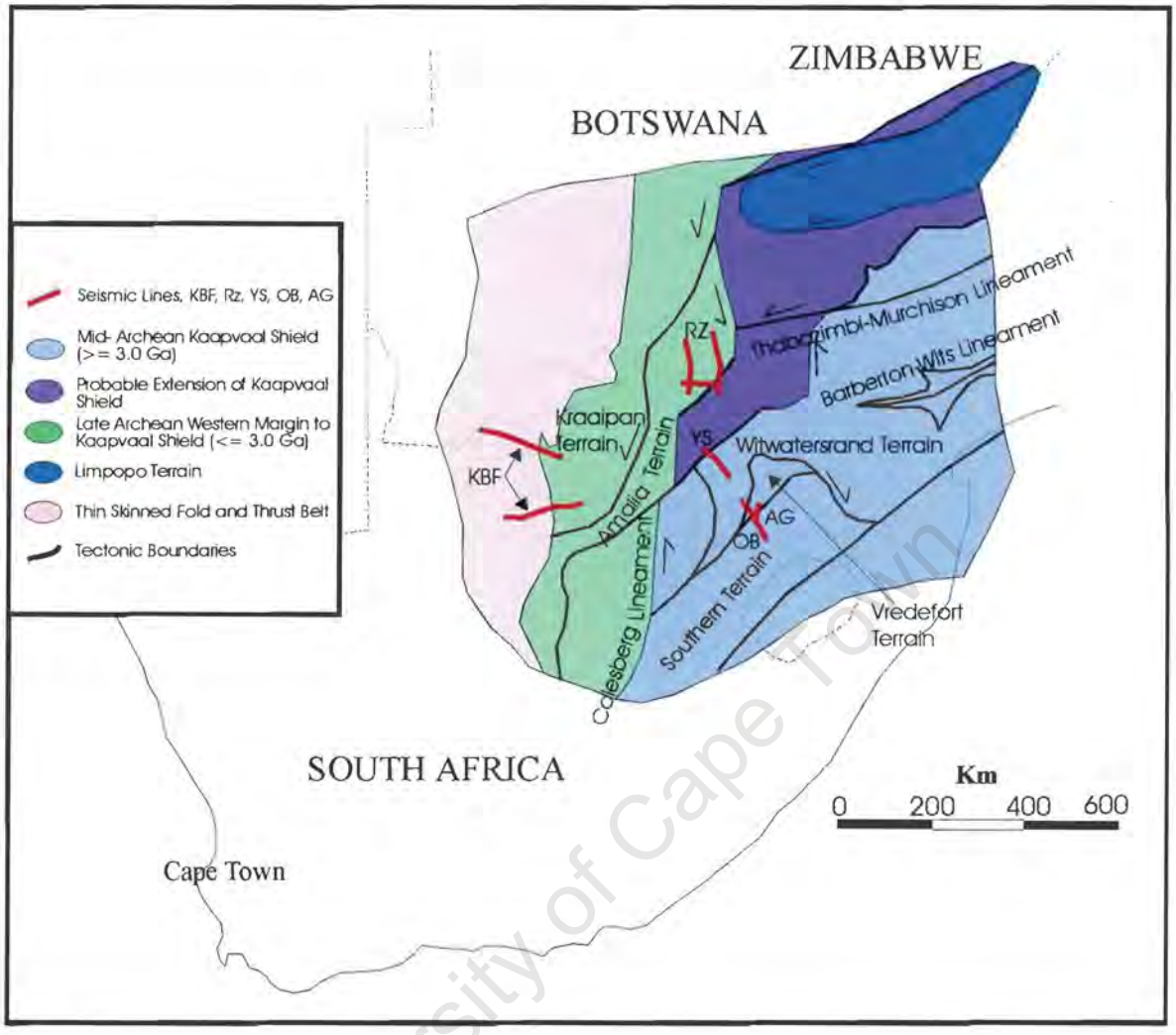

University of Cape Town

Figure 1.3: Map of the Kaapvaal Craton showing the location of the seismic reflection profiles relative to the Archean crustal subdomains (modified after de Wit *et al.*, 1992).

1.2.2. The Western Margin of the Kaapvaal Craton

The KBF Seismic Profiles: The Kheis Subprovince

Lines KBF03A and 01 extend near the western margin of the Kaapvaal Craton, towards the Kheis Subprovince. The Kheis Subprovince is a belt of low-grade, Archean-Proterozoic, arenitic and metavolcanic rock that forms a tectono-metamorphic transition zone between the high-grade rocks of the Namaqua-Natal mobile belt and the Kaapvaal

Craton (Moen, 1999). Many authors refer to a 'Kheis orogeny' involving thin-skinned fold and thrusting of these rocks. Beukes and Smit (1987) assign an Eburnian age of ~2200 to 2000 Ma to the Kheis orogeny. A younger age for the Kheis Subprovince of around 1800 Ma is suggested by Stowe (1986), and is further supported by an ^{39}Ar- ^{40}Ar metamorphic age for the Groblershoek Schist Formation (Olifantshoek Sequence) of 1780 Ma (SACS, 1980; Schlegel, 1988).

There is no agreement on the lateral extent of the Kheis Subprovince. Its eastern boundary has been suggested to coincide with the Blackridge thrust system (figure 1.4) (Beukes and Smit, 1987). Moen (1999) contests this position of the eastern boundary; he prefers to put it at the Dabep Fault (figure 1.4). This fault separates the Olifantshoek Supergroup, which has certainly undergone Eburnean-aged deformation, from the metamorphosed rocks of the Brulpan Group of uncertain age. The Dabep Fault marks the eastern limit of pervasive regional foliation, and thus, according to Moen (1999) should be taken as the eastern boundary between the Kaapvaal Province and the Kheis Subprovince.

Stowe (1986) places the western boundary of the Kheis Subprovince at the transition between ~ 1.1 Ga main Namaqua foliation and the > 1750 Ma 'Kheis' foliation. Whole rock isotope data indicates that the isotopic imprint of the Namaqua orogeny extends much further to the east than previously thought (Moen, 1999). Moen (1999) concludes from geochronology and structural data that there is no recognizable Eburnean-aged deformation in the Kheis Subprovince, (west of the Dabep Fault). He goes further to suggest that the Kheis Subprovince is in fact a subdivision of the Namaqua-Natal Province. The deformation of Eburnean age, east of the Dabep Fault, according to Moen (1999) appears to record an on-craton or craton-edge event.

University of Cape Town

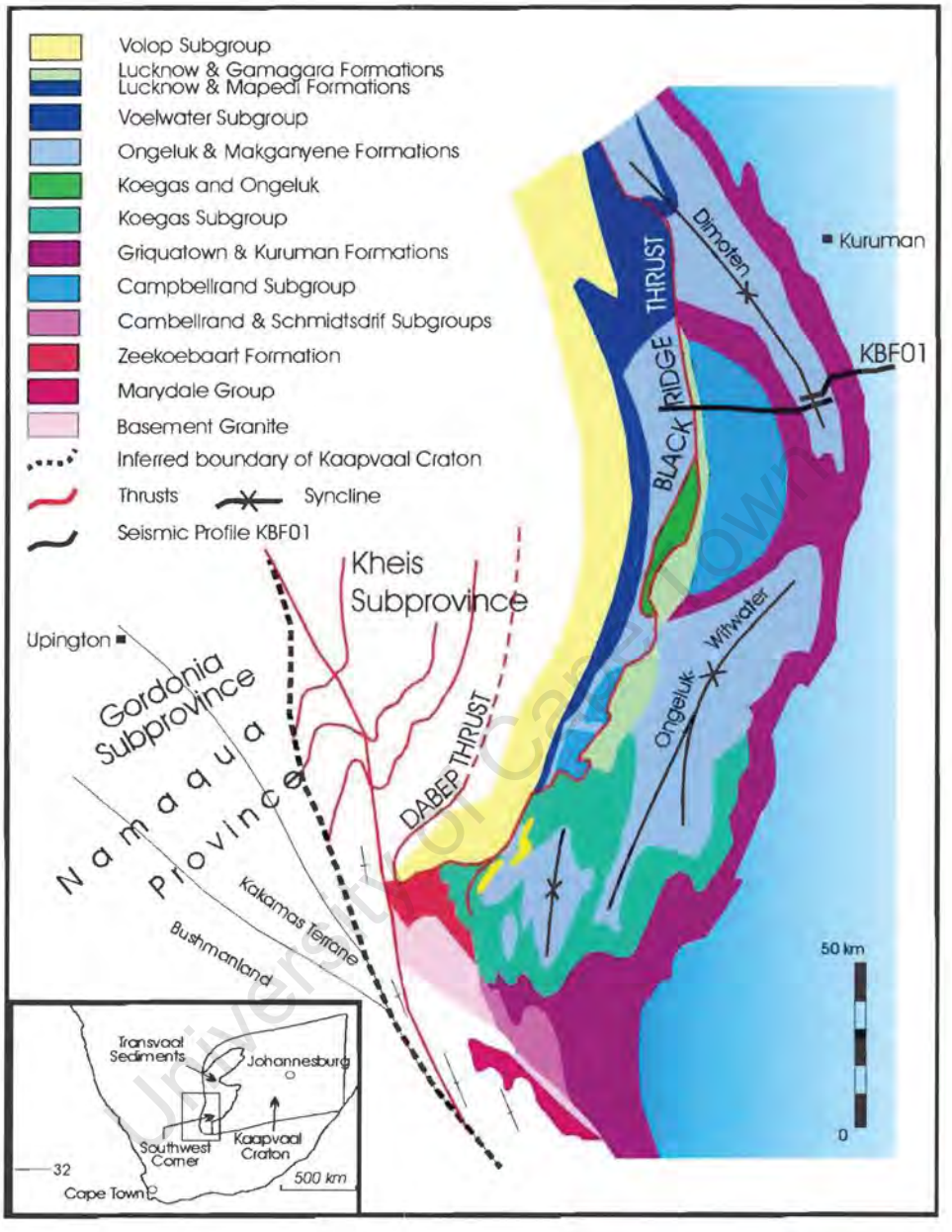

Figure 1.4: Simplified geology along the southwest margin of the Kaapvaal Craton showing bordering tectonic blocks and the location of the Blackridge and Dabep Thrusts (modified after Altermann and Hälbich, 1991).

1.3. Stratigraphic Overview

Figure 1.5 shows the location of the seismic profiles relative to the Witwatersrand, Ventersdorp and Transvaal Basins and extent of the Kaapvaal Craton. Figure 1.6 shows the seismic profiles plotted on a more detailed geological map.

1.3.1. Dominion Group (3.1 Ga)

The Dominion Group may represent a protobasinal phase of the Witwatersrand basin. It unconformably overlies Archean granitic basement and is preserved over an area of 15 000 km^2 (Tankard *et al.* 1982). It is up to 2200 m thick and is composed of quartzites and conglomerates overlain by volcanic mafic-felsic rocks (Armstrong *et al.*, 1991) (Table 1.1).

Group	Formation	Age	Method	Reference	Characteristics
Dominion	Syferfontein	< 3104 ± 3 Ma	U/ Pb on detrital zircons	Robb *et al.* (1990)	* Approximately 1550 m thick. Conformable with the underlying Renosterhoek Formation. * Consists of rhyolites, silicic tuffs, volcanic breccias and subordinate andesitic lavas (Burke *et al.*, 1986).
	Renosterhoek				* Contains up to 1100 m of basaltic andesites and tuffs, plus paleosols and sandstone interbeds (Burke *et al.*, 1986).
	Renosterspruit				* Contains up to 60 m of sandstone with minor conglomerate and argillaceous horizons. * Deposited in a braided stream environment (Burke *et al.*, 1986).

Table 1.1: Generalized Stratigraphy of the Dominion Group.

University of Cape Town

1.3.2. The Witwatersrand Supergroup (3.1 – 2.7 Ga)

The Witwatersrand Supergroup is almost entirely composed of clastic sediments and is divided into the West Rand and Central Rand Groups. The West Rand Group, with a maximum thickness of 7500 m (Clendenin *et al.*, 1988), conformably overlies the Dominion Group and extends over an area of at least 42 000 km^2 (Tankard *et al.*, 1982). A gravity anomaly associated with this basin suggests that its original extent may have been much greater. The successive Central Rand Group occupies a smaller area of 9750 km^2 (Tankard *et al.*, 1982). It is unconformable with the West Rand Group and attains an

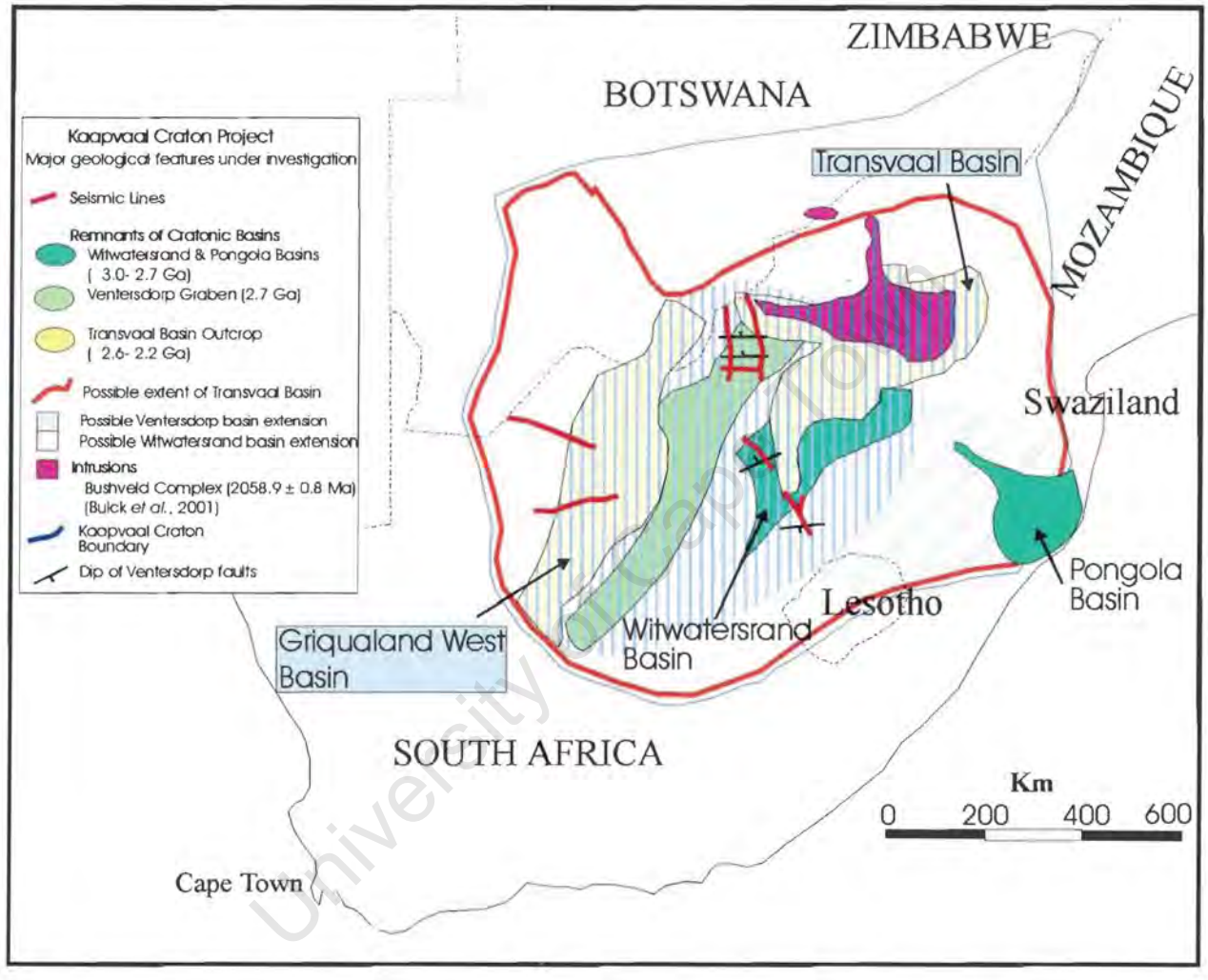

Figure 1.5: Location of the seismic reflection profiles studied in this thesis relative to the extent of the Kaapvaal Craton, Witwatersrand, Pongola, Ventersdorp and Transvaal Basins

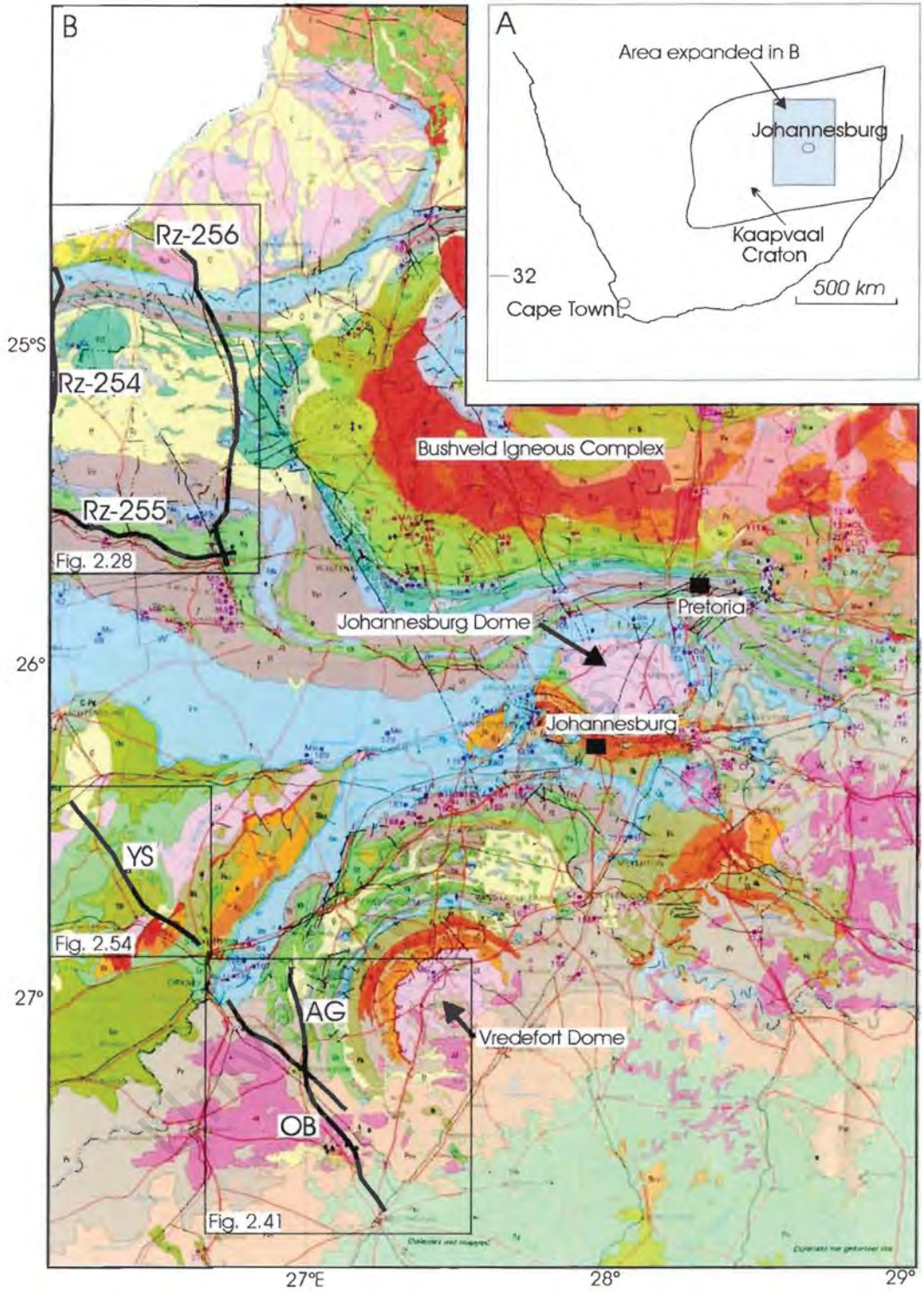

Figure 1.6: Geological map showing the location of seismic lines Rz-254 to 256, YS, AG and OB. (Geological Map of South Africa, Transkei, Bophuthatswana, Venda and Ciskei and the Kingdoms of Lesotho and Swaziland. 1: 1 000 000, 1984, *Geol. Surv. of S. Afr.)*

average thickness of 2900 m (Clendenin et al., 1988). The Central Rand Group contains predominately coarse-grained greywackes, conglomerates and interbedded quartz arenite, shales and siltstones. The Booysens shale Formation separates the Johannesburg and Turffontein Subgroups.

Supergroup	Group	Subgroup	Age	Method	Reference	Characteristics (Burke *et al.*, 1986)
Witwatersrand	Central Rand	Turffontein	< 2909 ± 3 Ma	U/ Pb, detrital zircons	Robb *et al.*, 1990	* Alluvial/ fluvial sands and conglomerate
		Johannesburg				* Alluvial/ fluvial sands and conglomerate, minor shale and lava
	West Rand	Jeppestown	< 3060 ± 2 Ma	U/ Pb, detrital zircons	Robb *et al.*, 1990	* Greywacke and shale, minor lava
		Government				* Magnetic and laminated shales, argillites and sandstones
		Hospital Hill				* Magnetic and laminated shales, argillites, graded sandstones, quartzites

Table 1.2: Generalized stratigraphy of the Witwatersrand Supergroup.

University of Cape Town

1.3.3. The Ventersdorp Supergroup (2.7 Ga)

The Ventersdorp Supergroup is an 8 km thick succession of volcanic and sedimentary rock which occupies 300 000km^2 area (Van der Westhuizen *et al.*, 1991). It is divided into the Klipriviersberg, Platberg and Pniel Groups. In the western part of the basin, an angular unconformity separates the Ventersdorp from the Witwatersrand Supergroup below (Tankard *et al.*, 1982). Elsewhere, the Ventersdorp succession is conformable with the underlying Witwatersrand Supergroup (Linton *et al.*, 1990).

The distribution of Ventersdorp Sequence across the craton is uneven. The basal Klipriviersberg Group outcrops only in the northeast and is between 1500 m and 2000 m thick (Myers *et al.*, 1990). The overlying Platberg Group outcrops intermittently but is absent from the northeast; on the other hand, the overlying Bothaville Formation of the

Pniel Group is laterally extensive. The Allanridge Formation lavas are present over large areas and are mostly covered by the Karoo Sequence (Van der Westhuizen *et al.*, 1991).

Supergroup	Group	Formation	Age	Method	Reference
Ventersdorp	Pniel	Allanridge			
		Bothaville			
	Platberg	Rietgat			
		Makwassie	2709 ± 4 Ma	U /Pb zircon	Walraven *et al.*, 1991
		Goedgenoeg			
		Kameeldoorns			
	Klipriviersberg		2714 ± 8 Ma	U/ Pb zircon	Armstrong *et al.*, 1991

Table 1.3: Generalized stratigraphy of the Ventersdorp Supergroup.

1.3.3.I. The Klipriviersberg Group

The Klipriviersberg Group is a repetitive sequence of alkali-rich, continental tholeiitic flood basalts (Tankard *et al.*, 1982) with high magnesium komatiitic basalt flows at its base (McIver *et al.*, 1981). Hatton (1995) relates the outpouring of Klipriviersberg flood basalts to the emplacement of a mantle plume beneath the Kaapvaal Craton.

The group has been divided into six formations based on lithology (Winter, 1976). The succession is mostly composed of sub-aerially extruded lava flows, that are generally amygdaloidal (Van der Westhuizen *et al.*, 1991). Palmer et al. (1986), Bowen et al. (1986), Myers et al. (1990) and Linton et al. (1990) have carried out geochemical analysis on these lavas. Myers et al. (1990) states that, in general, geochemical subdivision can be related to the subdivision of Winter (1976) and that lithological breaks conform to chemical breaks (Van der Westhuizen *et al.*, 1991). Linton *et al.* (1990) however question whether lithostratigraphy can be correlated over such large distances.

1.3.3.II. The Platberg Group

An unconformity separates the Klipriviersberg Group from the Platberg Group, which was deposited in a wide, north east/ south west trending extensional terrain, terminating against the Thabazimbi/Murchison Line to the north (Martin *et al.*, 1998). Platberg rock types vary greatly from chemical and clastic sediments, to mafic and acid volcanics (Van

University of Cape Town

der Westhuizen *et al.*, 1990). At the base of the Platberg Group is the Kameeldoorns Formation which consists of the sediment fill of deep intermontane graben basins (Buck, 1980). Sediments range from coarse material in scree and debris flow alluvial fan deposits, to fine grained terrigenous and chemical sediments in a more distal environment (Buck, 1980). Andesitic, porphyritic lavas of the Goedegenoeg Formation overlie these sediments. The lavas are in turn overlain by Makwassie felsic volcanics with a dacitic to rhyolitic composition (Van der Westhuizen *et al.*, 1991). The Rietgat Formation conformably overlies the Makwassie Formation in some places, and disconformably in others. It is composed of mafic and often porphyritic lavas and intercalated sediments (Van der Westhuizen *et al.*, 1991).

1.3.3.III. The Pniel Group

Separating the Pniel Group from the underlying Platberg Group is a pronounced unconformity (Winter, 1976, Cheney *et al.*, 1990). The base of the Pniel Group is the arenaceous Bothaville Formation. The Allanridge Formation, consisting of predominately green amygdaloidal basaltic lava (Winter, 1976), forms the top of the Pniel Group, that terminates the Ventersdorp Supergroup. Hatton (1995) and Martin *et al.* (1998) suggest that the Allanridge flood basalt, like the Klipriviersberg Group, is related to the emplacement of a mantle plume beneath the craton. Where the Bothaville Formation pinches out against paleohighs, the Allanridge Formation is in direct contact with the underlying Rietgat Formation (Van der Westhuizen *et al.*, 1991).

2.6 to 2.2 Ga saw the development of two major basins on the Kaapvaal Craton, namely the Transvaal and the Griqualand West Basin. Subtle differences between these basins exist, however the history of siliciclastic sedimentation, followed by chemical sedimentation and finally a return to siliciclastic sedimentation is shared. In this section the stratigraphy of these basins is discussed separately with particular reference to those formations encountered in the seismic profiles. Table 1.4, detailing the suggested correlation between these two basins is included in pages 1-14 and 1-15.

University of Cape Town

Griqualand West Supergroup						Transvaal Supergroup				
Group	**Subgroup**	**Formation**	**Age**	**Method and Reference**	**Lithology**	**Group**	**Subgroup**	**Formation**	**Age**	**Method and Reference**
					Volcanics and clastics	Rooiberg				
					Clastic sediments and volcanics	Pretoria		Rayton/ Woodlands		
								Magaliesberg		
								Silverton		
								Daspoort		
Postmasburg		Mooidraai	2394 ± 26 Ma	Bau *et al.* (1999) Pb/Pb whole rock isochron				Strubenkop		
		Hotazel						Dwaalheuwel		
		Ongeluk	2222 ± 13 Ma *	Cornell *et al.* (1996) Pb/Pb whole rock isochron				Hekpoort	2224 ± 21 Ma	Referenced in Eriksson *et al.* (1993) Rb/Sr
		Makganyene						Boshoek		
								Timeball Hill	2263 Ma	Referenced in Eriksson *et al.* (1993) Rb/Sr
								Rooihoogte		

Table 1.4: Possible correlation, highlighted by colours, between the Griqualand West and Transvaal Basin sequences. Geochronologic data, where available, is included. * The correlation between the Ongeluk and Hekpoort lava, as well as their respective dates is disputed (see page 1-22 for further explanation).

University of Cape Town

Griqualand West Supergroup					Lithology	Transvaal Supergroup				
Group	Subgroup	Formation	Age	Method and Reference		Group	Subgroup	Formation	Age	Method and Reference
Ghaap	Koegas				Chemical sediments: carbonate and iron formation	Chuniespoort		Duitschland		
	Asbesheuwels	Griquatown	2489 ± 33 Ma	Trendall unpubl. Referenced in Nelson *et al.* (1999) U/Pb zircon SHRIMP				Penge	2480 ± 6 Ma	Trendall unpublished, referenced in Nelson *et al.* (1999) U/Pb SHRIMP
		Kuruman	2465 ± 7 Ma	Armstrong pers. comm. Referenced in Martin *et al.* (1998) U/Pb Zircon						
	Campbellrand	Gamohaan	2521 ± 3 Ma	Summer and Bowring (1996) U/Pb Zircon			Malmani	(Oaktree)	2583 ± 5 Ma	Martin *et al.* (1998) U/Pb Zircon SHRIMP
		Kogelbeen							2588 ± 7 Ma	Martin *et al.* (1998) U/Pb Zircon SHRIMP
		Klippan								
		Papkuil							2550 ± 3 Ma	Walraven and Martini (1995) Pb evap -Zircon
		Klipfontein								
		Fairfield								
		Kamden Member								
		Reivilo								
		Monteville	2555 ± 19 Ma	Altermann and Nelson (1998) U/Pb Zircon SHRIMP						
	Schmidtsdrif	Lokammon a			Clastic sediments			Black Reef		
		Boomplaas								
		Vryburg	2642 ± 3 Ma	N. Beukes, pers. Comm. Pb evap- Zircon						

Table 1.4: Continued. Colours highlight suggested correlations between the Griqualand West and Transvaal Basins.

University of Cape Town

1.3.4. The Transvaal Supergroup (2.6- 2.2 Ga)

1.3.4.I. The Black Reef Formation

The Black Reef Formation is a thin layer of siltstone, sandstone and lava (Eriksson *et al.*, 1993), which rests unconformably on the Archean gneisses, granites and greenstone belt, Ventersdorp volcanics, Witwatersrand sediments and the Wolkberg Group (in the north east). Today the Black Reef Formation outcrops around the present day margin of the Transvaal Basin. The thickness of this unit varies from from a couple of meters to thirty meters to a maximum of 60m in eastern Botswana (Henry *et al.*, 1990 in Eriksson, 1993). The Black Reef starts as an upward fining sequence with varying lithologies from clast and matrix supported conglomerates, through cross bedded to planar bedded arenites and laminated carbonaceous mudstone (Button, 1986, Henry, 1990). Where the conglomerates rest directly on mineralised Witwatersrand sediments they can be auriferous (Button, 1986). Above the upward fining sequence is a coarsening upward succession. The carbonaceous mudstones at the top of the succession grade into the overlying dolomites of the Malmani Subgroup, Chuniespoort Group (Button, 1986).

Henry *et al.* (1990) interprets the successive coarsening upward sequence as prograding braid delta environment. The mudstone forming the top of the succession may have been deposited in a tidal flat setting, the precursor to the development of the epeiric marine carbonate platform and formation of the Malmani carbonates (Eriksson *et al.*, 1993).

1.3.4.II. The Chuniespoort Group

1.3.4.II.a. The Malmani Subgroup

The Malmani dolomite, which hosts important mineral deposits of gold, lead, zinc and manganese amongst others (Button, 1973; Beukes, 1986), comprises a succession of stromatolitic carbonates with interbedded chert, with minor shale and quartzite (Button, 1973). Five regionally persistent lithological units exist; these are recognized on the basis of the colour of the dolomite as well as the proportion of chert, limestone banded iron formation, mudstone and quartzite interbedded with the carbonate (Button, 1973).

University of Cape Town

A basic tidal paleoenvironment is suggested for the deposition of the Malmani Subgroup (Truswell and Eriksson, 1973). Columnar stromatolites are indicative of an intertidal environment, oolites of a high energy zone above wave base and domal stromatolites and mounds indicative of a subtidal environment (Eriksson *et al.*, 1993). Clendenin (1989) extends this earlier model of a tidal paleoenvironment further, calling for a tectonic steepening of a carbonate ramp by syndepositional tectonics. Facies distribution was controlled by water depth, which varied during five main transgressions and regressions of the proposed epeiric sea (Eriksson *et al.*, 1993).

1.3.4.II.b. Penge Iron Formation

Iron-formations on the whole are less well developed and less abundant in the Transvaal area than in the Griqualand west basin. The Penge Iron-Formation is the only known iron formation in the Transvaal Basin and has been correlated to the Asbesheuwels Subgroup of the Griqualand West succession (Beukes, 1983). The Penge Iron-Formation succeeds the Malmani Subgroup and attains a maximum thickness of 600 meters (Beukes, 1986). It is composed of alternating macro, meso and micro banded iron-formation and carbonaceous shale members. Minerals include quartz, magnetite, hematite, stilpnomelane, riebeckite and iron-carbonates amongst others (Beukes, 1986).

Due to the lack of mechanical sedimentary structures and lateral continuity of layers, the Penge Iron-Formation is believed to have formed below wave base in a very stable marine shelf (Beukes, 1986). Altermann and Halbich (1990) dispute this proposed stable environment. They present evidence of tectonic displacement and karstification of iron-formations and underlying carbonate rock (referred to in Eriksson *et al.*, 1993). The origin of the Kgwakgwe breccias is another point of debate. Eriksson *et al.* (1993) propose that tectonic instability of the basin margin resulted in uplift and subaerial exposure giving rise to brecciation of silica gels and non-deposition of iron formation. The Penge Iron Formation was deposited during a transgressive phase of the epeiric sea.

University of Cape Town

1.3.4.II.c. The Duitschland Formation

Subsequent regression produced an erosional unconformity at the base of the Duitschland Formation. Renewed transgression resulted in the deposition of Duitschland carbonates. The final regression of the epeiric sea led to basin contraction and a landward shift of facies, the deposition of the Duitschland conglomerates and diamictites (Eriksson *et al.*, 1993). The location of the Duitschland Formation, in the northeastern Transvaal suggests that the final regression took place in a north east direction across the craton.

1.3.4.III. The Pretoria Group

The Pretoria Group consists of alternating mudstones and sandstones with minor volcanic horizons and diamictites and conglomerates (Eriksson *et al.*, 1993). Unlike the chemical sediments of the Chuniespoort Group, the Pretoria group sediments cannot be as easily correlated between the Transvaal and Griqualand West Basins. It is for this reason that various authors have proposed that these two groups developed in separate basins (Crockett, 1972, Eriksson *et al.*, 1988, 1991 and Eriksson and Clendenin, 1990).

The base of the **Rooihoogte Formation** comprises chert breccia and conglomerates possibly formed by the reworking of older material by a transgressive sea (Beukes, 1986). A radically different depositional environment comprising alluvial fans and fan deltas is proposed by Eriksson (1998). The conglomerates and breccias grade upward into mudstones and finally into arenites (Eriksson *et al.*, 1993).

The **Timeball Hill Formation** consists of carbonaceous mudstones at its base, grading into ferruginous mudrocks and fine-grained sandstones. The suggested environment of deposition is a relatively deep basin in turn filled by fluvio-deltaic complexes from the north, northwest and east, with preservation only of the distal deposits (Eriksson *et al.*, 1993). **The Boshoek Formation** follows the **Timeball Hill Formation**. Boshoek conglomerates and sandstones and the diamictites of the upper Timeball Hill Formation are correlated with the Makganyene diamictites of Griqualand West. Visser (1971) interprets these diamictites as glacial, glaciofluvial and glaciomarine in origin.

University of Cape Town

The lavas of the **Hekpoort Formation** have a basaltic to andesitic chemistry (Sharp *et al.,* 1983 and Beukes, 1986) and extruded into both a marine and non-marine setting, in the case of the Machadorp Volcanic Member (Beukes, 1986). However, Eriksson *et al.,* 1993, believes the lack of pillow lavas and mudrock interbeds to be indicative of subaerial extrusion. Lack of pillow lavas, however, cannot alone be used as evidence for a non-marine setting.

Conglomerates and immature sandstones and minor mudstones of the **Droogedal/ Dwaalheuwel Formations** overlie the Hekpoort lavas. According to Eriksson *et al.* (1993) these represent sheets and lobes of sediment entering the Transvaal basin. They thin towards the direction of Pretoria where the Hekpoort lavas are followed directly by the mudstones and sandstones of the **Strubenkop Formation** (Eriksson *et al.,* 1991). In this model, the Strubenkop Formation represents a distal, lacustrine basin into which the Droodedal/ Dwaalheuwel sandstone and conglomerates were deposited. Structures including ripple marks, mud cracks and flute casts amongst others are all consistent with a shallow water setting, be it lacustrine or tidal flat (Eriksson *et al.,* 1993).

The **Daspoort Formation** consists of cross and planar bedded sandstones and overlies the Strubenkop mudstone (Eriksson *et al.,* 1993). In the west of the Transvaal basin the Daspoort Formation is known as the **Ditlhojana Formation** and directly overlies thin mudstones above the Hekpoort lavas (Key, 1983). There is no agreement as to the depositional setting of the Daspoort Formation. Suggested paleoenvironments vary from shallow marine (Button, 1973 in Eriksson *et al.*, 1993), fluvial-beach (Visser, 1969 in Eriksson *et al.,* 1993) to distal fan-fluvial braidplain (Eriksson *et al.*, 1993).

The **Silverton Formation** consists of a thick sequence of mudtones that contain intercalations of chert, sandstone, carbonate and tuff. Eriksson and Clendenin (1990) propose that the Silverton Formation shales developed in a lacustrine, deltaic environment. In this model the overlying **Magaliesberg sandstones** are interpreted as the shoreline of the basin. This is consistent with the uniform thickness of both above formations across the basin (Eriksson et al., 1993). Thinning of the Magaliesberg sandstones isopachs towards the centre of the basin have led Eriksson *et al.* (1990) to

University of Cape Town

propose an onset of doming in the basin, perhaps thermal in nature, due to the rising Bushveld plume. This concept of doming is consistent with paleocurrent estimates (Schreiber, 1991). Doming may have led to the retreat of the Silverton 'sea' away from the Magaliesberg shoreline sands, which may have been fluvially reworked (Reczko *et al.*, 1992).Doming may have resulted in the development of the two separate basins in post Magaliesberg times (Eriksson *et al.*, 1993). The **Rayton/Woodland's** mudstones, sandstones, tuffs, carbonates and cherts were subsequently deposited.

1.3.5. The Griqualand West Supergroup (2.6 – 2.2 Ga)

The Griqualand West Supergroup is divided into two groups: the Ghaap Group, composed predominately of chemical sediments overlain by the mostly clastic Postmasburg Group.

1.3.5.I. The Ghaap Group

At the base of the Ghaap Group is the Schmidtsdrif Subgroup, which is overlain by the Campbellrand and Asbesheuwels Subgroups.

1.3.5.I.a. The Schmidtsdrif Subgroup

The **Vryburg Formation**, the basal unit of the Griqualand West Supergroup, unconformably overlies Ventersdorp lava. The formation consists of shales, quartzites, siltstones and lava (Altermann and Nelson, 1998). It is correlated with the Black Reef Formation of the Transvaal Supergroup and is, at its maximum, 100 m thick (Altermann and Wotherspoon, 1995). Dolomites, limestones, oolites and shales of the **Boomplaas Formation** overlie the Vryburg Formation (Altermann and Wotherspoon, 1995). These are in turn overlain by the **Lokammona Formation** consisting of shales, tuffs, carbonates and chert (Altermann and Nelson, 1998).

The quartz arenites of the Schmidtsdrif Subgroup were deposited in a fluvial, shallow marine and intertidal environment. They are succeeded by a carbonate platform sequence which interfingers with a carbonate basinal shale in places (Beukes, 1986). Thus the

University of Cape Town

Schmidtsdrif Subgroup is understood to have formed in a transgressive environment in gradually increasing water depth.

The Schmidtsdrif Group, according to Clendenin *et al.* (1988), records the onset of thermal subsidence of the Ventersdorp rifting event and differential uplift due to thermal inflation resulting from hotspot related break up.

1.3.5.II.b. The Campbellrand Subgroup

The Campbellrand Subgroup, at least 1800 m thick, consists of stromatolitic dolomite and limestone platform facies which interfinger, basinwards with limestone and dolomite (Beukes, 1986). Further into the basin, turbiditic carbonates have been ankeritized and partially replaced by silica. The interior platform carbonate sequence has mostly been dolomitized. Limestone is preserved along the margin of the carbonate platform, where there was water circulation (Beukes, 1986).

Beukes (1987) separates the carbonates into two major lithofacies assemblages namely a basinal, non-stromatolitic laminated carbonate and shale sequence (off craton to the west) and a shallow water stromatolitic carbonate sequence on craton (Beukes, 1987). The upper part of the succession sees the development of a rimmed carbonate shelf causing the formation of mudflats and lagoons with a deep basin to the west.

The basal unit of the Campbellrand Subgroup is the **Monteville Formation**. It is interpreted as a shelf deposit (Beukes, 1987) and has an average thickness of 200 m (Altermann and Wotherspoon, 1995). It is overlain by the **Reivilo Formation** which is up to 900 m thick and consists of giant stromatolite domes intercalated with columnar stromatolites and oolites beds (Altermann and Wotherspoon, 1995). Carbonates are interspersed with banded iron formation (Kamden Member), oolite beds, algal mats and chert through the **Fairfield, Klipfontein, Papkuil, Klippan, Kogelbeen** and **Gamohaan Formations**.

University of Cape Town

Drowning of the carbonate shelf was followed by the deposition of the thick iron formations of the Asbesheuwels Subgroup.

1.3.5.I.c. The Asbesheuwels Subgroup

The basal microbanded **Kuruman Iron-formation** of the Asbesheuwels Subgroup conformably overlies the carbonates of the Gamohaan Formation, Campbellrand Subgroup (Hälbich *et al.*, 1993). It is between 150 to 750 m thick (Hälbich *et al.*, 1993) and represents an upward-shallowing sequence consisting of chemical sediments deposited in a euxinic basin, transitional euxinic (anoxic) basin/ open shelf, open shelf, slope of shallow water platform and shallow water platform environments (Beukes, 1986). The Kuruman Iron-Formation is overlain by the **Griquatown Iron-Formation**, a clastic-textured unit of 200 to 300 m (Hälbich *et al.*, 1993), deposited in a shallow epeiric sea (Beukes, 1986).

1.3.5.I.d. The Koegas Subgroup

The Griquatown Iron-Formation grades upward into the **Koegas Subgroup** which is composed of chloritic mudstone, siltstone and quartz wacke (Beukes, 1986). Beukes (1984) suggests a fresh-water lake depositional environment for the Koegas Subgroup.

1.3.5.II. The Postmasburg Group

The Ghaap sediments were uplifted and eroded to produce an unconformity that separates this group from the Postmasburg Group above. The **Makganyene Formation** is a diamictite, considered to be of glacial origin Visser (1971). The successive **Ongeluk Formation** has been correlated with the Hekpoort lavas of the Transvaal Basin. The correlation is based on Rb-Sr and Pb-Pb whole rock model ages as well as geochemical similarities. Moore *et al.* (2000) contests this correlation claiming that the age data is unreliable, and that the similarity of trace element compositions of all basaltic extrusions between 3000 and 2100 Ma makes discrimination on geochemical grounds unreliable (Moore *et al.*, 2000).

University of Cape Town

The Ongeluk Formation is a shallow-marine volcanic sequence of pillow lava, lava flows and hyaloclastite (Cornell *et al.*, 1996). Palaeomagnetic work has resulted in an 11 ± 5° depositional latitude estimate for the lavas (Evans *et al.*, 1997). The underlying Makganyene glacial deposits were therefore probably deposited within tropical latitudes, perhaps indicating that the earth's global climate system may have been fundamentally different in the Precambrian (Evans *et al.*, 1997).

The Ongeluk lavas are overlain by jasper, jaspilite and sedimentary manganese deposits of the **Hotazel Formation** and the clastic-textured dolomite and stromatolitic dolomite of the **Mooidraai Formation** (Beukes, 1986). These two formations compose the **Voëlwater Subgroup**.

1.3.6. The Olifantshoek Group

The Olifantshoek Group unconformably overlies the Griqualand West Supergroup (Table 1.6). The base of this group is the 10 to 1500 m thick **Mapedi Formation**, composed of shale, quartzite, lava and a basal iron-rich conglomerate (Beukes and Smit, 1987). Succeeding the Mapedi Formation are the 450 m **Lucknow** arenites (Beukes and Smit, 1987). In the Malmani dome area these two formations are collectively known as the **Gamagara Formation**. The lavas of the **Hartley Formation** have an average thickness of 700 m, and were extruded over the lower Olifantshoek sediments. They are dated at 1928 ± 4 Ma (Cornell *et al.*, 1998). It is an amygdaloidal, andesitic lava with interbedded sediments (SACS., 1980). The **Volop Subgroup** completes the Olifantshoek Group; it is a 3500 m unit of quartzites (Beukes and Smit, 1987).

University of Cape Town

Supergroup	Subgroup	Formation	Age	Method	Reference
Olifantshoek	Volop	Verwater			
		Glen Lyon			
		Ellis Rus			
		Fuller			
		Hartley	1928 ± 4 Ma	Pb-Pb Zircon (Kober method)	Cornell *et al.* (1998)
		Lucknow			
		Mapedi			

Table 1.5: Stratigraphy of the Olifantshoek Group

1.3.7. The Karoo Supergroup (350 – 180 Ma)

The Karoo Supergroup was deposited in the Main Karoo and Kalahari basins as well as several other subsidiary basins of southern Africa (Johnson *et al.*, 1996). The Supergroup outcrops over an area of 300 000 km^2 extending to a maximum thickness of 8000 m (Smith *et al.*, 1993). The strata of the main Karoo basin range in age from Late Carboniferous to Early Jurassic (Johnson *et al.*, 1996). The Karoo sequence accumulated under a wide range of climatic regimes and within a variety of tectonically controlled settings (Smith *et al.*, 1993). Depositional environments include glacial, deep marine, shallow marine, deltaic, fluvial, lacustrine and aeolian (Johnson *et al.*, 1996). The Supergroup is divided into the Dwyka, Ecca, Beaufort, Stormberg and Drakensberg Groups.

The **Dwyka Group** consists of glacial deposits, grading upward into mudrock deposited in marine and fresh water environments of the lower **Ecca Group** (Turner, 1999). Upper Ecca and Lower **Beaufort Group** sand dominated fluvio-deltaic deposits were formed contemporaneously with the mudrock by progradation into the basin from the north east and south (Turner, 1999). Non-marine deposits including the upper Beaufort Group and **Stormberg Group** exist in the central part of the Karoo basin (Turner, 1999). Capping the Stormberg Group is 1400m of basaltic lava of the **Drakensberg Group**. This has been radiometrically dated at 183 ± 1 Ma, (Duncan *et al.*, 1997), and is thought to represent a plume generated sequence during the onset of early rifting of Gondwana (Turner, 1999). Karoo strata are almost flat lying in the north. The southern margin strata have been folded and thrusted by the deformation causing the formation of the Cape Fold Belt. Isostatic uplift of the Cape Fold Belt may have created a southerly source for the sediments of the Main Karoo Basin up until the extrusion of the Drakensberg lavas (Turner, 1999).

Much of the stratigraphic interpretation of particularly the Transvaal and Griqualand West basin is controversial. Age constraints are poor, there is little paleoenvironmental agreement and regional correlations are unreliable. Seismic reflection data may help to solve some of the unknowns, which is what this thesis sets out to do.

University of Cape Town

Chapter 2 : Seismic Stratigraphy

2.1. Introduction

The seismic reflection profiles were interpreted with the aid of the following:

- *Charisma seismic interpretation software*, Geoframe version 3.6, developed by Geoquest, Schlumberger. This software is tailored specifically for:
  - Delineating reflections, unconformities and faults using *horizon and fault picking* tools.
  - Correlating distinctive reflectors across faults, and between seismic profiles using the *seismic correlation* tool.
  - Enhancing weaker reflectors and revealing structure using the *seismic attribute* tool.
  - Viewing small-scale structure using the *zoom* function.
- *Comparison to published seismic reflection data across the craton*. Although there have been several hundred thousand kilometres of seismic reflection data acquired over the Kaapvaal Craton, little has been published. The few profiles that are published are located near the Vredefort Dome, Carletonville and Welkom areas (Durrheim, 1986; Durrheim *et al.*, 1991); the Kheis Tectonic Province (Stettler *et al.*, 1998 a,b) and the Witwatersrand Basin (Pretorius *et al.*, 1987, 1994; Weder, 1994). They transect varying stratigraphy including the West Rand Group through to the Olifantshoek Group. Seismic reflection profiles are used to gain familarity with the seismic reflection character of the various stratigraphic groups across the craton.
- *Use of published P wave velocities* (table 2.1). P wave velocity values allow time/ depth approximations to be made.
- *Outcrop*. Wherever possible, the 1:250 000 and 1:1 000 000 geological maps are used to tie surface geology to the seismic reflection interpretation at depth. Where there is little or no outcrop, for example seismic profile KBF03A, comparison is made to other seismic lines through similar stratigraphy and better outcrop.

University of Cape Town

- *Boreholes.* Three interpreted boreholes, A, along seismic profile OB, B and C along seismic profile YS, are used to check the stratigraphic interpretation.

Group/ Formation	P wave average internal velocity (m/s)	Approximate reflection coefficients *
Karoo Sequence	3195	+ 0.336
Hekpoort Formation (acid lavas)	6083	- 0.068
Timeball Hill Formation (shales)	5513	+ 0.143
Malmani Subgroup (dolomites)	6834	- 0.061
Pniel Group (basic lavas)	6159	- 0.028
Platberg Group (sediments)	5827	+ 0.033
Klipriviersberg Group (basic lavas)	6230	- 0.065
Central Rand Group (quartzites)	5779	+ 0.025
West Rand Group (quartzites and shales)	5748	- 0.032
Basement Granite	5693	

Table 2.1: Typical P wave velocities and reflection coefficients for the Witwatersrand, Ventersdorp, Transvaal and Karoo rocks. * Density data derived from geophysical well-logs (from Pretorius *et al.*, 1987).

The seismic profiles fall into three main regions based on location (figure 1.1):

- *The Western Lines*, KBF03A and 01, which transect the western margin of the Kaapvaal craton.
- Rz-254, 255 and 256 are situated in the Northern and North West Provinces, close to the Botswana border. They transect a major syncline trending east-west involving mainly Transvaal-aged rocks and sporadic Bushveld outcrop, hence are termed the *Bushveld Lines*.
- The *craton interior lines*: OB and AG to the west of the Vredefort dome and YS to the north west.

Below, data for each line are divided into descriptive, interpretative and discussion sections. Stratigraphic groups are labelled with the same symbols used in the interpretation, but with interpretative detail omitted. Features of interest are located using common depth point (CDP) numbers listed along the top of each profile and the

University of Cape Town

two way time (TWT). The TWT interval in which the stratigraphic unit occurs is referred to as its 'thickness' though actual depth estimates are only given occasionally.

Reflection character is described using the following terms:

- *Reflection amplitude*: Divided into the categories of high, medium and low. Low amplitude reflections are often referred to as weak, whereas high amplitude reflections are described as strong or bright.
- *Reflection continuity*: Categories of reflection continuity are highly continuous, semi-continuous, and discontinuous. Where reflections are completely discontinuous they may be referred to as chaotic.

2.2. The Western Margin

2.2.1. Seismic Profile KBF03A

2.2.1.I Introduction

The seismic reflection profile KBF-03A is located in the Northern and North West Provinces and trends WNW to ESE (figure 2.1). Outcrop is minimal in this area due to extensive Kalahari cover of up to 180 m thickness. The few units that crop out do so predominately in the east. From east to west, only Archean granitic basement, the Vryburg Formation (Schmidtsdrif Subgroup), the Asbesheuwels Subgroup and the Ongeluk lava (Postmasburg Group) crop out (figure 2.1). Figure 2.2 is the stacked and migrated seismic profile of KBF03A. The profile is displayed with east to the right and west to the left and extends over a total horizontal distance of approximately 155 km.

2.2.1.II Description (see figure 2.2)

Profile KBF-03A shows a succession of strata that thickens from 0 km in the east where the Archean basement outcrops to > 17 km in the west. Since the reflections extend beyond the depth of the profile, the total thickness of sediments in the west is almost certainly thicker than this.

University of Cape Town

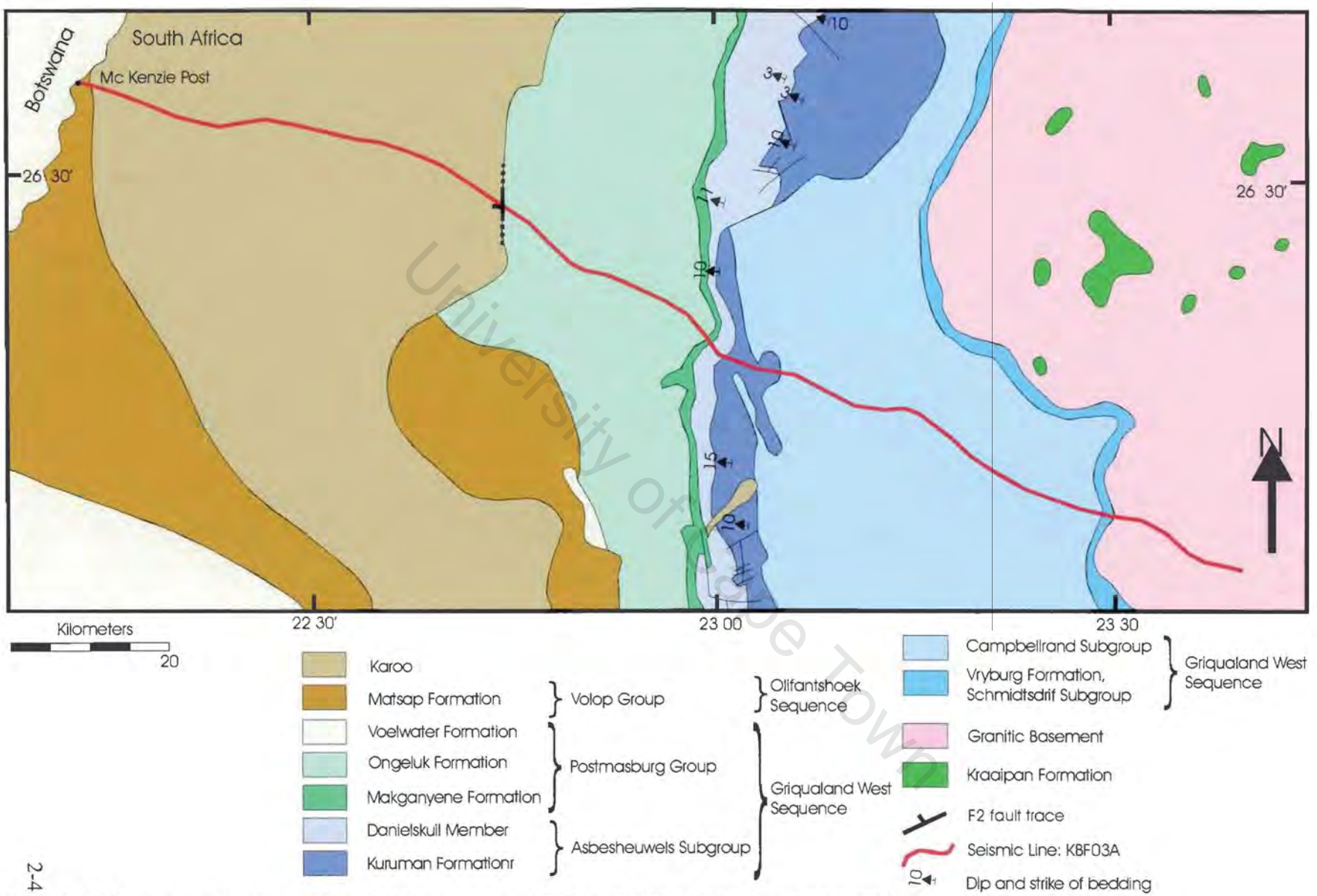

University of Cape Town

Figure 2.1: Subcropping Geology of the Morokweng Area * More than 90% of the surface is covered by Kalahari sand of thickness varying from 0 to 180 m (Geology simplified from the Geological Map of South Africa, Transkei, Bophuthatswana, Venda and Ciskei and the Kingdoms of Lesotho and Swaziland . 1: 1 000 000, 1984).

A dominant feature at CDP 4900 to 5400 is interpreted as a master normal listric fault (marked F2), which is near vertical in orientation above 1 s TWT and shallows to near horizontal below 3 s TWT. The fault has resulted in a displacement of the hanging wall relatively downward to the west. The extent of this displacement, as well as the timing of movement is discussed in greater detail in the interpretation section below.

The first continuous reflection marks the sediment/basement interface and has been marked on the profile as **S/B**. East of a fault zone (F1) at CDP 2500, unit $\mathbf{G_s}$ overlies the basement. West of this zone unit $\mathbf{G_s}$ continues above unit $\mathbf{V_b}$ and $\mathbf{V_s}$.

West of CDP 2750 unit $\mathbf{V_s}$ lies directly on the basement. Reflectors onlap a slight basement rise between CDP 2850 and 2700 and thicken, west of the main listric fault (F1), to a maximum of around 2000 m (P wave velocity approximately 5827 m/s, see table 2.1). The reflection character of $\mathbf{V_s}$ varies laterally from medium to high amplitude, semi-continuous reflections between CDP 5100 and 4700, to an almost transparent section at greater depth further west. Within unit $\mathbf{V_s}$ are several sequences and at least one channelised unconformity. The listric fault F2 has displaced unit $\mathbf{V_s}$ downward in the west.

Unit $\mathbf{V_b}$ is a transparent unit that succeeds $\mathbf{V_s}$. $\mathbf{V_b}$ is around 0.38 s TWT or 1170 m (P wave velocity of 6159 m/s) thick in the east and thins to 840 m at CDP 3900. Further west, it thickens again to a maximum of 1140 m. West of F1, a medium-amplitude, semi continuous reflection roughly bisects the unit. In the east $\mathbf{V_b}$ terminates against the F1 fault zone.

Unit $\mathbf{G_s}$ is the interval following the first medium to strong reflection succeeding the transparent unit $\mathbf{V_b}$. Unit $\mathbf{G_s}$ is distinct due to its medium to high amplitude reflections which are semi-continuous. Unit $\mathbf{G_s}$ outcrops between CDP 1700 and 1550. In the east $\mathbf{G_s}$ overlies granitic basement. In this area unit $\mathbf{G_s}$ has been displaced by normal faults with apparent dips to the west and east. This unit thickens westwards from ~500 m to 1410 m (P wave velocity estimated at 5800 m/s).

Unit $\mathbf{G_c}$ is conformable with the underlying unit $\mathbf{G_s}$. It maintains a thickness of ~1600 m to 1700 m (P wave velocity of 6834 m/s). In the east between CDP 3600 and 2650

University of Cape Town

it is truncated by the erosional unconformity $\mathbf{K_{unc}}$. It is displaced by F2 between CDP 5000 and 5300 and continues, plunging steeply to the west to reach unknown depths beyond the end of the profile. Unit $\mathbf{G_c}$ is composed of two sub-units of quite different reflection character. The lower unit, about 0.2 s TWT or ~680m thick, is mostly transparent though rare, weak, fairly continuous reflections are present. Reflections in the upper portion of unit $\mathbf{G_c}$ have greater amplitudes and are continuous over long distances. The top of unit $\mathbf{G_c}$ is the first very bright, high amplitude reflection.

Two reflectors of very high amplitude mark the base of unit G_{ak}. The seismic character of unit $\mathbf{G_{ak}}$ varies laterally from high amplitude, bright reflections to weaker ones. $\mathbf{G_{ak}}$ increases in thickness west of CDP 4400 and then is fairly constant at ~1450 m across the profile (average P wave velocity of 5800 m/s).

The top of $\mathbf{G_{ak}}$ is truncated in places by the successive unit $\mathbf{G_o}$. $\mathbf{G_o}$ unconformably overlies $\mathbf{G_{ak}}$ and maintains an equal thickness of around 0.35 s TWT or ~1060 m across the profile. Unit $\mathbf{G_o}$ is distinctive due to its transparency. The few weak, continuous reflections that are present are evenly spaced towards the lower boundary of the unit. $\mathbf{G_o}$, like the units below, is displaced by F2. Unit $\mathbf{G_o}$ is the upper most unit of the down-faulted sequence to be repeated on both sides of F2. It is truncated east of F2 by the erosional unconformity $\mathbf{K_{unc}}$. At the western extent of the profile, unit $\mathbf{G_o}$ is at a maximum depth of 4 s TWT, roughly 11.5 km.

East of F2, reflectors within units $\mathbf{V_s}$, $\mathbf{V_{fb}}$, $\mathbf{G_s}$, $\mathbf{G_c}$, $\mathbf{G_{ak}}$ and $\mathbf{G_o}$ dip westwards at an increasing angle into F2. West of F2, these units plus unit $\mathbf{O_{ml}}$ above bend (roll over) into the F1 plane.

Unit $\mathbf{O_{ml}}$ succeeds $\mathbf{G_o}$ only to the west of F2. $\mathbf{O_{ml}}$ is offset by numerous normal faults dipping to the east and west. Several of the faults extend beyond the $\mathbf{O_{ml}}$ interval into the units $\mathbf{G_o}$, $\mathbf{G_{ak}}$, $\mathbf{G_c}$, and $\mathbf{G_s}$ below (faults marked F3). Other faults (F5) displace units that succeed $\mathbf{O_{ml}}$. As a result of this intense faulting, the thickness variation of $\mathbf{O_{ml}}$ is difficult to ascertain though it does appear to thicken westward of CDP 5500 to reach a maximum of 1 s TWT or ~2750 m.

University of Cape Town

An erosional unconformity ($\mathbf{N_{unc}}$) separates $\mathbf{O_{ml}}$ from $\mathbf{O_h}$ above. It distinctly truncates $\mathbf{O_{ml}}$ reflectors between CDP 5350 and F2. The absence of truncation of reflectors to the west may signify a conformable succession. Alternatively, $\mathbf{N_{unc}}$ may be bedding parallel. $\mathbf{O_h}$ is a transparent unit marked at its top by a high amplitude reflector, **T**. Unit $\mathbf{O_h}$ has been duplicated at least three times by faulting (low-angle thrusting) as shown by the repetition of reflector **T**. The base of the thrusts is seemingly along $\mathbf{N_{unc}}$. Thus the unit $\mathbf{O_h}$ has been thickened through structural duplication by approximately 300% between CDP 5200 and 4900.

Unit $\mathbf{O_v}$ succeeds the tectonically thickened $\mathbf{O_h}$ unit and reflector **T**. $\mathbf{O_v}$ is mostly transparent, though weak reflections are noted. Reflector $\mathbf{K_{dunc}}$ truncates $\mathbf{O_v}$ reflectors between CDP 5950 and 6550. The unconformity, $\mathbf{K_{dunc}}$, also cuts across the underlying thrusts between CDP 5900 and 4850. Unit $\mathbf{K_d}$ above $\mathbf{K_{dunc}}$, consists of parallel and evenly spaced, medium amplitude reflections occupying large depressions of an apparent width of 400 to 500 CDP's (10 to 12.5 km). Reflector $\mathbf{K_{unc}}$ truncates these $\mathbf{K_d}$ reflectors. Unit $\mathbf{K_c}$ follows the unconformity, $\mathbf{K_{unc}}$ and is composed of weak though fairly continuous reflections. $\mathbf{K_c}$ extends over the entire profile with the exception of a few discrete patches where units below outcrop.

2.2.1.III Stratigraphic Interpretation (see figure 2.3)

2.2.1.III.a. Ventersdorp Sediments and Basalts (V_s and V_b) [2.71 - 2.64 Ga]

The Klipriviersberg mafic volcanics at the base of the Ventersdorp Supergroup are limited to the northeast of the Ventersdorp depository (Van der Westhuizen *et al.*, 1991) and are therefore unlikely to be present along seismic profile KBF 03A. The Ventersdorp sequence along this line can be roughly divided into a sedimentary package (V_s) followed by basalts (V_b). The distinction has been made primarily by consideration of seismic reflection character. The sedimentary unit is far more reflective than the overlying basalt unit.

The first Ventersdorp reflection fills in basement topography i.e. lows and onlaps the basement in the east. The onlap shows that this local basement-high is an earlier feature and also explains why the Ventersdorp does not outcrop in this area. At some

University of Cape Town

localities within the Ventersdorp sedimentary unit there are preserved sequences and channels. The best examples are illustrated in figure 2.4.

The lateral variation in reflection character from medium to high amplitude, semi-continuous reflections to almost transparent areas is perhaps due to lateral lithological shifts. A more proximal environment of deposition results in coarser sediment, the distal areas in fine sediment. These lateral changes in lithology may result in variation in density and acoustic impedance, causing laterally discontinuous reflections.

The sedimentary unit of the Ventersdorp Supergroup thickens to the west, reflecting a greater creation of accommodation space towards the craton edge. The progradation of sequences in apparent westward direction is consistent with this (figure 2.4). Sequence 2 cuts down into sequence 1. The position of sequence 2, west of sequence 1, suggests that the transport direction of sediment was to the west. The master listric fault F2 has resulted in the downward displacement of the Ventersdorp sedimentary unit to the west. Thus some of the apparent 'thickening' to the west may be due to duplication of the reflectors as the listric fault approaches the horizontal.

Extruded onto the Ventersdorp sediments are the Ventersdorp basalts (V_b), which may be associated with a period extension, associated with rifting along the Kaapvaal Craton's western edge. The transition from Ventersdorp sediments to basalt produces a significant density contrast, thus a large difference in acoustic impedance. This results in a reflector that is easy to identify due to its high amplitude and lateral continuity. Characteristically, the basalt unit is acoustically transparent suggesting a constant and uniform outpouring of basaltic material. The one distinct reflector, visible primarily to the west of F1 (CDP 5400) may result from a brief break in eruption, or perhaps it reflects a late stage intrusion.

University of Cape Town

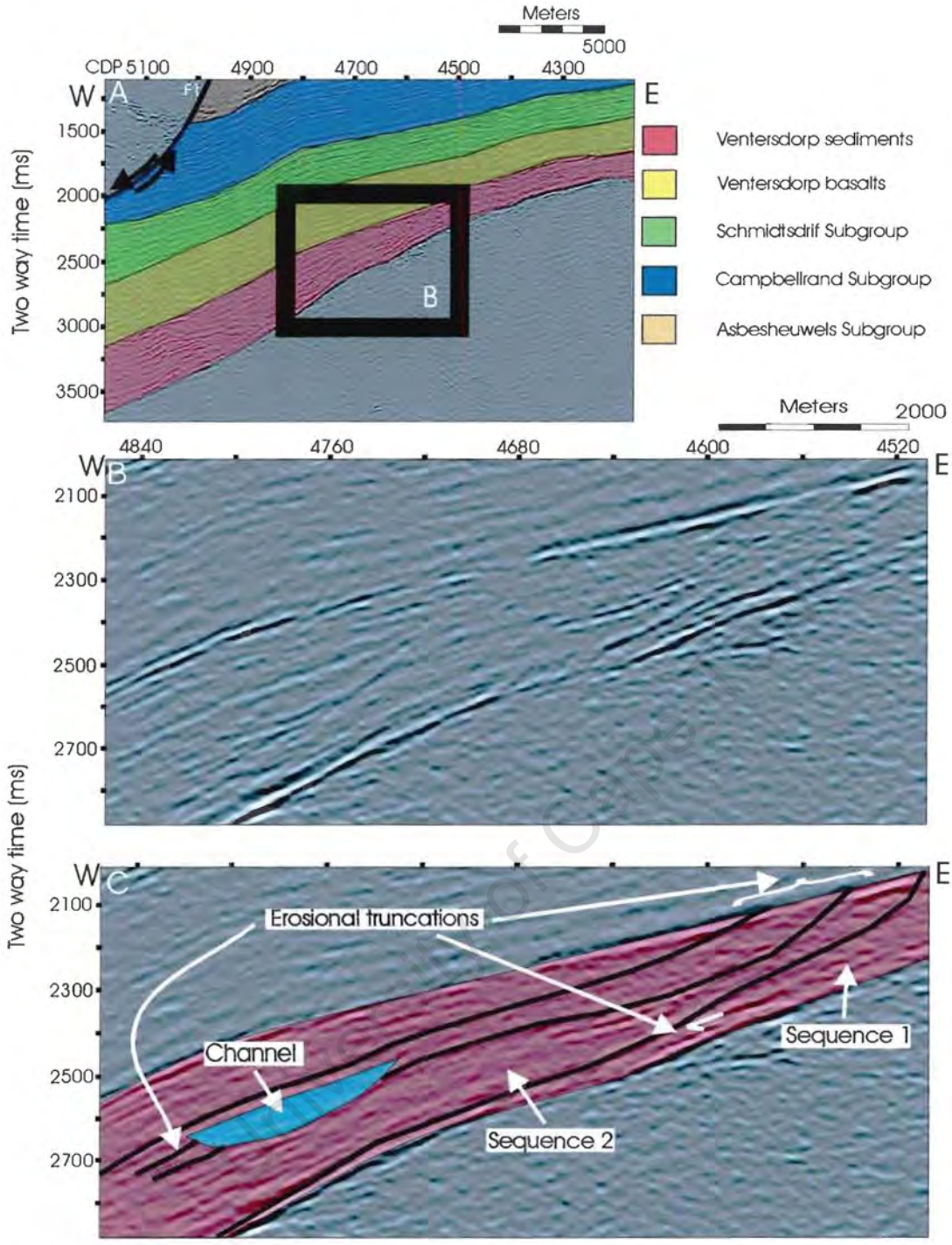

Figure 2.4: Sequences and channels in the Ventersdorp sedimentary unit along the central section of the line KBF03A. Sequence 2 erodes into sequence 1, and is located westwards of 1. Therefore, sediment transport is probably approximately to the west. Reflectors of sequence 2 are truncated by a channel (blue). The erosional truncations are particularly noticeable on the western channel edge. The top of the Ventersdorp sedimentary unit has been eroded. Box in A is enlarged: B is uninterpreted, C interpreted.

2.2.1.III.b. The Griqualand West Sequence (G_s, G_c, G_{ak} and G_o)

The Ghaap Group

The Ghaap Group is the lowest stratigraphic group in the Griqualand West Sequence. It is subdivided into the Schmidtsdrif (G_s), Campbellrand (G_c), Asbesheuwels and Koegas (G_{ak}) subgroups. Of these the Schmidtsdrif (CDP 1600) and Asbesheuwels (4200) Subgroups outcrop.

A. SCHMIDTSDRIF SUBGROUP (G_s) [2.64 – 2.59 GA]

The Schmidtsdrif Subgroup, succeeding the Ventersdorp flood basalts, thickens westward from ~500 m to ~1410 m. The high reflectivity of the Schmidtsdrif Subgroup may be indicative of the superposition of alternating lithologies. Shale and sandstone of the Vryburg Formation outcrops in the east where it as been deposited directly onto the basement. Absence of the Ventersdorp Supergroup east of F1 is discussed in section 4. East of F1, normal faults (figure 2.5) dipping both to the east and west, have displaced the Schmidtsdrif Subgroup.

B. CAMPBELLRAND SUBGROUP (G_c) [2.59 – 2.52 GA]

The Campbellrand carbonates succeed the Schmidtsdrif Subgroup. Unlike the Schmidtsdrif Subgroup and Ventersdorp Supergroup, the Campbellrand Subgroup maintains an equal thickness across the extent of the profile. The subgroup is composed of two units with differing reflection character. At basal unit (~ 680 m thick) is acoustically transparent which may indicate uniformity in composition. The unit above is marked by laterally continuous reflections of low to medium amplitude. The bright or high amplitude reflections towards the top of the Campbellrand Subgroup suggest a greater degree of interbedded material.

C. ASBESHEUWELS AND KOEGAS SUBGROUP (G_{AK}) [2.52 – ~2.46 GA]

The transition from the shales and carbonates of the Campbellrand Subgroup to the Banded Iron Formation of the Kuruman Formation, Asbesheuwels Subgroup is marked by a strong impedance contrast and therefore a very high amplitude, continuous reflection. The seismic character of unit G_{ak} varies laterally from brighter reflectors, high in amplitude, to weaker reflections.

University of Cape Town

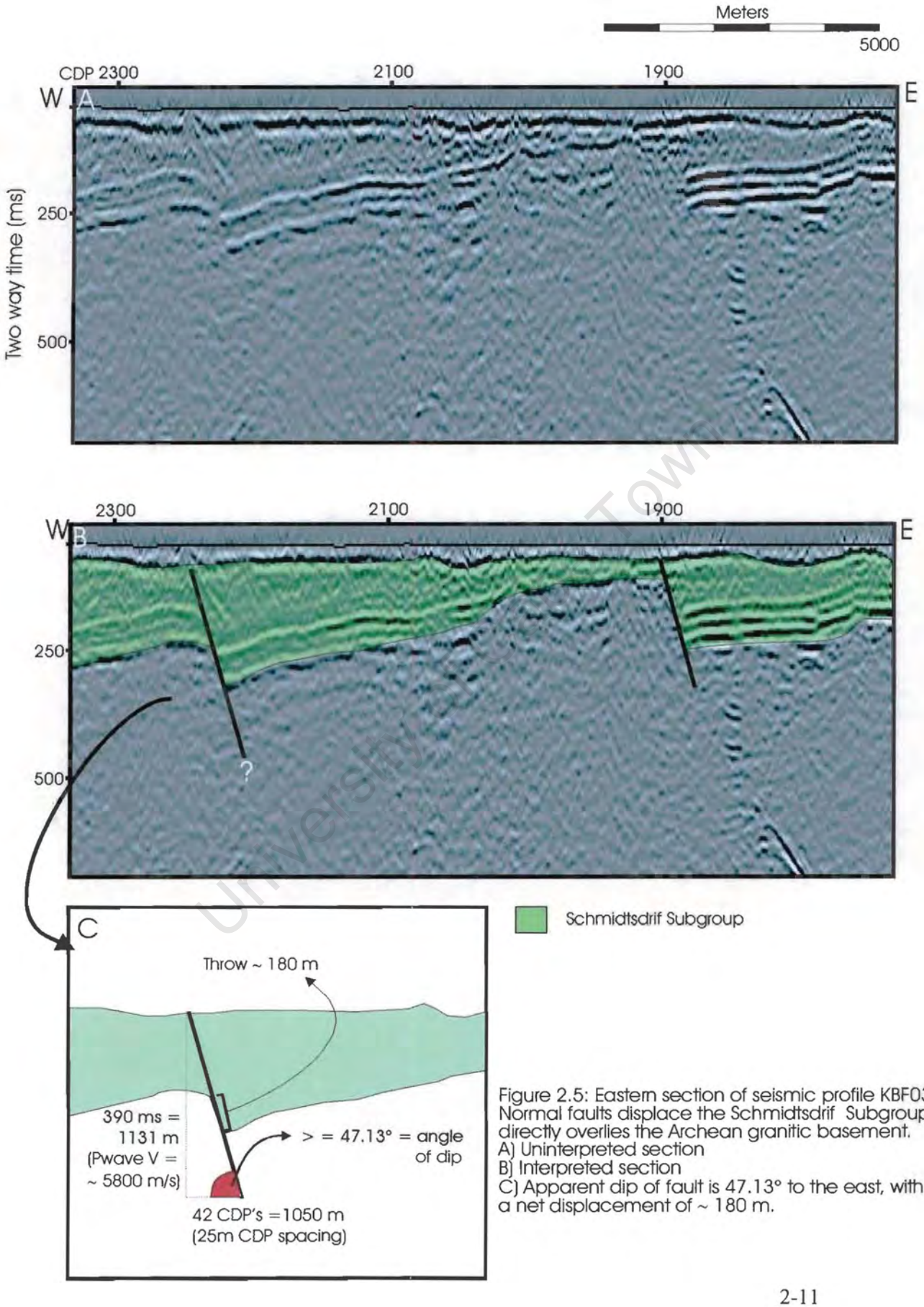

Figure 2.5: Eastern section of seismic profile KBF03A. Normal faults displace the Schmidtsdrif Subgroup, which directly overlies the Archean granitic basement.
A) Uninterpreted section
B) Interpreted section
C) Apparent dip of fault is 47.13° to the east, with a net displacement of ~ 180 m.

There is a general trend towards higher amplitude reflections westwards. This may be due to increased incidence of chert and shale interbeds at greater water depth.

Postmasburg Group

The Postmasburg volcanic-sedimentary sequence follows the chemical sediments of the Ghaap Group. The Postmasburg Group is stratigraphically divided into the Makganyene and Ongeluk Formations and Voelwater Subgroup. The Makganyene, below the Ongeluk Formation, is not identifiable on the seismic section. This is perhaps due to its thickness of only 50 to 150 m (Beukes and Smit, 1987). According to Altermann and Halbich (1991) the Ongeluk lava unconformably overlies the Makganyene Formation. The erosional unconformity is not identifiable on the seismic section KBF03A, however this may be due to the transparency of the overlying Ongeluk.

D. ONGELUK LAVA (G_o) [2.2 GA?]

Unit G_o is interpreted to be the Ongeluk Formation for two reasons:

1) It outcrops at CDP 4200.
2) It is transparent on the seismic section. On the Kaapvaal Craton seismic profiles basaltic units of uniform composition appear seismically transparent.

The transparent seismic reflection character of the Ongeluk unit is likely due to the uniformity in composition of the lava. The Ongeluk lava is the uppermost unit that is repeated on both sides of the listric fault, F2. Figures 2.6 to 2.8 show a comparison of two subsections from the west and east side of F2 in an attempt to verify the equivalence of the Ongeluk Formation and those units below that have been down thrown to the west. This test clearly indicates that the unit can be traced across the master listric fault, F2, with confidence. This also allows the calculation of a net slip of 6.5 km along the fault (see figure 2.9).

The first group of discontinuous reflections above the transparent Ongeluk Formation is interpreted to be the Voelwater Subgroup. These reflectors are discontinuous possibly due to intense faulting or lateral lithological variations. Structural complexity may have obscured the well-documented erosional unconformity truncating the

University of Cape Town

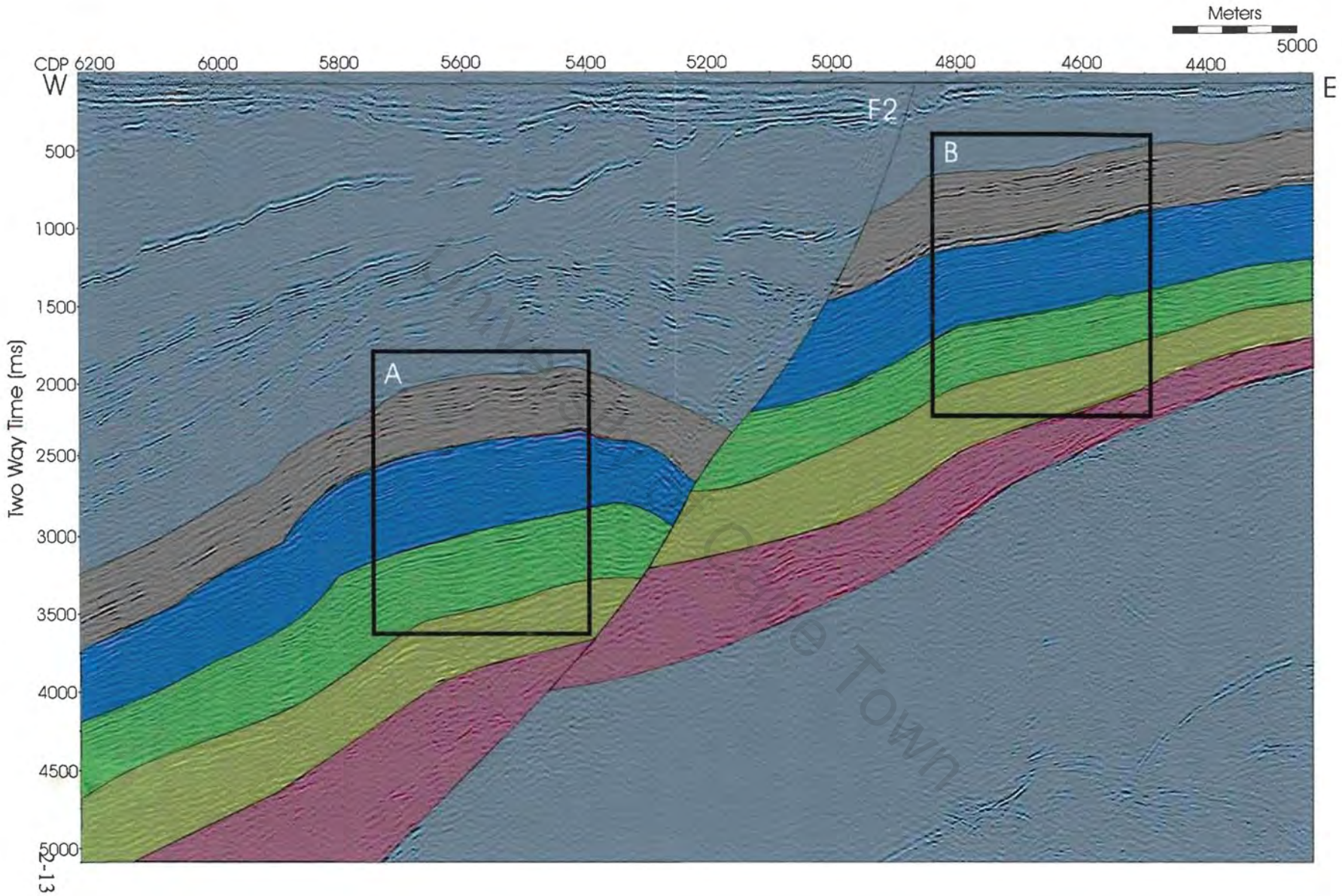

Figure 2.6: Displacement along main listric fault, F2. Box A and B are expanded in figure 2.7 and 2.8 to verify the correlation of units across F2.

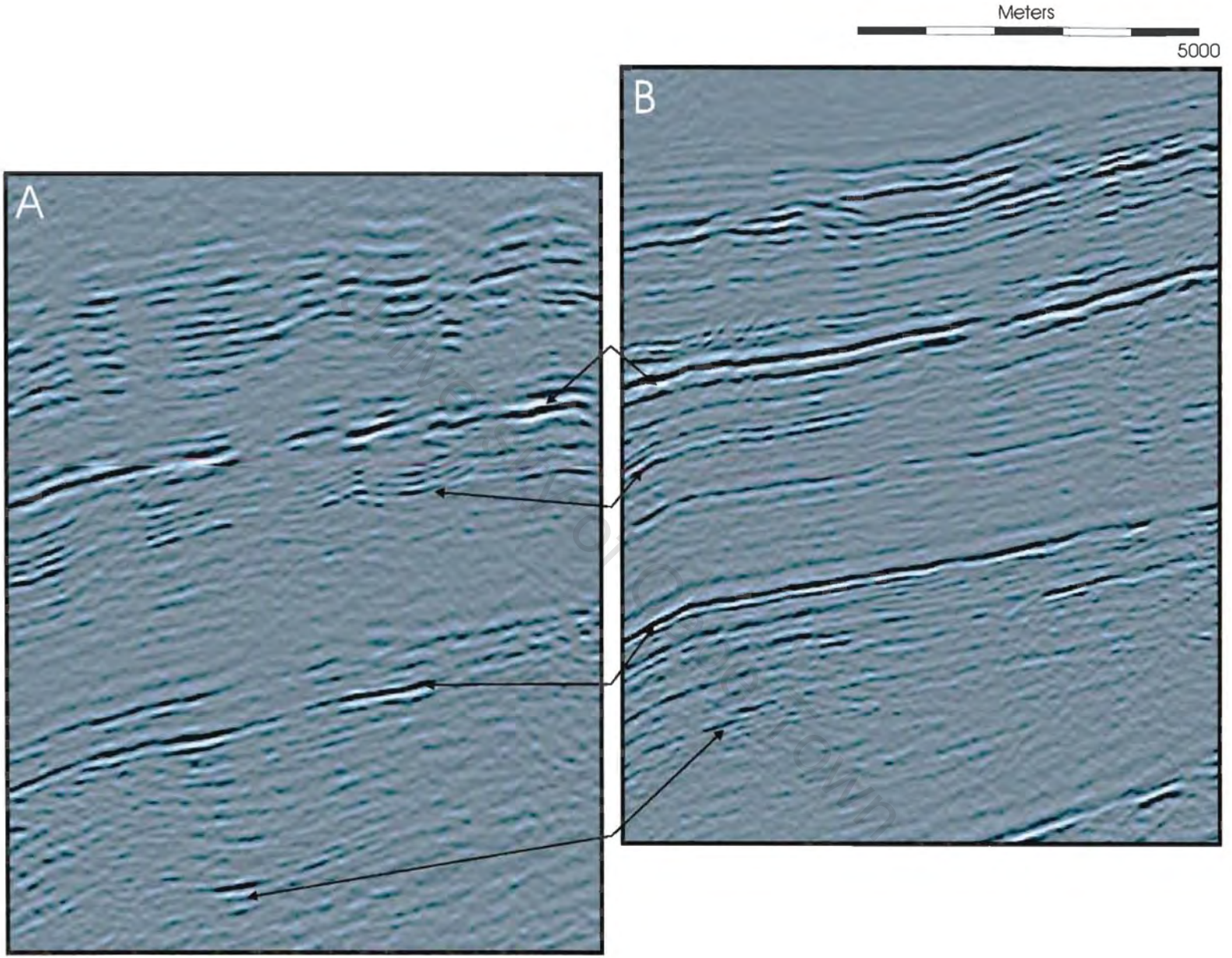

Figure 2.7: Box A and B from figure 2.6, uninterpreted, to illustrate the correlation of units across the listric fault, F2. Arrows mark the correlation of specific reflectors.

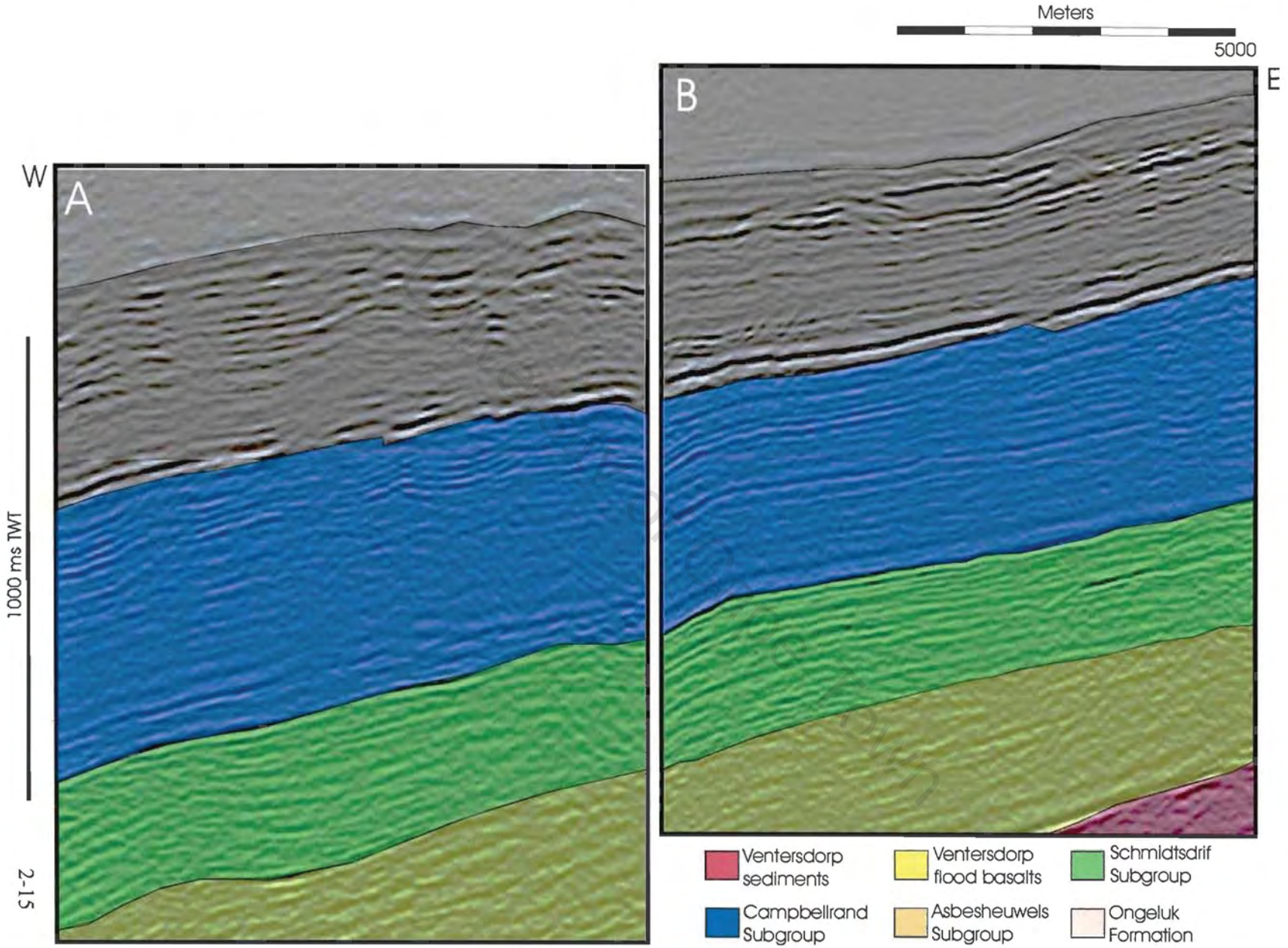

Figure 2.8: Box A and B from figure 2.6, interpreted, to verify correlations of units across listric fault, F2.

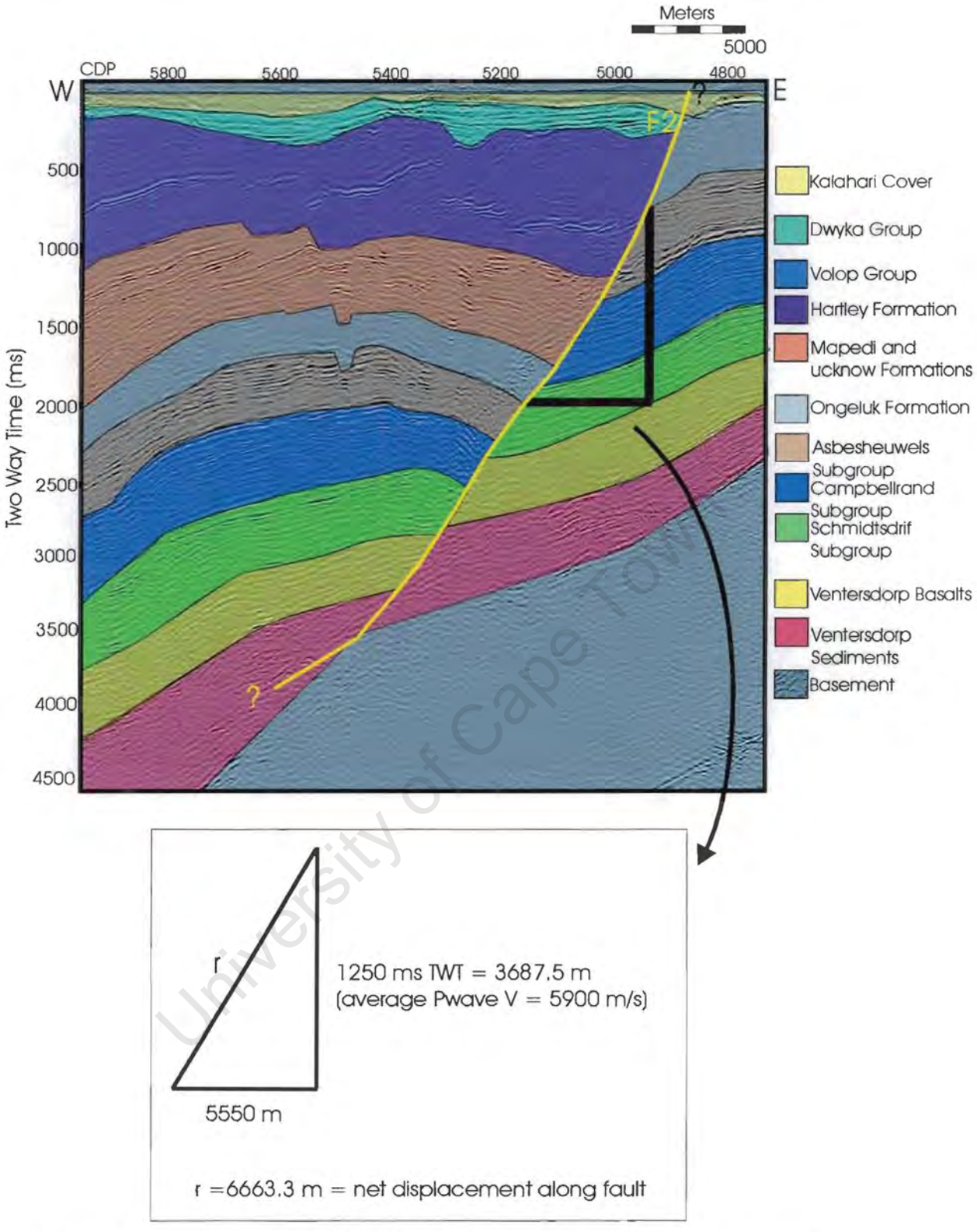

University of Cape Town

Figure 2.9: Estimate of net vertical displacement along the fault, F2. Displacement of ~ 6.5 km is measured from the offset of the Asbesheuwels/ Ongeluk transition, along the steepest portion of F2. Because there has been a reversal of motion along F2 (see section 2.2.1.IV.), the normal displacement calculated is a minimum.

Voelwater subgroup, and forming the base of the successive Olifantshoek sequence. This unconformity is not apparent in line KBF03A.

2.2.1.III.c. The Olifantshoek Sequence (O_{ml}, O_h and O_v)

Above the Postmasburg Group, stratigraphic detail is difficult to establish. This is due to lack of outcrop and borehole control and the complexity of deformation. To establish stratigraphic detail above the Ongeluk lava on KBF03A, it was necessary to use published structure and stratigraphy of areas ~ 150- 200 km to the south of KBF03A, where there is good outcrop control. (Grobbelaar *et al.* 1995; Barton *et al.* 1986; Stowe 1986; Schlegel 1988; Cornel 1987; Altermann et al.1992; Altermann and Halbich, 1990 and Moen, 1999). The published thicknesses of the Olifantshoek units were compared to the two way time intervals of KBF03A using P wave velocities given in table 2.1. This proved a means of checking the validity of the assignation of established stratigraphic names to the seismic profile. The seismic reflection character was also checked against what was expected for each unit.

The Olifantshoek Sequence consists of four formations and a group, the Mapedi, Lucknow and Hartley Formations and Volop Group. For the purpose of this work, the sequence has been treated here as two main units separated by N_{unc}, named the Neylan Unconformity (first recognised by H.S van Niekerk, RAU, pers. comm. 2000). Below the unconformity are the Mapedi and Lucknow Formations (O_{ml}) and above are the Hartley Formation (O_h) followed by the Volop Group (O_v).

A. The Mapedi and Lucknow Formations (O_{ML})

Succeeding the Ongeluk lavas are the Mapedi and Lucknow Formations (O_{ml}). Complex normal faulting has resulted in the displacement of several of the Mapedi and Lucknow reflectors. The similarity of some reflectors within this unit, suggests possible repetition caused by thin-skinned thrusting. Unfortunately this is difficult to verify.

The Mapedi and Lucknow Formations of the Olifantshoek as well as the Ongeluk basalts, Asbesheuwels and Campbellrand Subgroup form an anticline, dipping

University of Cape Town

westwards west of CDP 5400, and eastwards, east of this point. This deformation has given rise to a localized relative uplift, and has subsequently been eroded to produce the Neylan unconformity (N_{unc}) (Figure 2.10). The Neylan basal conglomerate, above the unconformity, forms the base of the Hartley Formation.

B. The Hartley Formation (O_H) [1.9 Ga]

The Hartley lava is distinguished by its transparent seismic character (similar to the Ongeluk basalt and Ventersdorp flood basalt). The top of the Hartley formation is marked by a prominent reflector marked T. The entire unit up to T has been repeated several times by low-angle thrusts with shallow dip to the west. The net result is a tectonically thickened section of the Hartley Formation by ~300%. The base of the thrusting is rooted in the Neylan unconformity, which may have acted as a décollement surface.

C. The Volop Group (O_V)

A small section of the arenaceous Volop Group overlies the Hartley Formation. It is almost completely transparent, though there are near horizontal, very weak reflectors towards the top of the unit. The horizontal orientation of these reflectors, relative to the dipping thrust reflectors cutting the Hartley Formation, seems to indicate that the Volop Group was deposited after thrusting, toward the hinterland (east). The transparency of the unit may be a reflection of its extremely uniform lithology.

2.2.1.III.d. The Karoo Supergroup (K_d) [350 – 300 Ma]

The Olifantshoek reflectors are truncated by a major unconformity, K_{dunc} (figure 2.11). This unconformity has cut into the underlying Olifantshoek-age thrusts and terminates against F2. The unconformity undulates as large, approximately 10 km wide depressions. Above this unconformity, and occupying the large depressions described above, is the Dwyka Group, Karoo Supergroup. The depressions are interpreted to be large glacial valleys which have been cut into the underlying rocks during the Permo-Carboniferous, Dwyka-aged glacial event (~350 to 300 Ma). Displacement of Karoo reflectors by the master listric fault, F2, indicates that this fault has a post-Karoo, pre Kalahari component of normal movement.

University of Cape Town

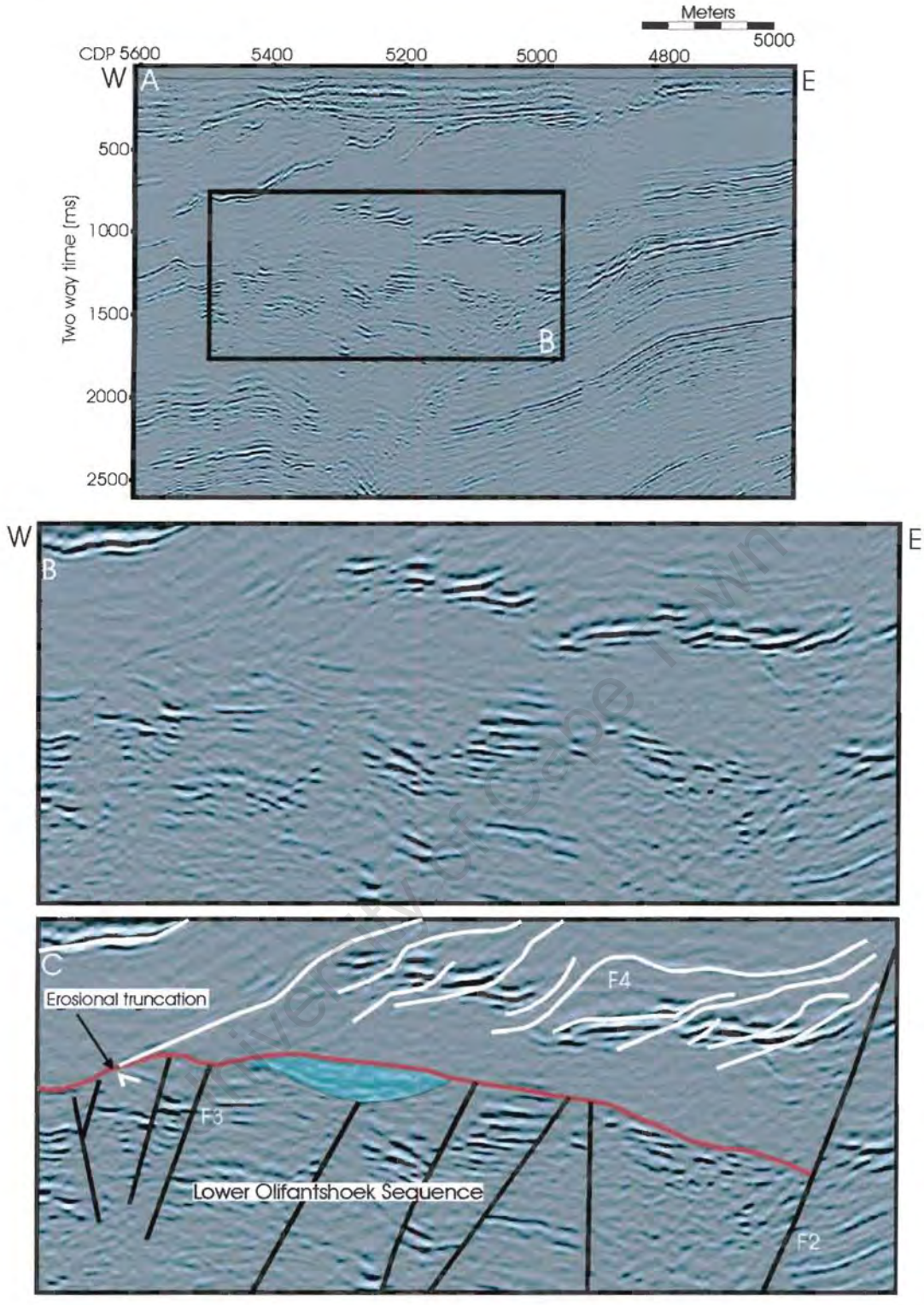

Figure 2.10: Central section of the seismic profile KBF03A. The Neylan Unconformity (red) erodes lower Olifantshoek reflectors. In blue is an interpreted channel. Normal faults are in black (F3), thrusts are white (F4). Box in A is enlarged: B is uninterpreted, C interpreted.

University of Cape Town

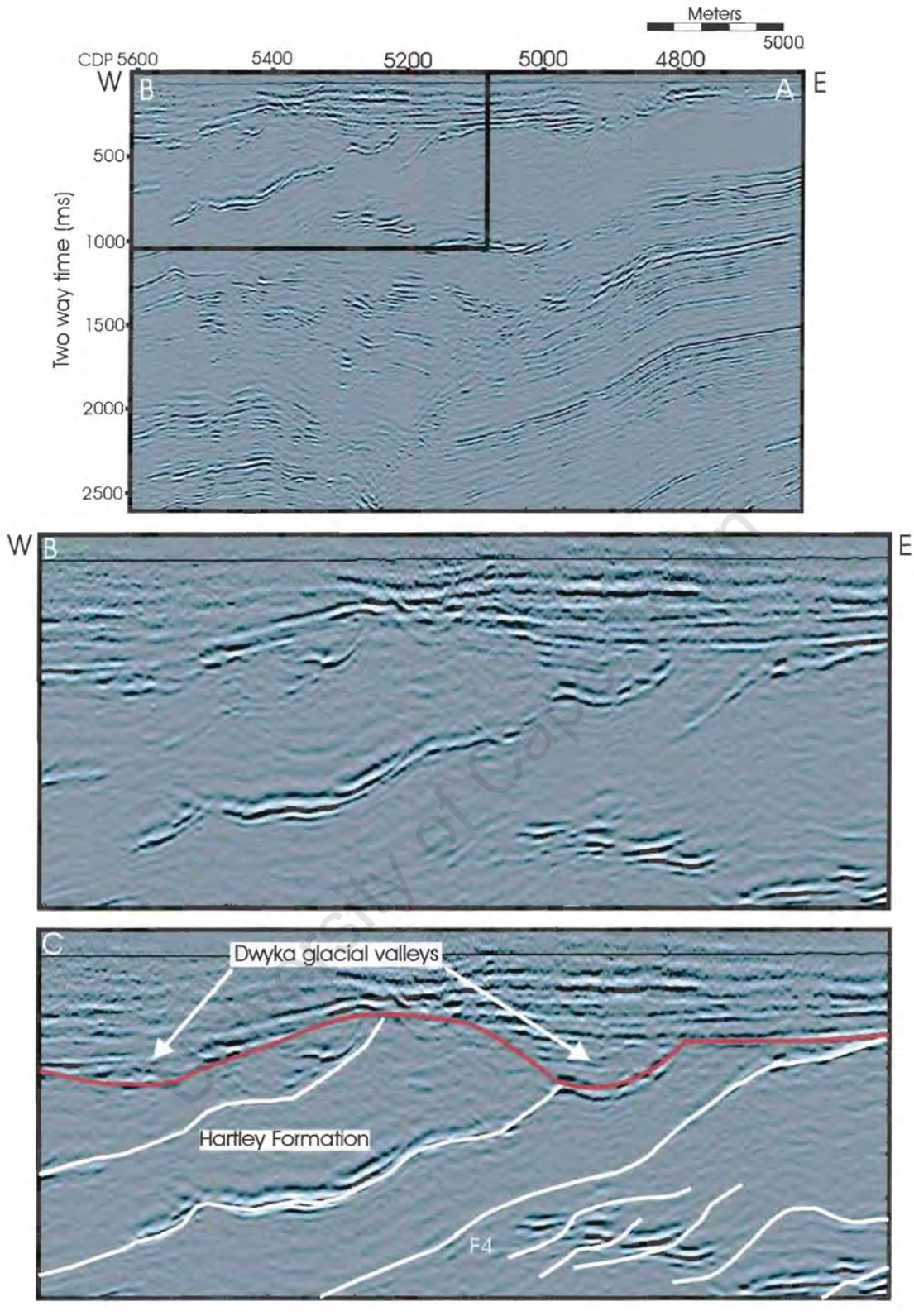

Figure 2.11: Central section of seismic profile KBF03A showing the Dwyka unconformity (red) eroding the Hartley Formation (F4), below. Box in A is enlarged: B is uninterpreted, C interpreted.

2.2.1.III.e. Kalahari Cover (K_c)

Dwyka reflectors are truncated by K_{unc}, named the Kalahari unconformity, which extends across the entire profile. In the east K_{unc} truncates the Ongeluk lavas and the underlying Asbesheuwels, Campbellrand and Schmidtsdrif Subgroups. The tertiary Kalahari cover is designated as K_c. The transparency of this unit is due to its uniform and its partially unconsolidated composition. Within this Kalahari unit at least one possible fluvial channel has been identified (figure 2.12).

2.2.1.IV. Tectonic model (Figures 2.16 to 2.18)

Profile KBF03A illustrates a complex structural history, which may help in the understanding of the tectonic history of the Kaapvaal Craton's western margin (see chapter 3.2.). The central section of seismic profile KBF03A has been structurally interpreted in figure 2.13. The structural history of line KBF03A is divided into four phases. These roughly correspond to:

1) Extension: Initial deposition in a rifted environment dominated by extension followed by thermal subsidence. Figure 2.14 gives an expanded view of the fault zone, F1, including the structural interpretation of this area.
2) Compression: Development of relative localized uplift and erosion of surfaces. Compression continued after a period of volcanic extrusion. This renewed compression resulted in the development of stacked thrust sheets.
3) Extension: Development of the master listric fault, F2, and numerous smaller scale faults, which displaced the thrusts of (2). There may be a strike-slip component to movement along F2 and smaller scale faults (figure 2.15). The net displacement along F2 is calculated to be 6.5 km (figure 2.9).
4) Finally the entire sequence was subject to two periods of uplift and erosion followed by deposition of the Dwyka Formation and Kalahari cover, resulting in today's land surface. Some movement along the master listric fault, F2, occurred post Karoo and pre Kalahari.

University of Cape Town

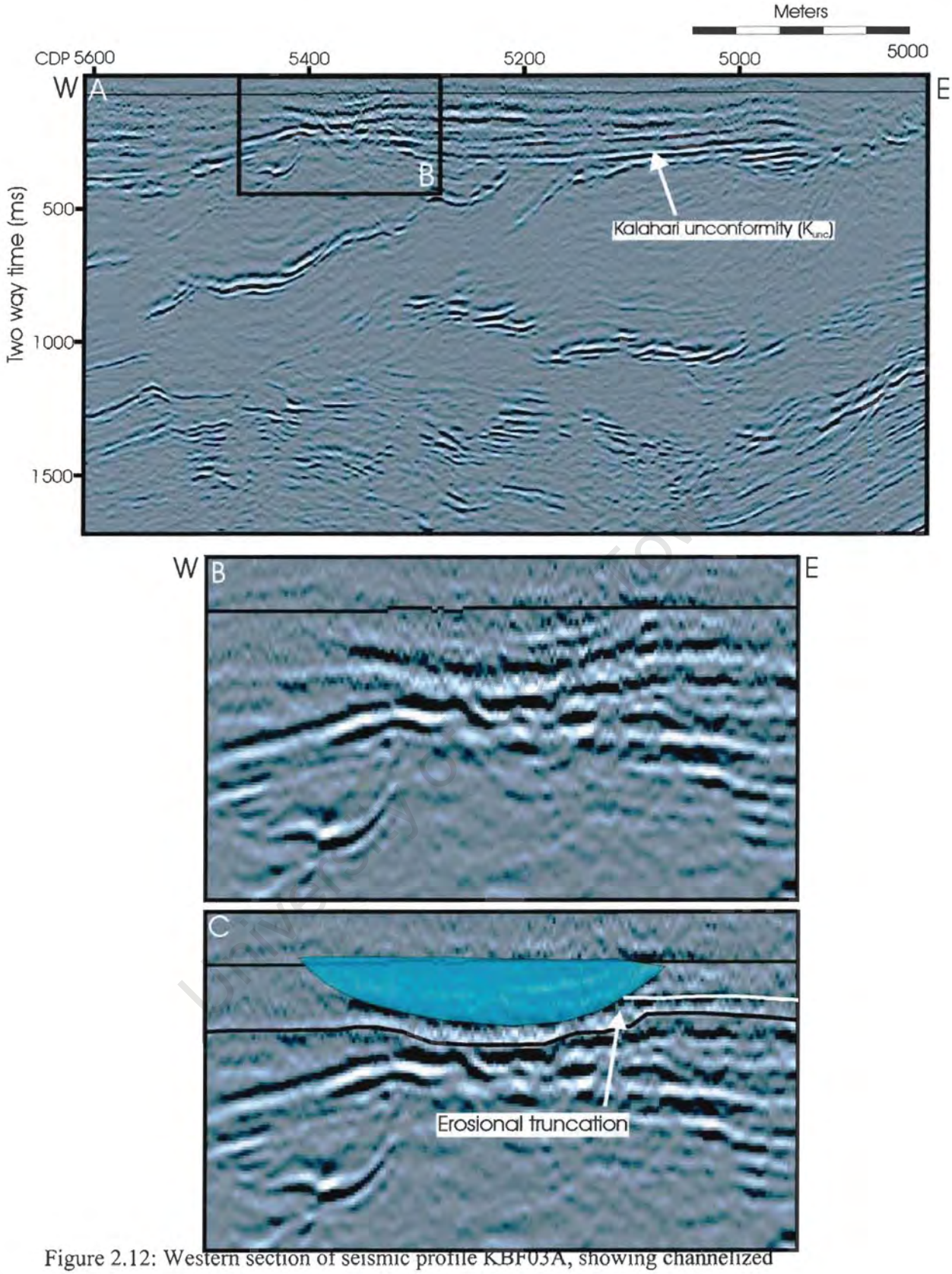

Figure 2.12: Western section of seismic profile KBF03A, showing channelized Kalahari unconformity. Note the truncation of a reflector by the eastern edge of the channel (blue). Box in A is expanded: B is uninterpreted, C interpreted.

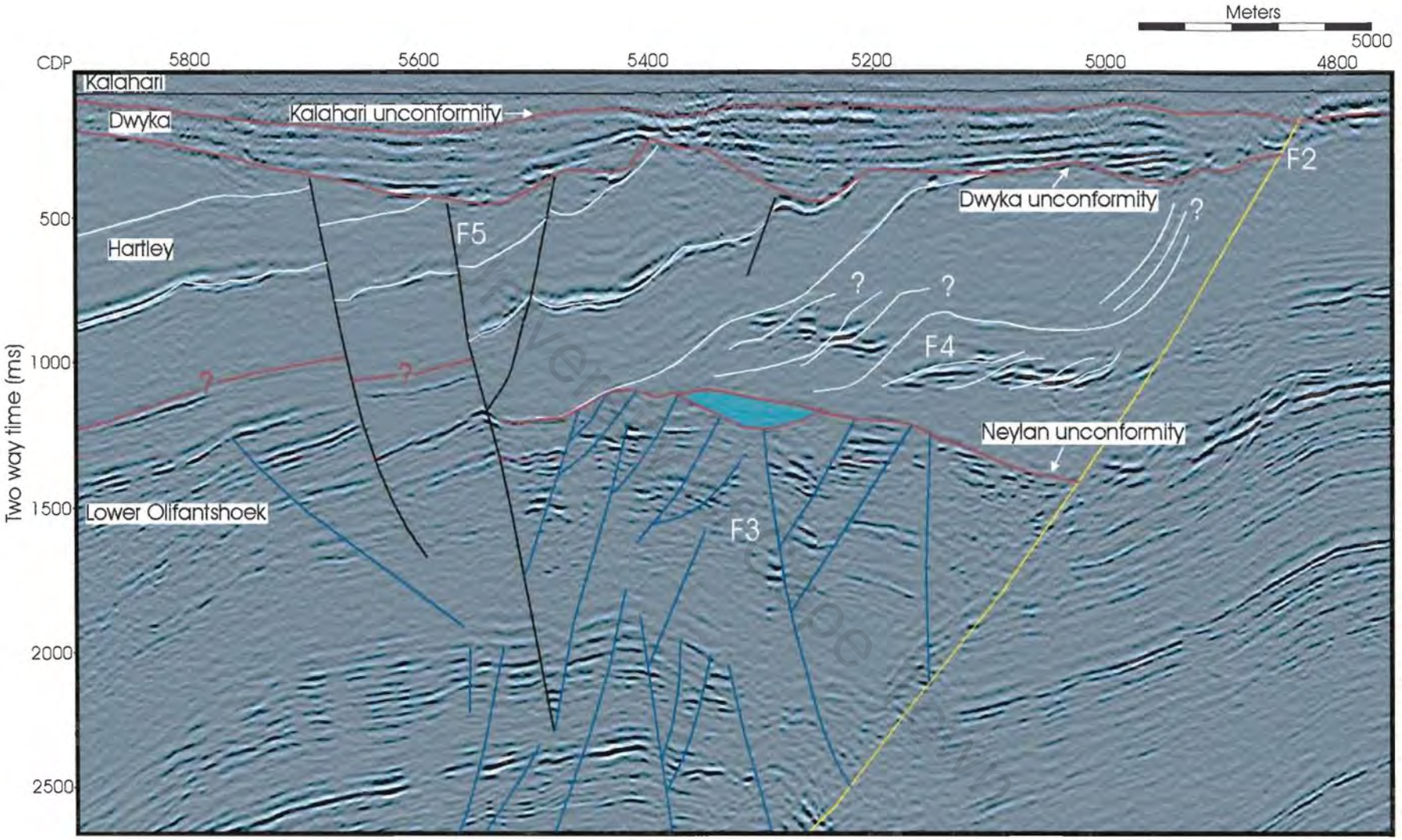

Figure 2.13: Structural interpretation of the Olifantshoek and successive Dwyka and Kalahari sequences. Phases of faulting are distinguished by various colours: The master listric fault (F2 in yellow); normal faulting within the lower Olifantshoek Group, prior to the formation of the Neylan unconformity (F3 in blue); thrusting of the Hartley Formation (F4 in white) and subsequent normal faults, which displace the thrusts (F5 in black). The Neylan, Dwyka and Kalahari unconformities are marked in red.

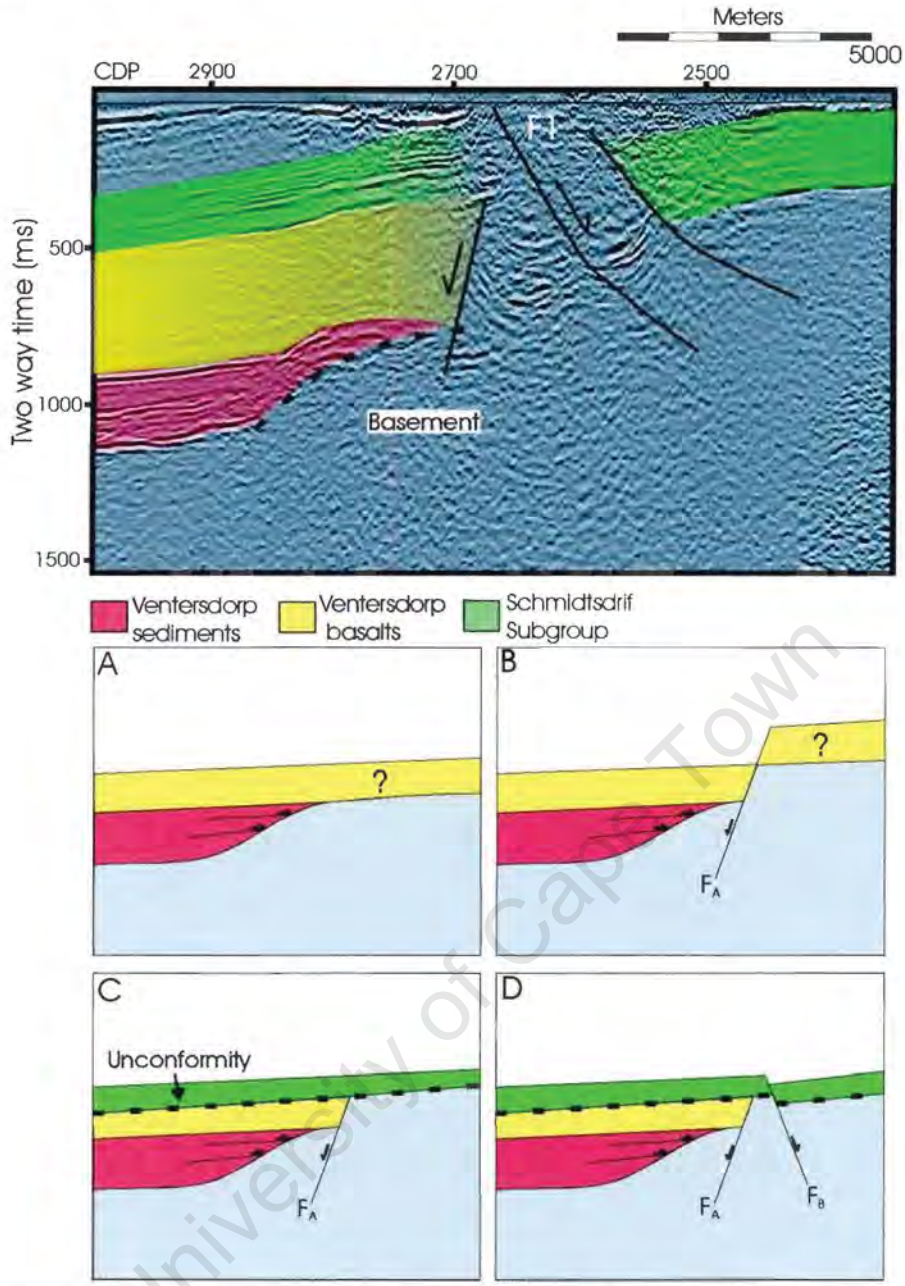

University of Cape Town

Figure 2.14: Top: Structural interpretation of the F1 fault zone. This zone is labeled 1, due to the fact that the displacement precedes Campbellrand carbonate deposition thus is one of the first phases of faulting recognized along KBF03A.
Bottom: Simplified 4-stage structural history.
A) The Ventersdorp sediments are deposited, onlapping a local basement high (black half arrow). The Ventersdorp basalts are then extruded. The original lateral distribution of the Ventersdorp basalts is unknown, hence marked '?'. There are two possibilities: 1) The basalts onlap the basement, and are not deposited to the east of F1, or 2) they have been eroded after initial movement along F1. The second interpretation is schematically shown above.
B) A normal fault (F_A) dipping to the west, displaced the Ventersdorp Supergroup relatively downward to the west.
C) Uplift and erosion preceded the deposition of the Schmidtsdrif Subgroup which lies directly on the basement in the east.
D) A second normal fault (F_B) dipping to the east then displaced the Schmidtsdrif Subgroup downward to the east. Initial F1 displacement is bracketed as post Ventersdorp and pre Schmidtsdrif Subgroup, with renewed extension, post Schmidtsdrif deposition.

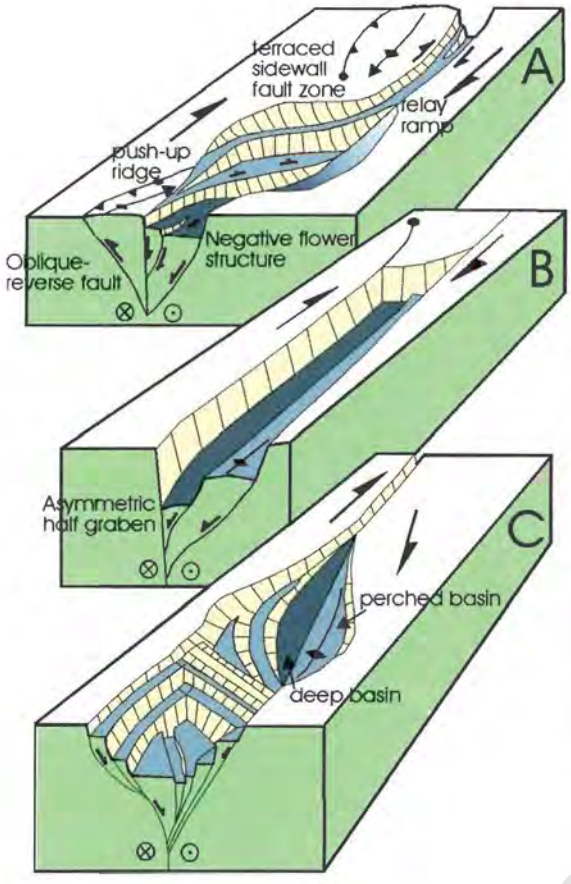

Figure 2.15: A, B and C show contrasting geometries of strike-slip basins in a dextral fault system.
A: Pull-apart basin resulting in negative flower structure oblique to the strike of the fault.
B: Transform parallel strike-slip basin
c: Marmara-type escape basin and symmetrical flower strucutre above buried master fault (after Aksu et al., 2000).
D: An expanded view of fault F2 (line KBF03A) and associated faulting, showing a geometrically similar distribution and orientation of associated faults to those of negative flower structures in A, B and C.

Thus there may be a repeated strike-slip component to the normal movement along F2 both during its initial movement (producing faults marked in blue) and its main secondary movement (producing faults marked in red). The vertical displacement along the master fault (F2 in yellow), is ~ 6.5 km.

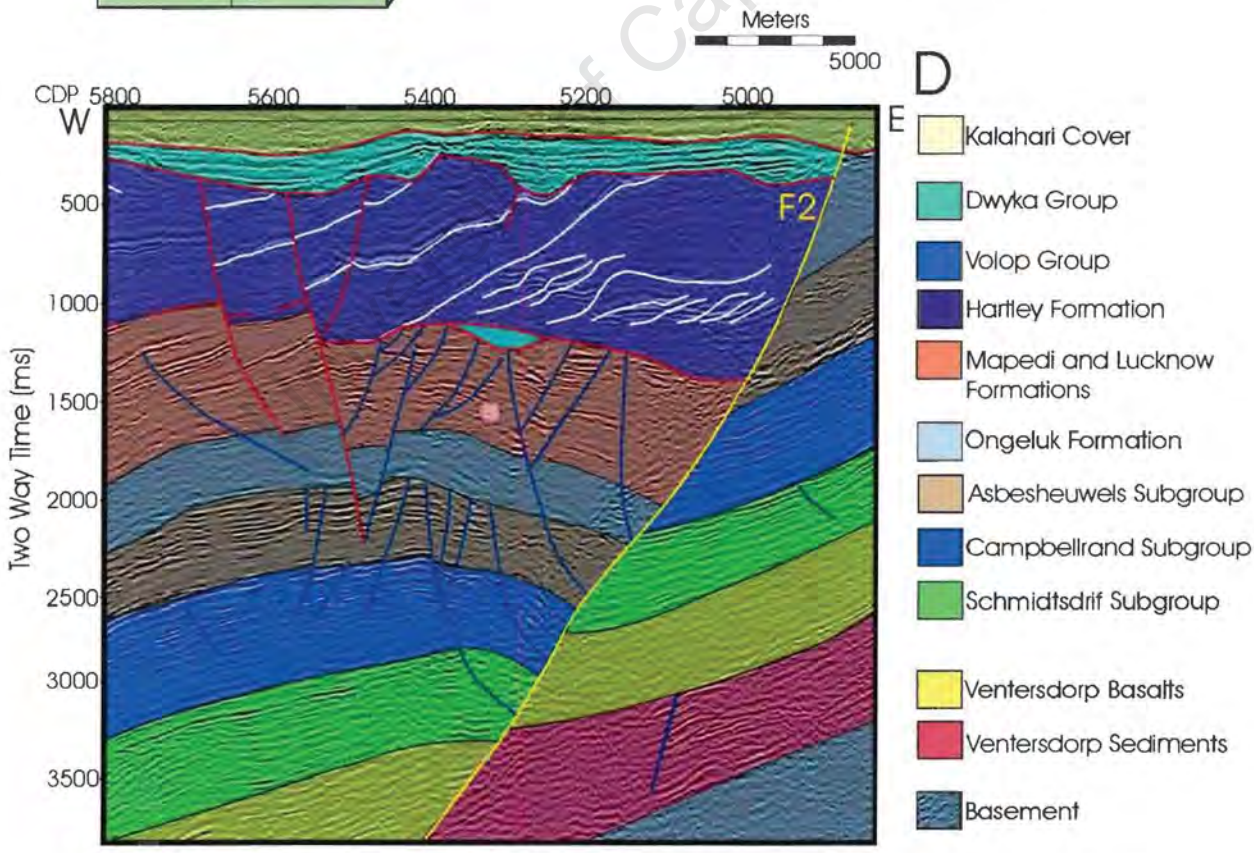

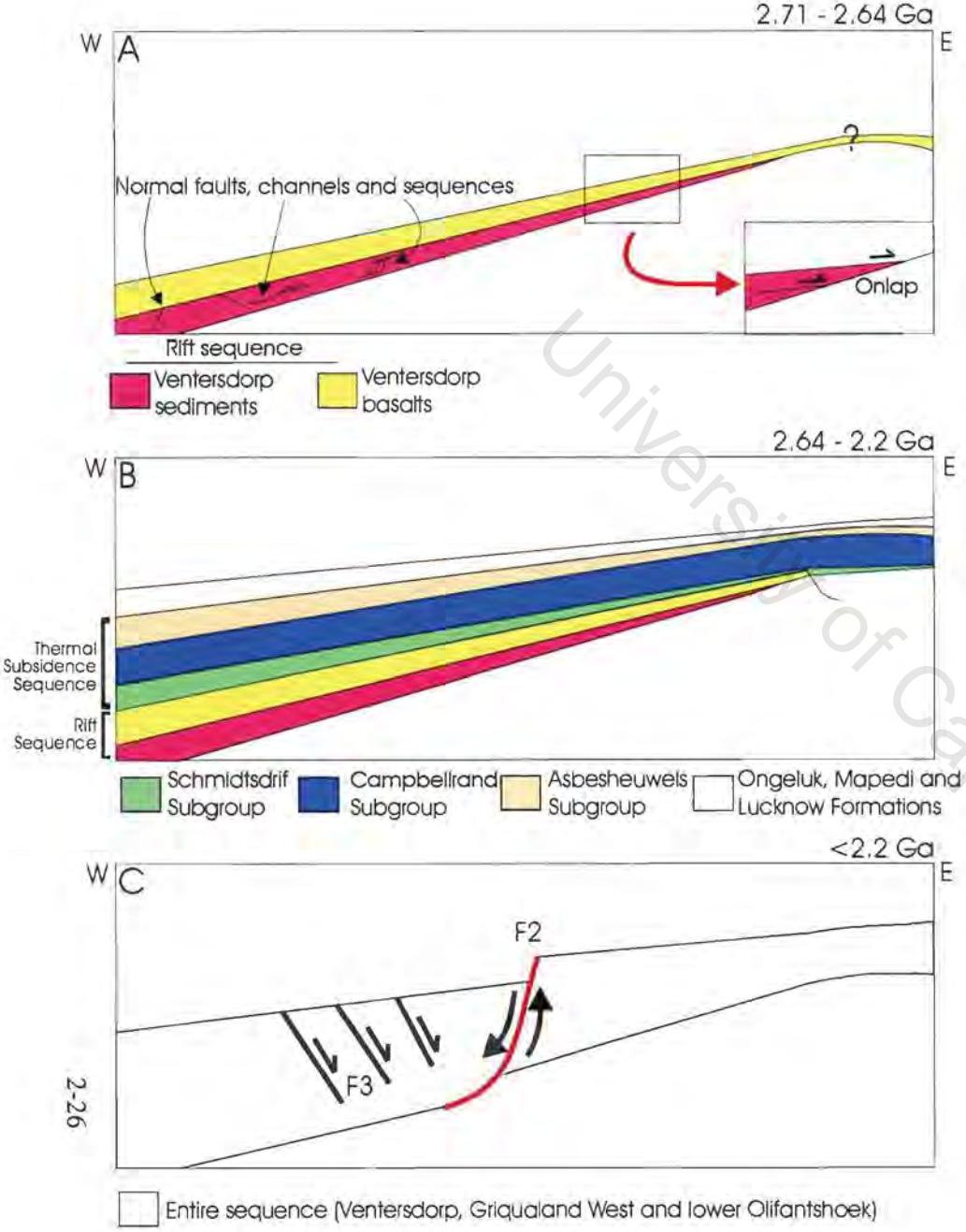

Figure 2.16: Schematic summary of the structural history from the interpretation of seismic profile KBF03A.

PHASE 1 - Extension and Subsidence

The Ventersdorp and Griqualand West Sequences were deposited during extension and subsidence related to rifting of an unknown fragment from the western margin of the Kaapvaal Craton. (Vertical scale is exaggerated).

A: Within the Ventersdorp sedimentary unit there are sequences, channels and steeply dipping normal faults causing minor displacement (figure 2.4). The Ventersdorp sediments and basalts (2714 ±3 Ma; Walraven, 1991) are interpreted as a rift sequence. Normal faulting occurs inland.

B: Thermal subsidence succeeded the rift related subsidence and resulted in the deposition of the Griqualand West Sequence, (siliciclastics, carbonates and banded iron formations) in the newly created accommodation space.

(Unconformably overlying this sequence are the lower units of the Olifantshoek Sequence. All units, except the Campbellrand Subgroup thicken westward toward the craton edge.)

C: Continued extension and the onset of normal movement along the listric fault, F2. Thus the age of this fault is <2222 ±12 Ma, the age of the Ongeluk lava, Cornell et al., 1996) but >1928 Ma (the age of the Hartley lava Cornell et al.,1998). (Some movement, however occurred post Karoo and pre Kalahari). Movement along F2 caused the development of a series of normal antithetic faults, dipping to the east (F3). There may be a component of strike-slip motion along F2 giving rise to a negative 'flower structure'- a splay of normal faults associated with strike-slip movement (figure 2.15).

University of Cape Town

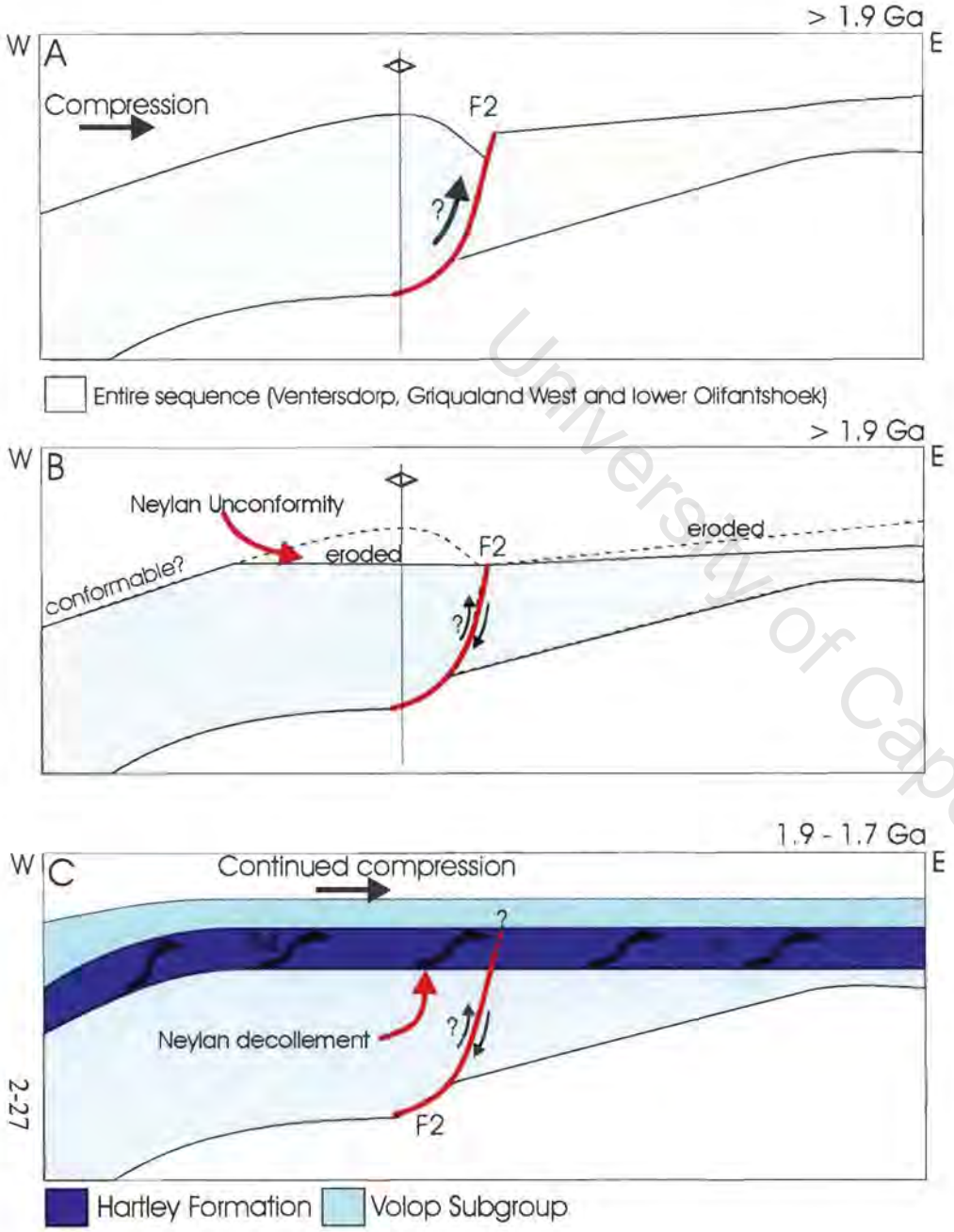

Figure 2.17: Schematic summary continued.

PHASE 2 - Compression

Phase 2: onset of compression, which may have resulted in bedding-parallel thrusts within the lower Olifantshoek Group, though this is difficult to verify.

A: Compression from the west folded the passive margin succession, producing an anticline bordered to the east by F2. This phase of compression may also have resulted in a reversal of motion along F2, from normal to thrust.

B: Folding caused localized uplift and the synchronous or subsequent erosion of this new topographic high resulted in the development of the Neylan unconformity. The Neylan unconformity possibly grades into a conformable sequence westward.

C: Following the extrusion of the Hartley basalts (upper Olifantshoek Group) thrusting of the upper Olifantshoek (F4) caused multiple duplication of these units. Thrusting was apparently directed from the west and décollement probably rooted along the Neylan unconformity (figure 2.10). The lateral extent of this thrusting is unknown. The development of thrust packages (duplexes) resulted in loading of the passive margin sequence causing it to flex downward to the west (chapter 3). Associated with this period of thrusting may have been further reverse motion along F2. It is uncertain whether the successive Volop Formation was deposited syn- or post- deformation.

University of Cape Town

Figure 2.18: Schematic summary continued.

PHASE 3 - Extension

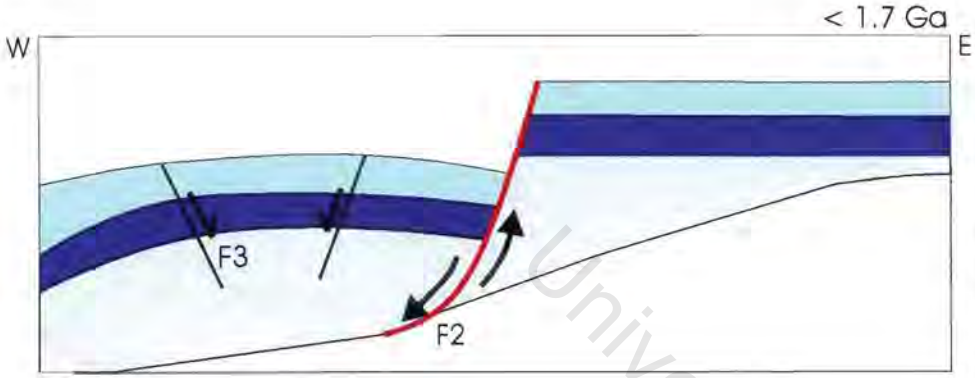

Phase 3: Onset of renewed extension. Major normal movement along F2 results in the displacement downward to the west of the passive margin sequence, together with the thrusted Hartley and successive Volop. Maximum displacement estimated in total is ~ 6.5 km (figure 2.9). Movement along this listric fault is accompanied by a pattern of monoclinal bending or 'roll over' of units into the fault and antithetic faulting (F3). The structures developed in the hanging wall are reminiscent of a 'flower structure', suggesting a significant strike-slip component.

This extensional period may have been the result of the movement of the thrust front to the east, leaving an extensional hinterland in its wake. Thus, the thrusts are displaced by subsequent normal faulting, F5 (figure 2.13).

PHASE 4 - Uplift

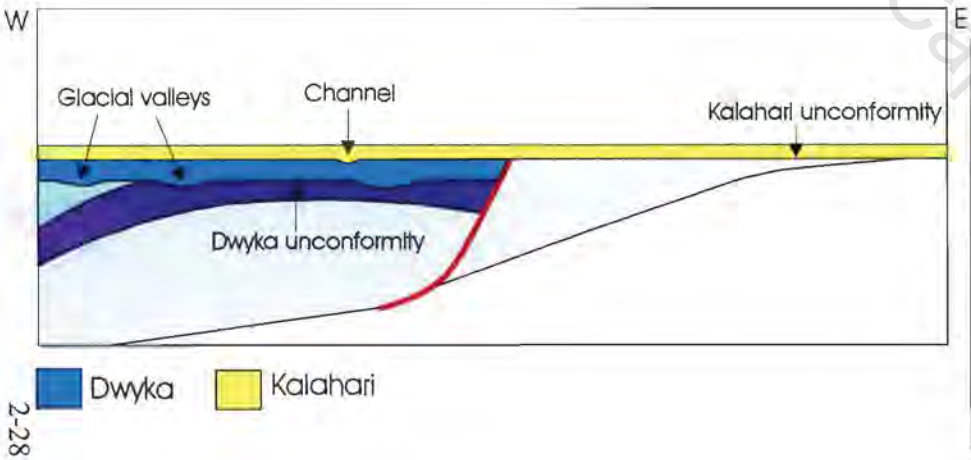

A period of uplift and glacial erosion (300 to 350 Ma) created the Dwyka unconformity which represents a considerable hiatus therefore of ~1500 to 2500 Myr. Large scale Dwyka glacial valleys have cut into the underlying late Olifantshoek-aged thrusts. The Dywka Formation is not repeated on the east side of the listric fault, F2 thus there has been post-Dwyka, normal reactivation of this fault.

Further uplift and erosion created the Kalahari unconformity upon which the Kalahari is deposited during the Tertiary. Again, a slight disturbance of reflectors by F2 suggests late stage reactivation of this fault.

University of Cape Town

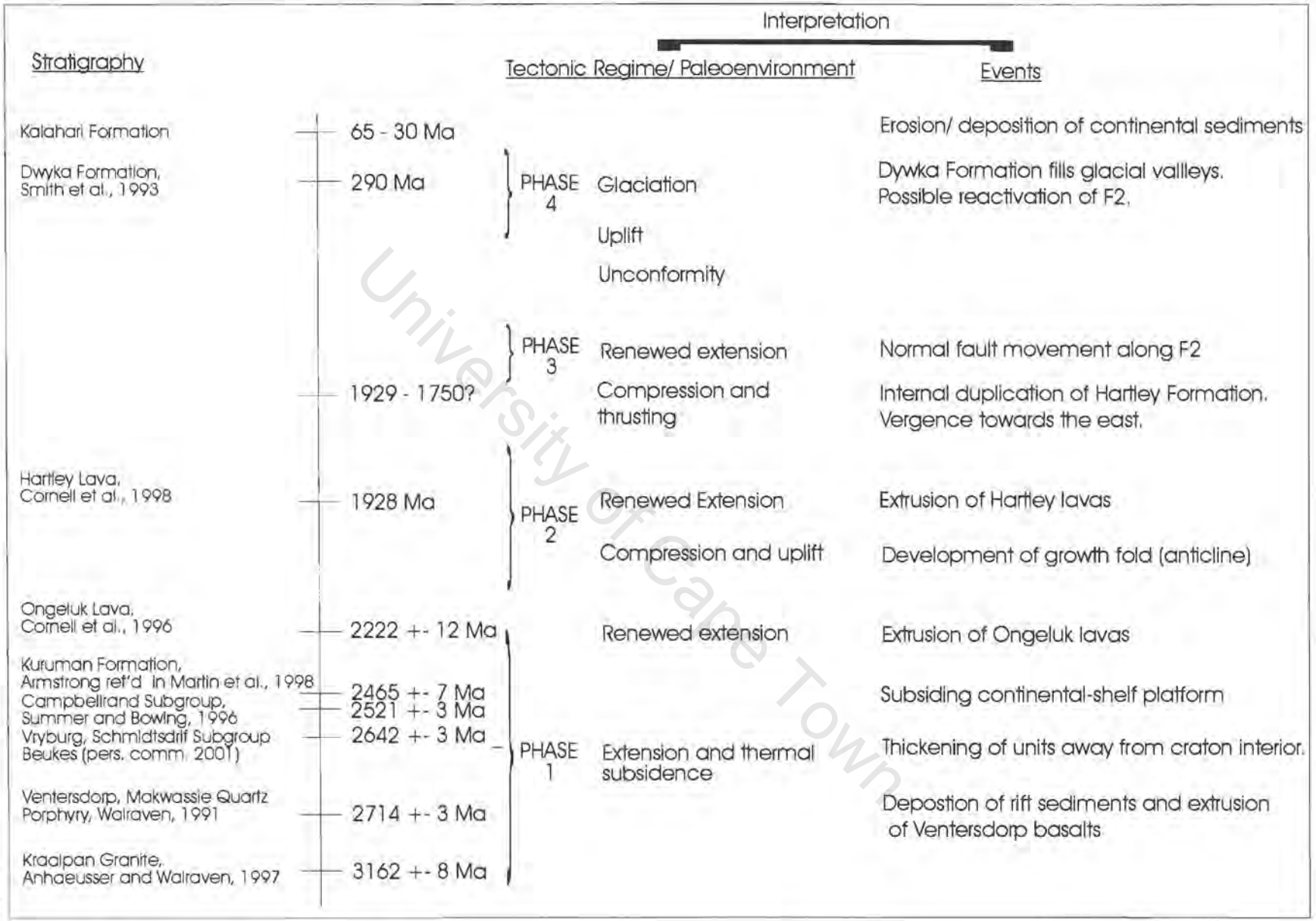

Table 2.19: Time line summary of the structural history of seismic profile KBF03A.

University of Cape Town

This sequence of events is included as a timeline in figure 2.19 and schematically summarized in figure 2.16 to 2.18.

2.2.1.V. Discussion

2.2.1.V.a. Why does the Schmidtsdrif Subgroup significantly thicken to the west (from ~500 m to ~1400 m)?

This is perhaps due to a higher rate of basement subsidence toward the edge of the craton. This subsidence is possibly thermally induced, related to the cooling of the aesthenosphere following rifting, and the extrusion of the Ventersdorp flood basalts. A higher subsidence rate at the craton's edge would create new accommodation space to be filled resulting in a transport of sediments westwards. Differing subsidence rates and associated sedimentation along line KBF 03A is discussed in chapter 3.1.

2.2.1.V.b. Why don't the Campbellrand Carbonates thicken to the west?

The Campbellrand Subgroup maintains an equal thickness across the extent of the profile. Unlike siliciclastic material, the formation of carbonate will only keep pace with subsidence if the water level remains within the window of carbonate production. If subsidence resulted in a relative rapid rise in sea level above this window, then the formation of carbonate may be inhibited. This is perhaps the reason for the lack of thickening of the carbonate unit in the west, where subsidence and consequently water depth has been proposed to be greatest. However, present day carbonate production can keep pace with subsidence rates of up to 5000 m/Ma (Altermann and Nelson, 1998), which far exceeds that calculated for this period along KBF03A (see chapter 3.1.).

2.2.1.V.c. Substantiation of stratigraphic interpretation

Published lithological descriptions of the Schmidtsdrif and Campbellrand Subgroups support the stratigraphic interpretation of the seismic profile KBF03A.

- The Schmidtsdrif Subgroup is composed of alternating shales, quartzites, siltstones, carbonates, chert and tuff (Beukes, 1987; Altermann and Wotherspoon, 1995; Altermann and Nelson, 1998). These alternating

University of Cape Town

lithologies produce high impedance contrasts, resulting in high amplitude reflections, which are apparent in the seismic profile KBF03A.

- The Reivilo Formation, at the base of the Campbellrand Subgroup, consists of various bioherm forms with only rare intercalations of shale and marl (Altermann and Nelson, 1998). Such uniformity in composition is apparent in the transparency of the formation in the seismic section. Towards the top of the Campbellrand Subgroup interbedded shale and carbonates of the Gamohaan Formation described by Altermann and Nelson (1998) may have caused increased reflectivity of the unit.

2.2.2. Seismic Profile KBF01

2.2.2.I. Introduction

Seismic profile KBF01 is located in the Northern Cape (figure 2.20) trends roughly east/west and consists of three slightly overlapping sections, which are treated here as one, ~150 km in length. Unlike line KBF03A to the north, there is far more rock outcrop in this area. The following units outcrop from east to west: Campbellrand dolomites, Asbesheuwels Subgroup, Ongeluk lava, Makganyene diamictite and the Gamagara Formation.

2.2.2.II. Description (figure 2.21)

The succession of reflective material overlying largely unreflective basement in seismic line KBF01, thickens from 0.5 s TWT in the east to 4.5 s TWT in the west. Both the thickness and degree of dip of individual units changes from east to west.

The sediment/ basement interface is a red dashed line in figure 2.21. The oldest unit overlying the basement is marked '**U**'. Unit **U** is divided into subsections, $\mathbf{U_A}$, $\mathbf{U_B}$ and $\mathbf{U_C}$ based on reflection character. $\mathbf{U_A}$ is characterised by low amplitude or weak, discontinuous reflections. In contrast, $\mathbf{U_B}$ is characterised by medium to high amplitude, semi-continuous to discontinuous reflections. Sub-unit $\mathbf{U_C}$, above, is transparent. Unit **U** thickens west of CDP 3700 to a maximum of 2.3 s TWT over a horizontal distance of around 45 km.

University of Cape Town

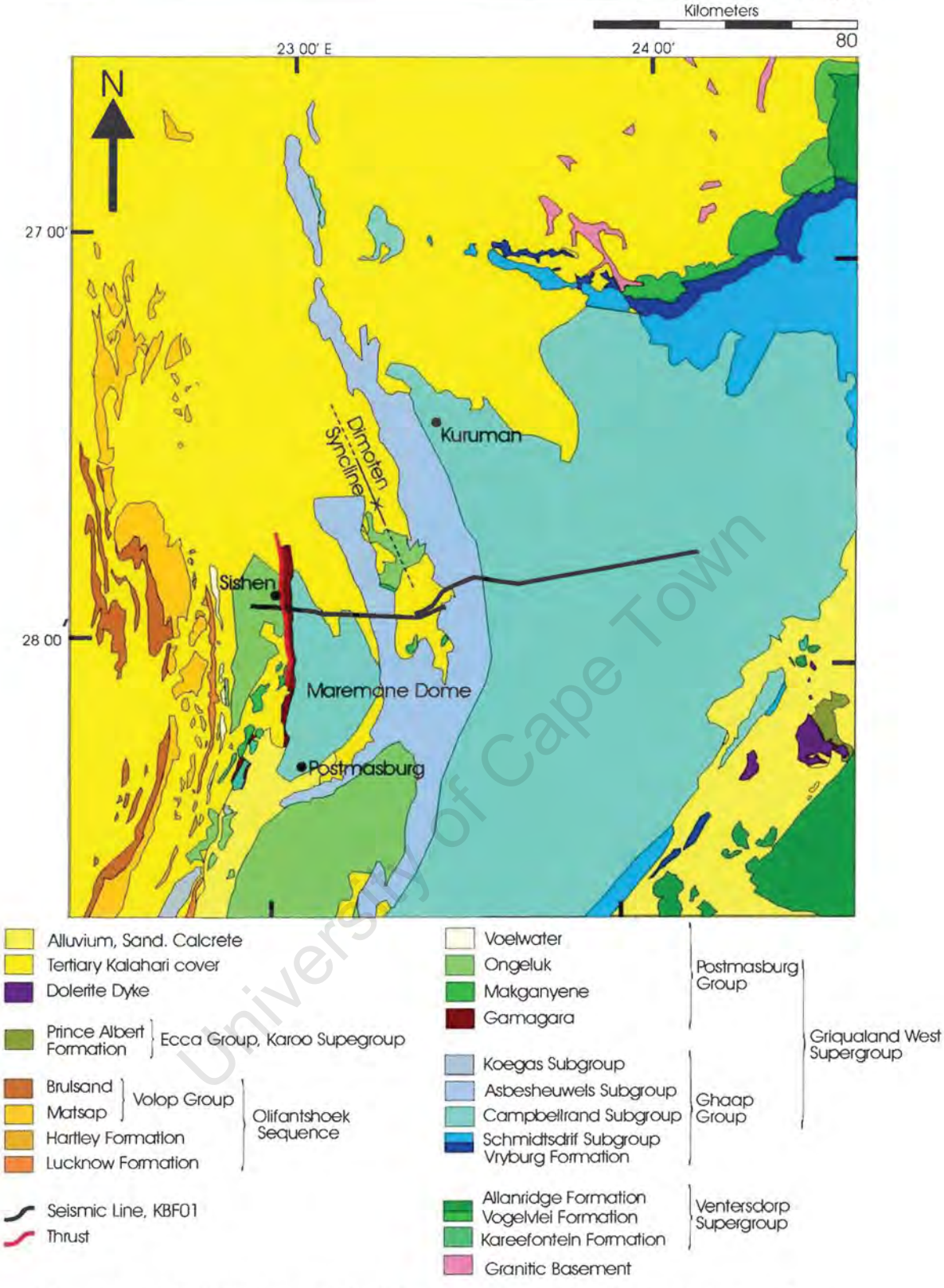

University of Cape Town

Figure 2.20: Geological map of the Maremane dome area, showing location of seismic profile KBF01 (geology simplified from the Geological Map of South Africa, Transkei, Bophuthatswana, Venda and Ciskei and the Kingdoms of Lesotho and Swaziland. 1: 1 000 000, 1984).

Unit $\mathbf{V_s}$ begins with the first reflection above the transparent unit $\mathbf{U_C}$. It is a unit composed of medium amplitude reflections that are semi-continuous. $\mathbf{V_s}$ reflectors have been displaced by numerous faults and show truncations both within the unit and by the successive unit, $\mathbf{V_b}$.

$\mathbf{V_b}$ is a thick transparent unit. In the west, it is divided into two subsections by a high amplitude, laterally continuous reflector. It thickens to the west from 0.3 s TWT or ~924 m to a maximum of 1.250 s TWT or ~3850 m (P wave velocity of 6159 m/s). Multiples, which have survived seismic processing, are most likely associated with the high amplitude reflectors of the unit $\mathbf{G_s}$ above. These give the false impression that $\mathbf{V_b}$ is highly reflective.

The basal reflector of unit $\mathbf{G_s}$ follows $\mathbf{V_b}$. Above this reflector, $\mathbf{G_s}$ is a distinctive unit, composed of very high amplitude, laterally continuous, parallel reflections that are evenly spaced. $\mathbf{G_s}$ thickens from a minimum of 0.05 s or ~145 m to 0.25 s or ~725 m (P wave velocity of 5800 m/s).

Unit $\mathbf{G_c}$, a transparent unit, is conformable with the underlying $\mathbf{G_s}$. Unit $\mathbf{G_c}$ outcrops east of CDP 2600 and west of CDP 4400. $\mathbf{G_c}$ maintains a constant thickness of around 0.5 s TWT or ~1708 m (P wave velocity of 6834 m/s). Both units $\mathbf{G_s}$ and $\mathbf{G_c}$ are truncated west of CDP 4950 by reflectors of the $\mathbf{O_{gl}}$ unit.

$\mathbf{G_{ak}}$ follows $\mathbf{G_c}$ and is composed of discontinuous and low amplitude reflectors. Like the units below, $\mathbf{G_{ak}}$ reflectors show minor displacement by pervasive normal faults. $\mathbf{G_{ak}}$ outcrops from CDP 2600 to 4300.

From the geological map (figure 2-20), it is known that a further group, $\mathbf{G_o}$, is present in the hinge of this syncline. It is impossible to isolate this unit on the seismic profile therefore an approximation of its location has been made in the seismic interpretation. $\mathbf{G_o}$ also outcrops west of CDP 5150. It truncates the unit $\mathbf{O_{gl}}$ below.

Unit $\mathbf{O_{gl}}$ outcrops between CDP 4950 and 5100 and again west of approximately CDP 5550. It is stratigraphically above and below unit $\mathbf{G_o}$. $\mathbf{O_{gl}}$ is a fairly transparent unit

University of Cape Town

though occasional medium amplitude, discontinous reflections do occur. One of these has been clearly truncated by unit $\mathbf{G_o}$.

West of CDP 5100, all units described above, dip steeply toward the west.

2.2.2.III. Stratigraphic Interpretation (figure 2-22)

2.2.2.III.a. Unit U

The stratigraphic interpretation of line KBF01 relies on outcrop information, which is abundant in this area. The basal unit U, however, does not outcrop. It forms a wedge that thickens rapidly to the west. U lies below the known Ventersdorp sediments and basalts, and is of questionable origin. Section 2.2.3.V.a. discusses possible origins of this unit.

2.2.2.III.b. Ventersdorp Sediments and Basalts (V_s and V_B)

Reflectors within the Ventersdorp sedimentary succession are semi-continuous due to their displacement by many normal faults. Faulting has resulted in horsts and grabens (figure 2-23). Within, and at the top of this unit, are several unconformities that have eroded into underlying reflectors (figure 2-24). The Ventersdorp sedimentary unit has similar features and is similar thickness to the same unit described in section 2.2.1.II KBF03A).

The Ventersdorp basalts are characteristically transparent, suggesting uniform composition. The reflector that cuts the unit west of CDP 2800 may be due to a late stage intrusion, or a temporary break in eruption. Section 2.2.1.II describes a similar reflection within the same group present on line KBF03A. The Ventersdorp basalt unit is variable in thickness, which may reflect either an uneven deposition or uneven erosion by the overlying Schmidtsdrif Subgroup.

Similarly to profile KBF03A, both the Ventersdorp sediments and basalts thicken to the west. This suggests an increased subsidence rate toward the craton edge in the west.

University of Cape Town

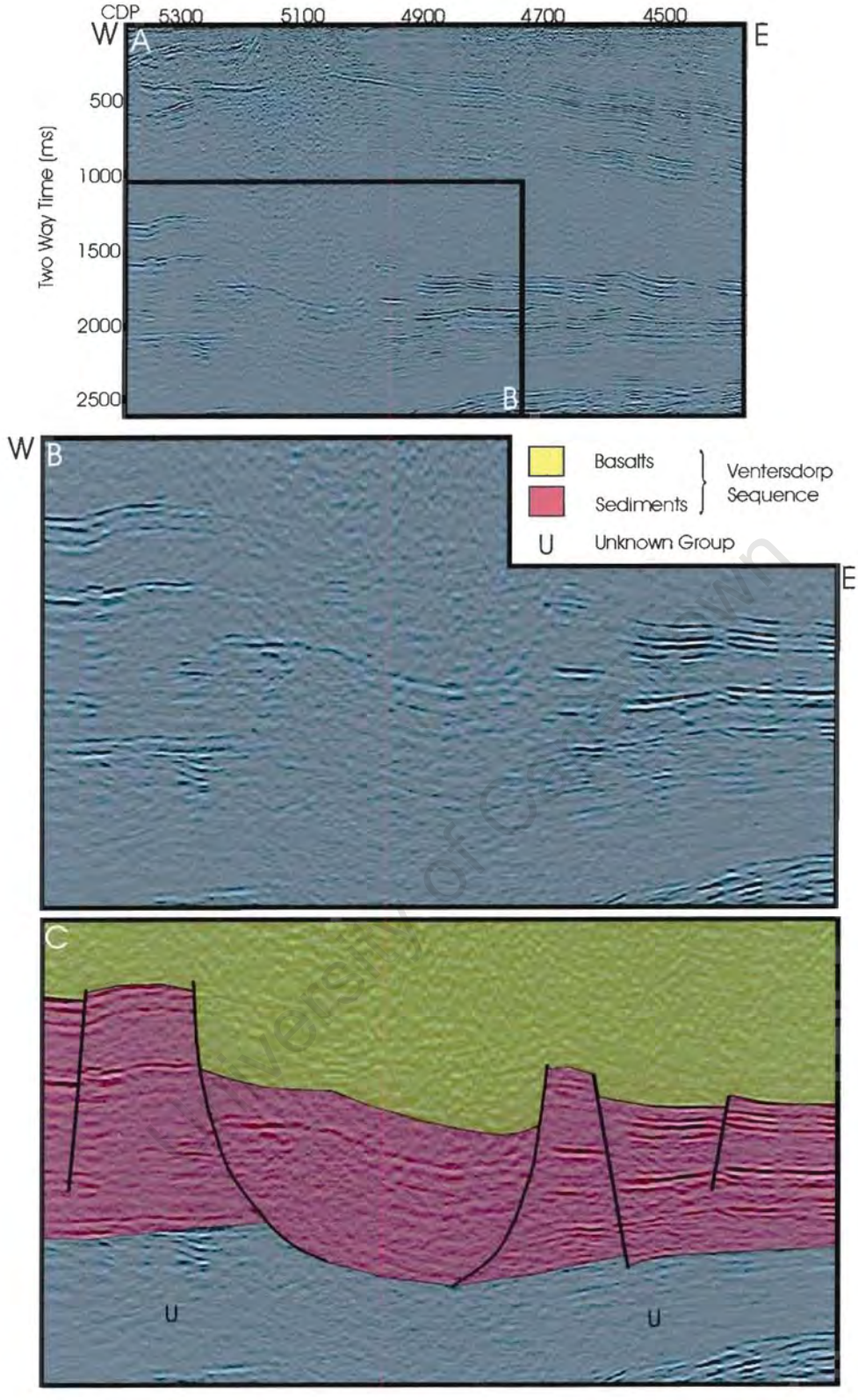

Figure 2.23: Seismic data is interpreted to show horst and grabens within the Ventersdorp Sequence. Box in A is enlarged: B is uninterpreted, C interpreted.

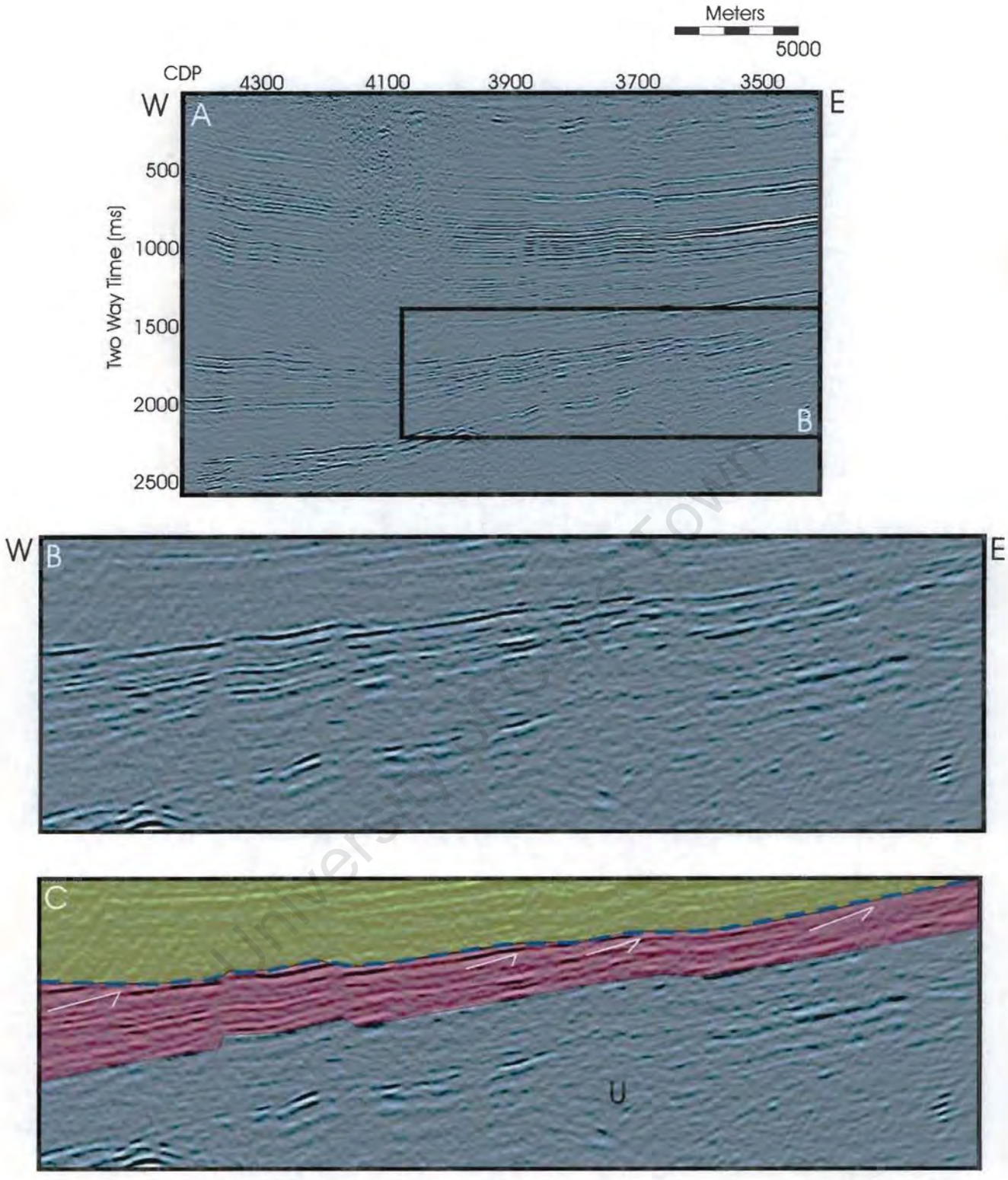

Figure 2.24: An unconformity (blue dashed line) truncates Ventersdorp sediments along KBF01. White arrows show reflection truncations. Box in A is enlarged: B is uninterpreted, C interpreted.

2.2.2.III.c. The Griqualand West Sequence (G_s, G_c, G_{ak} and G_o)

The Ghaap Group

A. The Schmidtsdrif Subgroup (G_s)

The Schmidtsdrif Subgroup thickens slightly to the west. The high amplitude, continuous reflectors suggest strong impedance contrasts perhaps reflecting laterally persistent lithologies. Like the underlying Ventersdorp units and overlying Campbellrand Subgroup, reflectors of the Schmidtsdrif Subgroup have been displaced by steeply dipping normal faults. The displacement along these faults is minor. The general seismic character of this unit is similar to that described in section 2.2.1.II (KBF03A).

B. The Campbellrand Subgroup (G_C)

The presence of multiples associated with the strongly reflective Schmidtsdrif unit obscures the fact that the Campbellrand Subgroup is acoustically transparent. This subgroup is uniform in thickness across the profile. West of CDP 4950 the Campbellrand dolomites outcrop adjacent to the lower Olifantshoek, Mapedi (Gamagara) and Lucknow Formations. This is due to the thrusting of the latter over the dolomites, described in fuller detail in section 2.2.3.IV, figure 2.26.

C. The Asbesheuwels and Koegas Subgroup (G_{AK})

An increase in reflectivity accompanies the transition from the carbonates (Campbellrand Subgroup) to iron formation (Asbesheuwels Subgroup). This may be due to acoustic contrasts arising from interbedded chert or shale within the iron formation. The Asbesheuwels and Koegas subgroups appear to be more faulted than the carbonates below. However, this may be due to the transparency of the Campbellrand carbonates, hence the difficulty in identifying faults.

The Postmasburg Group

D. The Makganyene and Ongeluk Formations (G_O)

These formations are only evident on the seismic profile to the west of CDP 5150. They are seismically indistinguishable from each other, therefore have been grouped as G_O. This unit truncates the underlying reflectors of the lower Olifantshoek

University of Cape Town

formations. This unconformity is interpreted as tectonic, forming as the Ongeluk and Makganyene Formations were thrust over the lower Olifantshoek sediments.

E. The Lower Olifantshoek Group (O_{GL})

The lower Olifantshoek sediments are seismically transparent, indicating uniform composition. One reflector, however, is truncated by the Ongeluk Formation above. The unconformity between the lower Olifantshoek Group and the Ongeluk and Makganyene Formations above is again interpreted as tectonic. Thus the position of the lower Olifantshoek Group both above and below the older Ongeluk Formation is explained by thrusting (section 2.2.3.IV., figure 2.26).

2.2.2.IV. Tectonic Model

The following structural observations are made:

- The Ventersdorp sediments and basalts, Ghaap Group and Ongeluk lava are folded into a syncline/ anticline pair.
- The syncline is asymmetric. The eastern limb has a shallower dip than the western limb. The apparent asymmetry may be due to the orientation of the profile relative to the strike of the fold.
- The lower Olifantshoek Group: Mapedi (Gamagara) and Lucknow Formations lie above and below the Makganyene and Ongeluk Formations. The thrusting of both the lower Olifantshoek over the Griqualand West Sequence and the Ongeluk and Makganyene over the lower Olifantshoek has caused the tectonic truncation of reflections (figure 2.25).
- A normal fault has displaced the thrusted Ongeluk Formation as well as the underlying Ghaap Group.

From these observations a tectonic model is proposed. This model consists of four main phases of deformation:

1) After the deposition of the Ongeluk Formation (< 2.2 Ga), the Ventersdorp, Ghaap and Postmasburg groups were folded to form a syncline/anticline pair (figure 2.26a).

University of Cape Town

2) Compression continued, resulting in the thrusting of the lower Olifantshoek Group sediments (Gamagara/ Mapedi and Lucknow Formations) over the Griqualand West strata (Schmidtsdrif and Campbellrand Subgroups) (figure 2.26b).
3) Thrusting continued, causing the duplication of the entire sequence (Ongeluk to Mapedi and Lucknow) (figure 2.26c).
4) A late stage extensive regime resumed, resulting in the displacement of a thrust by at least one normal fault.

2.2.2.V. Discussion

2.2.2.V.a. Origin of unit U

This wedge may be composed of:

1. Stratigraphically older material (perhaps equivalent to the Dominion and or/ Witwatersrand Group).
2. Ventersdorp units that have been duplicated by thrusting.
3. Thickened Ventersdorp basalts and sediments along the craton edge.

Ventersdorp deposition is associated with craton-wide extension, resulting in normal and strike-slip faulting. In addition, there is no evidence for Ventersdorp aged thrusting in seismic profile KBF03A, further north along the Kaapvaal Craton's western margin. The Ventersdorp sediments are interpreted to be a rift sequence deposited during extension along the margin. Therefore, option 2 seems unlikely.

Without outcrop or boreholes it is difficult to choose between option 1 and 3. However, this wedge of material thickening toward the cratonic margin may be compared to similar modern extensional margins elsewhere. Seaward dipping reflector wedges are described from the east Antarctic coast (Hinz and Krause, 1982; Jokat *et al.*, 1996) and off the eastern margin of Greenland and the western margin of Norway (Courtillot *et al.*, 1999, Reemst and Cloetingh, 2000). The Hatton and Edoras bank, Rockall continental margin, are two further examples of seaward dipping reflectors arising from volcanic flows, associated with continental break up (Barton and White, 1997).

University of Cape Town

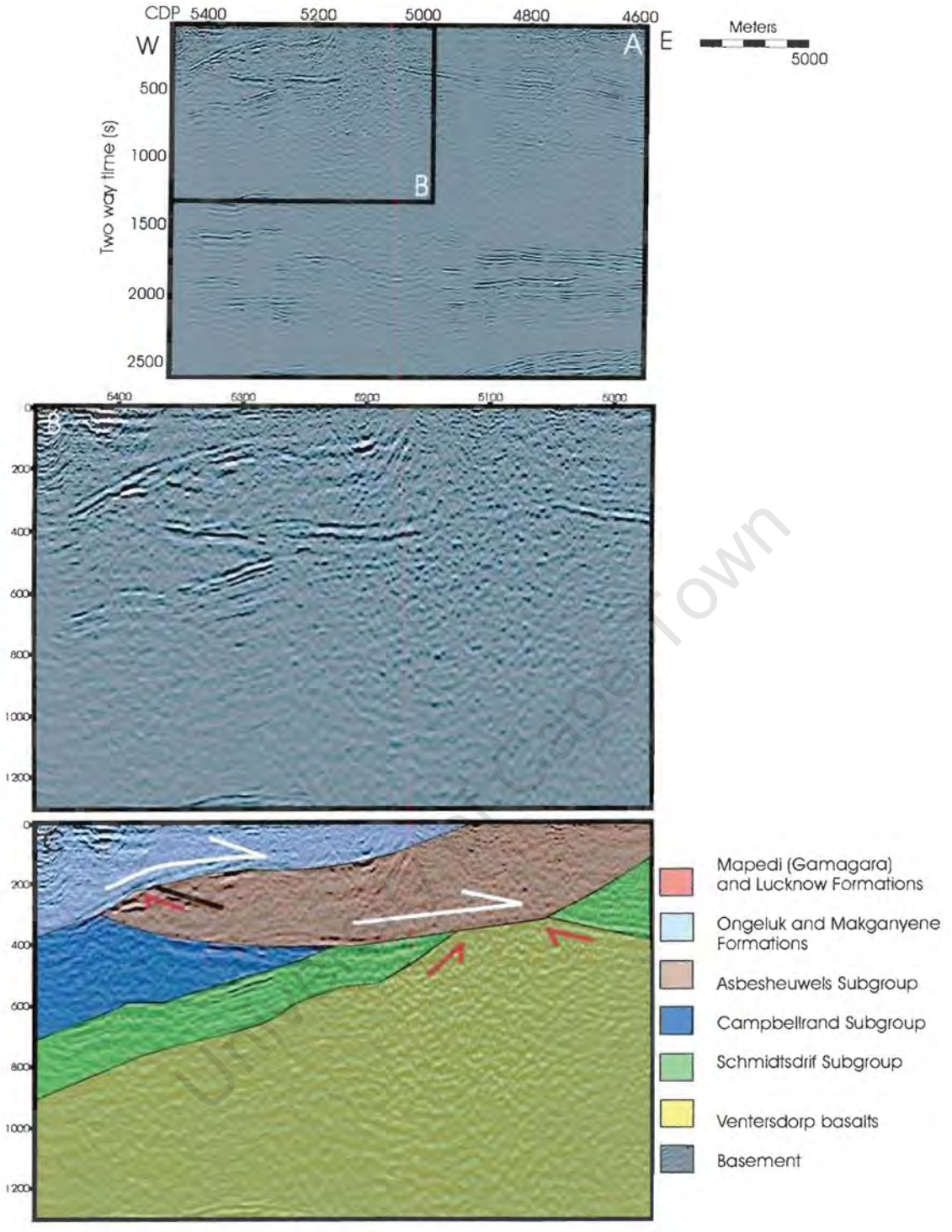

Figure 2.25: Western section of line KBF01. Box is enlarged: B is uninterpreted and C interpreted. The lower Olifantshoek (Gamagara and Lucknow) is thrust over, and truncates the underlying Griqualand West Sequence. The lower Olifantshoek is in turn truncated by the stratigraphically older thrusted Ongeluk and Makganyene Formations. White arrows show apparent direction of thrusting. Red arrows mark reflection truncations.

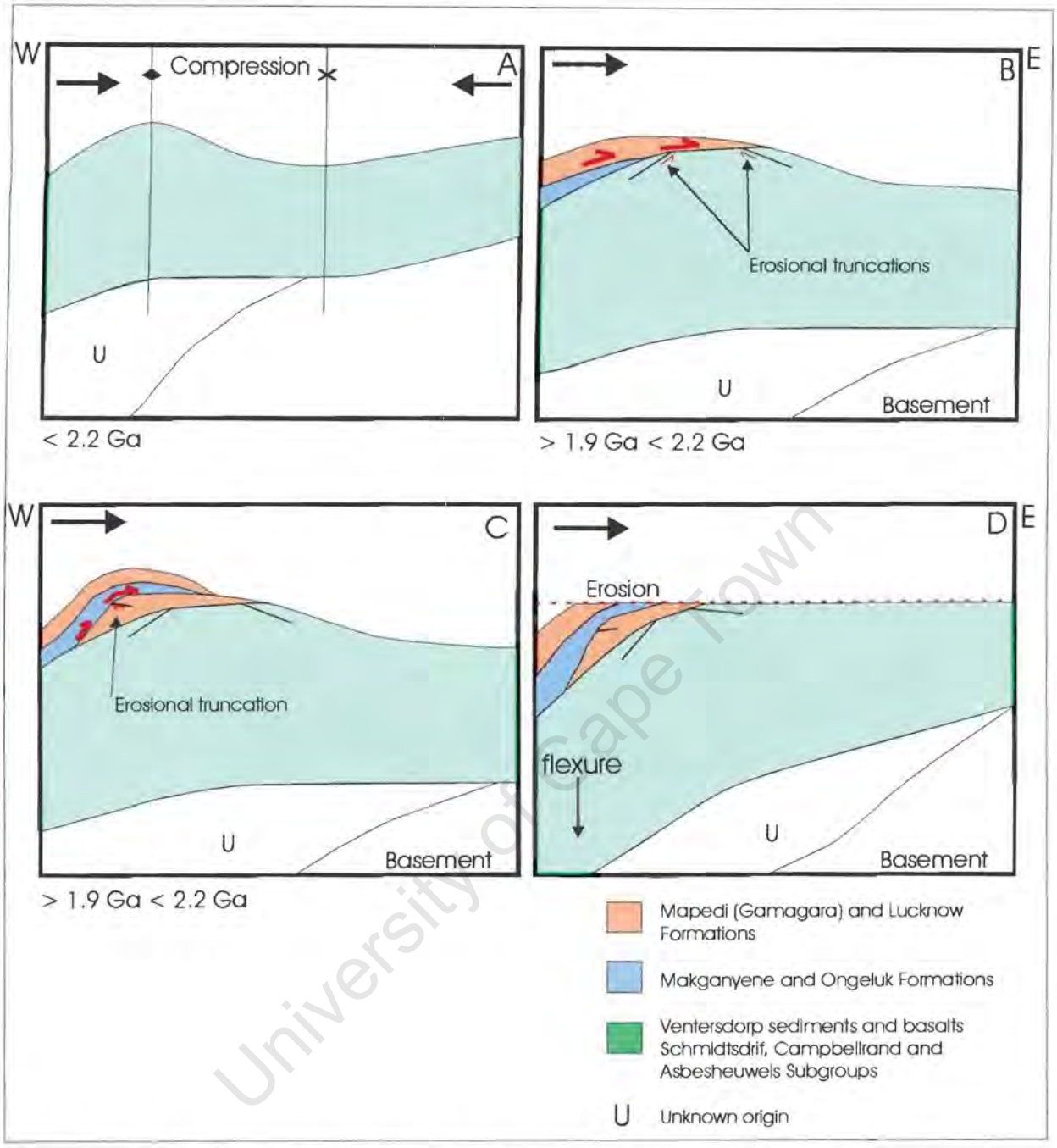

University of Cape Town

Figure 2.26: Schematic interpretation of the structural history of the western section of line KBF01.

A: Compression results in folding. B: Lower Olifantshoek units (Mapedi/ Gamagara and Lucknow Formations) thrust over Ventersdorp and Griqualand West Sequence. C: Continued thrusting of entire sequence (Ongeluk and Olifantshoek) across previously duplicated lower Olifantshoek and formation of distinct duplexes. D: Additional load may have resulted in flexure of foreland down to the west. Sediments are now eroded to present land surface.

The maximum thickness of unit U is 2.3s TWT which equates to ~7080 m if composed entirely of basalt (P wave velocity of 6159 m/s, see table 2.1). The seismic character of this unit is not uniform however, which suggests a mixed composition of roughly 50% basalt, 50% sediment. Again ignoring compaction, a thickness of ~6870 m is estimated using this mixture (P wave velocity of 5800 m/s for the Ventersdorp sediments). These Archean thicknesses are similar to the ~8 km thickness estimated for offshore continental-edge basaltic volcanic sequences associated with Mesozoic continental break up in the North Atlantic (Courtillot *et al.*, 1999).

2.2.2.V.b. Stratigraphic position of the Gamagara Formation

The stratigraphic position of the Gamagara Formation is debated. Historically (pre 1967) the Gamagara has been interpreted to be the equivalent of the Mapedi Formation, hence included as part of the lower Olifantshoek Group. The stratigraphic column was subsequently revised and the Gamagara is now regarded to be part of the Griqualand West Sequence. Beukes and Smit (1987) propose that the former interpretation is correct. Line KBF01 substantiates this claim.

Two structural interpretations are shown in figure 2.27. In figure 2.27a, thrusts result in the duplication of Gamagara and lower Olifantshoek strata. Figure 2.27b lacks these thrusts suggesting rather the presence of several unconformities between the various units. Structural observations of line KBF01 (figure 2.25) show that the Gamagara and Ongeluk Formations have indeed been thrust over the Transvaal sediments. Thus, this evidence supports the proposition that the Gamagara is a correlative of the Mapedi Formation (lower Olifantshoek). Hence it is younger than, therefore cannot be a part of the Griqualand West Sequence (figure 2.26a).

2.2.2.V.c. Possible flexure induced by loading

Thrusting involving the Postmasburg and lower Olifantshoek Group resulted in the loading of the Ghaap and Ventersdorp Groups below. The emplacement of this load may have caused the latter to be deflected or flexed downward to the west. Thus the steep westerly dips of the Ventersdorp and Ghaap Groups may be related to this thrusting.

University of Cape Town

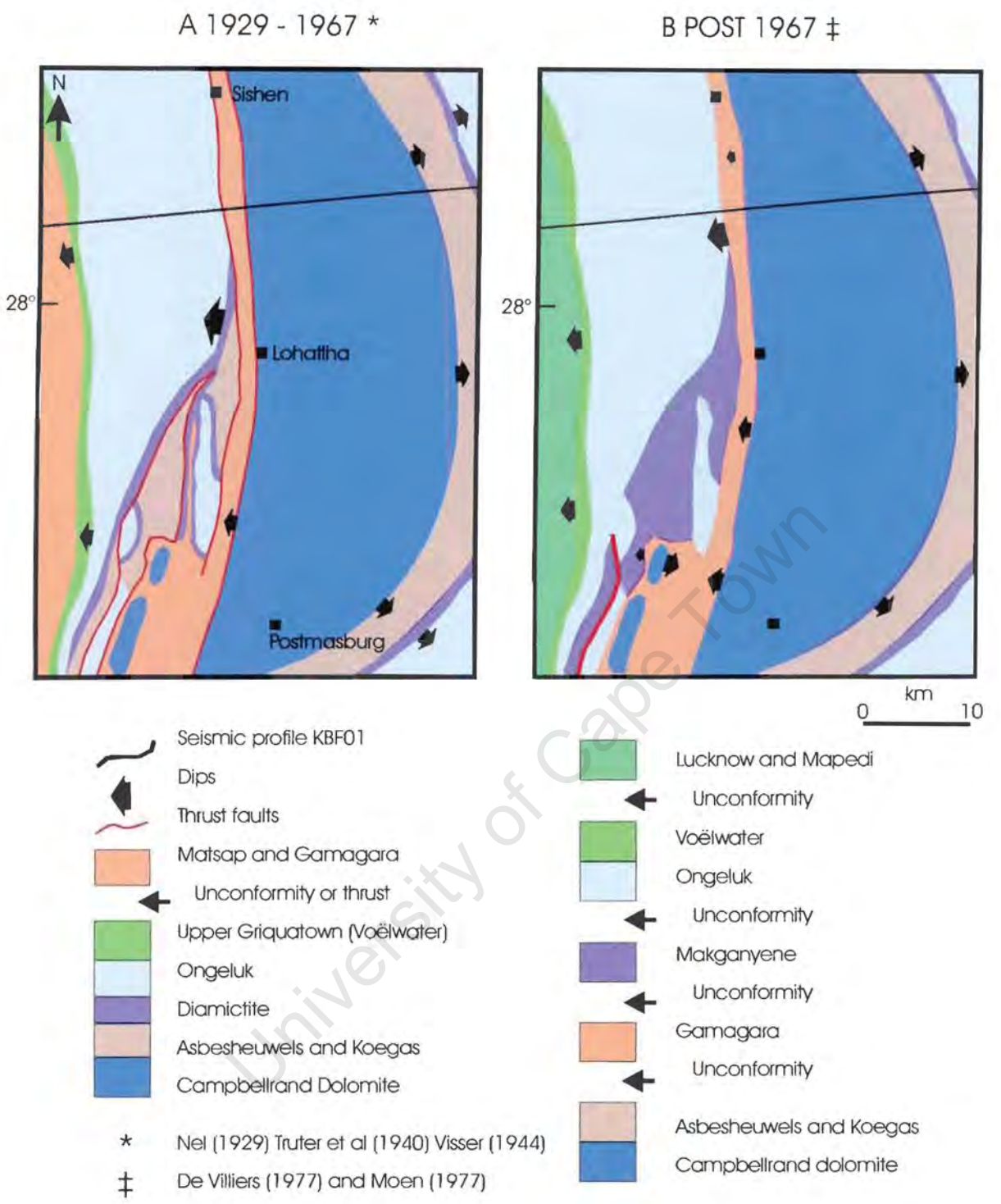

University of Cape Town

Figure 2.27: Two different interpretations, A and B, of the stratigraphic sequence in the Maremane Dome area. A: The Gamagara Formation forms part of the lower Olifantshoek Sequence and has been thrust over younger Griqualand West sediments. B: The Gamagara Formation is older, forming part of the Griqualand West Sequence (from: Beukes and Smit, 1987).

2.3. The Bushveld Profiles

2.3.1. Introduction

Lines Rz-254, 255 and 256 are located in the Northern and North West Province, east of the Botswana border (figure 2.28). They traverse a large syncline that is oriented east-west and is composed of sediments and lava belonging to the Transvaal Supergroup. Remnants of Bushveld sills form scattered outcrops within its hinge. Rz-254 extends 105 km north/south. Rz-256 is semi-parallel to Rz-254 and is 115 km long. These two lines are connected by Rz-255, which is 72 km in length and orientated parallel to the strike of the fold, thus east-west.

2.3.2. Description (figures 2.29, 2.30, 2.31)

The sediment/basement interface has been marked as a red line on figures 2.29 to 2.31. Question marks and dashed line segments signify uncertainty in the placement of this line. The sediment/ basement contact is irregular. The successive unit, **V** occupies discrete areas where the sediment/basement contact is deep. **V** has a highly variable seismic character. Reflections are generally weak with poor continuity though occasionally semi-continuous reflectors do occur (for example, line Rz-255, east of CDP 2700). The unit attains maximum thickness in line Rz-256 of 1400 ms TWT or ~4195 m, between CDP 700 and 1400 (average P wave velocity for Ventersdorp sediments and basalts estimated at 5993 m/s).

A high amplitude, laterally continuous reflector, marked **Br**, terminates the reflections of unit **V**, below. Unit $\mathbf{C_m}$ lies conformably above **Br**. Its seismic character and thickness of around 500 ms TWT or ~1700 m (P wave velocity of 6834 m/s) is uniform in all three lines. $\mathbf{C_m}$ grades from medium amplitude, continuous reflectors at the bottom, to weaker reflectors, and in some areas, transparency, towards the top.

The first strong reflector marks the top of $\mathbf{C_m}$ and the bottom of the successive unit $\mathbf{P_t}$. $\mathbf{P_t}$ has brighter reflectors than $\mathbf{C_m}$ below. Reflectors range from continuous to semi-continuous. They onlap and downlap and in some cases truncate, older reflectors within the unit.

University of Cape Town

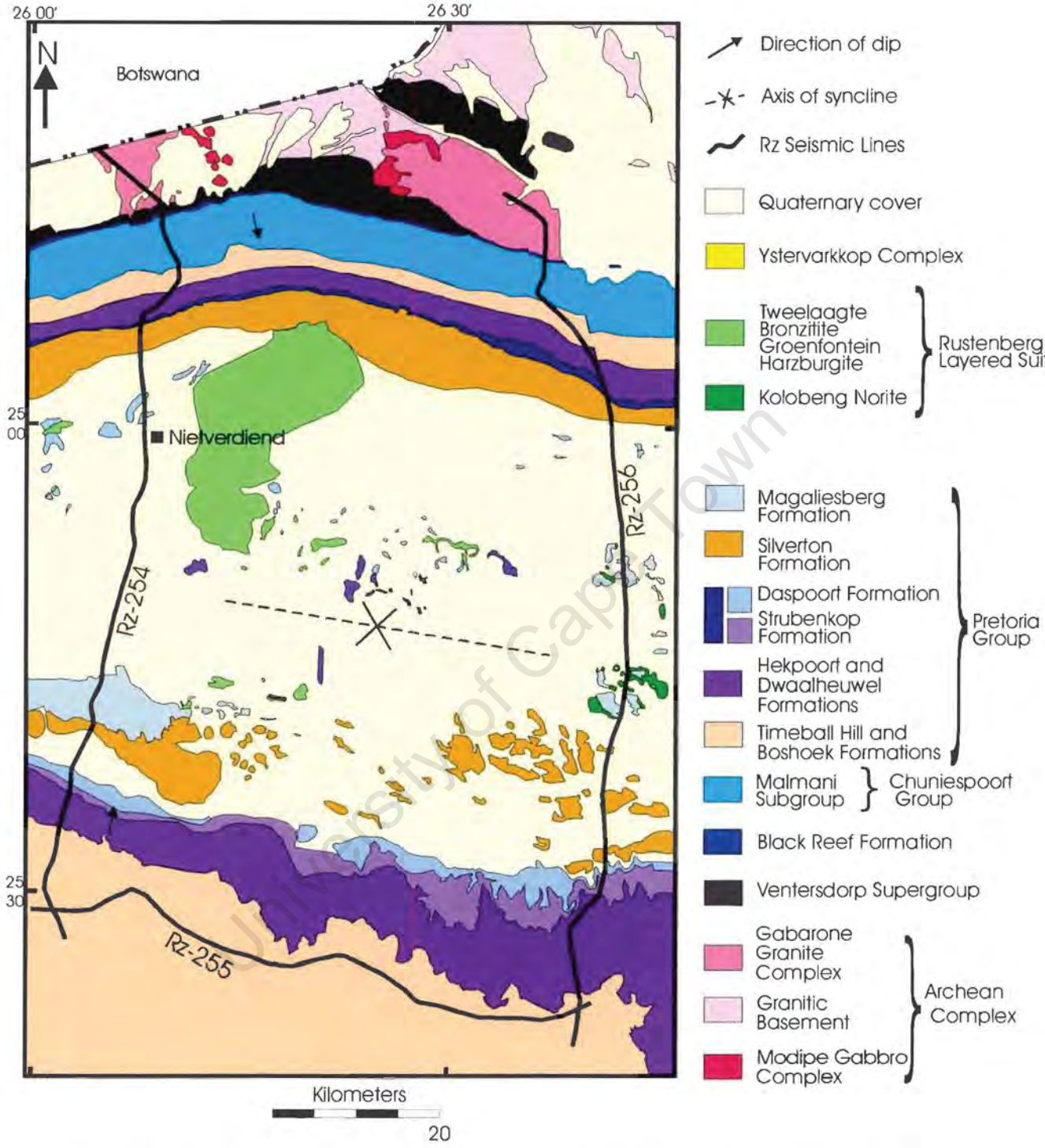

University of Cape Town

Figure 2.28: Geological map of Thabazimbi and Rustenberg areas showing location of seismic profiles Rz-254, 255 and 256 (geology simplified from Geological Map of South Africa, Transkei, Bophuthatswana, Venda and Ciskei and the Kingdoms of Lesotho and Swaziland. 1: 1 000 000, 1984).

Unit $\mathbf{P_h}$ and the successive units $\mathbf{P_{sds}}$ and $\mathbf{P_m}$ are only present in lines Rz-254 and 256. Unit $\mathbf{P_h}$ is mostly transparent, though occasional, medium amplitude reflectors do occur towards its top. It is similarly thick in these two lines, 250 ms (~760 m) to 300 ms TWT (~912 m) in line Rz-256 and 254 respectively (P wave velocity of 6083 m/s). With the transition from unit $\mathbf{P_h}$ to unit $\mathbf{P_{sds}}$ above, there is an increase in reflectivity. High amplitude reflectors mark the base of the unit. Reflectors are semi-continuous and onlap, downlap and truncate other reflectors within the unit. The thickness of unit $\mathbf{P_{sds}}$ varies from 350 ms TWT or ~960 m in line Rz-256 to 450 ms TWT or ~1240 m in line Rz-256 (P wave velocity of underlying Timeball Hill Formation is 5500 m/s).

The transparent unit $\mathbf{P_m}$ follows $\mathbf{P_{sds}}$. The youngest unit, **P?,** is identified on the basis of seismic character. The unit is characterized by semi- to discontinuous, folded reflectors. The top of this unit is transparent. In both seismic lines Rz-254 and 256, a very thin veneer of quaternary cover, **Q**, obscures the sediments below. It is unidentifiable on the seismic line, thus its approximate position has been marked from the geological map (figure 2.28).

All units in lines Rz-254 and 256, except **V**, dip inward to the center from the northern and southern extent of the lines. Units $\mathbf{C_m}$ and $\mathbf{P_t}$ of line Rz-255 are almost horizontal.

2.3.3. Stratigraphic Interpretation (figures 2.32 to 2.34)

The stratigraphic interpretation of the Rz lines is based on outcrop (figure 2.28).

2.3.3.I. Ventersdorp Supergroup (V)

The Ventersdorp Supergroup fills listric fault-bounded, discrete basins along the three seismic profiles. Bounding normal faults strike predominantly east-west, and dip to the north and south. Line Rz-255 shows an along strike view of a Ventersdorp basin between CDP 3300 and 2700. The width of this particular basin is estimated at ~16 km, and its depth at 1050 ms or ~3.15 km (average P wave velocity for Ventersdorp sediments and basalts is 5993 m/s). The across strike dimensions of the Ventersdorp basins may be estimated from the lines oriented north-south, Rz-254 and 256. Thus,

University of Cape Town

due to the perpendicular orientation of the seismic profiles to one another, it is possible to make 3D approximations of the geometry of these basins. Figure 2.35 is a box diagram of the three Rz lines, and offers a 3D perspective of the Ventersdorp basins, and Transvaal sediments and basalts above.

Of the Ventersdorp Supergroup, only the Allanridge andesites and the Bothaville sediments outcrop in the vicinity of the Rz-lines. However, the similarity of basin geometry to the Platberg basins described in section 2.4 suggests that older Platberg sediments may also be deposited in these discrete basins.

2.3.3.II. Transvaal Supergroup (C_m, P_t, P_h, P_{sd}, P_m and P?)

2.3.3.II.a. Black Reef Formation (Br) [2642 ± 3 Ma]

(Age for correlative Vryburg Formation, U-Pb, Beukes, pers. comm. 2001)
The Black Reef Formation forms a distinctive marker reflector on the three seismic profiles. It appears very bright due to a strong impedance contrast between it and the carbonates above. The Black Reef Formation has eroded into the underlying the Ventersdorp sediments, resulting in a prominent unconformity (figure 2.36). A preserved channel is located within this unit, along seismic profile Rz-254 (figure 2.37).

2.3.3.II.b. Chuniespoort Group

Malmani Dolomite (C_m) [2583 ± 5 Ma] (U-Pb, upper Oak Tree Formation, Martin *et al.*, 1998)
The Malmani dolomite has constant thickness across the three seismic profiles. It is also of similar thickness to the correlative Campbellrand dolomite described in the Griqualand West sub-basin along the western margin of the craton (section 2.2.1.II). Malmani reflections may be caused be interbedded chert or sediment or by the intrusion of sills, possibly Bushveld in age (2060 Ma).

University of Cape Town

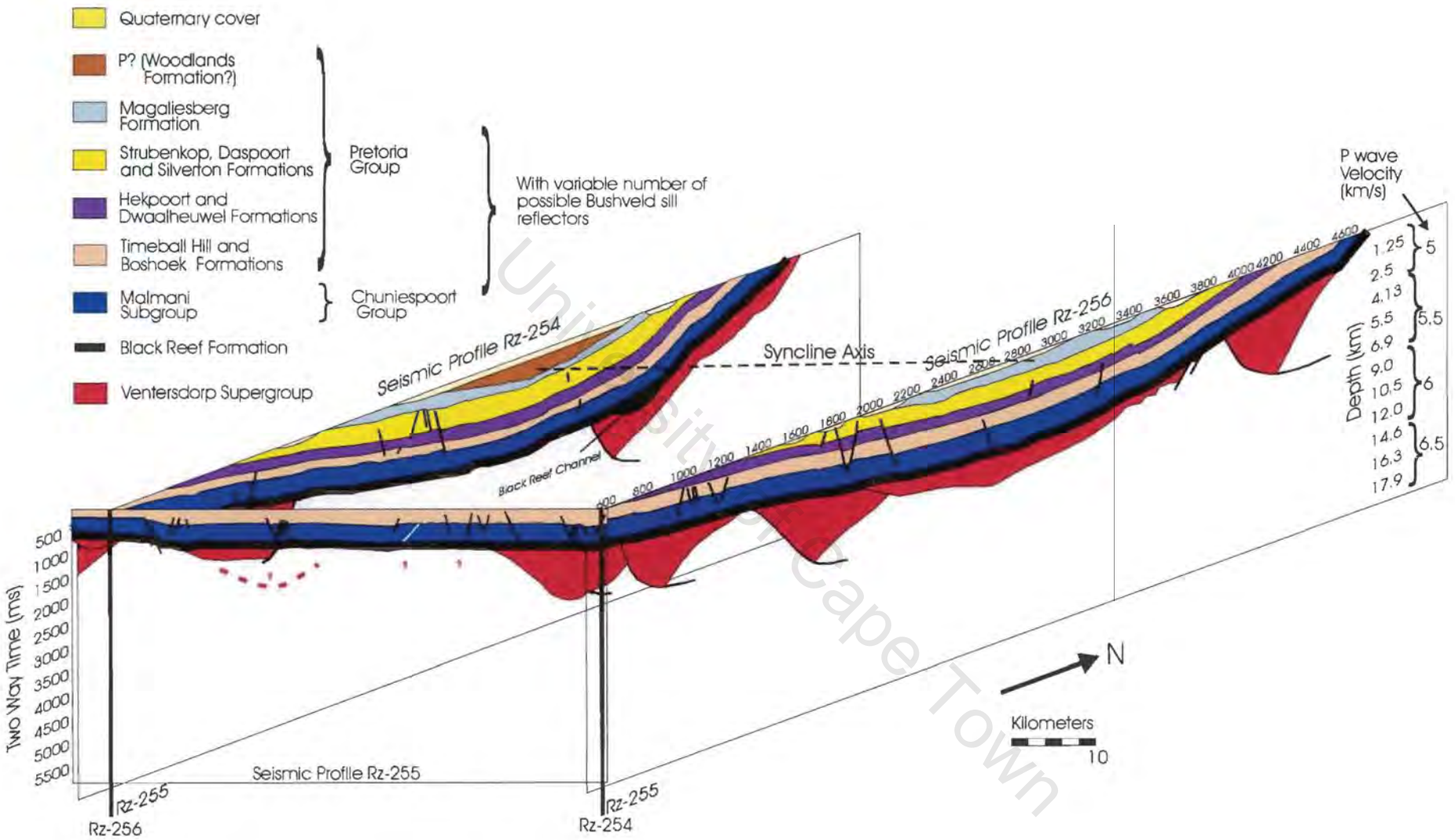

University of Cape Town

Figure 2.35: Three dimensional view of the Rz lines. Two way time in ms has been roughly converted to depth in km, using increasing estimated P wave velocities due to increasing compaction with depth. Ventersdorp Supergroup occupies half grabens with boundary normal faults trending east/west and predominately dipping to the north. The Black Reef Formation truncates these faults..

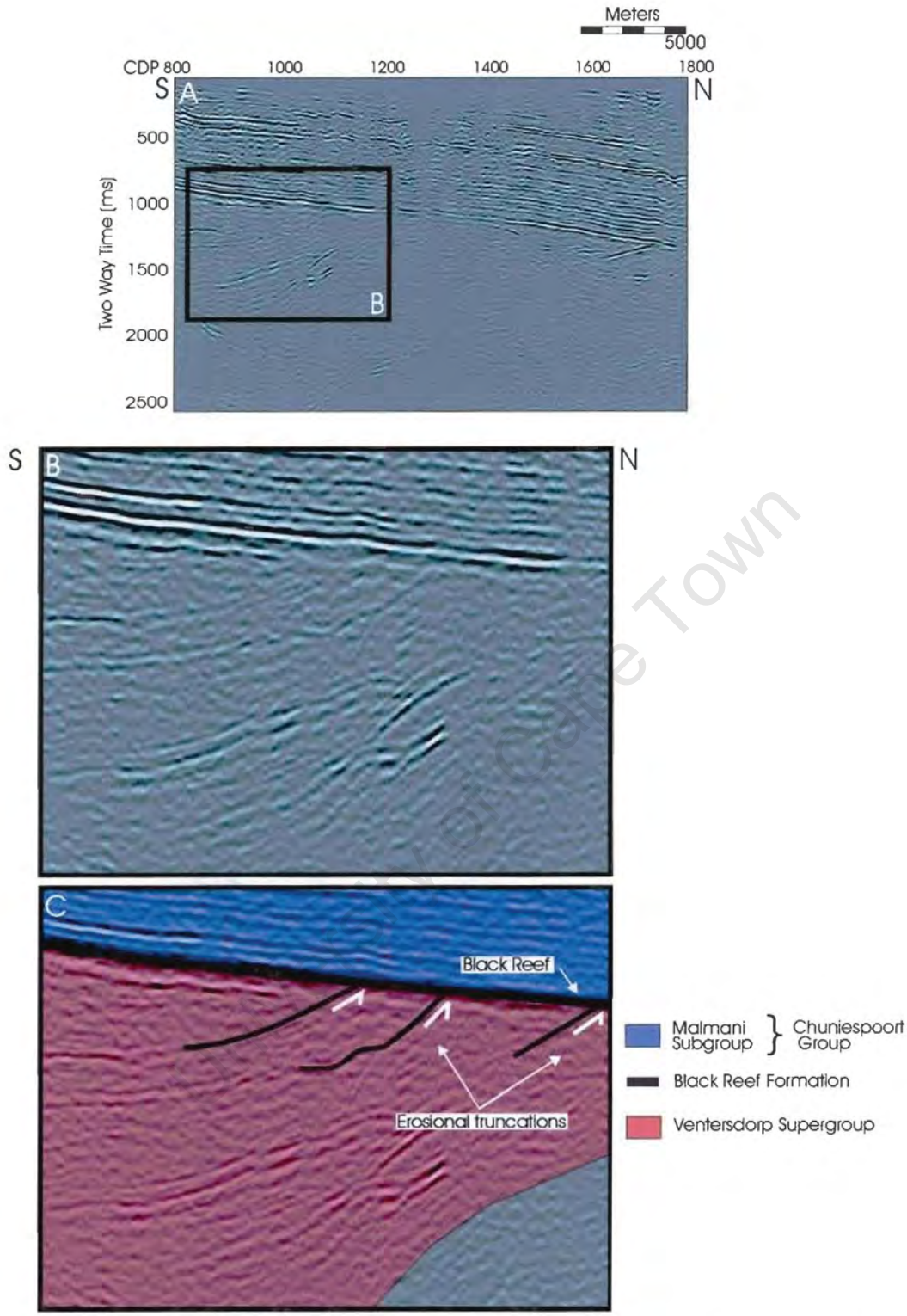

University of Cape Town

Figure 2.36: Erosional truncation of Ventersdorp reflectors by Black Reef Formation, Transvaal Supergroup (line Rz-256). Box in A is expanded: B: uninterpreted, C interpreted.

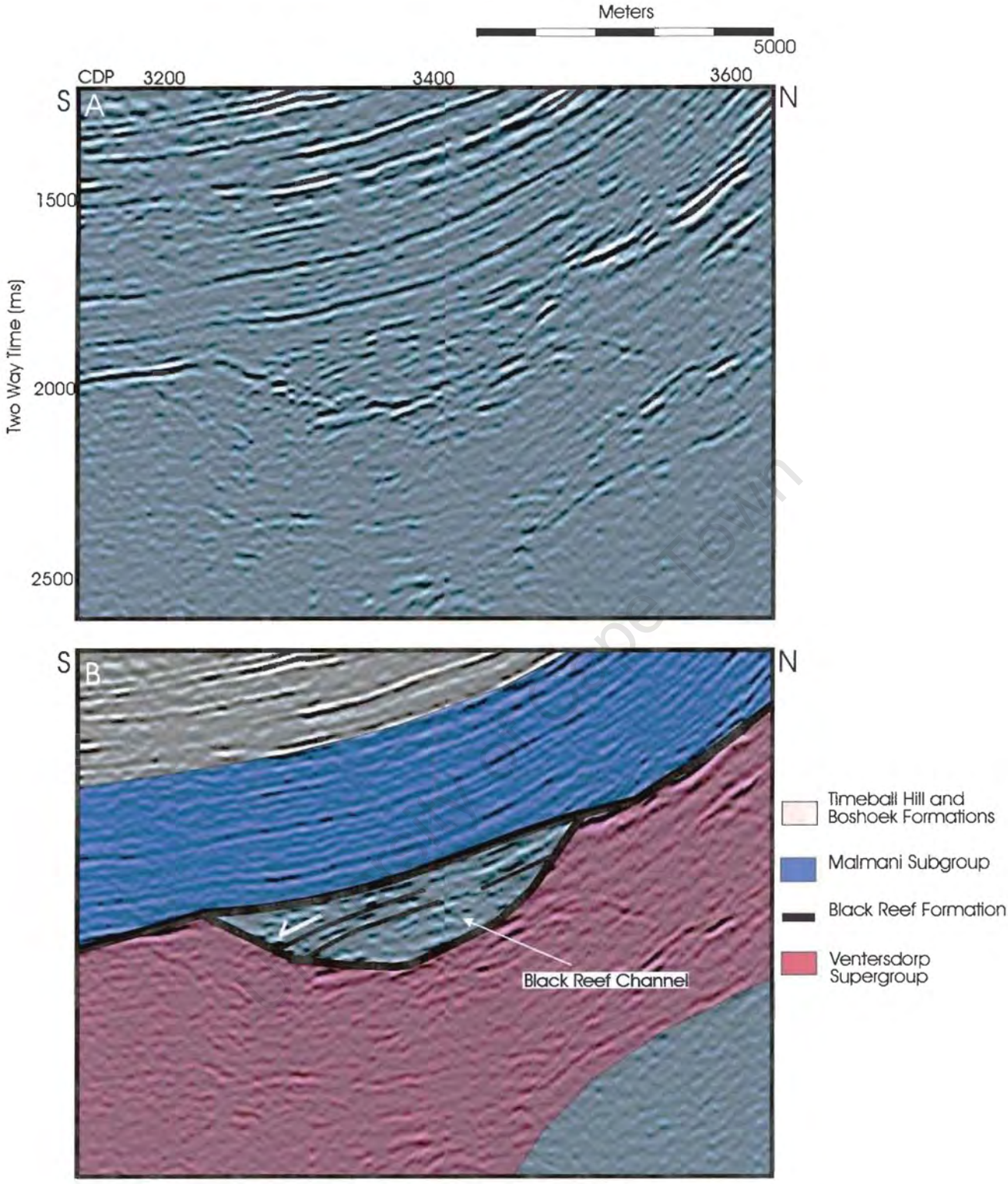

Figure 2.37: Channel in Black Reef Formation (line Rz-254). Channel fill reflectors onlap channel walls. A is uninterpreted, B interpreted.

2.3.3.II.c. Pretoria Group

A. Timeball Hill and Boshoek Formations [2263 Ma; Rb-Sr, Referenced in Eriksson *et al.*, 1993]

The onlap and downlap of reflectors (figure 2.38) within this unit suggests lateral transport of sediment and the development of sequences. Vertical and lateral lithological changes cause density, therefore impedance contrast and result in reflections. Alternatively, Bushveld-aged mafic sills may cause reflections. Apparent reflection truncations may be sills 'stepping up' through the stratigraphy.

B. Hekpoort and Dwaalheuwel Formations [2223 ± 13 Ma; Rb-Sr, Cornell *et al.*, 1996]

The transition from the Timeball Hill and Boshoek sediments to the Hekpoort andesitic lavas is marked by an increase in transparency. This lack of reflections suggests uniform lithology. The reflectivity of this unit increases from the transparent Hekpoort Formation lavas to the Dwaalheuwel Formation sediments. Again, Bushveld-aged sills may cause these reflections.

C. Strubenkop, Daspoort and Silverton Formations

These formations are grouped together due to their similar seismic character. Similarly to the Timeball Hill and Boshoek Formations, reflections onlap and downlap other reflectors within the unit. Again, this suggests lateral sediment movement and the development of sequences, or the presence of sills (figure 2.39). These reflections are the brightest of all units in both profile Rz-254 and 256, indicating that density and impedance contrasts are the greatest within these formations.

D. Magaliesberg Formation

Top reflectors of the Silverton Formation are truncated by the transparent Magaliesberg Formation above (see figure 2.40). Again, the transparency of the Magaliesberg Formation suggests a uniform composition. In line Rz-256 weak, folded reflections are noted.

University of Cape Town

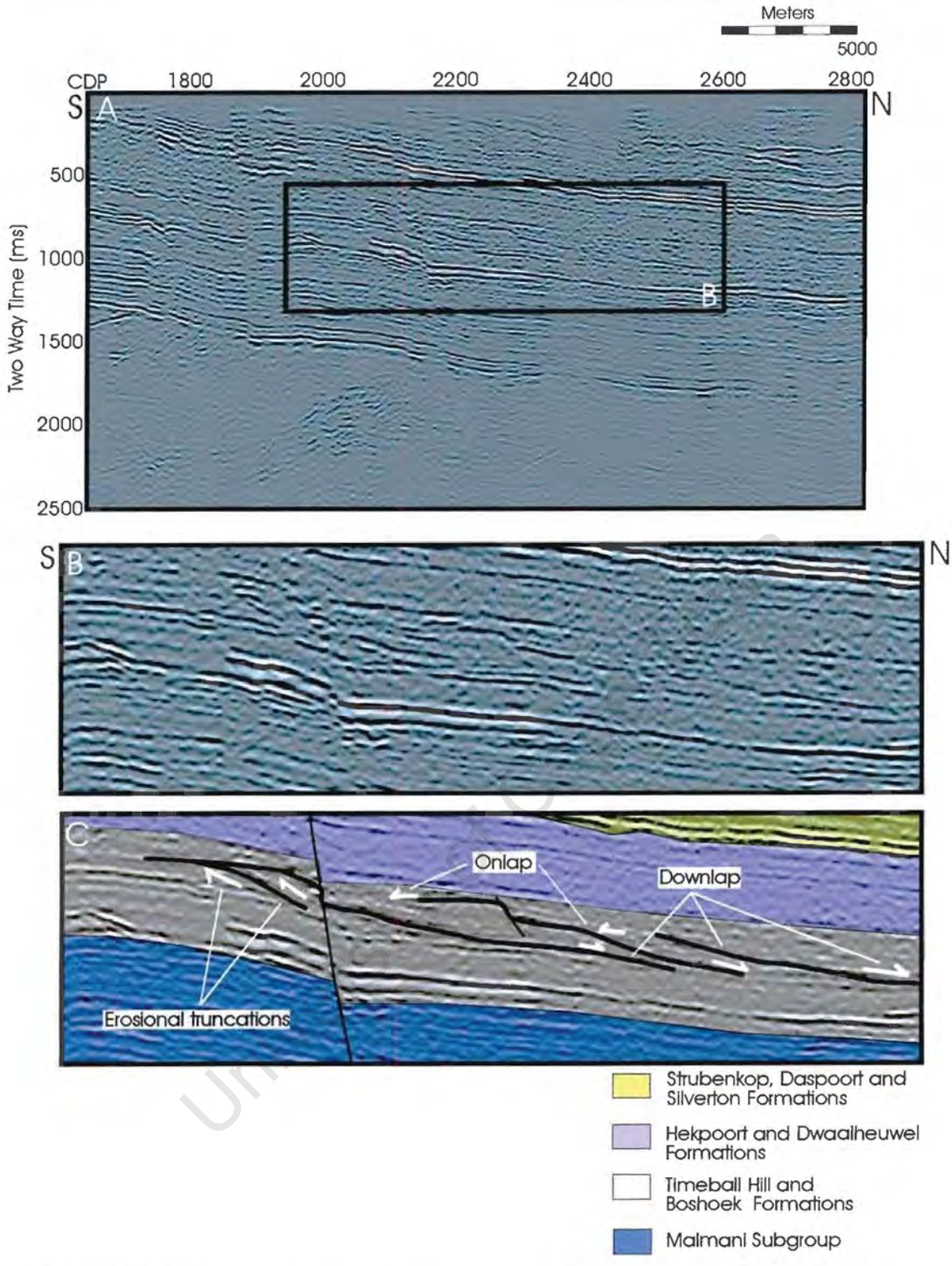

Figure 2.38: Onlap and downlap of reflectors suggesting the movement of sediment, therefore the development of sequences within the Timeball Hill and Boshoek Formations (line Rz-254). Alternatively, reflection terminations may be due to intrusive sills, of possible bushveld age, 'stepping up' through the stratigraphy. Box in A is enlarged: B is uninterpreted, C interpreted.

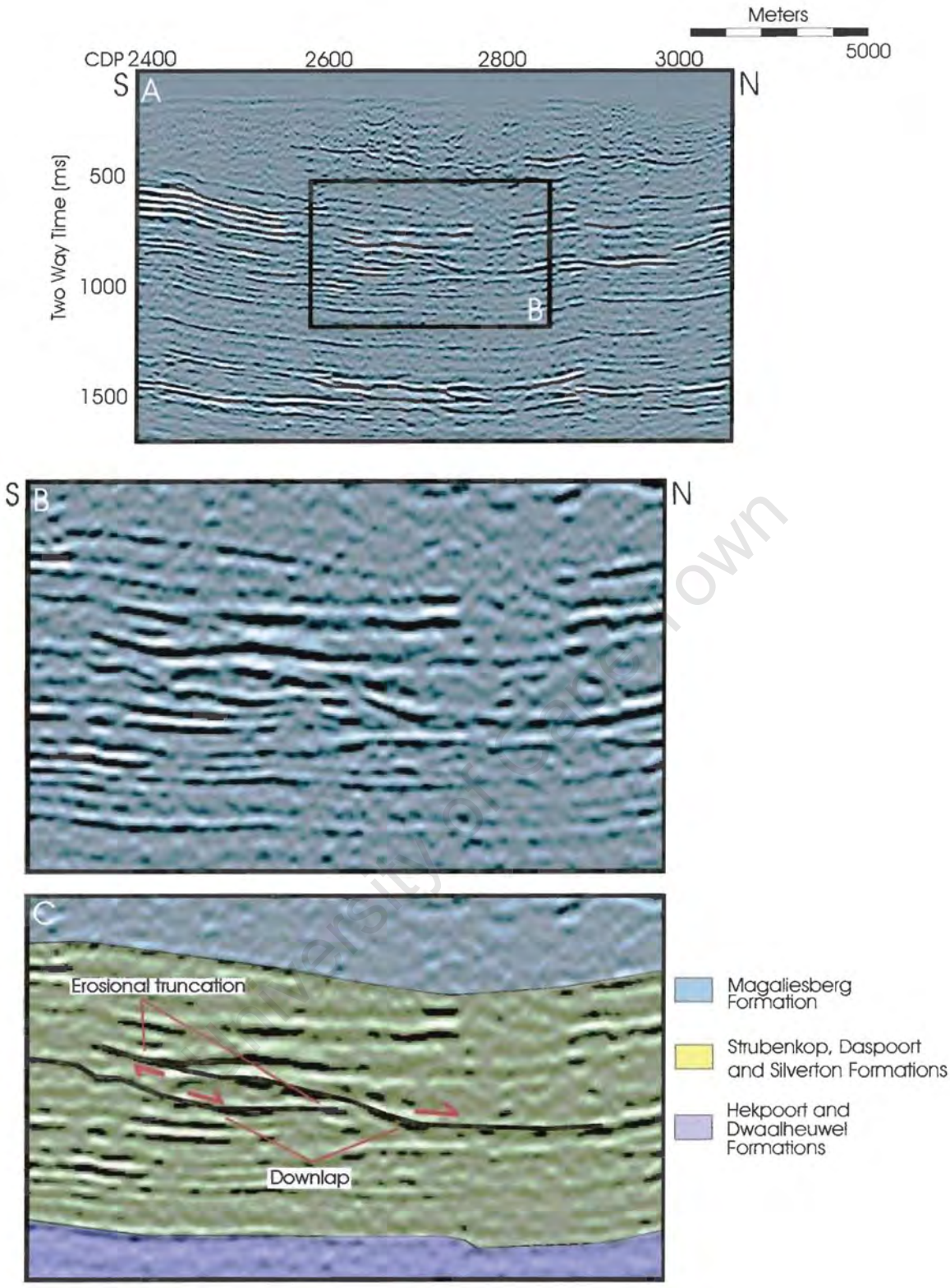

University of Cape Town

Figure 2.39: Erosional truncation and downlap of reflectors within the upper Pretoria Group sediments (line Rz-254). Box in A is enlarged: B is uninterpreted, C interpreted.

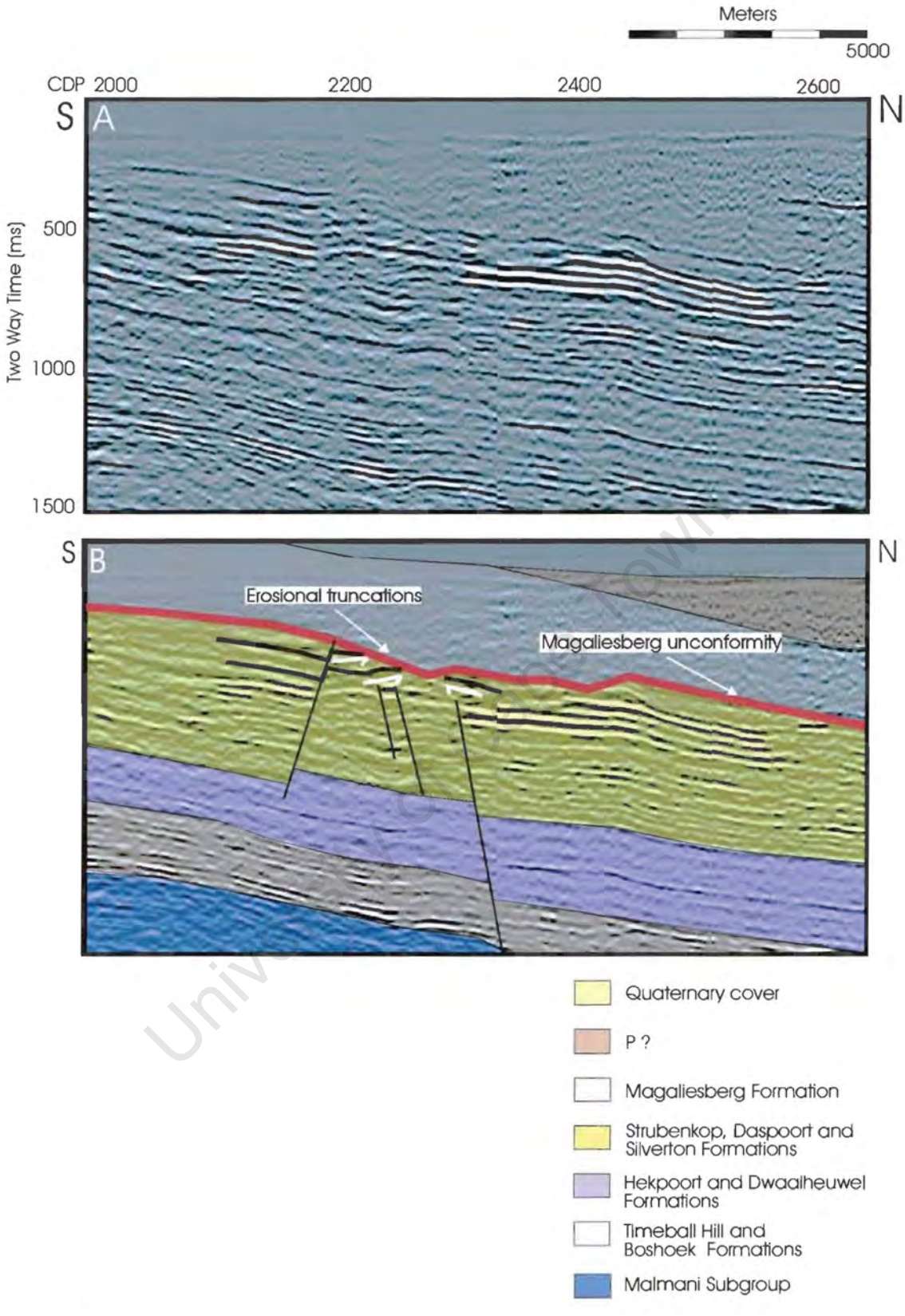

Figure 2.40: Silverton reflectors truncated by Magaliesberg Unconformity (line Rz-254). A is uninterpreted, B interpreted.

E. P? (LINE RZ-254)

A general increase in reflectivity accompanies the transition from the Magaliesberg Formation to the unit P? above. The stratigraphic name of this unit is uncertain, hence the '?' (see discussion below). Like the Magaliesberg Formation in line Rz-256, the unit's basal reflectors are folded (section 4). The upper section of P? is transparent, suggesting uniform lithology.

2.3.3.III. Quaternary Cover

A thin veneer of quaternary cover covers the hinge of the syncline.

2.3.4. Structural Observations and Tectonic Model

The following structural observations are made (oldest to youngest):

- Deposition of the Ventersdorp Supergroup is controlled by listric normal faulting. The faults, bounding half grabens, trend predominately east-west, ~ parallel to the Thabazimbi-Murchison line, and dip to the north. Minimum vertical displacement along these faults ranges from ~3 km (Rz-254) to ~6 km (Rz-256).
- Formations at the northern end of lines Rz-254 and 256 dip to the south, and those at the southern end, dip to the north. Thus both lines are structurally dominated by a large syncline.
- The syncline strikes east-west and extends over 100 km. Line Rz-255 is oriented along strike.
- The thickness of all formations involved in the folding does not change through the syncline. Therefore folding, which must postdate the youngest formation, is post Pretoria Group in age (< 2.2 Ga)
- Minor normal faulting has displaced reflectors of most formations.
- Small scale folding is present within the P? unit and Magaliesberg Formation.

Thus, the interpreted tectonic history of this area is as follows:

1) *Extension*: Ventersdorp extrusion and sediment deposition in small, discrete, predominately listric fault-bounded half grabens (2.6 Ga)

University of Cape Town

2) Deposition of Chuniespoort carbonates followed by Pretoria clastics in extensive regime as evident from numerous small-scale normal faults (2.6-2.2 Ga).

(Bushveld Igneous Intrusion- 2060 Ma)

3) *Compression*: Development of east-west striking syncline. Reflectors within Magaliesberg and P? Formation more intensely folded perhaps due to lower competency.

2.3.5. Discussion

2.3.5.I. The origin of the unit 'P?'

Thin Quaternary cover obscures older material making up the hinge of the syncline. There is thus uncertainty as to what this older material is. Two possibilities are: 1) Magaliesberg and Silverton Formations intruded by Bushveld sills, or 2) the Woodlands Formation.

Eriksson *et al.* (1998) proposed that the Woodlands Formation, which outcrops in the eastern Botswana, might continue into South Africa, under the Quaternary cover. The Woodlands Formation is suggested to form the top of the Pretoria succession. Eriksson *et al.* (1998) attributes the lack of outcrop in this area to the Woodlands Formation sediment composition, namely mudrocks and recrystallised quartzitic sandstones. Unit P? has a maximum thickness in line Rz-254 of 500 ms (~1000 m, estimated P wave velocity of 4000 m/s). This thickness is comparable to that estimated by Key (1983) of 1200 m, but much thicker than the 100 m suggested by Eriksson *et al.* (1998).

From seismic evidence a distinctive change in reflection character between the transparent underlying Magaliesberg quartzites and the more reflective P? is apparent. This increase in reflectivity may be attributed to the intrusion of Bushveld sills, which outcrop in this area. Without borehole control, it is difficult to distinguish between the first possibility and the second.

University of Cape Town

2.4. The Craton Interior

2.4.1. Seismic Profiles OB (A and B) and AG

2.4.1.I. Introduction

The 'Karoo lines' are located in the Free State, south west of the Vredefort dome and at the northern extent of the great Karoo basin (figure 2.41). OB-A trends roughly NNE-SSW and extends as line OB-B to the SSE. Together they are around 85 km in length. Line AG trends NW-SE for 40km and intersects line OB-A near the town of Viljoenskroon. The Timeball Hill, Boshoek and Hekpoort Formations (Pretoria Group), Ecca Group and the Beaufort Group (Karoo Sequence), and post-Karoo, dolerite intrusions outcrop.

2.4.1.II. Description (figure 2.42 and 2.43)

The basement/ sediment interface is judged as the first appearance of semi-continuous reflections. This interface is irregular, thus has not been marked in figures 2.42 and 2.43. Unit **W + D** is composed of medium to high amplitude reflections and has a maximum thickness of 2.5 s TWT or ~7.2 km (P wave velocity of West Rand Group is 5748 m/s). Reflectors within this group are discontinuous.

Above this reflective unit is a transparent section **CRG** which is cut roughly in half by a high amplitude reflector couplet, **B**. Topping this transparent section in some places, is a high amplitude, continuous reflection. The unit $\mathbf{V_k}$, above is transparent and is also capped by a laterally continuous reflector.

Large-scale normal faults have displaced all units described thus far. Displacement along these faults varies (see section 2.4.1.IV.). The result of these normal faults is a series of horsts and grabens into which, for example line AG, CDP 1300 to 1600, a mostly transparent to weakly reflective unit $\mathbf{V_p}$ has been deposited. This infilling unit has a maximum thickness of 700 ms TWT or ~2040 m (P wave velocity of 5827 m/s).

University of Cape Town

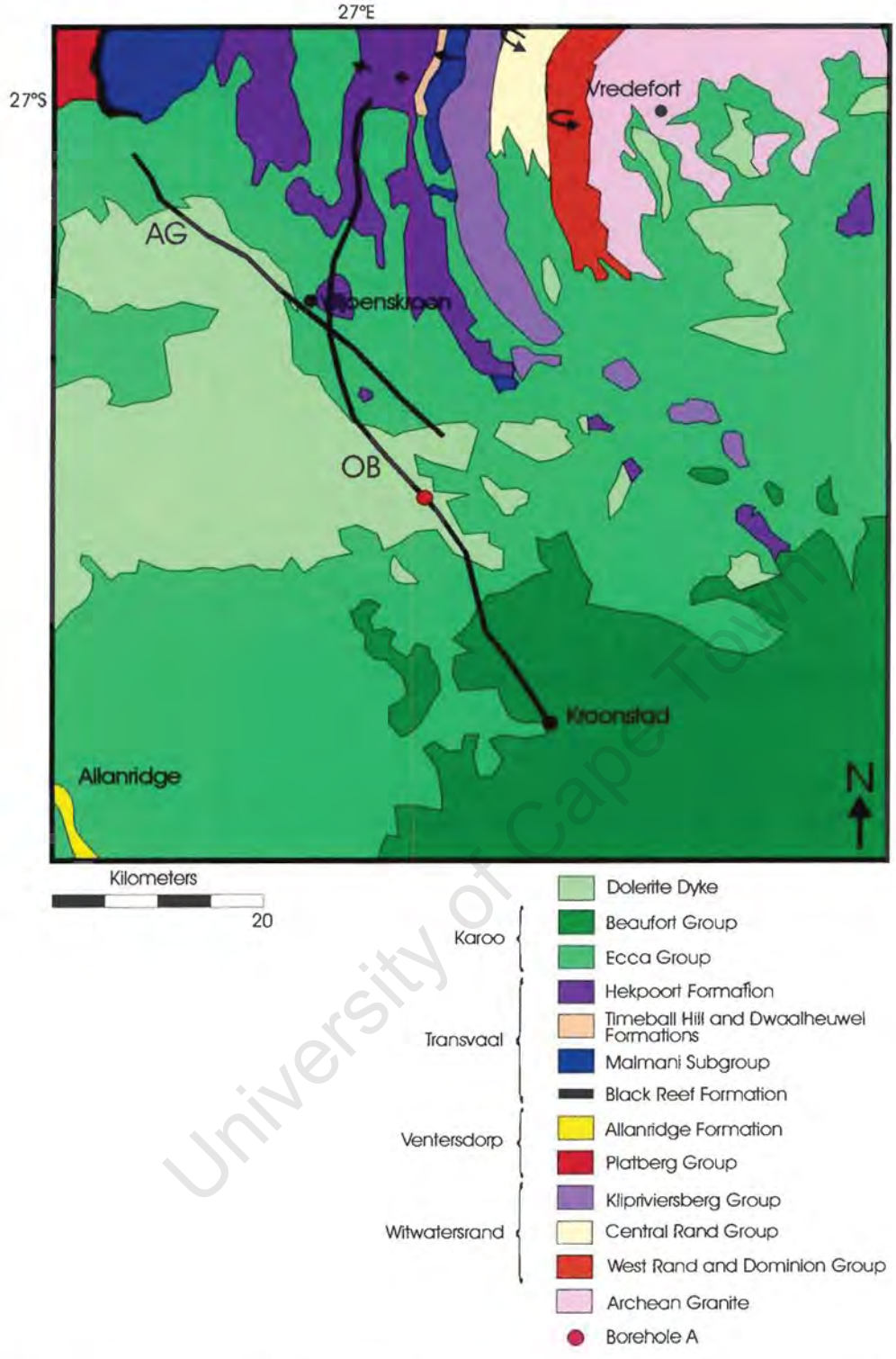

University of Cape Town

Figure 2.41: Geological map of the Bothaville/ Vredefort area showing location of the Karoo lines, OB and AG. (Geology simplified from Geological Sheet of Bothaville/ Vredefort (2726B/ 2727A), 1962 and Geological Map of South Africa, Transkei, Bophuthatswana, Venda and Ciskei and the Kingdoms of Lesotho and Swaziland. 1: 1 000 000, 1984).

The basal reflector of the successive unit $\mathbf{V_{pn}}$, truncates the underlying $\mathbf{V_p}$, $\mathbf{V_k}$ and **CRG** units. $\mathbf{V_{pn}}$ is composed of medium amplitude, semi-continuous reflectors. It is variable in thickness up to 250 ms or ~770 m (P wave velocity of 6159 m/s).

A continuous reflector, **Br**, is distinctive on all three lines and truncates the units below. This second unconformity is the base of $\mathbf{C_m}$ which is uniformly 500 ms or ~1700 m thick (P wave velocity of 6834 m/s). $\mathbf{C_m}$ is mostly transparent, though weak continuous reflections do occur.

$\mathbf{P_t}$ succeeds $\mathbf{C_m}$. It is distinctive on the seismic line due to its high amplitude, continuous reflectors. The unit $\mathbf{P_h}$ above is characteristically transparent and outcrops between CDP 2300 and 2500 and north east of CDP 2800 in line OB, and between CDP 550 and 800 in line AG. It is up to 300 ms or ~900 m thick (P wave velocity of 6083 m/s). $\mathbf{P_h}$, $\mathbf{P_t}$, and $\mathbf{C_m}$ have been folded resulting in undulations of approximately 700 CDP's or ~17.5 km in wavelength.

$\mathbf{K_e}$, a transparent unit, follows a weak continuous reflection that truncates reflectors of the units below. It outcrops on both lines. On line OB, units $\mathbf{K_e}$, $\mathbf{P_h}$, $\mathbf{P_t}$, $\mathbf{C_m}$ and $\mathbf{V_{pn}}$ are truncated by a high amplitude, continuous basal reflector of unit $\mathbf{K_b}$. This is a transparent unit and outcrops south east of CDP 800 on line OB only.

2.4.1.III. Stratigraphic Interpretation (Figure 2.44 and 2.45)

This interpretation is based upon borehole and outcrop data along with an applied knowledge of the reflection characteristics of the various groups from published interpreted profiles (Pretorius *et al.*, 1987) and those presented in this thesis. A three-dimensional view of seismic profiles OB and AG is included as figure 2.46.

Borehole A is located along line OB. Figure 2.47 shows the various lithologies that the borehole intersects along with an interpretation of their stratigraphic position. The borehole has been drilled through a horst block bordered to the SE and NW by large-scale normal faults possibly extending to a depth of to 3.5 s TWT or 10 km. Thus the borehole intersects the Central Rand Group, Witwatersrand Supergroup at a relatively shallow depth of around 0.7s TWT (from profile) or 2.53km (from borehole).

University of Cape Town

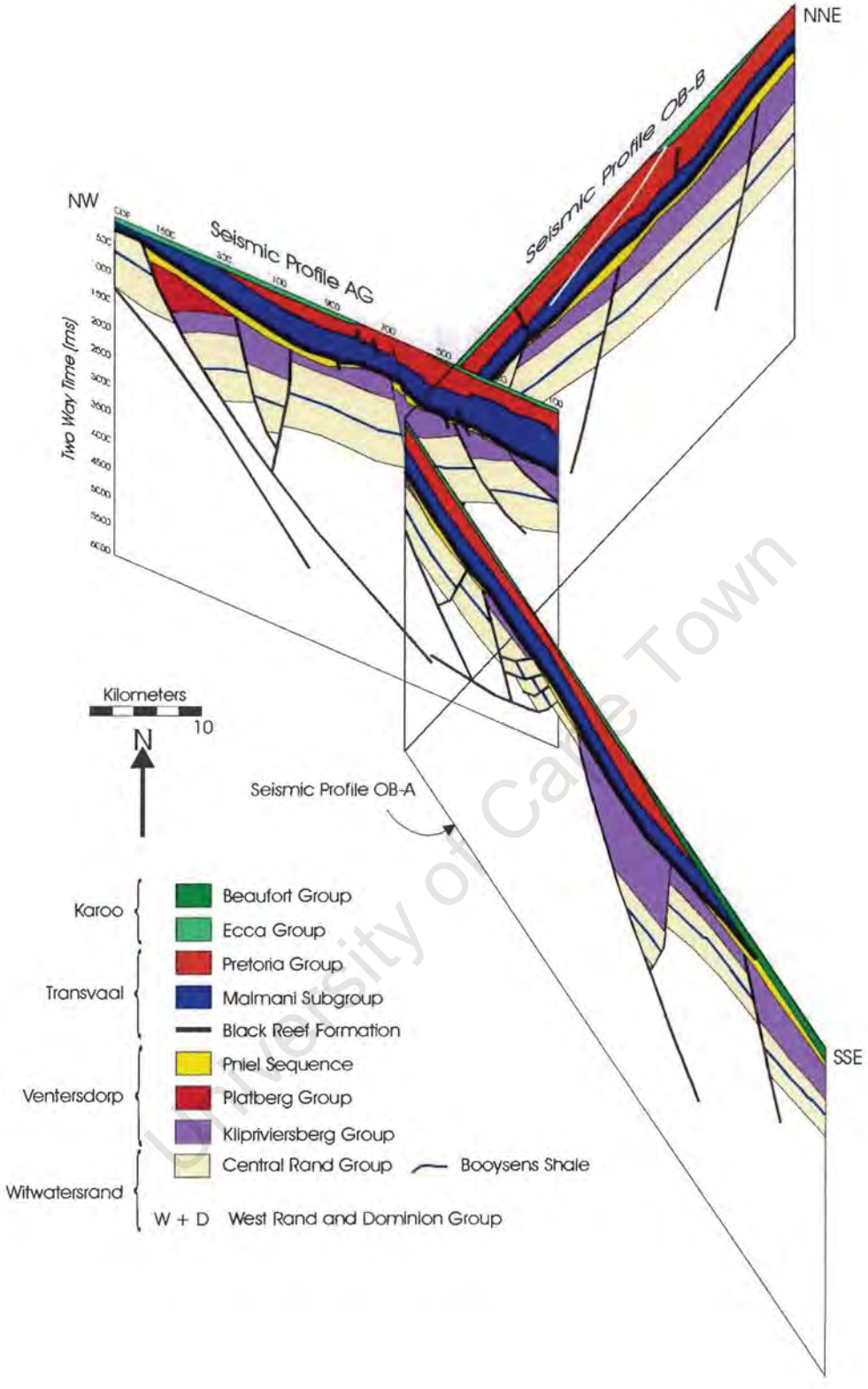

University of Cape Town

Figure 2.46: Three dimensional view of the craton interior lines, OB-A and B and AG. Normal faults trend east/west to north east/south west but dip to the south.

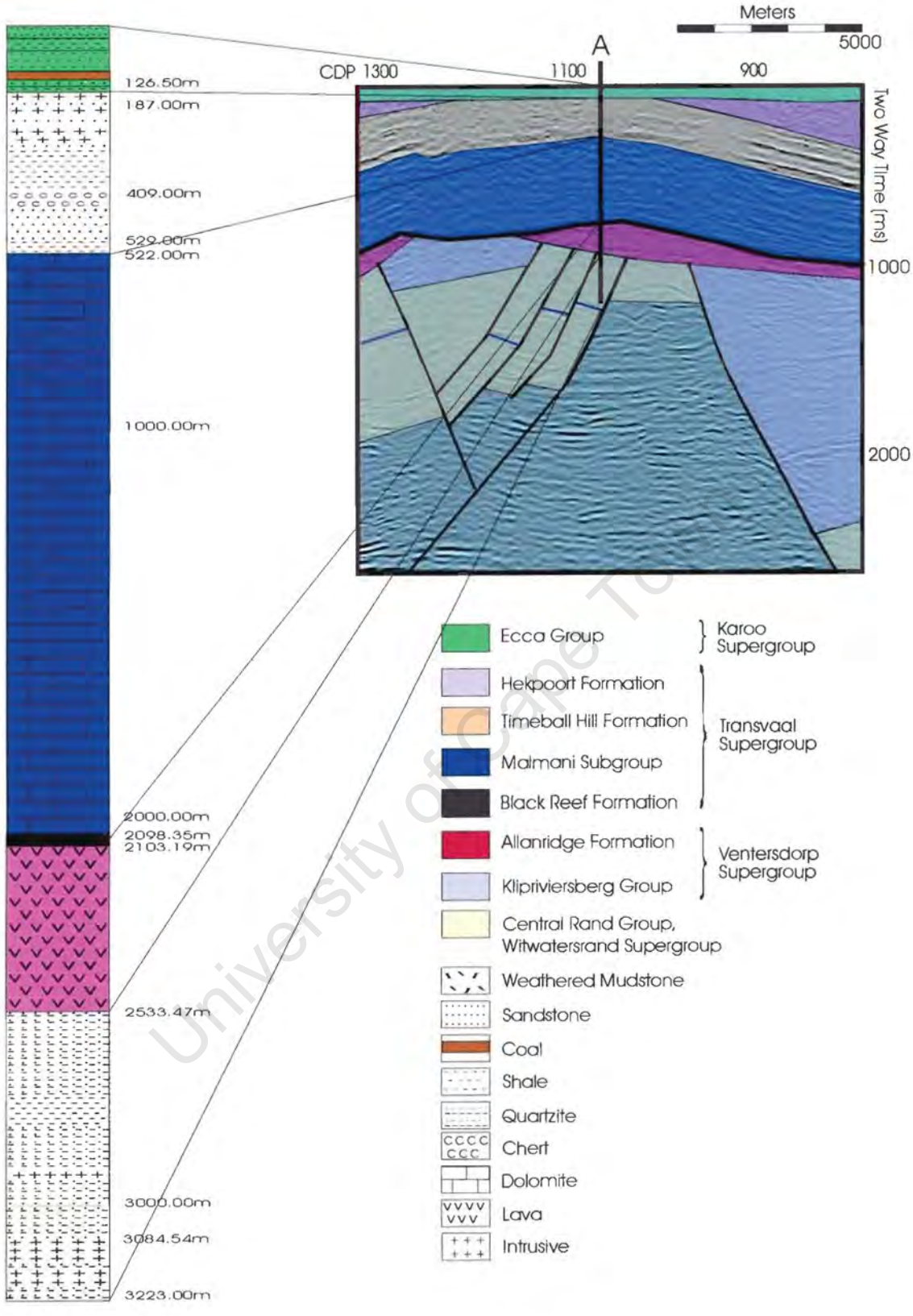

Figure 2.47: A comparison of borehole A to seismic interpretation of line OB.

The stratigraphic interpretation of lines OB and AG is in chronological order, from the oldest groups to the youngest. The sediment/basement interface varies in depth below surface due to displacement by numerous faults. The relative age of this faulting will be discussed later in section 2.4.1.IV.

2.4.1.III.a. The West Rand and Dominion Groups (W+D)

The West Rand and Dominion Groups are characterised by continuous to discontinuous, high amplitude reflections. The lack of continuity of reflectors may be due to numerous small-scale faults. Like the underlying granitic basement, the West Rand and Dominion Group interval has been displaced by numerous large-scale normal faults and therefore is situated at variable depths.

2.4.1.III.b. The Central Rand Group (CRG)

The transition from West Rand Group to Central Rand Group is marked by a change in reflection character. The Central Rand Group is acoustically transparent, indicating lack of impedance contrast. Its total thickness varies between around 600 ms (~1700 m) to 1000 ms (~2800 m) TWT (P wave velocity of 5779 m/s). Through the centre of this interval is a strongly reflective couplet interpreted to represent the Booysens shale (B).

2.4.1.III.c. The Ventersdorp Supergroup (V_k, V_p, V_{pn})

Like the Central Rand Group below, the Klipriviersberg Group (V_k) is semi-transparent though in some places, particularly along line AG, low amplitude fairly continuous reflections do occur. Large-scale listric and normal faults have displaced all units described thus far.

The Platberg Group, V_p, is distinguished from the older, transparent, Klipriviersberg Group below by its weak reflectors. This implies that the group's composition is not as uniform as that of the Klipriviersberg Group. The Platberg Group is only present in one location along line AG. It forms a wedge of sediment, between CDP 1300 and 1600, that thickens into a bounding listric fault. The Platberg Group, in this example, is filling in accommodation space adjacent to a listric normal fault. The movement

University of Cape Town

along this bounding fault was probably incremental, causing the Platberg reflectors to 'fan out'. Figure 2.48 calculates the minimum throw along this fault. The relative age of this block faulting can be estimated as post-Klipriviersberg, thus < 2714 ± 8 Ma (U-Pb, Armstrong *et al.*, 1991) and syn-Platberg deposition. The relative age of Ventersdorp faulting is consistent with that observed from the Rz seismic profiles (syn-Platberg, pre-Black Reef).

The basal reflector of the successive Pniel Sequence (V_{pn}) above truncates the underlying Platberg, Klipriviersberg and Central Rand Groups. Thus an erosional unconformity separates the Pniel Sequence from the older strata below (figure 2.49). Borehole A (figure 2.47) intersects only the Allanridge andesites (Pniel Sequence) of the Ventersdorp Supergroup. As figure 2.47 shows, the borehole was drilled through the top of a horst block, thus it is likely that the older Klipriviersberg Group was eroded from this uplifted area, prior to the extrusion of the Allanridge andesites of the younger, Pniel Sequence.

2.4.1.III.d. The Transvaal Supergroup (Br, C_m, P_b, P_h)

A. THE BLACK REEF FORMATION [2642 ± 3 MA; Age for correlative Vryburg Formation, U-Pb, Beukes, pers. comm, 2001]

The Black Reef Formation forms the base of the Transvaal Sequence and is correlated to the Vryburg Formation, Griqualand West Sequence. Borehole A intersects it at a depth of 2098.35m where it is only 5 m thick. Even though the Black Reef Formation is a very thin unit in this area, it appears as a high amplitude, continuous reflector on both seismic lines. The reflector marks an erosional unconformity, as shown by its truncation of the older units below (figure 2.50).

B. CHUNIESPOORT SUBGROUP

Malmani Subgroup [2583 ± 5 Ma; U-Pb, Martin *et al.*, 1998]

Above the Black Reef is a 1500 to 1700 m succession of Malmani dolomite. The reflection character of the Malmani Subgroup is predominately transparent, thus implying a fairly even composition. Occasional reflections within this unit may be

University of Cape Town

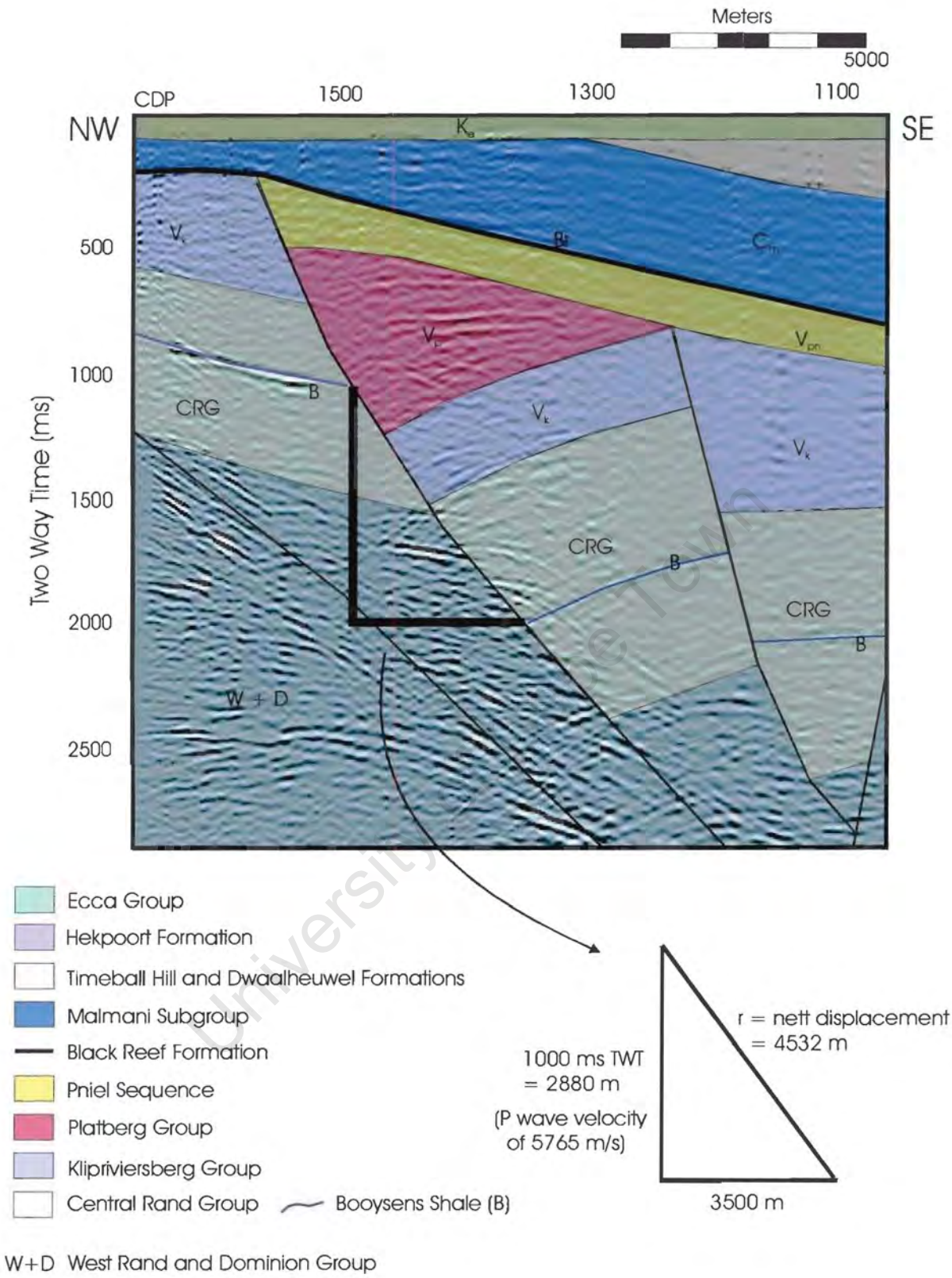

Figure 2.48: Calculation of throw along listric normal fault, line AG. Booysens shale marker reflector is displacement relatively downward to the south east by ~4532 m.

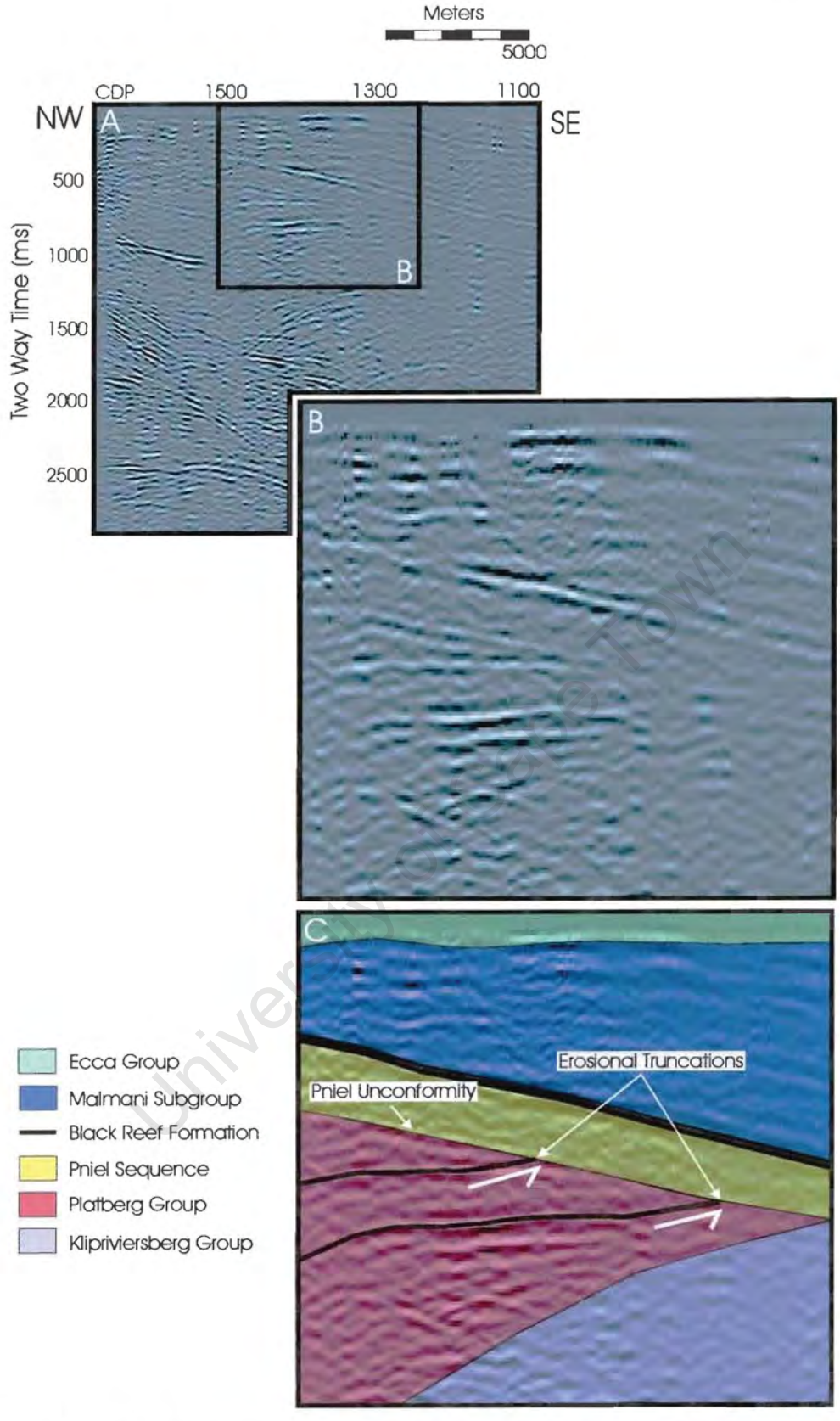

University of Cape Town

Figure 2.49: Basal Pniel reflector truncates Platberg reflectors below (line AG). Box in A is expanded: B is uninterpreted, C interpreted.

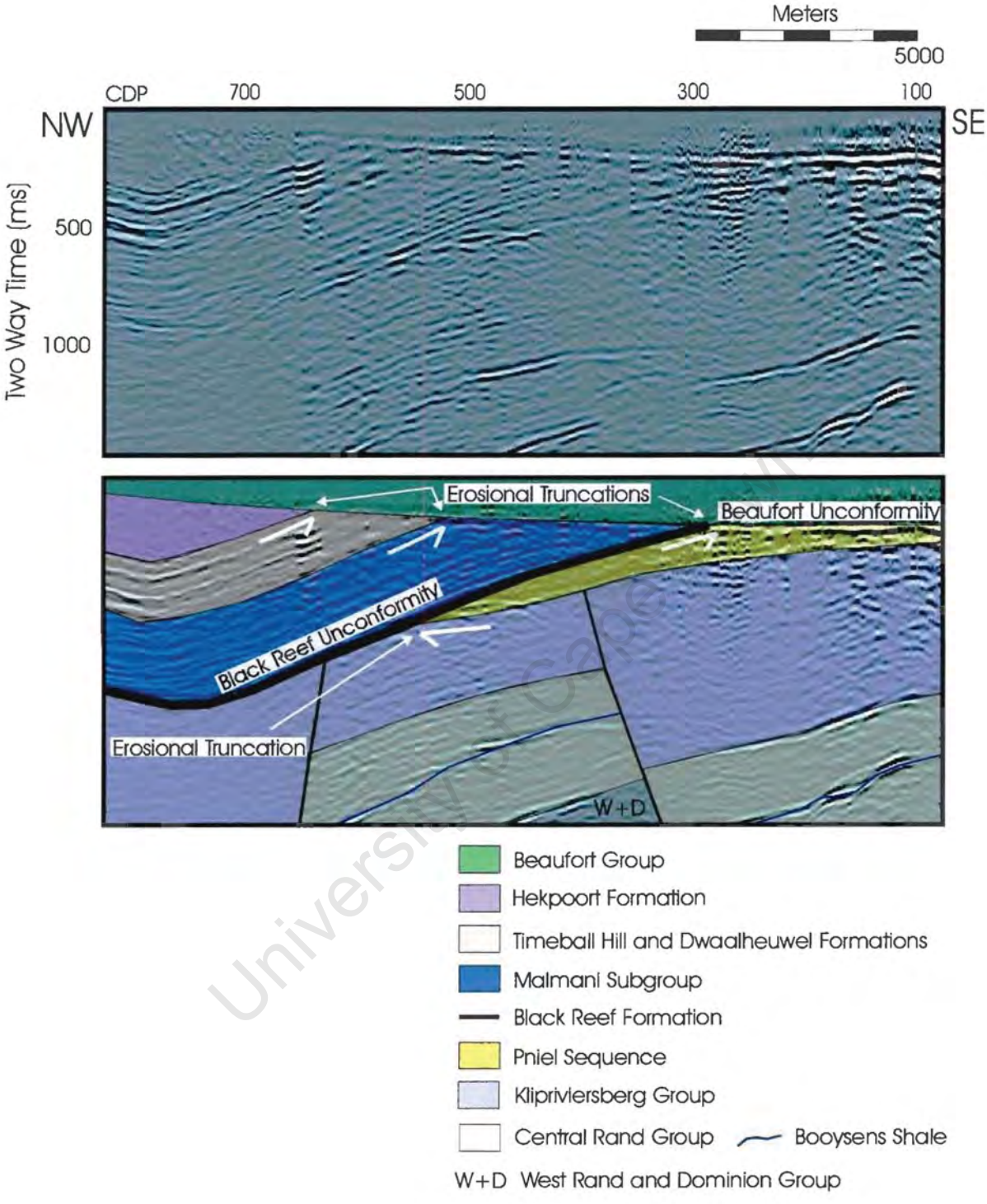

Figure 2.50: The Black Reef and Beaufort Unconformities (line OB). A is uninterpreted, B interpreted.

caused by changes in carbonate facies, from shallow water carbonate, to deeper water laminated carbonate interbedded with chert and shale.

C. THE PRETORIA GROUP (P_T, P_H)

Timeball Hill and Boshoek Formations (P_t) [2263 Ma; Rb-Sr, Referenced in Eriksson *et al.*, 1993]

The Pretoria Group sediments of the Timeball Hill and Boshoek Formations, succeed the Malmani dolomites. The high amplitude reflection marking this transition is indicative of a large impedance contrast between the Malmani dolomites and the sediments above. The high amplitude, continuous reflections within this group may result from changing lithologies within this group. This interpretation is supported by borehole A, which shows rapid changes from shales to sandstones to chert (figure 2.47). Three separate intrusions into this unit which were intersected by borehole A, may also have given rise to its high reflectivity.

Hekpoort Formation (P_h) [2223 ± 13 Ma; Rb-Sr, Cornell *et al.*, 1996]

The transition from the sediments of the Timeball Hill Formation below, to the Hekpoort andesites is marked by a decrease in reflectivity. This may indicate a greater uniformity in composition of the Hekpoort Formation.

The Pretoria Group, Chuniespoort Subgroup and Pniel Sequence have been gently folded into long wave undulations seen on both seismic profiles (see section 2.4.1.IV).

2.4.1.III.e. The Karoo Supergroup

A. THE ECCA GROUP

A thin veneer of the Ecca Group overlies the Pretoria Group. The Ecca Group is composed of shale, coal, quartzite and mudstone (deduced from borehole and outcrop information). In all three lines the Ecca Group appears as a transparent unit up to 250 ms TWT or ~400 m thick (P wave velocity of 3195 m/s). Although the Ecca Group appears transparent in the seismic section, a reflector marks the contact between it and the underlying Pretoria Group. The erosional truncation of older reflectors by this reflector shows that there is an unconformity between these two Groups. The hiatus represented by this unconformity is approximately 2 Ga.

University of Cape Town

B. The Beaufort Group

A very high amplitude reflection marks the base of the Beaufort Group that outcrops at the SE extent of line OB. This reflector is a prominent unconformity truncating the Ecca, Pretoria and Malmani Groups below (figure 2.50). Like the Ecca, the Beaufort group is mostly transparent. A maximum thickness of the Beaufort group is around 200 ms TWT or 319 m (P wave velocity of 3195 m/s).

2.4.1.IV. Tectonic Model

The following structural observations are made (oldest to youngest):

- Numerous small-scale faults have displaced the West Rand and Dominion Group.
- Large-scale block faulting of the granitic basement, Dominion, West and Central Rand and Klipriviersberg Groups has resulted in horst and grabens.
- The Pniel unconformity truncates strata below. Its development may be associated with the degradation of the horsts, and the peneplanation of the landscape (see section 2.4.1.V).
- The successive Transvaal strata are displaced by normal and reverse faults (figure 2.51).
- The Transvaal Supergroup has been folded. Fold axes trend approximately east/west.
- The Ecca and Beaufort Groups truncate underlying strata.

The tectonic and depositional history of this area is interpreted as follows (oldest to youngest):

1) *Deformation* of the West Rand and Dominion Groups
2) *Deposition* of the Central Rand and Klipriviersberg Groups
3) *Extension*: Block faulting of all units with synchronous deposition of infilling Platberg Group.
4) *Uplift and erosion* of horsts and levelling of land surface.
5) *Extrusion* of Allanridge andesites.
6) *Uplift and erosion*: development of Black Reef Unconformity
7) *Deposition* of the Transvaal Supergroup

University of Cape Town

8) *Folding*: north-south directed compression *
9) *Faulting*: both normal and reverse (see figure 2.51).
10) *Uplift and erosion*: development of Ecca unconformity
11) *Deposition* of Ecca Group
12) *Uplift and erosion*: development of Beaufort unconformity
13) *Deposition* of (terrestrial) Beaufort Group.

* This direction of compression is only a rough estimate due to the two dimensional nature of the profile. Folding occurred post Hekpoort extrusion (< 2223 ± 13 Ma, Rb-Sr, Cornell *et al.*, 1996) and pre Karoo (300 Ma).

2.4.1.V. Discussion

2.4.1.V.a. The Welkom Gold Field

Buck's study of the Welkom gold field area (1980) reveals several similarities to the area seismically imaged in this study. He, too, documents the degradation of horst blocks and accompanying infilling of sediments of the Klippan Formation, Platberg Group (figure 2.52). The De Bron and Arrarat faults in figure 2.52 have the same relative age to those of lines AG and OB. Faulting post dates deposition of the Klipriviersberg and is synchronous with the deposition of the Platberg Group. The De Bron horst in this case is degraded, providing infilling Platberg material.

The Bothaville sediments are suggested to have accumulated on a broad fluvial-plain after being transported and deposited by braided streams (Buck, 1980). Thus perhaps they never fully covered the degraded horsts. This could be the reason for the absence of the Bothaville Formation in borehole A, drilled into the top of a horst. This non-deposition of the Bothaville Formation is shown in plan for the Welkom gold field area in figure 2.53 (Buck, 1980).

University of Cape Town

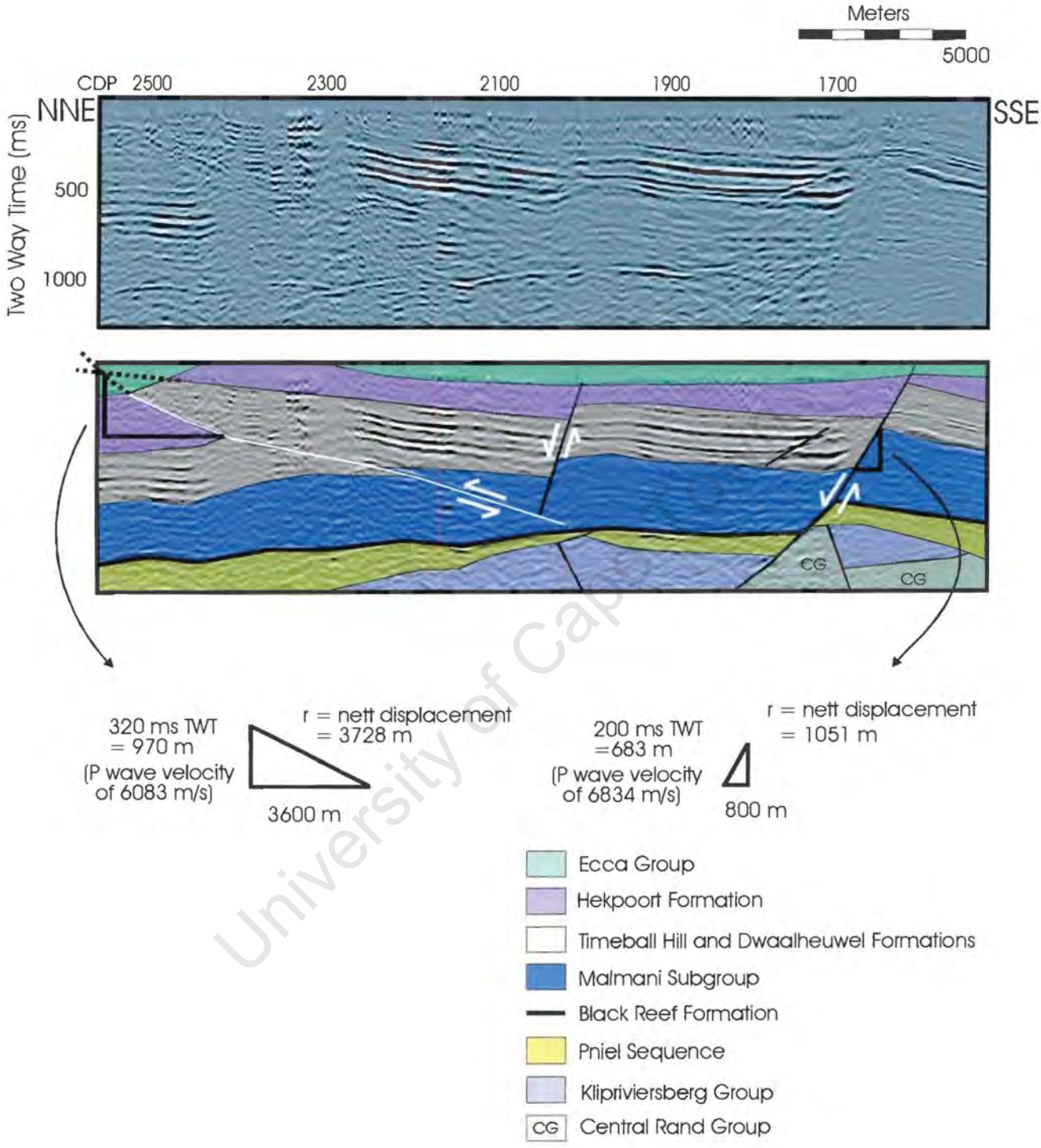

University of Cape Town

Figure 2.51: Calculation of throw along normal and reverse faults, which displace the Transvaal Supergroup (line OB). Thrust is marked in white, normal faults in black. A is uninterpreted, B interpreted.

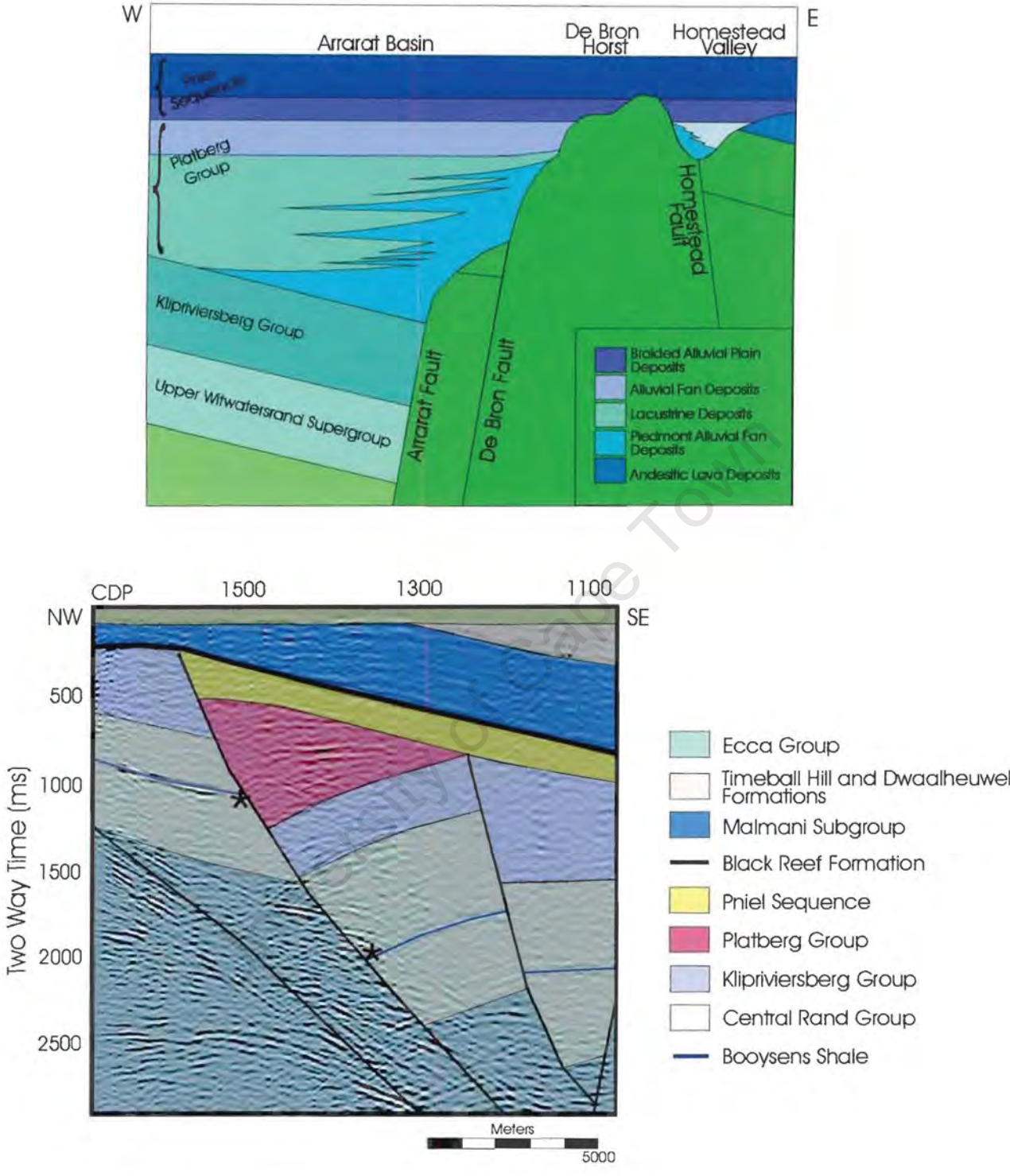

Figure 2.52: Schematic section through the De Bron Horst, Welkom Gold Field (after Buck, 1980) and a comparison to the seismic section AG. The Booysens shale has been displaced ~4532 m down to the south east (calculated in figure 2.48).

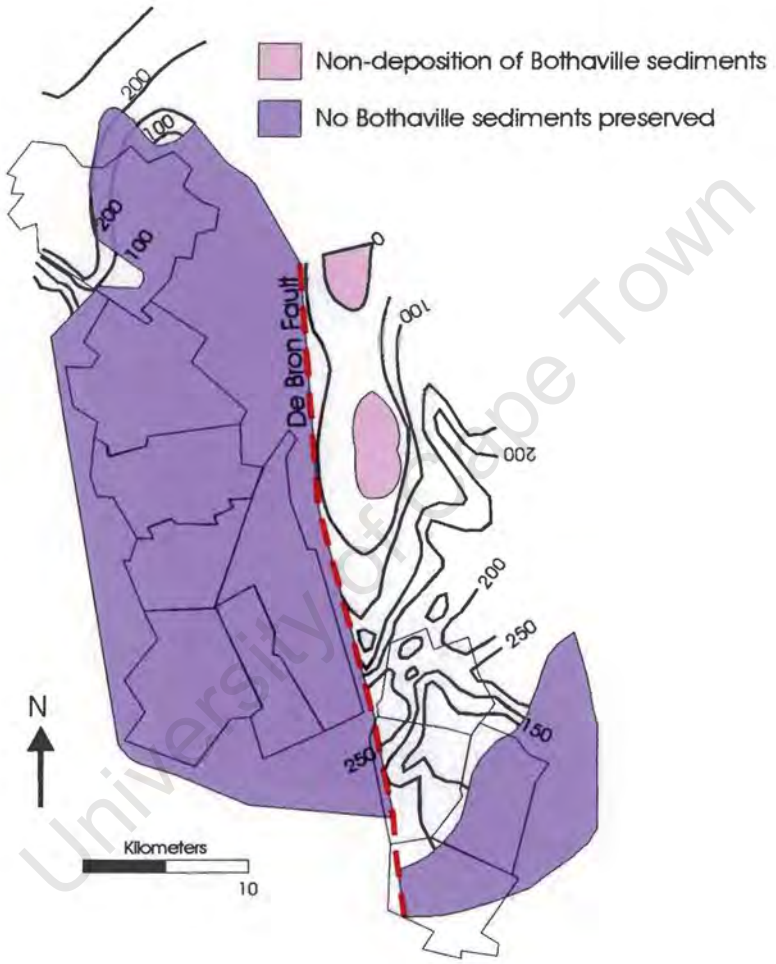

University of Cape Town

Figure 2.53: Topographic elements and isopach plan of the Bothaville Formation (after Buck, 1980). Lines OB and AG lie 100 km to the north west.

2.4.2. Seismic Profile YS

2.4.2.I. Introduction

Line YS, approximately 65 km long, trends NW/SE in the North West Province (figure 2.54). The processed, uninterpreted profile is included as figure 2.55.

Archean granitic basement, Dominion Group sediments and volcanics, West Rand Group, Hospital Hill quartzites and Government shales, Ventersdorp Platberg sediments, and Bothaville gravels (Pniel Sequence) outcrop in this area. The geological map of the area (figure 2.54) shows younger Platberg sediments juxtaposed against older Archean basement rock in the NW and SE near Hartebeesfontein. Likewise in the southeast, the Witwatersrand Supergroup outcrops adjacent to the Archean basement. The young Platberg sediments reappear at the southeastern extent of line YS.

2.4.2.II. Description (figure 2.55)

The basement is mostly transparent though occasional strong, high-amplitude reflections do occur. The basement outcrops north west of CDP 700 and between CDP 2250 and 2350.

Bordering basement outcrop are reflections of different acoustic character. Between CDP 700 and 1000 a thin veneer of unit $\mathbf{V_k}$ and $\mathbf{V_p}$ covers the Archean basement. Unit $\mathbf{V_p}$, is composed of continuous reflections with variable amplitude and extends laterally 38 km to the south east. These reflections dip towards a large listric fault marked F. The reflections are rotated towards the horizontal with decreasing depth below surface.

Outcrop observations show that the contact between the unit **W + D** and the basement occurs around CDP 2400. This contact is seismically very poorly resolved. Further to the southeast, however, there is a clear transition to a unit of higher reflectivity, marked **W + D**. Reflections are parallel and have been displaced by two normal faults, dipping to the southeast.

University of Cape Town

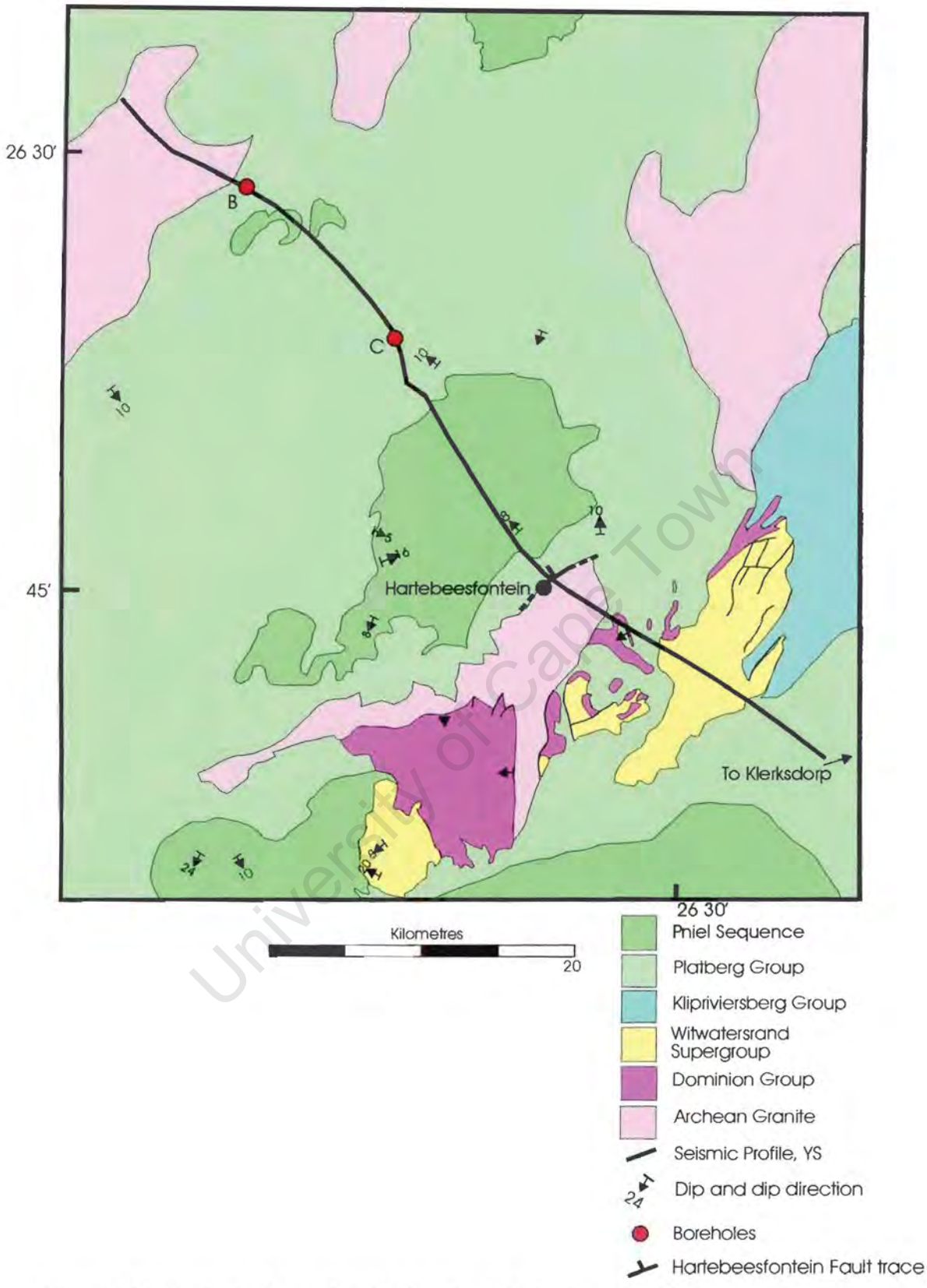

University of Cape Town

Figure 2.54: Geological map showing location of seismic profile YS (geology simplified from Geological Sheet of West Rand (2626), 1986).

Unit $\mathbf{V_p}$ reappears at this southeastern extent of the profile. Its basal reflector truncates the underlying **W + D** unit. The medium amplitude reflections within unit $\mathbf{V_p}$ unit, southeast of CDP 2700, are unlike those towards the centre of the profile, in that they are discontinuous.

Unit $\mathbf{V_{pn}}$ outcrops twice along seismic profile YS (figure 2.54), however, it can only be isolated on the seismic profile between CDP 1700 and 1950. The contact between $\mathbf{V_p}$ and $\mathbf{V_{pn}}$ is a weak reflector and unit $\mathbf{V_{pn}}$ above is transparent.

2.4.2.III. Stratigraphic Interpretation (figure 2.56)

Stratigraphic interpretation has relied heavily on borehole (figure 2.57) and outcrop (figure 2.54) information.

2.4.2.III.a. Boreholes A and B (figure 2.57)

An 800m thick succession of Alberton and Loraine lavas of the Klipriviersberg Group deposited on granitic basement were encountered in borehole B (figure 2.57). These are succeeded by ~ 250 m of Rietgat lava, Platberg Group.

Further to the southeast, borehole C was drilled. Depth of hole is over 1800 m, of which 1462 m is through the Platberg Group. The Klipriviersberg Group is absent from this location, either due to its non-deposition or its erosion prior to Platberg deposition. The lower-most Platberg formation, the Kameeldoorns Formation is separated by granitic basement below by a 300 m intrusive sill. The Goedenoeg, Makwassie and Rietgat Formations succeed the Kameeldoorns Formation.

2.4.2.III.b. West Rand and Dominion Groups (W + D) [3060 ± 2 Ma; detrital zircons in the West Rand Group, U-Pb, Robb *et al.*, 1990]

On the stratigraphic interpretation (figure 2.56), the Witwatersrand Supergroup and Dominion Group have been collectively marked with a W + D. The contact between these two groups and the Archean basement is unclear, hence it is marked as a dashed line in figure 2.56. Reflectors of the West Rand and Dominion Groups are high in

University of Cape Town

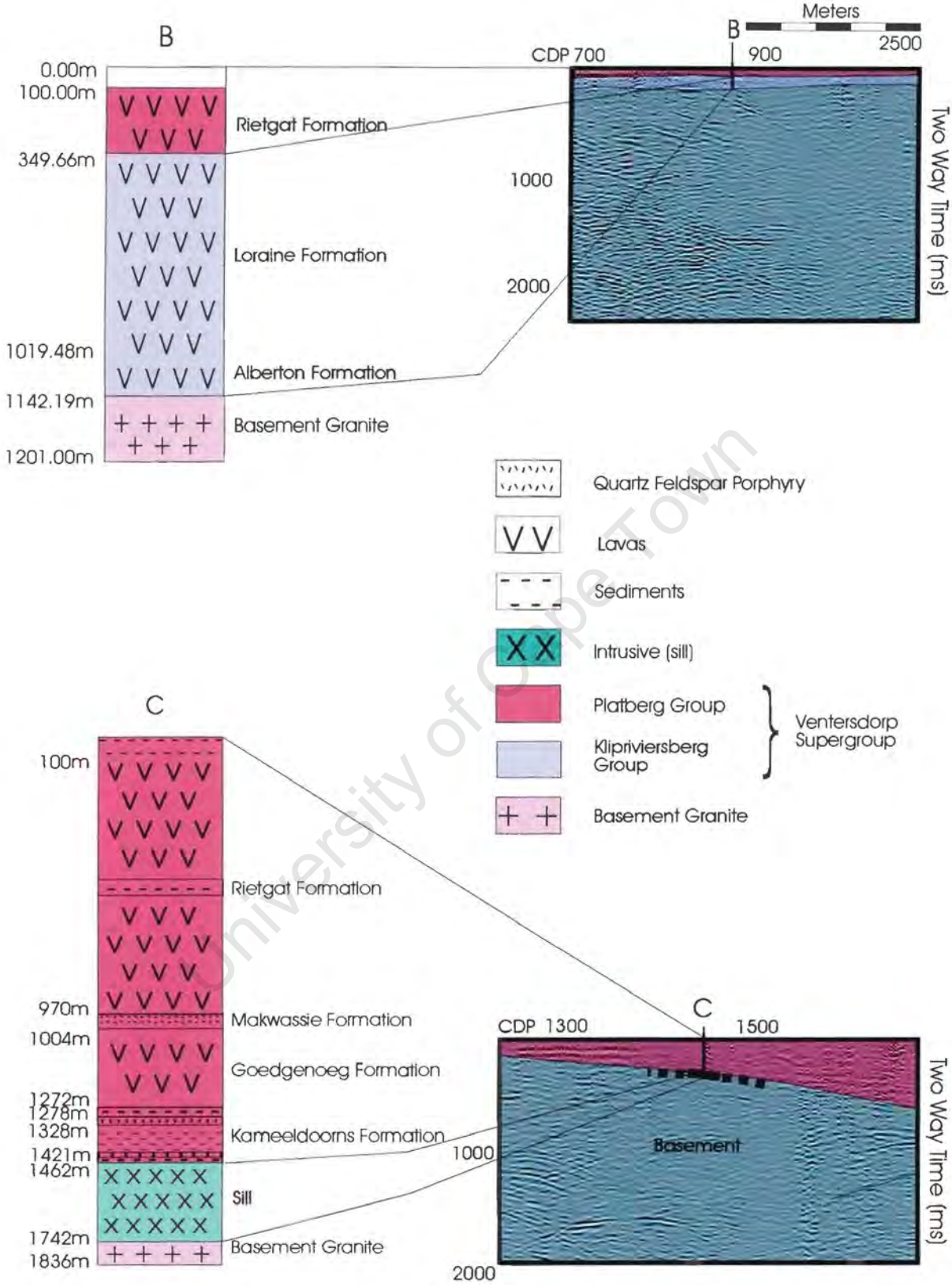

Figure 2.57: Borehole data (B and C) tied to seismic profile YS.

University of Cape Town

amplitude and are continuous, southeast of CDP 2500. The basal reflector of the successive Platberg Group (V_p) truncates the West Rand Group reflectors.

2.4.2.III.c. Ventersdorp Supergroup (V_k, V_p, V_{pn})

A. KLIPRIVIERSBERG GROUP (V_K) [2714 ± 8 MA; Alberton tuffs, U-Pb, Armstrong *et al.*, 1991]

The Klipriviersberg Group is impossible to isolate on the seismic profile YS. From borehole A, however, it is known that the Klipriviersberg Group is ~800 m thick in this area. Its absence from borehole B suggests that it pinches out to the southeast. Thus, its rough location has been marked as a lens on figure 2.56.

B. PLATBERG GROUP (V_P)

The Platberg Group is preserved in two locations along seismic profile YS, southeast of CDP 2700 and between CDP 700 and 2250. At the southeastern extent of the line the Platberg Group unconformably follows the West Rand Group. The discontinuity of reflections in this location perhaps reflects the sedimentary environment; a proximal source and lateral shift in facies. Lateral facies changes produce lateral changes in rock density and corresponding changes in acoustic impedance. Reflections, therefore, tend to be discontinuous.

The Platberg Group is also preserved in the centre of seismic profile YS, in a large-scale basin (figure 2.58). The basin is bounded by a listric growth fault, the Hartebeesfontein fault, extending to 2 s TWT. It has an apparent dip to northwest ranging from a steep dip to near horizontal at depth. As the movement along the fault continued, the space gradually filled, resulting in a series of reflectors that dip at a decreasing angle towards the fault with the top most sediments semi-horizontal (stratal rotation). This is shown diagrammatically in figure 2.59 and further explained in section 2.4.2.V.

The extension of the Hartebeesfontein fault to the surface is difficult to isolate on the seismic profile. Listric faults by definition increase in steepness towards the surface. Since seismic reflection profiling does not resolve steeply dipping features well, it is not

University of Cape Town

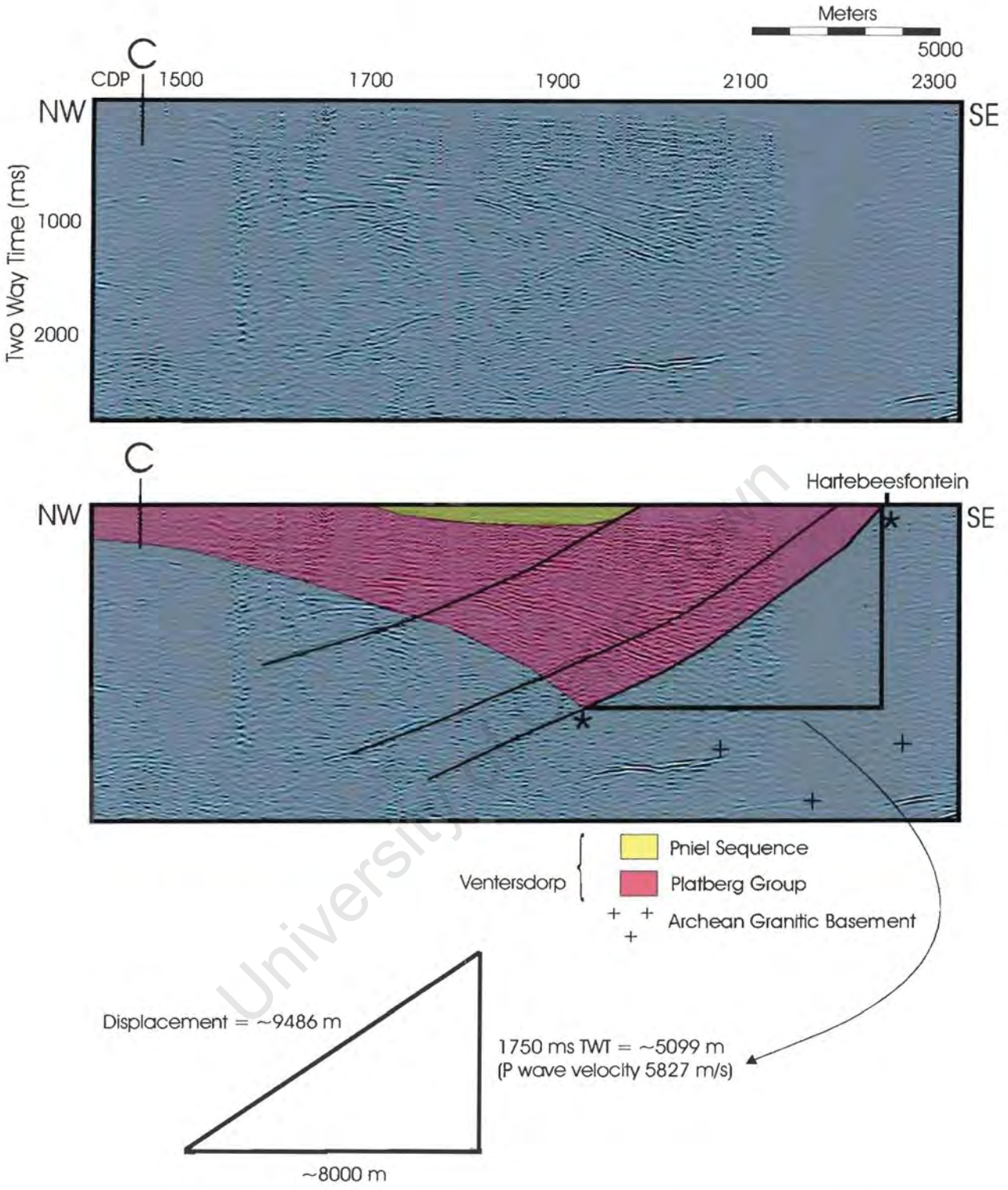

Figure 2.58: Platberg sediments fill syntectonic accommodation space produced by gradual normal movement along listric growth faults. Borehole C is marked. Minimum throw along the Hartebeesfontein fault (between *'s) is ~9500 m.

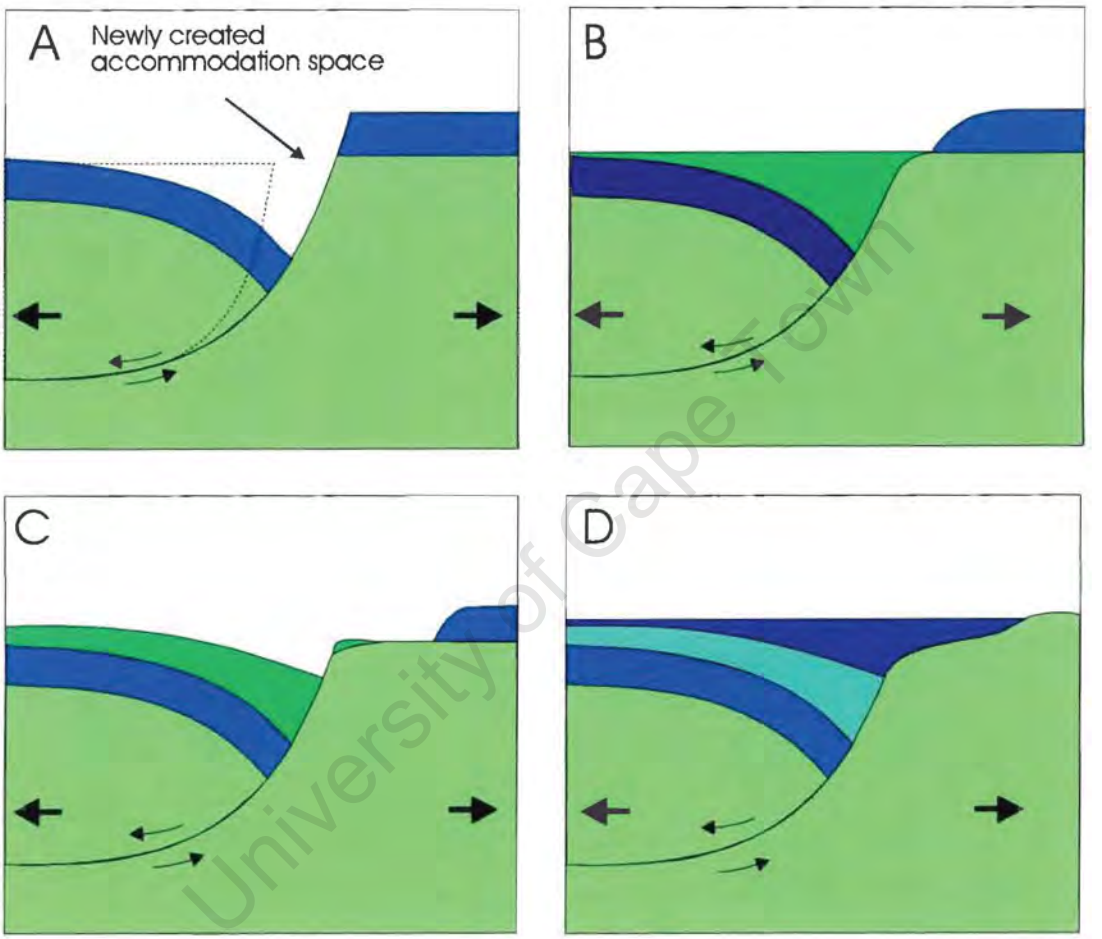

University of Cape Town

Figure 2.59: Cross-sectional sketches showing the rotation of strata (roll over) displaced by a listric fault (modified from Anderson *et al.*, 1983).

clear exactly where the fault nears the surface. In addition some faulted material may have been eroded from the surface.

The in-filling Platberg sediments of the main central basin are continuous, with individual reflectors traceable up to 10 km in length. Their uniform spacing and continuity suggests a low energy environment of deposition with perhaps seasonal (climatic) variations in sediment supply. A reduction in siliciclastic sediment input into the basin promotes carbonate or evaporite formation. Cyclically varying lithologies would produce the evenly spaced reflectors shown in line YS.

C. The Pniel Sequence (V_{PN})

The Bothaville Formation outcrops twice along seismic profile YS. It is seismically imaged as a thin veneer of transparent material and can only be isolated in one position along the profile. The relation between the Bothaville Formation and the underlying Platberg sediments is unclear from the seismic data.

2.4.2.IV. Tectonic Model

- Discontinuity of West Rand and Dominion Group reflectors caused by numerous small-scale faults.
- Two stages of normal faulting, 1) pre-Platberg and 2) synchronous with Platberg deposition.
- Seismic profile is dominated by large listric fault-bounded half grabens into which Platberg sediments are deposited (Minimum throw of ~9.5 km and dipping to the north west).
- Successive Bothaville sedimentation follows Pniel unconformity.

From these observations the following tectonic model is proposed:

1) *Deformation*: (3.1 – 2.9 Ga) small-scale faulting within West Rand and Dominion Groups.
2) *Extension*: (post-West Rand and pre-Platberg Group) normal faulting displaces West Rand and Dominion Groups.

University of Cape Town

3) *Extension*: syn-tectonic Platberg sedimentation in discrete basins of presumably of the same age as the Ventersdorp grabens in the Bushveld lines (section 2.3).
4) *Uplift and erosion*: Deposition of the Bothaville sediments above Pniel Unconformity.

2.4.2.V. Discussion

2.4.2.V.a. Listric Growth Fault Basins

The geometry of slip on a concave upward listric fault requires that horizontal extension is greater than one would expect from the steep near surface part of the fault. Thus accommodation space forms adjacent to the fault and the size of the resultant 'void' is dependent on the curvature of the fault and the amount of slip (Anderson *et al.*, 1983). To solve the space problem, listric faults are accompanied by a "conspicuous pattern of downbending or flexing of the basin-fill strata into the fault (so-called reverse drag or roll over) and/or antithetic faulting as well as an associated growth fault pattern of sedimentation" (Anderson *et al.*, 1983, 1056). The listric fault of line YS, which dips to the north west and has a minimum throw of > 9 km, shows the growth fault pattern.

A geometrically similar basin to the Platberg basin in YS, is located in the northern Basin and Range province of Nevada. A seismic profile through Dixie Valley (Nevada) is included and compared to the listric fault bounded basin of line YS (figure 2.60). The Dixie Valley basin, however, lacks the rotation of strata and subsequent downbending characteristic of listric faults, hence the bounding fault is a relatively planar normal fault (Anderson *et al.*, 1983). The Dixie seismic line was shot across strike of the basin. The similarity between it, and the seismic profile YS suggests that this latter profile may also be oriented across the basin's strike.

University of Cape Town

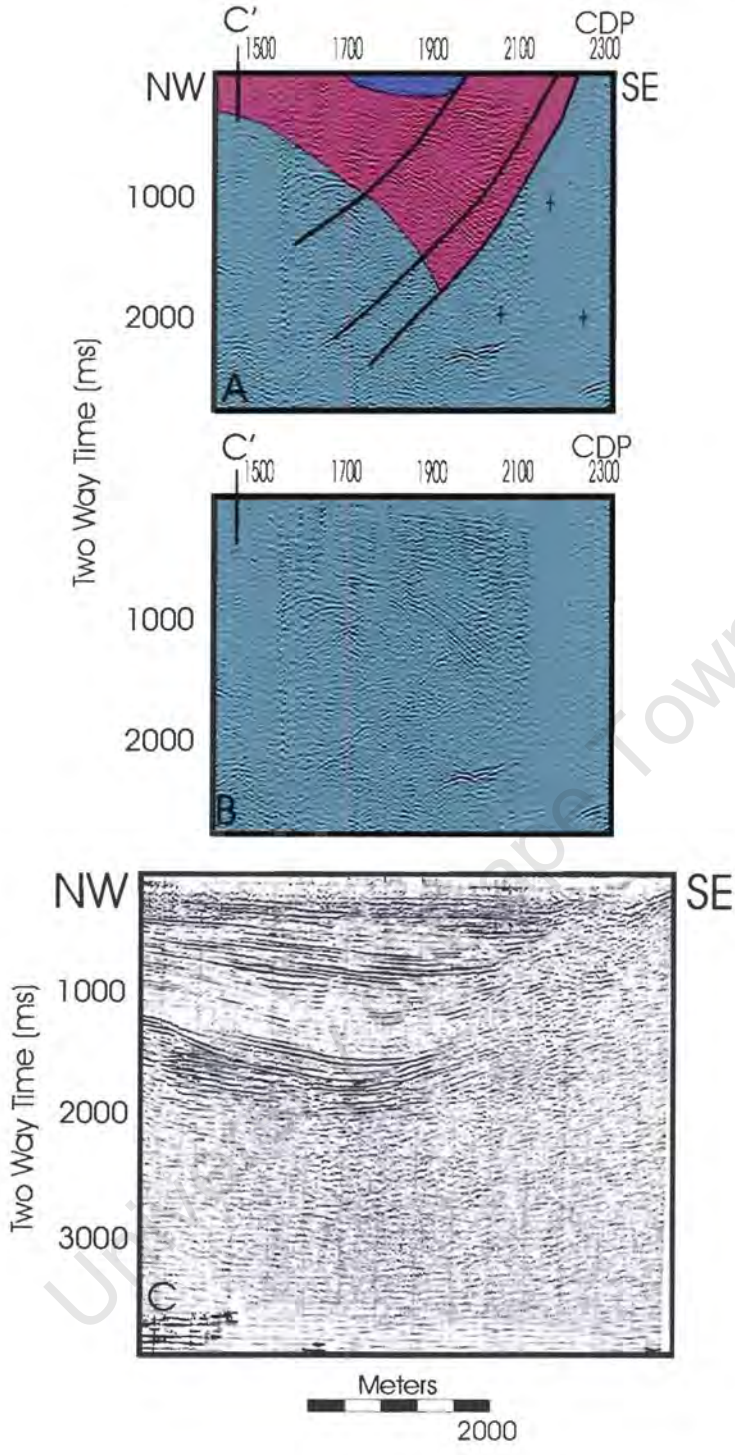

Figure 2.60: A comparison of the Platberg basin, seismic profile YS (A, interpreted, B uninterpreted), to a profile from Dixie Valley, Nevada (C) (from Anderson *et al.*, 1983). Vertical and horizontal scales equivalent. The Dixie line is across strike of the basin. Its similarity to the seismic line YS, suggests that the latter is also across the strike of the basin. Borehole is marked C'. Note: in A (B) reflectors bend down into the fault, in C, reflectors are bent up.

2.5. Discussion

The following three points arising from sections 2.2 to 2.4 are explored in this chapter:

1) The Ventersdorp sediments and basalts are different both in terms of their seismic character and their depositional environment, from craton interior to craton edge.
2) Analysis of the orientation of the listric faults that displace the Ventersdorp Supergroup allows a rough estimate of the direction of extension at 2.7 Ga; N-S to NW-SE and is almost perpendicular to the western craton margin.
3) High amplitude, continuous basement reflectors are identified at depth generally greater than 2 s TWT, or ~5 km.

2.5.1. The Ventersdorp Supergroup: Seismic character

The Griqualand West and Transvaal Basins are correlated on the basis of litho- and limited chronostratigraphy. Correlation is supported by the similarity of the seismic characteristics of various formations. For example, the Campbellrand/ Malmani carbonates are similarly transparent towards their base, and reflective towards their top in both the Transvaal and Griqualand West Basins. In addition their thickness appears mostly constant over hundreds of kilometers. Similarly, the Schmidtsdrif/ Vryburg Subgroup/Formation is highly reflective in all of the seismic profiles interpreted.

The Ventersdorp Supergroup, however, varies in terms of its seismic character and interpreted depositional environment, according to location on the Kaapvaal Craton. Along the western margin of the craton, Ventersdorp sediments and basalts gradually thicken to the west to > ~3 km over a distance of > 150 km. In the craton interior, the Ventersdorp Supergroup sediments are deposited in discrete, E-W, (NE-SW) fault-bounded, half graben basins. Reflection character varies from high amplitude, continuous reflections (line Ys) to low amplitude, discontinuous reflections (the western extent of KBF03A).

University of Cape Town

This suggests that, unlike the Transvaal/Griqualand West Basins, the Ventersdorp Supergroup was not deposited across the Kaapvaal craton in a uniform manner or even in related tectonic depositories. However, Ventersdorp sediments and basalts along the western margin of the craton are contemporaneous with the craton interior fault-bounded Ventersdorp extrusion and sedimentation. The Ventersdorp Supergroup of line KBF03A and 01 is interpreted as a rift sequence associated with the rifting of an unknown fragment from the western margin of the Kaapvaal Craton. This occurred during craton-wide extension also responsible for the formation of discrete fault bounded basins, which were depositories for the Ventersdorp sediments and basalts, evident in seismic profiles Rz, YS, OB and AG.

2.5.2. Orientation of Ventersdorp boundary faults (figure 2.60)

In the seismic profiles Rz-254, 255, 256, OB and AG, the listric and normal boundary faults of the Ventersdorp Basins have a similar east-west strike, dipping both to the north and south. The observations below are schematically shown in figure 2.61:

- The bounding faults identified in the Rz lines (in the north) trend east-west and dip to the north.
- Towards the craton interior, east-west trending normal faults identified in seismic lines OB and AG, dip predominately to the south.
- Seismic profiles KBF03A and 01, show a thickening of both Ventersdorp sediments and basalts on a regional scale from east to west.

(The dips and strike direction is apparent only, due to the two dimensional nature of the seismic profiles).

From these observations it seems that the stretching pattern of extension was complex during the deposition of the Ventersdorp Supergroup, but the extension direction was approximately N-S, perpendicular to E-W direction of extension, proposed for the craton's western margin.

University of Cape Town

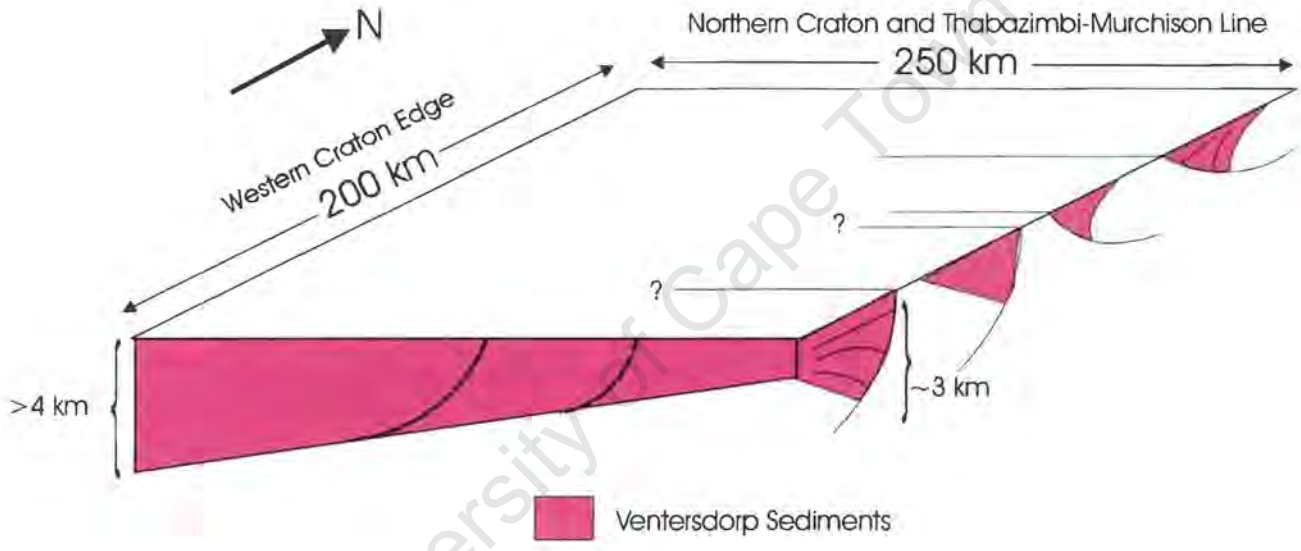

University of Cape Town

Figure 2.61: Schematic representation of the complex pattern of extension during Ventersdorp deposition across the Kaapvaal craton, from the centre to the western edge. Note: normal faults trend uniformly east-west, though they dip northwards in the north and northwards and southwards in the south (craton interior). The Ventersdorp Supergroup thickens on a regional scale from east in the interior to west, towards the craton margin.

2.5.3. Basement Reflections

World wide, the upper crystalline crust is mostly devoid of reflections even though studies of well logs have shown that the appropriate changes in impedance do exist (Mooney and Brocher, 1987). This is explained by the proposition that the impedance changes are not well laminated, or are not of long enough scale length to cause reflections. This has been explained as a consequence of the brittle behaviour of the upper crust producing short, steeply dipping features that are difficult to image. Alternatively the transparency of the upper crust may be due to the seismic method itself for reasons outlined in Mooney and Brocher (1987).

However, high amplitude, continuous reflectors are identified on several of the seismic profiles, generally below 2 seconds TWT or 5 km depth. Thus, given that the upper crystalline crust is often transparent, the observation of these basement reflections is unexpected. The reflectors are almost certainly real features, as opposed to artifacts of the data for two reasons:
They do not have the same structure as shallower prominent reflectors, therefore are not likely to be ghosts or multiples.
They occasionally onlap and truncate other basement reflectors.

Blundell and Raynaud (1986) Klemperer *et al.* (1987), Durrheim *et al.* (1991) and Durrheim (1998) have noted similar reflections within upper crystalline crust. Durrheim *et al.* (1991) observe these basement reflections on a deep seismic reflection profile, parallel and east of line Ys. Durrheim *et al.* (1991) state: "The observation of strong, continuous reflectors in the upper crystalline crust of the Ventersdorp dome is [thus] unexpected, especially when the lengthy tectonic history of the area is considered".

A number of possible origins have been suggested for basement reflections including primary igneous layering, mafic sills, ductile strain banding and contrasts in physical qualities including fluid content in banded rocks. Geologic structures that may cause such reflections include igneous intrusions, diapiric upwelling, strongly folded surfaces or extensive faulting (Durrheim *et al.*, 1991). Corner (1998) mentions regional magnetic anomalies arising from sources within the granite-gneissic

University of Cape Town

basement which suggest anomalous magnetization at depth. This increased level of magnetisation may be the result of the interaction of fluids, with an elevated oxygen fugacity, with iron in the basement, causing it to crystallize to magnetite in the middle to lower crust (Corner, 1998). This magnetization may be the cause of the basement reflections evident in the seismic lines of this study.

Due to the large lateral extent of the reflective zones, Durrheim *et al.* (1991) suggest that they may signify reconstitution of the crust during basin formation either through metamorphism of ductile deformation together with the intrusion of sills. The basement reflectors of line YS differ from those described in the profile presented in Durrheim *et al.* (1991). The former shows no obvious parallelism to the supracrustal strata above whereas Durrheim *et al.* (1991) note a strong similarity in orientation between basement reflectors and supracrustal strata. The parallelism of the reflectors with the base of the Dominion Group strata, has been used to suggest that the eruption of the Dominion lavas could have produced the metamorphism responsible for the basement reflectors (Durrheim *et al.,* 1991). They mention too, Ventersdorp and Bushveld intrusion (sills) as alternative responsible events.

Basement reflectors are the most numerous, and of the greatest amplitude in seismic profile, Rz-254. This may be due to the proximity of the Rz lines to the Bushveld Igneous Intrusion, strengthening the argument that the reflectors arise from intrusive sills and/or their thermal metamorphic effects at depth. The basement reflector truncations noted in seismic profile YS, may arise from the successive intrusion of sills cutting previous intrusions. Alternatively intruding sills would disturb the pre-existing metamorphic texture, perhaps causing the complex reflector patterns evident in line YS.

University of Cape Town

Chapter 3 : Tectonic Synthesis

The tectonic and sedimentary history of the Kaapvaal Craton's western margin is the focus of further exploration in this chapter. Particularly,

1) *Sediment accumulation rates*: An assessment of how sediment accumulation rates vary across seismic profile KBF03A gives insight into the creation of accommodation space across the margin. It is interesting to compare these rates with Archean and Paleo-Proterozoic rates calculated elsewhere, as well as with modern sedimentation rates.
2) *Structural and tectonic history (2.7 - 1.8 Ga)*: The Kaapvaal Craton's western margin is largely obscured by Tertiary Kalahari cover. Seismic profiles KBF03A and KBF01 offer a glimpse of what lies beneath this cover, and allow for the northwards projection of mapped structural detail in the south.
3) *Lithospheric elastic thickness*: Seismic profile KBF03A offers the unique opportunity to calculate lithospheric elastic thickness for that section of the craton's western margin between 1.9 and 1.7 Ga. This estimate may be compared to the same region's present day estimated elastic thickness, and to that of other regions of convergence world-wide. Comparing a paleo-elastic thickness to the present day thickness in this area, allows insight into changes of lithospheric elastic thickness over a ~2.0 Ga time period.

University of Cape Town

3.1. Sediment accumulation rates across profile KBF03A

3.1.1. Introduction

The Ventersdorp and Griqualand West Supergroups with the exception of the Campbellrand Subgroup increase in thickness westwards, away from the craton. This implies that the creation of accommodation space is greatest in the west, allowing for the maximum thickness of sediment to be deposited there. This increase in accommodation space may have resulted from a relative sea level rise caused by local subsidence or alternatively may be the result of a eustatic sea level rise. Both scenarios would result in a

marine transgression, an increase in accommodation space, and a corresponding increase in sediment thickness offshore to the west.

All of the Griqualand West sediments, except the banded iron formation, were deposited at, or near sea level. Thus, assuming sufficient sediment supply, sediment accumulation rate is equivalent to subsidence rate, or the increase in accommodation space with time. Although we cannot choose between the above scenarios, it is possible to quantify the increase in accommodation space to the west by assessing sediment accumulation rates for various time intervals across the profile, KBF03A. These calculations are first order approximations only. With little spatial and temporal constraint all estimates of Archean/ Paleoproterozoic sediment accumulation rates need to be treated with caution.

3.1.2. Method

Three vertical sections have been chosen to calculate sediment accumulation rates and to compare the creation of accommodation space across profile KBF03A. The first section, A, is in the east, where sediment thickness is at a minimum. A second section B is just east of the main listric fault. Section C is to the west of the listric fault where the sedimentary succession is the thickest (figure 3.1). Age data to constrain the sediment accumulation rate is taken from a variety of sources, but preference is given to ages calculated using the U/Pb technique on zircons, and to those samples collected at closest proximity to line KBF03A. This particularly applies to the ages used in the calculation of the Campbellrand Subgroup sediment accumulation rate.

Sediment accumulation rate is calculated using the equation,

$$cSR = h(x) / t$$

where cSr is the compacted sediment accumulation rate, h (x) is the compacted thickness, and t is the duration of deposition (Altermann and Nelson, 1998). Table 3.1 lists the thicknesses estimated for the Ventersdorp sediments and flood basalts, the Schmidtsdrif Subgroup, the Campbellrand Subgroup and the Kuruman Formation, Asbesheuwels Subgroup as well as appropriate ages. These thicknesses were calculated by converting TWT to depth using the P wave velocities given in table 2.1.

University of Cape Town

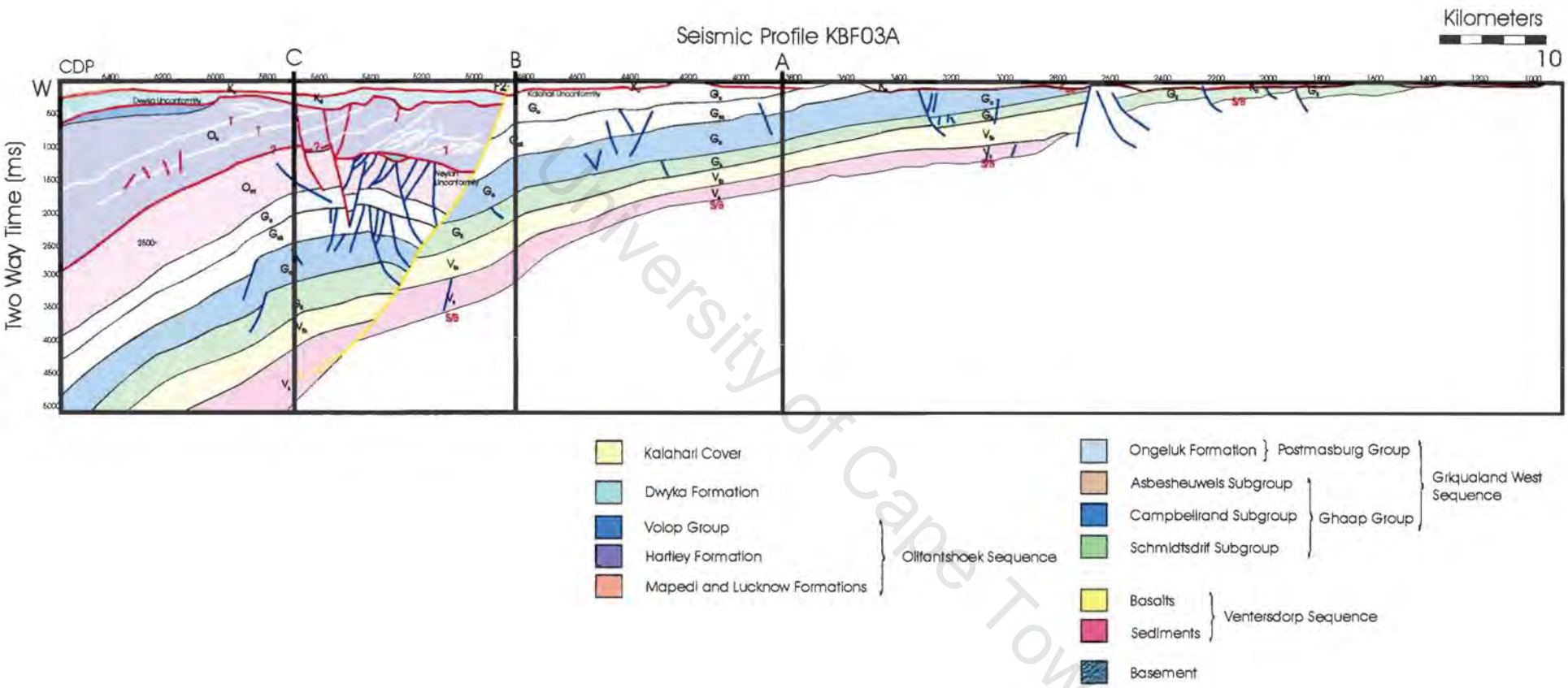

Figure 3.1: Location of vertical sections A, B and C, used to calculate sedimentation rates along seismic profile KBF03A.

University of Cape Town

Unit	Thickness (m) from Kathu Borehole section (Altermann and Nelson, 1998)	Thickness in meters (corrected for dip) - calculated from seismic profile KBF03A (this work)			Dated Unit	Age and method	Reference
		Sub-locations along seismic profile KBF03A					
		A	B	C		Ma	
					Ongeluk Lava	2222 ± 13 Ma? Pb/Pb whole rock isochron	Cornell *et al.*, 1996 Contested by Moore *et al.*, 2000 – 2.4 Ga (section 1.3.5.II.)
Kuruman Formation, Asbesheuwels Subgroup		815.63	1314.1	1540.6	Upper Kuruman Iron Formation	**2465 ± 7 Ma** U/Pb- SHRIMP	R.A. Armstrong pers. comm. (1996).- referenced in Martin *et al.* (1998)
Campbellrand Subgroup	2830	1655.2	1815.3	1868.7	Upper Gamohaan Formation	**2516 ± 4 Ma (1)** U/Pb- SHRIMP	Altermann and Nelson, 1998
					Upper Monteville Formation shales	**2555 ± 19 Ma (2)** U/Pb - SHRIMP	Altermann and Nelson, 1998
Schmidtsdrif Subgroup	517	589.06	951.56	1359.4	Vryburg Formation	**2642 ± 3 Ma** U/Pb- zircons	Beukes pers. comm. (2001)
Ventersdorp Flood Basalts		769.88	1299.2	1251.0			
Ventersdorp Sediments		728.38	1138.1	2185.1	Kareefontein Formation	**2714 ± 3 Ma** U/Pb	Walraven, 1991

Table 3.1:Summary of thicknesses and geochronology of various units measured from the seismic profile KBF03A. Age data from Altermann and Nelson (1998). Note that in the case of the Campbellrand carbonates ages were selected from samples close to line KBF03A. (1) Sample WA 92/4 from Kuruman Kop peak. (2) Sample WA 93/41 from the farm Suiversfontein (between Douglas to Niekerkshoop).

University of Cape Town

Units	Time Span	Calculated Sedimentation Rate (m/Ma) (this study) *				Sedimentation rate from Altermann and Nelson (1998) (m/Ma)
			Sub-locations of seismic profile KBF03A			
	Ma		A	B	C	
Top of the Campbellrand Subgroup (Gamohaan Formation) to the top of the Kuruman Formation (at roughly half of the Asbesheuwels Subgroup total thickness)	40 - 62	Banded Iron Formation	6.578 – 10.20 (ave: 8.289)	10.60 – 16.43 (ave: 13.52)	12.42 – 19.26 (ave: 15.84)	60
Bottom of the Campbellrand Group (Monteville Formation) to the top of the Campbellrand Subgroup (Gamohaan Formation)	24 - 54	Predominately stromatolitic carbonates with shale, micrite and chert intercalations	30.65 – 68.97 (ave: 49.81)	33.62 – 75.64 (ave: 54.63)	34.61 – 77.86 (ave: 56.24)	40 – 150
Bottom of the Schmidtsdrif Subgroup to the bottom of the Campbellrand Subgroup (Monteville Formation)	73 - 101	Predominately shales, minor quartzites, carbonates, oolites and tuff beds	5.832 - 8.069 (ave: 6.951)	9.421 – 13.04 (ave: 11.23)	13.46 – 18.62 (ave: 16.04)	20
Bottom of the Ventersdorp Supergroup to the bottom of the Schmidtsdrif Subgroup	66 - 78	Quartzites and shales succeeded by basalt	19.21 - 22.70 (ave: 20.96)	31.25 – 36.93 (ave: 34.09)	44.05 – 52.06 (ave: 48.28)	NA

Table 3.2: Subsidence rates calculated for the depositional intervals shown above. * Note: rates are calculated without knowledge of compaction. NA = not available.

University of Cape Town

Table 3.2 lists the rates calculated for these time intervals with comparisons to those published in Altermann and Nelson (1998).The sediment accumulation rates calculated here are rough approximations only because:

1) The thickness of units is estimated from TWT read from the seismic profile, then converted to depth using published P-wave velocities (table 2.1. Thickness is approximated by taking into account the apparent dip of the unit. The section is two-dimensional, therefore this thickness is apparent only.
2) Due to the lack of lithological control, for example well data, the calculations ignore the effect of compaction, which causes increased seismic velocity with increasing depth. Thus the calculations result in minimum thicknesses.
3) The Transvaal Sequence lacks detailed chronological control. Age data is sparse and in some instances controversial (section 1.3.5.II.). Thus the sediment accumulation rates are averaged over long time spans. One such depositional interval is up to 100 Ma long.
4) Subtle discontinuities including periods of non-deposition and erosion have been ignored.

3.1.3. Results

Results are graphed and compared to those obtained in Altermann and Nelson (1998) in figure 3.2.

- During the deposition of the Ventersdorp sediments and basalts, sediment accumulation rates vary widely across the profile. In the east the sediment accumulation rate during this time is estimated at 20 m/Ma. This increases by 150 % to the west where the Ventersdorp Supergroup sediments were deposited at a rate of around 50 m/Ma.
- The Schmidtsdrif Subgroup was deposited at a more even rate across the entire section than the Ventersdorp Supergroup. Again though, the highest rate calculated for this group is in the west. On average the sediment accumulation rate for this subgroup of shales and carbonates is slow, at ~ 7 to 16 m/Ma.
- Sediment accumulation rates increase across the entire profile to around 50 m/Ma as Campbellrand carbonates are deposited. The clustering of rates

University of Cape Town

calculated from A, B and C shows an even rate of carbonate accumulation across the profile, though the rate calculated at C (in the west) does show an elevation in rate of ~13 % relative to A.

- The deposition of the banded iron formations of Kuruman Formation, Asbesheuwels Subgroup, occurred at a markedly reduced rate from the carbonates below. The calculated rate falls to around 8 to 16 m/Ma. Again there seems a clustering of sediment accumulation rates suggesting that sedimentation during this time occurred at a fairly even rate across the profile.

3.1.4. Discussion

3.1.4.I. Comparison of results with rates from Altermann and Nelson (1998)

Altermann and Nelson (1998) divide the Griqualand West basin into two sub-basins, the Prieska and Ghaap Plateau sub-basins. For the carbonates of the Nauga Formation, Prieska sub-basin, these authors estimate a sediment accumulation rate of up to 10 m/Ma. Closer to line KBF03A, in the Ghaap Plateau sub-basin, their calculated sedimentation rate increases to between 40 and 150 m/Ma. A rate estimate of 20 m/Ma is suggested for the Schmidtsdrif Subgroup and up to 60 m/Ma for the Kuruman BIF (Altermann and Nelson, 1998). In the above calculations, these authors have made the first attempt to take into account the effect of compaction as well as that of erosion and non-deposition when calculating sedimentation rates. This was particularly difficult to achieve for the Kuruman BIF, due to the lack of standard figures for BIF compaction (Altermann and Nelson, 1998).

Rates calculated by Altermann and Nelson (1998) are compared graphically to those calculated in this study (figure 3.2). From this comparison, the following points emerge:

- Rates calculated in this study are 3 to 7 times lower for the Schmidtsdrif, Campbellrand Subgroup and Kuruman Formation than those calculated in Altermann and Nelson (1998).
- This reduction in rate is perhaps partially due to the fact that this study did not take compaction or the effect of periods of non-deposition and erosion into account, hence values reflect minimum rates.

University of Cape Town

Sediment Accumulation Rates (m/Ma)
(This Study)

Age (Ma)	A (east)	B	C (west)	Altermann and Nelson (1998)
2714				
	20.96	34.09	48.28	
2642				
	6.951	11.23	16.04	20
2555				
	49.81	54.63	56.24	40 - 150
2516				
	8.289	13.52	15.84	60
2465				

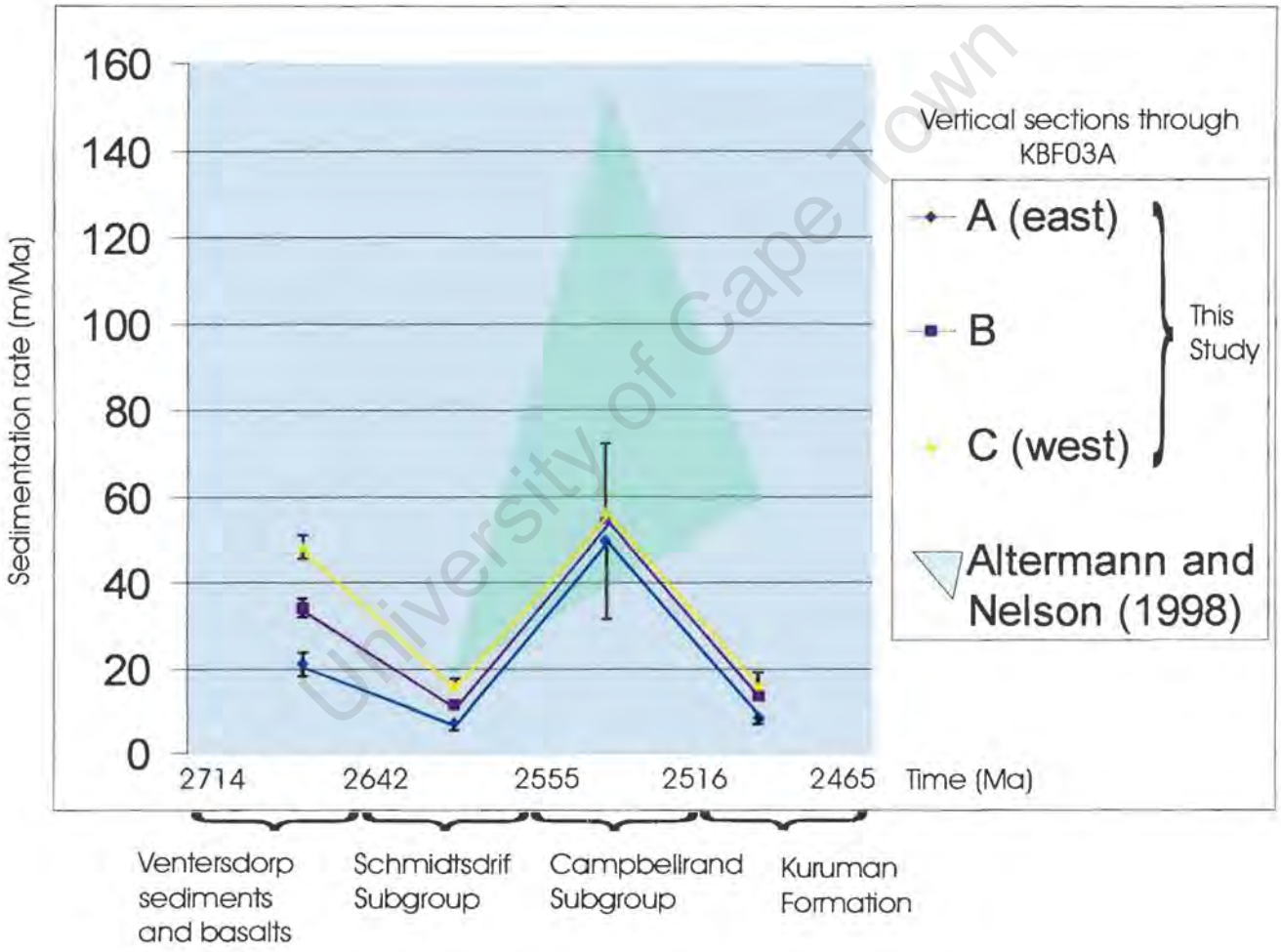

University of Cape Town

Figure 3.2: Comparison of sediment accumulation rates calculated in this study to those of Altermann and Nelson (1998).

- The greatest rate difference is for the chemical sediments, the carbonates and the BIF.

3.1.4.II. Comparison to other rates calculated for the Kaapvaal and Pilbara Cratons (figure 3.3)

Barton *et al.* (1994) have calculated a sedimentation accumulation rate for the Nauga Formation (upper Campbellrand Subgroup) of carbonate, shale and BIF at 2-4 m/Ma. This calculation is based upon a then newly acquired U-Pb age of 2552 ± 11 Ma for a zircon separated from a banded-tuff horizon in the Nauga Formation. Barton et al. (1994) propose therefore that rock accumulation rates in the late Archean- Early Proterozoic may have been greatly reduced from those of younger lithologically equivalent deposits.

Barton et al. (1994) estimate a sediment accumulation rate for the Campbellrand and Schmidtsdrif Subgroup by dividing the thickness of 1700m of mainly carbonates, by the time interval estimated from available ages. These are the maximum age of the Schmidtsdrif (Jahn *et al.*, 1990) and the newly acquired upper Campbellrand age of 2551 ± 11 Ma (Barton *et al.*, 1994). This gives a minimum rate of 26 m/Ma. Subsequently, improved dating of the Schmidtsdrif Subgroup, in particular of the Vryburg Formation at 2642 ± 3 Ma (Walraven *et al.*, 1999), results in a considerably faster rate of deposition of the Campbellrand and Schmidtsdrif Subgroup.

Higher in the stratigrapy, when the BIF's are encountered, published estimates of sediment accumulation rates differ widely. This is partially because the chronostratigraphy of the Asbesheuwels banded iron formations is sketchy. Better age data exist for the Hammersley Group, Western Australia which makes comparisons between these two, perhaps stratigraphically equivalent groups (Cheney, 1996, Martin *et al.*, 1998, Zegers *et al.*, 1998), useful.

Arndt et al. (1991) found a slow rate of accumulation, similar to that estimated by Barton *et al.* (1994) of 3-4 m/Ma for the Hamersley Group of the Pilbara craton in Western Australia. This rate of 3-4 m/Ma is contested by Barley et al. (1997) on the basis of newly

University of Cape Town

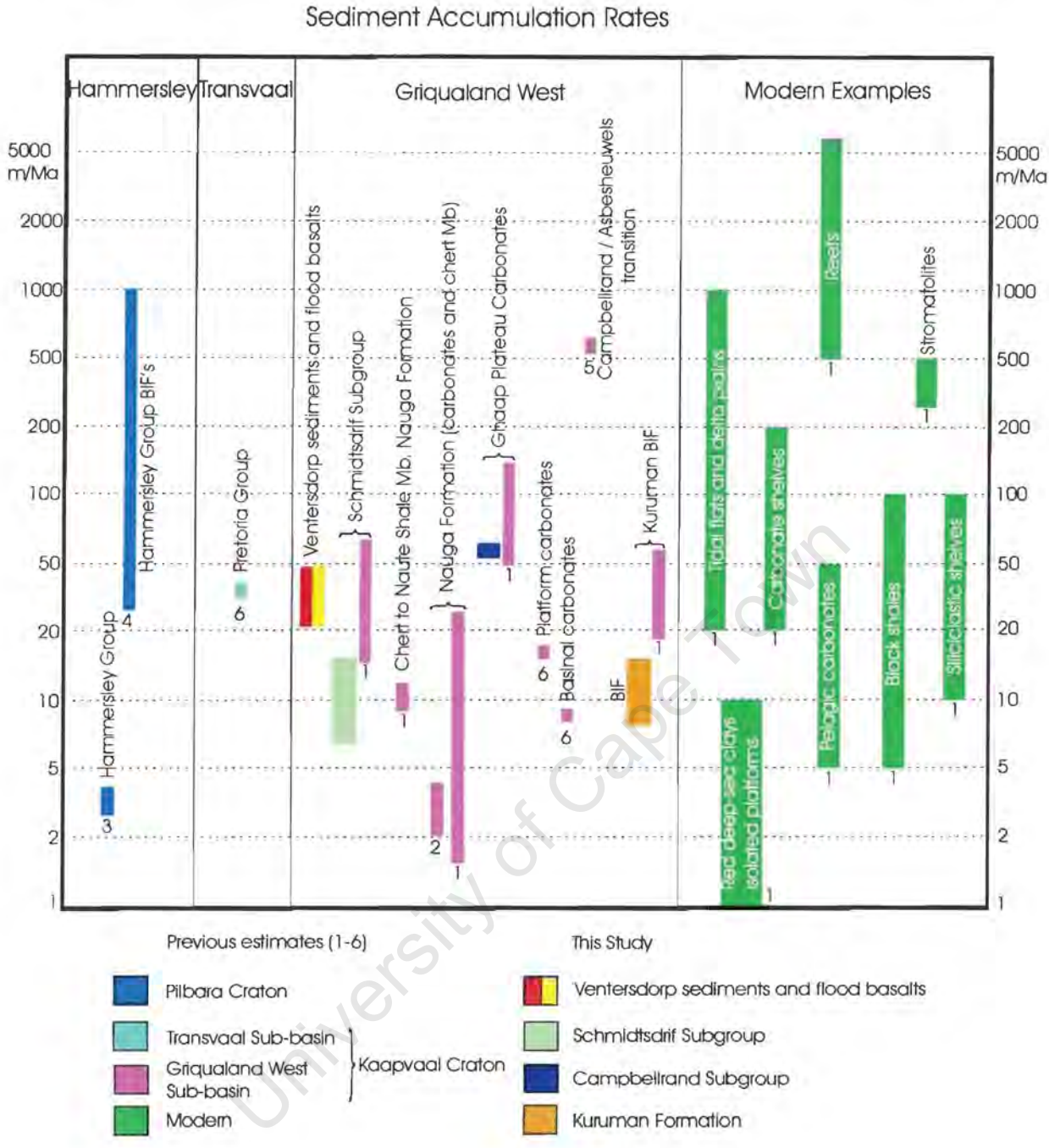

University of Cape Town

Figure 3.3: A comparison of sediment accumulation rates between the Archean/ Proterozoic and modern environments, and between the Pilbara and Kaapvaal Cratons. Several authors have suggested a stratigraphic correlation between the Kaapvaal and Pilbara cratons based on similar litho- and chronostratigraphy (Cheney, 1996; Martin *et al.*, 1998; Zegers *et al.*, 1998). Numbers correspond to the data's source: 1. Altermann and Nelson (1998) 2. Barton *et al.* (1994) 3. Arndt *et al.* (1991) 4. Barley *et al.* (1997) 5. Klein and Beukes (1989) 6. Walraven and Martini (1995).

acquired SHRIMP data. They claim that the BIF of the Australian Hamersley Group must have been deposited at a rate considerably faster than that suggested by both Arndt et al. (1991) for the same group, and Barton et al. (1994) for the Campbellrand Subgroup, Griqualand West. Barley *et al.* (1997) suggests a depositional rate of greater than 30 m/Ma for the Hamersley Province BIF's. Even greater rates of between 100 to 1000 m/Ma are mentioned when possible role of periods of nondeposition or very slow deposition reflected by sequence boundaries and organic shales respectively are considered (Barley *et al.*, 1997). These rates are far greater than the 8 to 16 m/Ma calculated for the Kuruman Formation in this study.

Klein and Beukes (1989) have calculated a sediment accumulation rate for the Campbellrand – Asbesheuwels transition zone at around 570 m/Ma on the basis of annual varves. This represents a considerable increase in rate from previous estimations of Campbellrand carbonate deposition. However it does fall within the estimate of rate of 100 to 1000 m/Ma by Barley *et al.* (1997). It is, however, an order of magnitude higher than the sediment accumulation rate calculated for the Campbellrand carbonates in this study.

Sediment accumulation rates for carbonate platform and basin facies have been calculated at 17 and 8 m/Ma respectively (Walraven and Martini, 1995). As new age data emerge, so will new estimates of sediment accumulation rates for both the carbonates and the BIF's of the Griqualand West Sequence.

3.1.4.III. Comparison to rates estimated for the modern environment

Figure 3.3 shows estimated sedimentation rates for the modern environment. Altermann and Nelson (1998) conclude from their estimates of sediment accumulation rates that Archean and Phanerozoic chemical and clastic sedimentation rates are comparable. This contradicts the view of Barton *et al.* (1994), working with older age data, that sedimentation rates during the late Archean- Early Proterozoic may have been greatly reduced.

University of Cape Town

Rates calculated in this study tend to support the conclusion of Barley et al. (1997), that Archean/ early Paleoproterozoic are not appreciably different from those estimated from Phanerozoic deposits. The average rate of just over 50 m/Ma calculated for the Campbellrand carbonates falls within the modern window for carbonate shelves of 20 m/Ma to 200 m/Ma. However it is an order of magnitude lower than that of modern reefs and at least 6 times less than modern stromatolites. This discrepancy may be due to the failure in this study to take compaction, non-deposition and possible different carbonate precipitation processes operating in the Archean into account. Grotzinger (1989) and Sumner and Grotzinger (1996) suggest a direct chemical precipitation of carbonate from seawater during the Archean and Precambrian. Therefore, perhaps the validity of comparisons between modern carbonate production and Archean carbonate deposition is questionable.

The rate calculated for the Kuruman BIF falls within the black shale window in figure 3.3. The rate for the Schmidtsdrif Subgroup is comparable to both the siliciclastic and pelagic carbonate environment (figure 3.3).

3.1.4.IV. Sediment accumulation rates reflective of passive margin subsidence?

The calculated sediment accumulation rates show more lateral variation across the profile for the older units, the Ventersdorp Supergroup and the Schmidtsdrif Subgroup than the younger, Campbellrand Subgroup and Kuruman Formation. This is apparent by the way the calculated rates converge as one progresses upward in the stratigraphy, or to the right in figure 3.2. In a passive margin environment initial subsidence is related to lithospheric thinning and associated passive rifting. The structural interpretation of line KBF03A (figures 2.16 to 18, section 2.2.1.IV.) indicates that the Ventersdorp sediments and basalts, possibly including the Schmidtsdrif Subgroup are deposited during this original stage of extension-related subsidence. With rifting occurring to the west of KBF03A it is likely that subsidence there was greatest, thus accommodation space was being created fastest in the west. Subsidence associated with rifting tends be localised which may explain why sedimentation accumulation rates are so much greater at C, in the west therefore closest to the rifting, than at A, in the east.

University of Cape Town

In a passive margin environment, thermal subsidence follows subsidence related to initial rifting. As the upwelled asthenosphere cools, a large area will be affected by this later staged thermal subsidence (McKenzie, 1987). The Campbellrand Subgroup and Kuruman Formation are both interpreted to have been deposited during such a period of thermal re-equilibration. Thus perhaps it is not surprising that these two units show the least lateral variation in sediment accumulation rate across the profile; both are deposited in accommodation space that is being created fairly equally across the profile.

3.2. Structural and Tectonic History

3.2.1. Introduction

The western margin of the Kaapvaal craton has undergone numerous phases of deformation. The complex tectonic history of this area may be unraveled from seismic profile KBF03A (in the north) and KBF01 together with geological mapping in areas of sufficient outcrop (in the south). This sub-chapter compares the tectonic history proposed from geological mapping in the south west, to evidence arising from seismic lines KBF03A and KBF01. Section 1.2.2. places lines KBF03A and KBF01 in their tectonic setting.

Figure 2.16 to 18 graphically illustrate an interpretation of the structural history of line KBF03A. This history involves four main phases:

1) *Extension* (2.7 – 2.2 Ga), development of a passive margin and the deposition of the Griqualand West sequence and lower Olifantshoek units. Initial normal movement along the listric fault (F2) dates from this time. It is unusual that a passive margin existed for 500 Ma. Modern margins span ~ 200 – 300 Ma.
2) *Compression* (>1.9 Ga) in an east-west direction with reversal or inversion of movement along F2 and the onset of folding. The formation of an anticline to the west of F2 resulted in localised uplift and erosion of the underlying sequence. The resultant unconformity separates the lower Olifantshoek Group (Mapedi and Lucknow Formations) from the upper units, and is termed the Neylan unconformity. Continued compression (1.9 – 1.7 Ga) caused

University of Cape Town

duplication and significant shortening of the Hartley Formation during thrusting from the west.

3) *Extension* in the hinterland (<1.7 Ga) and renewed inversion along the listric fault F2, with a possible strike-slip component.
4) *Uplift and erosion* during two separate episodes (at 300 Ma and <30 Ma respectively) left prominent unconformities evident in line KBF03A. The first represents glacial erosion during the deposition of the Karoo-aged Dwyka. The second unconformity probably represents erosion during the tertiary uplift of Southern Africa. Kalahari sediments were deposited onto this Kalahari Unconformity.

Line KBF03A transects very little outcrop due to Kalahari cover of varying thickness (0 to 200 m). Further to the south, however, solid outcrop has allowed researchers to unravel the structural history of the Kaapvaal craton's western and southwestern margin. This sub-chapter will compare structural observations made predominately in the south to those made from line KBF03A, further north.

3.2.2. Structural observations made at surface along the Kaapvaal Craton's western margin (table 3.3)

There is much debate about the stratigraphy of the Griqualand West Sub-basin. This is largely due to the general lack of understanding of the role of thrust faulting along this western margin. Several thrusts have been identified along the southwestern margin, where outcrop is better, but the lack of precise geochronology impedes analysis of the tectono-stratigraphy. Thrusts have resulted in duplication of strata, which, according to some authors, has resulted in overestimation of the original lithostratigraphy. Beukes and Smit (1987) in particular contest the stratigraphic position of the Gamagara red beds (see figure 2.27). Stratigraphic duplication, they claim, is due to a zone of low angled thrust faults called the Blackridge fault zone (figure 1.4). Altermann and Hälbich (1990) also recognized the need for a review of Griqualand West stratigraphy, due to complexity of structure along the southwestern margin of the Kaapvaal Craton. However, lack of precise ages hampers any further analysis.

University of Cape Town

Sequence	Group	Subgroup	Formation	Age	Reference	Structural Observations					
						Stowe (1986)	Beukes and Smit (1987)	Altermann and Halbich (1991)	Grobbelaar (1995)	This Study -KBF03A	This Study -KBF01
	Kalahari									Uplift and erosion- Kalahari unconformity	
Karoo	Dwyka									Uplift and erosion- Dwyka unconformity	
Late Namaqua (~ 1 Ga)						N trending normal faults			Relaxation of shears into normal faults in new tensional stress field	Renewed extension causing normal movement along F2 with possible strike-slip component. Displacement of thrusts by normal faults	Estimate age of late-stage extension resulting in displacement of thrusts by normal fault-
						NNW wrench faults		Wrench faulting along Doornberg Lineament	Major transcurrent dextral shearing due to north directed compression		
Namqua Orogeny (1.2 – 1 Ga)						Open folds at SW margin Tight Z folds and renewed thrusting			Open folding		

Table 3.3: A suggested correlation of structural observations made by Stowe (1986), Beukes and Smit (1987), Altermann and Hälbich (1991) and Grobbelaar et al. (1995) along the southwestern margin of the Kaapvaal Craton, to those made further north (this study).

University of Cape Town

Sequence	Group	Subgroup	Formation	Age	Reference	Structural Observations					
						Stowe (1986)	Beukes and Smit (1987)	Altermann and Halbich (1991)	Grobbelaar (1995)	This study - KBF03A	This Study - KBF01
Olifantshoek		Volop						Upright to E vergent folds and limited brittle thrusts trending N-S			
			Hartley	1928 ± 4 Ma- U-Pb	Cornell et al. (1998)	E to SE vergent recumbent isoclines and thrusts	Thin skinned tectonic deformation possibly related to Kheis-Korannaberg orogeny resulted in duplication of strata by thrust faults dipping gently to west-Blackridge thrust zone. Crustal shortening estimated at 35-55 km	S to SE verging near horizontal thrusts and folds in Boegoeberg Dam area	Thrusting defined by single sole thrust striking N/S and dipping ~ 10 degrees to the west. Imbricate thrusting occurs within this nappe structure-Blackridge Thrust, renamed Kheis Thrust.	Thin-skinned thrusting of the Hartley Formation due to E/W directed compression. Thrusting causes loading and flexure of the passive margin sequence downward in the west	Thrusting of lower Olifantshoek Group (Gamagara/ Mapedi and Lucknow Formations) over Griqualand West strata (Schmidtsdrif and Campbellrand Subgroups)
			Lucknow							Folding of the lower Olifantshoek units to the west of F2. Subsequent erosion leads to the Neylan Unconformity.	

Table 3.3: (continued)

University of Cape Town

Sequence	Group	Subgroup	Formation	Age	Reference	Structural Observations					
						Stowe (1986)	Beukes and Smit (1987)	Altermann and Halbich (1991)	Grobbelaar (1995)	This study -KBF03A	This Study- KBF01
Griqualand West	Postmasburg	Voëlwater	Mapedi								
			Mooidraai	2394 ± 26 Ma- Pb/Pb	Bau et al. (1999)		Folding and peneplanation of strata prior to deposition of Olifantshoek		Folding and erosion prior to Olifantshoek deposition, subsequent block faulting and the development of horsts and grabens		Ventersdorp, Ghaap and Postmasburg groups folded to form a syncline/anticline pair
			Ongeluk	* 2222 ± 12 Ma	Cornell et al. (1996)					Initial normal movement along F2.	
	Ghaap	Koegas						Recumbent fold zones, thrusts, imbricates and decollements in BIF- movement to SE, E and NE. Uitkoms Thrust- movement to east		Possible unconformity truncates BIF	
		Asbesheuwels	Griquatown	2489 ± 33 Ma	Trendall unpub. Ref in Nelson et al. (1999)					Development of a passive margin during an extensional environment	
			Kuruman	2465 ± 7 Ma- U-Pb	Armstrong pers. comm. (1996) ref in Martin et al. (1998)						
		Campbellrand	Gamohaan	2516 ± 4 Ma- U-Pb 2521 ± 3 Ma- U-Pb	Altermann and Nelson (1998) Summer and Bowring (1996)						Thermal Subsidence
			Monteville	2555 ± 19 Ma- U-Pb	Altermann and Nelson (1998)						Rift
		Schmidtsdrif	Vryburg	2642 ± 3 Ma- U/Pb	Beukes pers. comm.. 2001						

Table 3.3: (continued). * Ongeluk age is contested (see section 1.3.5.II.)

University of Cape Town

Altermann and Hälbich (1990, 1991) identify a deformational event in the field. Structural features identified include bedding-parallel thrusts within the BIF, one of which is named the Uitkoms Thrust (Altermann and Hälbich, 1991). It predates the Ongeluk lava and thus is > 2222 ± 12 Ma (Pb-Pb whole rock isochron age, Cornell *et al.*, 1996) and postdates the Koegas Formation. This Ongeluk age is contested (section 1.3.5.II.). A diagenetic age for the Mooidraai dolomite (stratigraphically above the Ongeluk lava) of 2394 ± 26 Ma (Pb-Pb isochron, Bau *et al.*, 1999) perhaps indicates that the deformational episode is 200 Ma older.

A second phase of deformation has been identified by Grobbelaar *et al.* (1995) and is correlated to structural observations made from line KBF01. In the mining areas around the Malmani dome, gentle, open folds of the Dimoten Syncline, Maremane Anticline and Ongeluk-Witwater Syncline are described. Grobbelaar *et al.* (1995) propose that this folding resulted in uplift and erosion to produce the unconformity upon which the Olifantshoek units were deposited. The age of this folding must be pre 1928 ± 4 Ma (Cornell *et al.*, 1998), the age of the Hartley Formation, lower Olifantshoek. Grobbelaar et al. (1995) also identify a phase of deformation involving block faulting and the development of a horst and graben structure. This too, is interpreted to precede the deposition of the Olifantshoek Supergroup (Grobbelaar *et al.*,1995). Similarly, in line KBF01 a normal fault is identified, which displaces the thrusted Ongeluk Formation. The age of this fault can only be estimated at < 2.2 Ga.

A third phase of deformation, described by Altermann and Hälbich (1990), postdates the Matsap, or lower Olifantshoek strata. It is associated with east-west compression producing mainly N-S trending duplexes and recumbent fold zones at a variety of scales (Altermann and Hälbich ,1991). This phase of deformation may be equivalent to that identified by Beukes and Smit (1987) and Coward and Potgieter (1983) which involved the development of the Blackridge Thrust Zone and the Boegeoberg-Doornberg Shear. These two structures postdate the Hartley lava, therefore, are younger than 1928 ± 4 Ma (Cornell et al., 1996). The amount of crustal shortening due to this thrusting has been estimated at around 35 to 55 km across the Blackridge thrust (Beukes and Smit, 1987) and a minimum displacement of 120 km is estimated across the Boegoeberg-Doornberg

University of Cape Town

Shear (Coward and Potgieter, 1983). Both tectonic features are possibly related to the Kheis orogeny and according to Beukes and Smit (1987) support thin-skinned tectonic deformation along the craton's western margin in the early Proterozoic. Grobbelaar *et al.* (1995) also recognize the possible relation of the Blackridge Thrust Zone to the Kheis orogeny. They claim the thrusting is defined by a single sole thrust, striking roughly N-S and dipping around 10 degrees to the west. They rename the Blackridge Thrust, the Kheis Thrust (Grobbelaar *et al.*, 1995). Altermann and Hälbich (1991) identify two further compressional phases in early Olifantshoek time that resulted in south and east verging folds and thrusts.

The Namaqua-Natal orogeny (1.0 – 1.2 Ga) resulted in deformation as far to the east as the Kaapvaal Craton's western boundary. Altermann and Hälbich (1991) claim that open folds observed along the southwestern margin of the craton are a result of this event. Namaqua-related compression also may have resulted in the development of strike-slip deformation around the margins of the craton. These shears are interpreted to reflect the last movements along the rim of the craton, occurring around 1.0 Ga (Altermann and Hälbich (1991).

Grobbelaar *et al.* (1995) also mention the development of lateral shears resulting from north directed late Namaqua compression. They state that compressive forces resulted in both the reactivation of pre-existing faults into dextral shears and the development of new faults and lineaments. A relaxation of this stress resulted in the development of a tensional stress field and the reversion of the shears into normal faults, forming horsts and grabens (Grobbelaar *et al.*, 1995).

Structural observations along the southwestern margin of the Kaapvaal craton are summarized as follows:

1) Bedding-parallel thrusts mainly within the BIF (Altermann and Hälbich, 1990, 1991), and other rocks older than the Ongeluk lava (2222 ± 12 Ma; Cornell *et al.*, 1998).

University of Cape Town

2) Folding and erosion prior to Olifantshoek deposition (Grobbelaar *et al.*, 1995). Block faulting and horst and graben structures also preceded Olifantshoek deposition according to Grobbelaar *et al.* (1995).
3) Recumbent folding and thin-skinned thrusting and the formation of the Blackridge/ Kheis Thrust. This structure is late Eburnean (~2.0- 2.2 Ga) in age and possibly related to the 'Kheis orogeny'.
4) The Namaqua-Natal orogeny open folding and subsequent strikeslip shearing in Kibaran times (1.0 – 1.2 Ga) (Altermann and Hälbich, 1991; Grobbelaar *et al.*, 1995).
5) Relaxation of the shear zones into normal faults (Grobbelaar *et al.*, 1995).

3.2.3 A comparison of surface observations to evidence from seismic profiles KBF03A and KBF01

1) Bedding-parallel thrusts within the BIF, described by Altermann and Hälbich (1990, 1991) may not represent the oldest tectonic event along the Kaapvaal Craton's western margin. Possible evidence for an older event is found in the seismic profile KBF01. The basal unit U may be the product of Ventersdorp-aged thrusting. If so, the oldest compression recognized along the craton's south western boundary is dated at around 2.6 Ga.

2) Bedding parallel thrusts are difficult to identify in seismic section. Thus, whether those described by Altermann and Hälbich (1990, 1991) are present in line KBF03A and KBF01 is uncertain. In addition, Altermann and Hälbich (1991) propose that trend of the thrusting is oriented mainly N-S, thus would not be easily identifiable in lines KBF03A and KBF01 which trend E-W.

3) Grobbelaar *et al.* (1995) describe gentle, open folds in the Maremane area which were subsequently eroded to produce the unconformity upon which the Olifantshoek Supergroup was deposited. Structural analysis of KBF01 identifies similar-style folding in the form of a distinct anticline/ syncline pair. However, in KBF01, the unconformity between the folded Griqualand West-aged units and the overlying Olifantshoek Group is

University of Cape Town

interpreted as tectonic. A breached anticline and resultant Neylan Unconformity is identified in seismic profile KBF03A. The age of this unconformity differs to that described by Grobbelaar *et al.* (1995). The Neylan unconformity marks the boundary between the Hartley and Lucknow Formations and is not at the base of the Olifantshoek Supergroup (Grobbelaar *et al.*, 1995).

4) Kheis thin-skinned thrusting of Eburnean age (Stowe, 1986), may be equivalent to thin-skinned thrusting of the Hartley lava, identified in line KBF03A. The compression direction is east-west (Altermann and Hälbich, 1990), as it is in line KBF03A. However, there is one important difference: The Blackridge/ Kheis structure thrusts Griqualand West strata over Olifantshoek strata (Beukes and Smit, 1987; Grobbelaar et al., 1995). Altermann and Hälbich (1990) describe similar thrusting of lower Griqualand West units in the Prieska- Boegoeberg Dam area. Thrusting in line KBF03A involves only Olifantshoek-aged units. This may be due to the Neylan Unconformity, which may have acted as an effective décollement, facilitating thin-skinned thrusting.

The age of the Kheis orogeny is debated. Ages range from 1750 to 2200 Ma. If the thin-skinned thrusting identified in line KBF03A is related to Kheis compression, the Kheis orogeny must be post-Hartley, therefore younger than 1928 ± 4 Ma (Cornell *et al.*, 1998).

5) Altermann and Hälbich (1991) and Grobbelaar *et al.* (1995) described Namaqua-Natal, Kibaran aged strike-slip motion along the rim of the craton. Evidence from line KBF03A also indicates a possible strike-slip component, perpendicular to the section, of movement along the master fault. This stems from the similarity of the pattern of normal faults associated with the master fault to a 'flower' structure. The late stage normal faults identified in line KBF03A may thus be related to the Kibaran aged shearing event.

5) The resumption of an extensive regime of late Kibaran age saw the relaxation of shears into normal faults (Grobbelaar et al., 1995). This may be correlated with phase three observed in line KBF03A, which sees the return of extension and the main normal movement along the master fault. In line KBF03A this extension is observed as normal displacement of thrusts. Grobbelaar *et al.* (1995) describe a similar scenario at Rooinekke

University of Cape Town

Mine, where the thrust is disrupted by N-S trending faults apparently related to the late Namaqua orogeny.

3.3. Modelling Archean-Paleoproterozoic lithospheric elastic thickness from observations of lithospheric flexure

3.3.1 Introduction

The western margin of the Kaapvaal craton, imaged in the seismic profile KBF03A, has a complex structural history involving at least a two stage tectonic environment. The lower succession comprises Ventersdorp and Griqualand West and lower Olifantshoek aged units, interpreted to have been deposited in a 'passive' continental margin environment. This would imply thermal subsidence following rifting of an unknown fragment away from the western margin of the Kaapvaal Craton (2.7 to 2.2 Ga). Following this, the 'passive' margin was transformed into an 'active' compressional margin. This compression created relative uplift and the subsequent erosion of this uplifted terrain produced the Neylan unconformity. Compression continued with the development of stacked thrust-packages and the loading of the passive margin sequence. The age of east-directed thrusting postdates the Hartley lava (1928 ± 4 Ma, Cornell *et al.*, 1998). Cornell *et al.* (1998) brackets regional Olifantshoek deformation between 1929 and 1750 Ma. Without an age for the overlying Volop quartzites, this is the best available approximation of the age of thrusting along KBF03A. The tectonic loading caused the foreland to be flexed downward to the west.

The structures identified of KBF03A provide new insight into the tectonic history of the Kaapvaal Craton's western margin. For example, the tectonic loading of the passive margin of the craton allows a rough determination of lithospheric elastic thickness at time of thrusting. Thus it is possible to calculate the strength of the lithosphere *after* the development of a passive margin.

University of Cape Town

What is elastic thickness?

The strength of the lithosphere can be expressed in terms of its rigidity (D). Elastic thickness is the term applied to the thickness of lithosphere that responds in an elastic manner to a load applied to it. The shape of flexure allows the estimation of flexural rigidity, hence lithospheric strength. It is of interest to see if elastic thickness (or rigidity of the lithosphere) changes over time and how it varies between different tectonic environments.

This sub-chapter outlines the application of an established method of the estimation of elastic thickness from observations of flexure related to external loading. We begin with a discussion of where this method has been applied followed by a description of the method as applied to structures identified on line KBF03A. To achieve this, it was necessary to isolate flexure associated with loading from that produced by earlier subsidence in the west during the development of the passive margin. Section 3.3.3.I. details how this is achieved. The results of the calculations are summarized in section 3.3.4. and are followed by a discussion (section 3.3.5) which aims at highlighting both the problems and assumptions associated with the calculations. An interpretation in terms of the broader context of late Archean and early Proterozoic tectonics follows.

University of Cape Town

3.3.2. Variations of elastic thickness in different tectonic settings

The calculation of lithospheric elastic thickness during compression in this study is made in the context of similar calculations in several locations of convergence world-wide. McNutt et al. (1988) has compiled varying elastic thickness values for continental thrust belts. The flexure of the European lithosphere beneath the Apennines, Carpathians and Alps has been extensively researched (Royden, 1988; Kruse and Royden, 1994; Zoetemeijer *et al.*, 1995; Stewart and Watts, 1997). Calculation of elastic thickness has also been carried out for the north eastern Australian margin flexed beneath the Papua New Guinea orogenic belt (Haddad and Watts, 1999) and for flexure associated with the Andes and Appalachians (Stewart, and Watts, 1997). Only few similar calculations have been made for older terrains. For example, Grotzinger and Royden (1990) calculate an

elastic thickness at 1.9 Ga of 12 ± 4 km along the north eastern margin of the Archean Slave Craton. This latter example has special significance for the Kaapvaal Craton's western margin due to its similar age of thrusting. In the above examples, data used to constrain timing and degree of flexure include gravity, seismic reflection profiles, wells and bio- and lithostratigraphy.

The elastic thickness of European lithosphere flexed beneath the Carpathians and Appenines is thin at 3 to 16 km (Royden, 1988; Kruse and Royden, 1994; Zoetemeijer *et al.*, 1995). Kruse and Royden (1994) modelled deflections of the Adriatic lithosphere beneath the Apennine thrust front incrementally. Their results are consistent with those obtained for total flexure (Kruse and Royden, 1994). Lateral changes in elastic thickness are reflected in the varying geometry of associated foreland basins. There have been a number of reasons suggested to explain lateral change in European lithospheric strength, one being a mechanical cause involving high curvature of flexure causing a reduction in elastic thickness (Kruse and Royden, 1994; Zoetemeijer *et al.*, 1999).

Elastic thickness calculated for the north-east Australian margin differs laterally from a maximum of 70 to 80 km to a minimum of just 8 km (Haddad and Watts, 1999). In the Australian case, local weakening of the lithosphere is suggested to be a result of thermal processes due related to late Tertiary volcanism (Abers and Lyon-Caen, 1990).

Stewart and Watts (1997) calculated the elastic thickness of the Andes lithosphere, which varies from 5 to 85 km across and along strike of the orogen. These variations are attributed to the inheritance of thermal and mechanical properties of the foreland lithosphere.

Decreasing lithospheric strength, calculated from flexure induced by loading during compression, may be influenced by the following factors.

1) Decoupling between the upper crust and mantle lithosphere (Burov and Diament, 1995,1996; Zoetemeijer *et al.*, 1995). Decoupling is illustrated in figure 3.4.
2) Heating of lithosphere from below during load emplacement.

University of Cape Town

3) Strong deformation and high plate curvature (Kruse and Royden, 1994; Zoetemeijer *et al.*, 1995, Stewart and Watts, 1997).
4) Increase in the depth to basement due to subsidence and deposition of new sediment by increasing the equilibrium thermal gradient in the basin. (Kominz and Bond, 1986).
5) Inheritance of thermal and mechanical properties of the foreland lithosphere results in great variations in elastic thickness (Stewart and Watts, 1997).

Though there may not be consensus regarding the mechanism(s) causing variations in lithospheric strength (perhaps different causes dominate in different tectonic settings) one point that is agreed upon is the extreme heterogeneity in plate strength reflected by elastic thickness.

3.3.3. Method

An adaptation of the method used in some of the examples above has the following aim: To constrain elastic plate thickness (Te) *at time of flexure* linked to loading of the foreland due to thrusting of Olifantshoek aged strata (1750 to 1929 Ma). Underlying the calculation is the assumption that the flexed lithosphere acts as an elastic sheet. It behaves neither in a brittle or ductile fashion in that pure elastic deformation is recoverable. The flexural equation is derived by considering all forces and torques acting on a flexed plate and relating those to stress and strain changes coupled with deflection. The flexural equation has been constructed to approximate the response of plates of variable elastic thickness under varying loads (Royden, 1988) (appendix B).

The method involves the substitution of various estimates of flexural wavelength (related to elastic thickness) into the flexural equation. For each estimate of flexural wavelength, a separate theoretical solution or flexural curve is generated from the calculation of the adapted flexural equation (see appendix C). The curve that best fits the data has the most realistic flexural wavelength (expressed) as an alpha value and represents the most realistic elastic thickness. In reality, a range of alpha values may present a possible fit to the data, yielding a range in elastic thickness. Traditionally, gravity data have been used to narrow the range of possible elastic thickness values and to offer an independent check

University of Cape Town

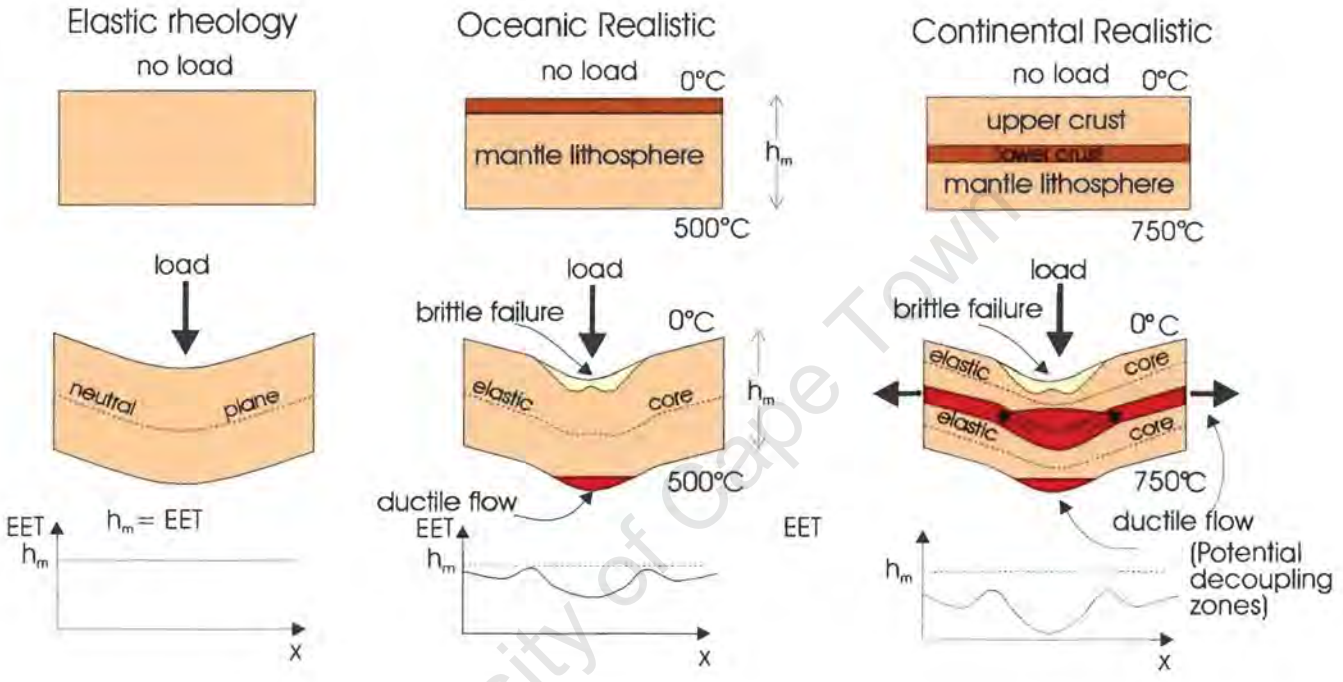

University of Cape Town

Figure 3.4: Illustration of the difference between an idealized elastic plate and realistic continental and oceanic plates. Plates are elastic until a load is added which produces areas of inelastic strain resulting in local weakening. In the continental case, a weak lower crust facilitates a mechanical decoupling between upper crust and mantle, thus weakening the plate and lowering the effective elastic thickness (after Burov and Diament, 1996).

on the validity of the results. Unfortunately the gravity data could not be used in this thesis.

3.3.3.I. Separating passive margin subsidence from flexure produced by loading during compression

The aim of the calculation is to calculate lithospheric elastic thickness *during time of flexure associated with loading* during a compressional regime. Thus flexure produced by loading of sediments during the development of a passive margin has to be separated from that produced by subsequent tectonic loading of these sediments during compression. To achieve this, a seismic reflector was chosen which is assumed to have been sub-horizontal, prior to load emplacement. The base of the Campbellrand Subgroup is assumed originally horizontal for two reasons:

1) The Campbellrand Subgroup is a platform carbonate sequence, likely to have formed in shallow water depths.
2) The Campbellrand Subgroup does not thicken substantially to the west across the seismic profile, indicating that any passive margin subsidence was similar across the margin.

Using this information, it is possible to isolate deflection of the passive margin sediments due to loading, from flexure produced by preferential subsidence and sediment accumulation in the west.

3.3.4. Results

Theoretical flexural curves for varying elastic thickness (5, 7.5, 10, 15, 20 and 30 km) were calculated and compared to the actual deflection noted from the seismic profile KBF03A (figure 3.5). The flexural wavelengths corresponding to these elastic thicknesses are 26, 36, 45, 67, 76 and 102 km respectively.

- In general, the smaller flexural wavelengths, thus thinner elastic thickness, offered a better fit to the observations.
- The shortest wavelength chosen, 26 km, is a poor fit for the following reasons:

University of Cape Town

1) At plate end (x = 0), the curve calculated for an elastic thickness of 5 km (flexural wavelength of 26 km), levels off. This does not match the deflection observations from the seismic line which increase by increasing amounts as x tends to 0.
2) 65 km from plate end, deflection for Te = 5 km is calculated at 0. The geological map (figure 3.6) indicates that the contact between the Schmidtsdrif and Campbellrand outcrops at 180.5 km from plate end. Therefore, the flexural curve calculated for an elastic thickness of 5 km results in an incorrect positioning of the flexural bulge. It is too narrow in width and lies too far to the west, toward plate end. The flexural wavelength is thus too short to adequately match the observations, therefore the *elastic thickness was greater than 5 km.*

- The three flexural curves generated for flexural wavelengths of 67, 76 and 102 km (elastic thickness of 15, 20 and 30 km) also show a poor fit to observations because:
    1) From plate end to 30 km all three flexural curves underestimate the observed deflection.
    2) From 30 to 90 km from plate end, the observed deflection is overestimated.
    3) In all three cases the flexural bulge falls too far to the east.
    4) The curves differ by 150 to 300 km from the two observations at 180.5 and 202.5 km from plate end. Thus at time of load emplacement, *elastic thickness was less than 15 km.*

- The remaining two curves plotted offer significantly better fits to the observations.
    1) From plate end to 45 km, both flexural curves for elastic thickness of 7.5 and 10 km closely fit the observed deflections.
    2) However, from 52.5 to 82.5 km both curves overestimate observed deflection. The elastic thickness curve of 7.5 km overestimates deflection to a lesser extent.
    3) The observation at 180.5 is best fit by the flexural curve representing an elastic thickness of 10 km. It differs by only around 7 m in this case.

University of Cape Town

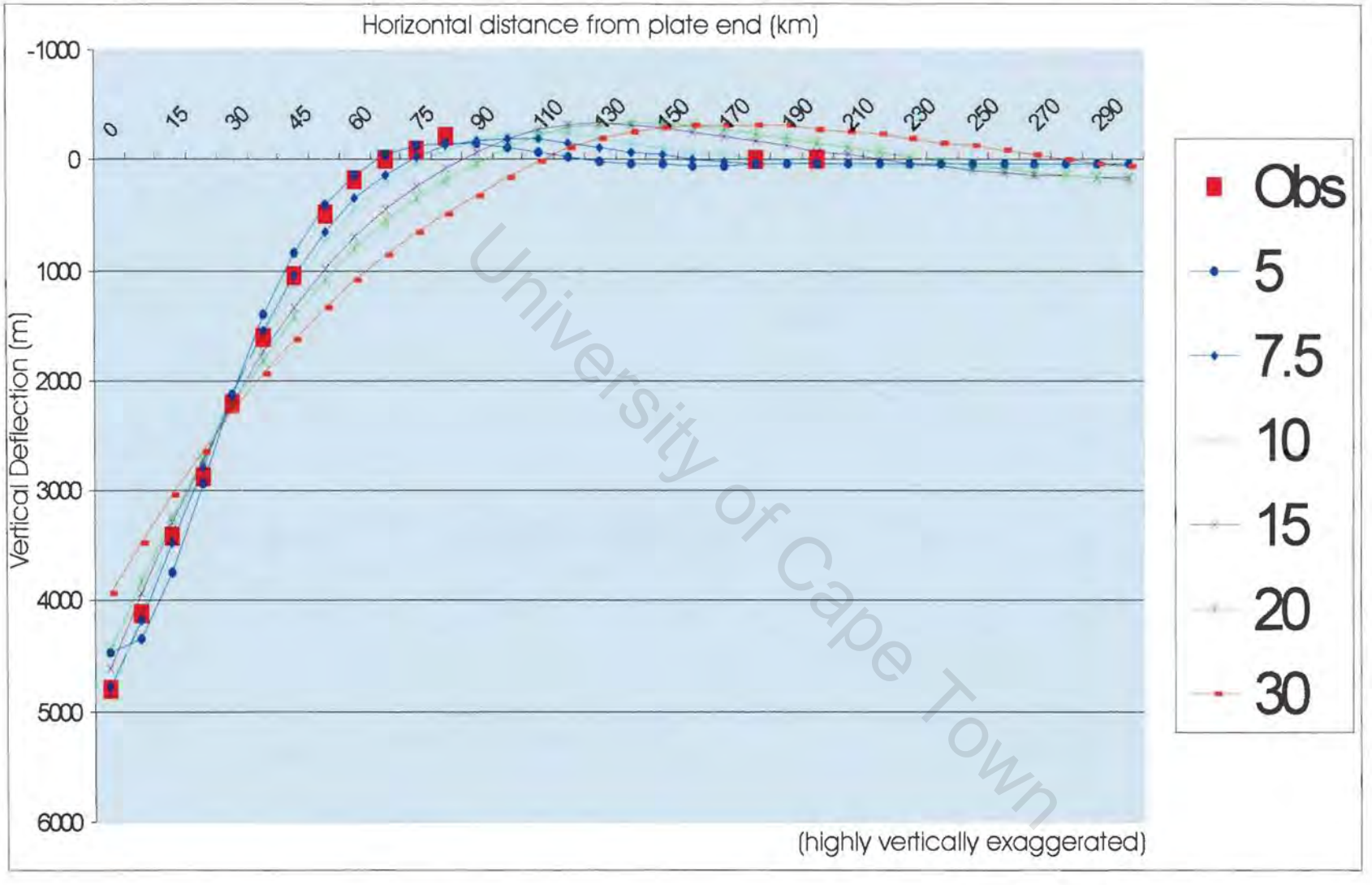

University of Cape Town

Figure 3.5: A comparison of theoretical curves, generated by calculation of the flexural equation for various estimates of elastic thickness. Flexures is caused by tectonic loading of Griqualand West and Olifantshoek Sequences during compression and is observed from seismic profile KBF03A (red squares).

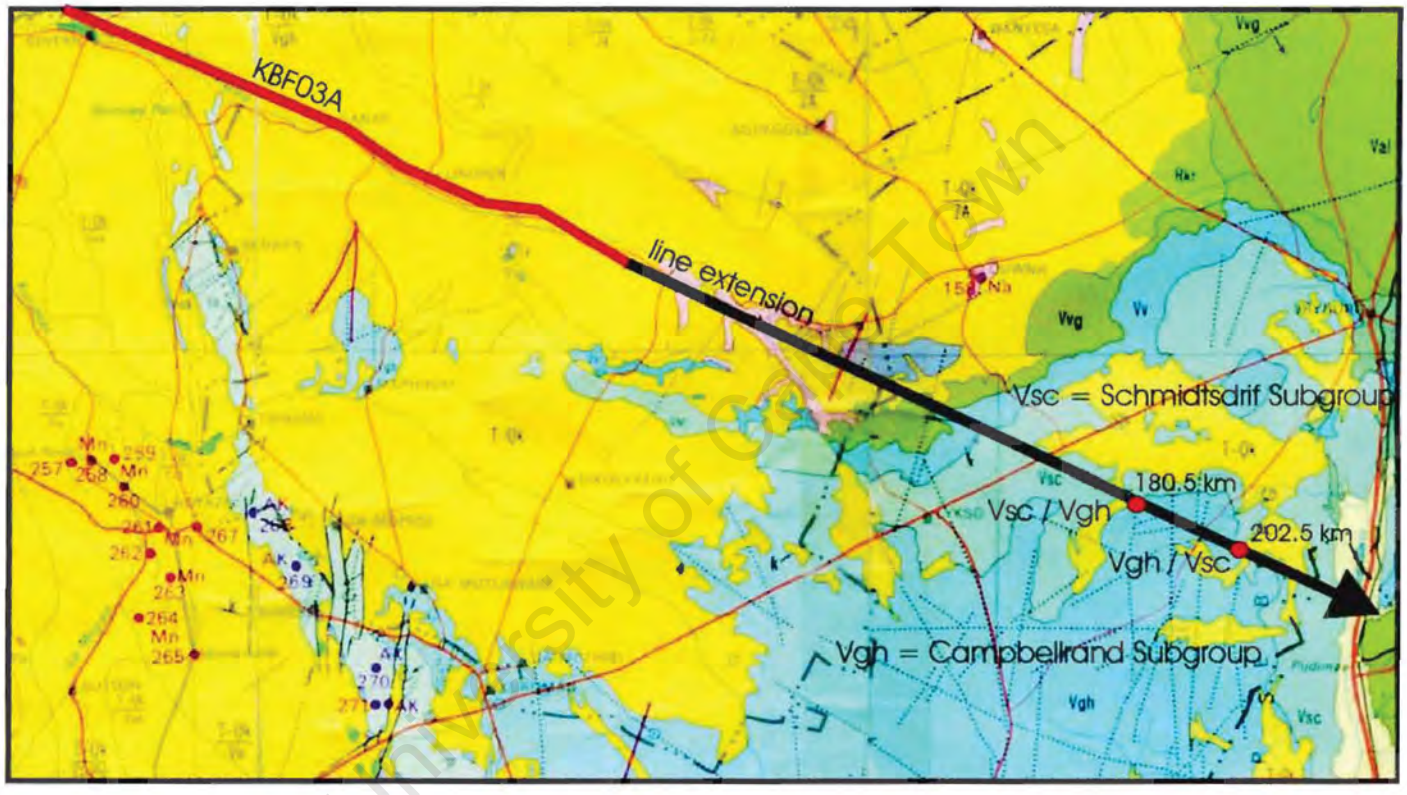

University of Cape Town

Figure 3.6: Geological map including the extension of line KBF03A to two observation points (marked in red).

With (so little difference between these two curves, the elastic thickness of the plate during time of flexure is estimated to have been in the range of 7 to 10 km.

3.3.5. Discussion

The elastic thickness of 7-10 km is suprisingly thin and it is important to evaluate this in light of a number of uncertainties.

1) Flexural observations made east of 52.5 km were calculated by adding an average thickness for the Schmidtsdrif Subgroup to the granitic basement / Schmidtsdrif contact. Since the Schmidtsdrif Subgroup thins to the east, the height of the contact above basement, estimated by taking an average thickness, may be overestimated in this area. However, both the theoretical curves calculated for an elastic thickness of 7.5 and 10 km also overestimate flexure in this interval, thus they may fit the true flexure better than the estimated observations would suggest.

2) There is uncertainty regarding the observational points at 180.5 and 202.5 km from plate end, east of the flexural bulge. These were established from a geological map (figure 3.6). The points fall within what has been described as the Takwan Trough (Beukes, 1986). Due to the 2 Ga age of flexure, there are likely to have been later tectonic events that may have effected this trough. Thus the compression that resulted in the Takwan Trough may have altered the position of the Campbellrand / Schmidtsdrif contact since flexure. In addition, the Campbellrand Subgroup in the Pering area, 25 km to the south east, is over 2000 m thick. This puts the Campbellrand / Schmidtsdrif contact at a considerably greater depth than that expected along the extension of the line KBF03A, at a distance of just 25 km.

Despite the uncertainty in the position of the observation points to the east of the flexural bulge, it remains true that the curves calculated for an elastic thickness of 7.5 and 10 km best fit the observed data to the west of the flexural bulge. Curves calculated for elastic thickness greater than 15 km are poor fits to this data.

University of Cape Town

3. Velocity/ Depth Conversion uncertainty. Observations were made by converting two way time to measure actual depth of contact. This conversion was achieved by using P wave velocities in table 2.1. There could be no correction for compaction due to lack of lithological control. The observations therefore must be regarded as maximum depths to the contact.

4. In modern examples of estimation of elastic thickness from flexural observations, it is possible to be sure that deflection observations are a direct result of a particularly tectonic conversion event. An Archean/ Proterozoic terrain such as the Kaapvaal craton's western margin, however, has been exposed to numerous subsequent tectonic events that may have distorted the primary flexural signal due to loading of the Olifantshoek aged thrusts

5. Lack of independent gravity constraint. In most of the applications of this type of calculation of elastic thickness, gravity data offer an important constraint on estimate of elastic thickness. The gravity profile expected to result from flexure associated with loading is included in figure 3.7. However gravity data provides only a present day signature. Since this region contains Archean aged sediments that have undergone a long complex structural history, it is difficult, without more detailed information, to back calculate the gravity anomaly pattern caused by flexure at 1.9 – 1.7 Ga. Thus, the gravity data could not be used as an independent measure of elastic thickness or be used to constrain values calculated from the observation of flexure. Without the independent constraint offered by gravity data, the results have to be treated with caution.

6. Assumption of uniform initial water depth. The method assumes a uniform initial water depth across the profile, KBF03A. The Campbellrand/ Schmidtsdrif Subgroup contact is regarded as initially sub-horizontal because the Campbellrand Subgroup formed as a carbonate platform sequence. However they may have been subtle differences in initial water depth over the long length of line, 200 km.

These uncertainties, however, would not significantly alter the results.

University of Cape Town

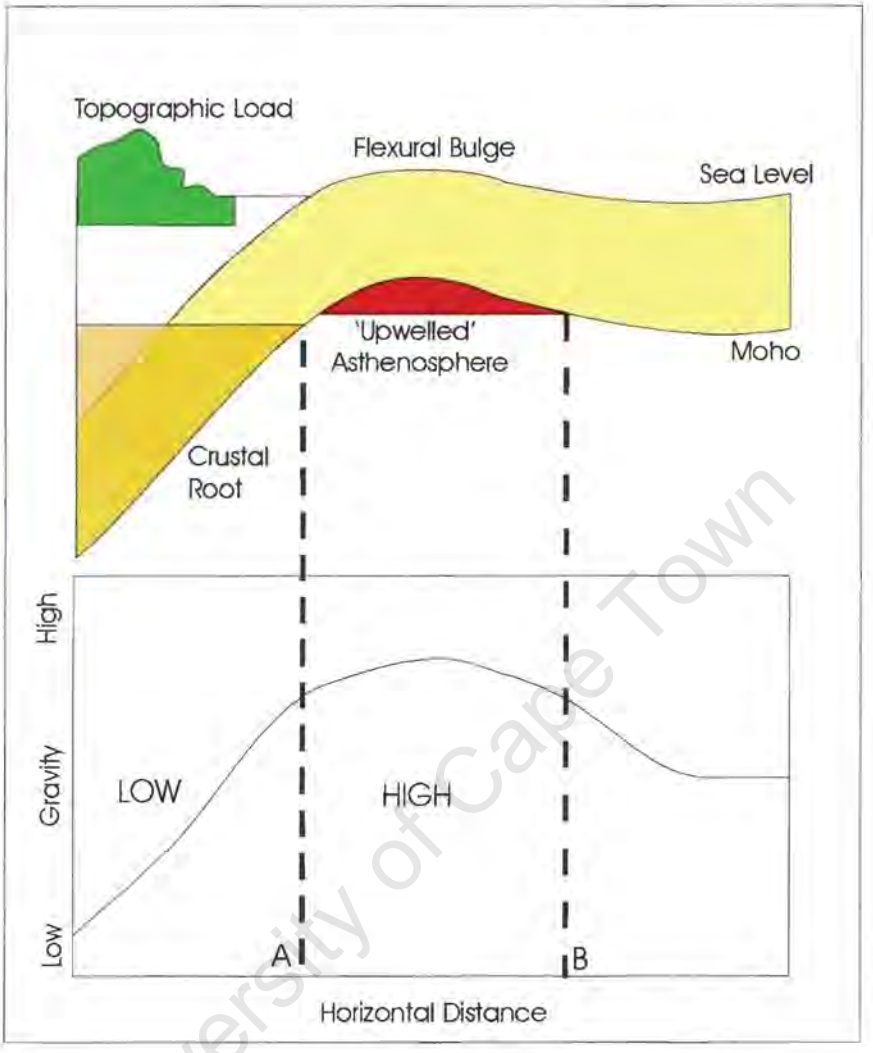

University of Cape Town

Figure 3.7: Schematic diagram to illustrate the expected gravity signature resulting from flexure induced by instantaneous loading. Gravity low, east of B, is associated with shallowing of granitic basement. Gravity high, between A and B, corresponds to where flexure of underlying units is mirrored by the Moho, which is relatively flexed upward. The latter results in dense asthenosphere being at relatively shallower depth thus causing the gravity high. The gravity low, to the west of A is due to thickened sediments in foreland basin as well as the depressed crustal root.

3.3.6. Implications

A thin lithospheric elastic thickness contrasts with a 60 – 70 km thick present-day lithosphere calculated for the craton as a whole (Doucouré *et al.*, 1996). It is therefore valuable to compare the thin value of lithospheric elastic thickness calculated here to present day estimates of the same region. Has there been lithospheric strength recovery? What are the possible explanations for such a low lithospheric elastic thickness at 1750 to 1929 Ma? What is the role of inherited passive margin lithospheric elastic thickness to that calculated during subsequent flexure induced by loading? How representative is this low lithospheric elastic thickness value for Paleo-Proterozoic lithosphere as a whole?

3.3.6.I. Comparison of calculated elastic thickness to present day estimates for the region

Doucouré *et al.* (1996) and Hartley *et al.* (1996) review the isostasy of southern Africa by calculating elastic thickness from Bouguer gravity data and topographic information. The highest elastic thickness values correlate with cratonic regions, the lowest with younger fold belts and rift systems. Figure 3.8a (Doucouré *et al.*, 1996) shows present-day elastic thickness for the area over which KBF03A was shot. From this figure, elastic thickness along line KBF03 is fairly constant from east to west at around 60 to 70 km. Figure 3.8b shows another estimate of present-day elastic thickness for this area (Hartley *et al.*, 1996). Line KBF03A lies in the elastic thickness interval of 40 to 60 km.

The estimated present day elastic thickness is at least seven to ten times greater than that calculated at 1750 to 1929 Ma. Thus elastic thickness may have remained thin for around 600 to 800 Ma, from the Kaapvaal craton's destabilization at 2600 Ma to 1750 to 1929 Ma. Since this Mesoproterozoic time, the elastic thickness of the craton has thickened to reach its present day value of 40 to 70 km. It is not known if the elastic thickness increased gradually or episodically.

University of Cape Town

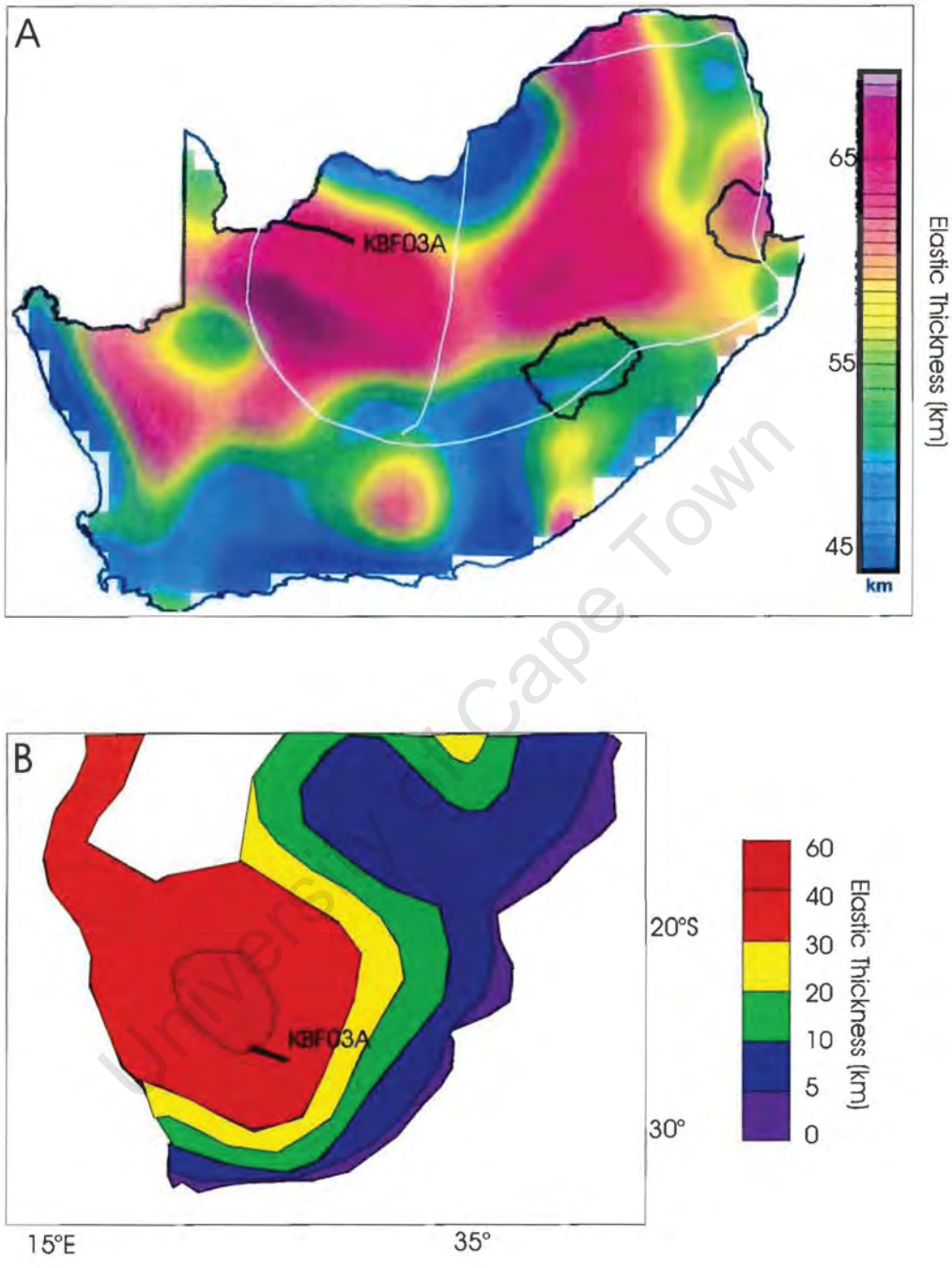

University of Cape Town

Figure 3.8: Lithospheric elastic thickness estimates. A: from Doucouré and De Wit. (2001) B: from Hartley *et al.* (1996).

3.3.6.II. Variation in continental elastic thickness: past and present

A relatively thin elastic thickness for Proterozoic terrain is not unique. In a flexural study of the Kilohigok Basin in the Archean Slave Craton an elastic thickness of only 12 ± 4 km was calculated (Grotzinger and Royden, 1990). Effective elastic thickness is 100 ± 25 km for the area today (Grotzinger and Royden, 1990). From this data the authors conclude that at 1.9 Ga the Slave Craton lacked the several hundred kilometre thick mechanical layer it has today, implying a significant thickening in the last 1.9 Ga. They also suggest that geothermal gradients were two to four times higher then than at present. This seems, as the authors point out, contrary to other cratonic data, for example from the Kaapvaal craton, that suggest the existence of thick mantle roots since Archean time (Boyd et al., 1985).

Present day elastic thickness of tectonically active areas, however, varies considerably, and elastic thickness is dependent on a number of different factors. It is not unrealistic to assume the similar if not greater varieties existed in the Proterozoic, since many of the factors controlling elastic thickness are equally likely to have been important then too. Locally, at least, heat flow may have been higher in the Archean due to a 3 to 6 times higher radiogenic heat production (Pollack, 1997).

The low elastic thickness during time of flexure along the Kaapvaal craton's western margin may have been inherited from earlier passive margin development. Some of the lowest elastic thicknesses have been observed at passive margins (Stewart and Watts, 1997). Reemst and Cloetingh (2000) note the resulting reduction in lithospheric strength following rifting on the Trondelag Platform, Voring Margin (mid-Norway). Minimum values of around 10 to 12 km for elastic thickness were obtained in the centre of the rift basin during extension (Reemst and Cloetingh, 2000). Recent research has shown that there may be significant rapid gradients from weakened, rifted lithosphere to stronger cratonic lithosphere.

Figure 3.10 shows elastic thickness gradients calculated for the Voring margin (Reemst and Cloetingh, 2000), the Andes margin (Stewart and Watts, 1997) and an inset of the

University of Cape Town

Kaapvaal craton and its western margin at a similar scale. The locations of the geophysical transects are shown in figure 3.9. Figure 3.10 demonstrates the variation in elastic thickness with distance from the margin, a characteristic of both passive and active tectonic settings. It is possible, therefore, that the thin elastic thickness calculated for this region of the Kaapvaal Craton, merely represents a marginal effect at 1.7 to 1.9 Ga. The margin may be weaker section within or along the margin of a strong lithosphere of far greater elastic thickness. "Lateral variations in elastic thickness are expected to exist as we move from margins toward the interior of continents" (Stewart and Watts, 1997). It is possible that further from the margin, the elastic thickness could increase to typical cratonic values as is evident from the Andes and Norway examples.

3.3.6.III. Lithospheric strength recovery?

Stewart and Watts (1997) claim that no low values of elastic thickness have been estimated from Paleozoic orogenies using standard methodology of flexural and gravity modelling. They infer that this is due to either of two reasons:

1) Weak orogens are preferentially destroyed in geological processes
2) Stretched and weak lithosphere is able to recover its strength.

Results from this study of the Kaapvaal Craton's western margin and those obtained for the Slave Craton (see section 3.3.6.II) are both examples where thin elastic thicknesses have been calculated for the Paleoproterozoic, in regions where present day values for the same terrain are now substantially higher. The Kaapvaal Craton's western margin is thus perhaps a prime example of the recovery of lithospheric strength. Greater sampling of older terrains is needed however, to further constrain which of the above two possibilities is more probable.

University of Cape Town

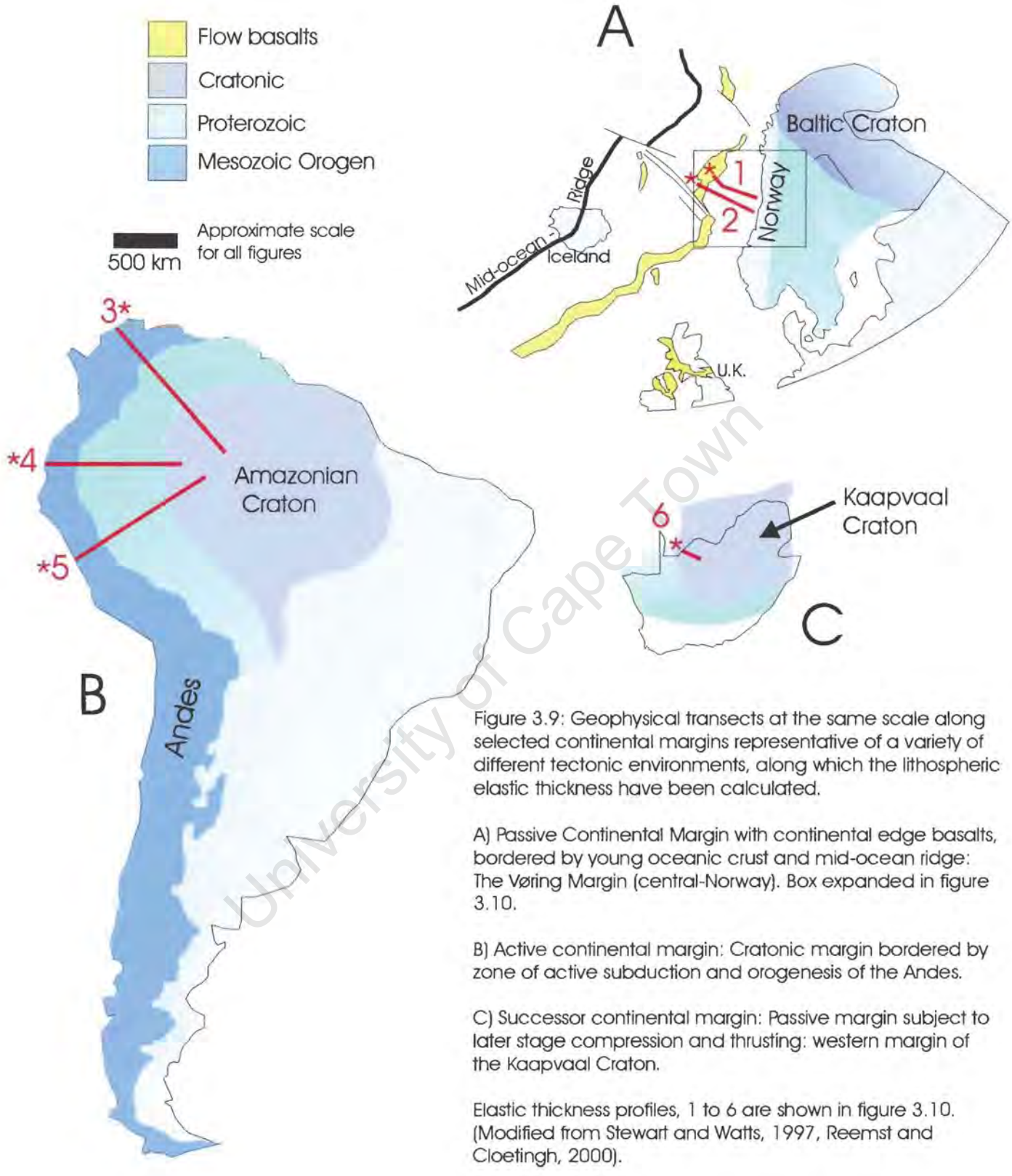

University of Cape Town

Figure 3.9: Geophysical transects at the same scale along selected continental margins representative of a variety of different tectonic environments, along which the lithospheric elastic thickness have been calculated.

A) Passive Continental Margin with continental edge basalts, bordered by young oceanic crust and mid-ocean ridge: The Vøring Margin (central-Norway). Box expanded in figure 3.10.

B) Active continental margin: Cratonic margin bordered by zone of active subduction and orogenesis of the Andes.

C) Successor continental margin: Passive margin subject to later stage compression and thrusting: western margin of the Kaapvaal Craton.

Elastic thickness profiles, 1 to 6 are shown in figure 3.10. (Modified from Stewart and Watts, 1997, Reemst and Cloetingh, 2000).

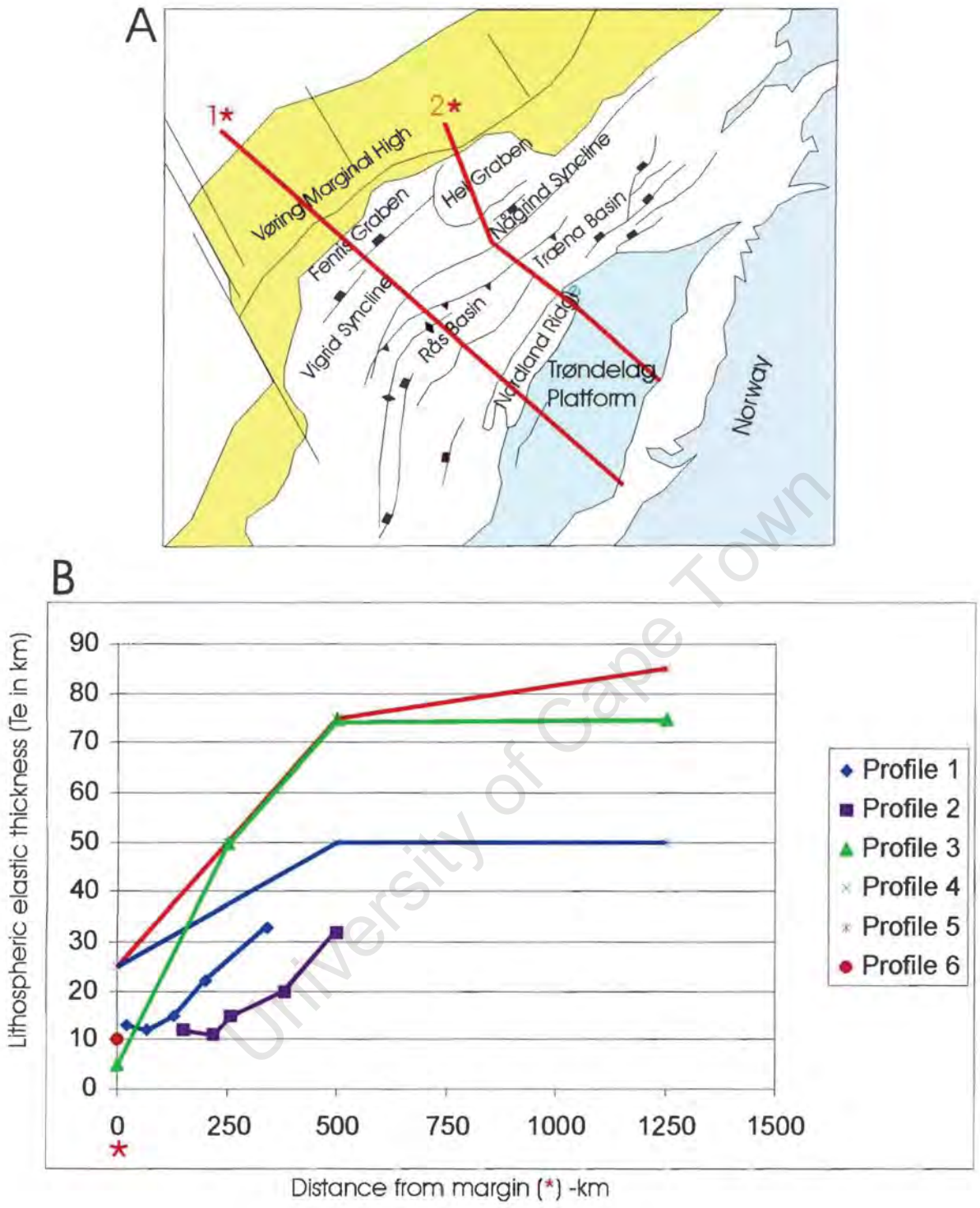

University of Cape Town

Figure 3.10: A) Expansion of box in figure 3.9 (from Reemst and Cloetingh, 2000). B) Variation of lithospheric elastic thickness across continental margins for profiles 1 to 6. Location of profiles shown in figure 3.9.

3.3.6.IV. Why is the estimated elastic thickness of the Kaapvaal Craton edge so thin at 1750 to 1929 Ma?

Thermal effect

Some authors consider heat flow to correlate inversely to elastic thickness (Zoetemeijer *et al.*, 1990; Hartley *et al.*, 1996). Thus thermal effects can alter elastic thickness, but not if separated from load emplacement by sufficient time. For example, Zoetemeijer *et al.* (1999), in their study of flexure beneath the Carpathians, expect little thermal influence of Jurassic rifting on subsequent evolution of the 'Neogene wedge', because theoretically the thermal equilibrium would have been reached. This represents a time gap of approximately 120 to 200 Ma.

The last two periods of volcanic activity in the Griqualand West basin prior to late Olifantshoek aged thrusting, involved the extrusion of the Ongeluk basalts at 2222 ± 12 Ma (Cornell *et al.*, 1996) and the extrusion of the Hartley Formation basalts and tuffs at 1924 ± 4 Ma (Cornell *et al.*, 1998). The thermal effect associated with the extrusion of the Ongeluk Formation is likely to have been re-equilibrated in the 200 Ma time gap between extrusion and loading. The maximum amount of time between the Hartley extrusion (1928 ± 4 Ma, Cornell *et al.*, 1998) and thrusting (bracketed at 1.9 to 1.7 Ga) is also 200 Ma. However, the extrusion of the Hartley lavas may predate thrusting by far less time than this maximum estimate. The thermal effect of this episode of volcanism could have had an influence on the elastic strength of the lithosphere, a reduction in elastic thickness. Heating weakens the lower crust, which may result in a decoupling of upper and lower parts of the lithosphere, thus causing a weakening of the plate (Abers and Lyon-Caen, 1990).

However, the link between volcanism and plate weakening is not fully understood. Abers and Lyon-Caen (1990) point out that it is difficult to assess whether heating due to igneous intrusion weakens the plate, or it is because the plate is weak that the intrusion reaches the surface. These authors also mention that without knowledge of the extent of the intrusion at depth it is difficult to ascertain whether heating due to volcanism is sufficient to reheat the lithosphere.

University of Cape Town

3.3.6.V. Relation of elastic thickness to tectonic style

It is proposed in Watts et al. (1995) that the strength of underlying lithosphere controls the tectonic style of the orogen and thin-skinned fold and thrust deformation and low angle decollement surfaces are related to advancement onto stronger lithosphere. Higher elastic thickness implies shallower deflections of the lithosphere when subject to loading. Stewart and Watts (1997) mention that the underthrust lithosphere will tend not to become incorporated in the deformation. Weaker lithosphere will result in greater deflection and the likely involvement of underthrust lithosphere in the deformation. This relationship between elastic thickness and tectonic style is supported by observations from southern Peru and Bolivia (Stewart and Watts, 1997).

Elastic thickness calculated along line KBF03A has shown that, at the time of thrusting, the underthrust lithosphere was relatively weak. This is apparent from the high deflection beneath the thrusts, and corresponding low elastic thickness. However, the thrusting is thin-skinned and a low angle decollement surface (Neylan unconformity) is apparent. In addition there has been very little or no involvement of the underlying passive margin material in the deformation. This is opposite to what is expected for loading by thrusting onto weak lithosphere as described above. A possible reason for this discrepancy is that only this narrow region is so weak. As described in 7.4 above, perhaps there is a rapid increase in elastic thickness, thus lithospheric strength, to the east of the profile, toward the centre of the craton. Rapid changes in lithospheric strength have been shown to occur craton-wards. 1.7 to 1.9 Ga sees the deposition of the Waterberg Sequence in fault-bounded basins spanning the Kaapvaal Craton interior. These brittle structures imply a stronger central cratonic interior, which may support the suggestion that the elastic thickness calculated here represents just a narrow transition to a much stronger craton. This area today has an effective elastic thickness of 60 to 70 km (Doucouré *et al.*, 1996). The mechanisms responsible for recovery of this elastic thickness are beyond the scope of this thesis.

University of Cape Town

Chapter 4 : Summary and Conclusions

The seismic profiles interpreted in this study roughly fall into three areas:

1) The Kaapvaal Craton's western margin (KBF03A, KBF01)
2) The Bushveld Lines within the confines of the 2.06 Ga Bushveld Complex Province (Buick *et al.*, 2001) (Rz-254, 255, 256)
3) The craton interior (YS, OB, AG).

Information gathered from the interpretation of these seismic profiles has given new insight into some of the stratigraphic and structural questions pertinent to these areas.

4.1. The Kaapvaal Craton's Western Margin

Tertiary Kalahari cover obscures most of the northwest margin of the Kaapvaal Craton. Geophysical techniques, including gravity and magnetics, are the only methods of observing structure along this part of the craton margin. The interpretation of newly released seismic reflection data has resulted in increased understanding of stratigraphic and structural detail of this area and the identification of many, previously undescribed features. Some of these features are:

- *The prominent listric fault, F2*, displacing the succession downward to the west, by > 6 km (<~2.2 Ga). This master fault has been reactivated during compression (~1.9- 1.7Ga) and post Karoo and pre Kalahari deposition. The similarity of antithetic faults associated with F2, to a 'negative flower structure' suggests a component of strike-slip motion.
- *The Neylan unconformity*, between the lower Olifantshoek succession and Hartley Formation above. To the west the unconformity either dies out, or becomes bedding parallel.
- *The tectonostratigraphic (duplexed) nature of the Hartley Formation*. Eastward verging thrusting is initially thin-skinned on craton, then involves the entire Hartley Formation resulting in tectonic thickening of ≥ 300 % (~1.9- 1.7 Ga).
- *The Dwyka unconformity*, formed as large glacial valleys cut into underlying basement thrusts during the Dwyka glacial event (~ 350 to 300 Ma).

University of Cape Town

- *The Tertiary Kalahari unconformity*, which is channelized and cuts into underlying Karoo, Olifantshoek and Griqualand West sequences.

The interpretation of seismic Profile KBF01, which traverses greater outcrop to the south of KBF03A, has resulted in the identification of:

- *The Maremane anticline and Dimoten syncline* in section.
- *An unknown unit at depth*. This unit may be composed of west dipping basalt reflectors of Ventersdorp age. This may indicate the presence of an oceanic-continental boundary along the western margin of the Kaapvaal Craton. Similarities were found between the unknown unit and those of extensional margins worldwide, in terms of orientation (reflectors dipping away from the continent), seismic character, and estimated thickness (up to 7 km).
- *Thrusting of lower Olifantshoek and upper Griqualand West strata*. Seismic data substantiated the stratigraphic position of the Gamagara Formation as correlative with the Madedi Formation (lower Olifantshoek Supergroup) as proposed by Beukes and Smit (1987).

These observations have led to the further discussion:

- Immediately apparent from the seismic profiles KBF03A and 01, is the rapid thickening of the sedimentary succession to the west (from basement outcrop to > 17 km along KBF03A). This implies a high and increasing amount of subsidence and creation of accommodation space westward, towards the craton edge. *Sediment accumulation rates* across the margin of the craton have been calculated and compared to modern day estimates and estimates from age-equivalent (and possibly correlated) basins for example the Hammersley Basin of western Australia. Sediment accumulation rates calculated from KBF03A average approximately two times less than those calculated for the same stratigraphic groups by previous authors and an order of magnitude lower than most modern carbonate depositional environments. This latter difference supports the suggestion that Archean carbonate deposition may have occurred by different processes to present day carbonate formation as proposed by Grotzinger (1989).

University of Cape Town

- A *tectonic history* of the craton's northwestern margin is proposed. This has been compared to previous models arising from structural mapping of better outcrop in the south. Many of the southern structural observations are confirmed by structural interpretations of the seismic data.
- It has been possible to calculate lithospheric elastic thickness at 1.9 to 1.7 Ga, from the analysis of lithospheric flexure produced by tectonic loading. Elastic thickness is estimated at 7 to 10 km, which is 7 to 10 times greater that estimates for the same area today, because present day elastic thickness for this area is ~60 to 70 km (Doucouré *et al.*, 1996). This implies that since 1.9 – 1.7 Ga, there has been lithospheric strength recovery. The unusually thin value for elastic thickness around 2.0 Ga, may reflect KBF03A's location near the craton margin. High gradients, from thick, strong cratonic lithosphere, to thin, weak lithosphere along the margins have been calculated elsewhere, for example, the Norwegian, Andean and Antarctic margins.

4.2. The Bushveld Lines

Interpretation of the seismic profiles, Rz-254, 255 and 256 resulted in the identification of the following:

- Ventersdorp listric basins, with east-west striking boundary faults.
- The prominent black reef unconformity, showing clear truncations of the underlying Ventersdorp Supergroup.
- A large scale, shallow syncline, involving the Transvaal Sequence and striking east-west over hundreds of kilometers.

The Bushveld intrusion was seismically unresolved, implying that it is extremely thin in this location. Reflections noted within the basement, however, may be sills related to the Bushveld intrusion. This proposition is supported by the fact that these basement reflections are of highest amplitude and number along Rz-254, relative to other interpreted lines on the western margin and craton interior.

University of Cape Town

4.3. The Craton Interior

The following features were noted from seismic profiles OB, AG and YS:

- *Horst and graben structures* composed of Dominion, Witwatersrand and lower Ventersdorp Supergroups (OB and AG).
- *Listric growth fault bounded Ventersdorp basins*. Bounding faults had a approximate east-west strike and dipped to the north and south (YS).
- The *Black Reef unconformity* is particularly prominent in its truncation of several units below.
- *Open folding of the Transvaal Supergroup*, with fold axes trending approximately east-west (OB and AG).
- The *distinctive Beaufort unconformity*, truncating several older groups (OB).

From the apparent east/ west strike of the listric faults bounding the Ventersdorp sedimentary deposition, it was tentatively proposed that extension was oriented north/ south at 2.7 Ga.

Thus, the interpretation of these seismic profiles has not only allowed new, previously undescribed stratigraphic and structural features to be identified, but has also allowed for the evaluation of existing tectonic models for the western margin, Northern Province, and craton interior. It has also revealed that, at least in places, lithospheric strength of the Archean terrain was not inherited from its inception, but was attained during younger lithospheric strengthening processes. The details of these processes remain to be revealed. As hopefully more seismic and borehole data becomes available, these models may be tested in great depth.

University of Cape Town

References

Aksu, A., Calon, T.J. and R.N. Hiscott, 2000, Anatomy of the North Anatolian Fault Zone in the Marmara Sea, Western Turkey: Extensional Basins Above a Continental Transform, *GSA Today*, June, pp. 3-7

Altermann, W. and D.R. Nelson, 1998, Sedimentation rates, basin analysis and regional correlations of three Neoarchean and Palaeoproterozoic sub-basins of the Kaapvaal Craton as implied by precise SHRIMP U-Pb zircon ages from volcanic sediments. *Journal of Sedimentary Geology*, **120,** pp. 225-256

Altermann, W. and J. McD. Wotherspoon, 1995, The carbonates of the Transvaal and Griqualand West Sequences of the Kaapvaal craton, with special reference to the Lime Acres limestone deposit, *Mineralium Deposita*, **30** (2), pp. 124-134

Altermann, W., Hälbich, I.W., Hortsmann, U.E., Ahrendt, H., Fitch, F.J. and J.A. Miller, 1992, The age of tectonogenesis and metamorphism of the southwestern Kaapvaal Craton *(Abstract). 29th IGC, Kyoto*, **2/3,** pp.261

Altermann, W. and I.W. Hälbich, 1991, Structural history of the southwestern corner of the Kaapvaal Craton and the adjacent Namaqua realm: new observations and a reappraisal, *Precambrian Research*, **52,** pp. 133-166

Altermann, W. and I.W. Hälbich, 1990, Thrusting, folding and stratigraphy of the Ghaap Group along the south-western margin of the Kaapvaal Craton, *S. Afr. J. Geol.* **93,** pp. 553-556

Anderson, R.E., Zoback, M.L. and Thompson, G.A., 1983, Implications of selected subsurface data on the structural form and evolution of some basins in the northern Basin and Range province, Nevada and Utah, *Geological Society of America Bulletin*, **94,** pp. 1055-1072

Armstrong, R.A., Compston, W., Reteif, E. and I.S. Williams, 1991, Zircon ion microprobe studies bearing on the age and evolution of the Witwatersrand Triad. *Precambrian Research*, **53,** pp. 243-266

Arndt, N.T., Nelson, D.R., Compston, W., Trendall, A.F. and A.M. Thorne, 1991, The age of the Fortescue Group, Hammersley Basin, Western Australia, from ion microprobe U-Pb zircon results. *Australian Journal of Earth Sciences* **38,** pp. 261-281

Barley, M.E., Pickard, A.L. and P.J. Sylvester, 1997, Emplacement of a large igneous province as a possible cause of banded iron formation 2.45 billion years ago. *Nature* (London) **385,** pp. 55-58

Barton, E.S. and R.S. White, 1997, Volcanism on the Rockall continental margin, *J. of the Geo. Soc.* **154,** (3) pp. 531-536

University of Cape Town

Barton, E.S., Altermann, W., Williams, I.S. and C.B Smith, 1994, U-Pb age for a tuff in the Campbell Group, Griqualand West, South Africa: implications for early Proterozoic rock accumulation rates. *Geology* **22,** pp. 343-346

Bau, M., Romer, R.L, Luders, V. and N. Beukes, 1999, Pb, O, and C isotopes in silicified Mooidraai dolomite (Transvaal Supergroup, South Africa): implications for the composition of Paleoproterozoic seawater and 'dating' the increase of oxygen in the Precambrian atmosphere, *Earth and Planetary Science Letters*, **174,** pp. 43-57

Beukes N.J., 1987, Facies relations, depositional environments and diagenesis in a major Early Proterozoic stromatolitic carbonate platform to basinal sequence, Campbellrand Subgroup, Transvaal Supergroup, Southern Africa. *Sediment. Geol.* **54,** pp. 1-46

Beukes, N.J and C.A. Smit, 1987, New evidence for thrust faulting in Griqualand West, South Africa: implications for stratigraphy and age of red beds, *S. Afr. J. Geol.*, **90,** (4) pp. 378-394

Beukes N.J., 1986, The Transvaal Sequence in Griqualand West. In. *Mineral deposits of southern Africa.* (eds.: Anhaeusser, C.R. and S. Maske) *Geol. Soc. S. Afr.* Johannesburg, pp. 519-528

Beukes, N.J., 1984, Sedimentology of the Kuruman and Griquatown Iron-Formations, Transvaal Supergroup, Griqualand West, South Africa, *Precambrian Research*, **24,** pp. 47-84

Beukes N.J., 1983, Palaeoenvironmental setting of iron-formations in the depositional basin of the Transvaal Supergroup, South Africa. In. *Iron Formations: Facts and Problems.* (eds.: Trendall, A.F. and Morris, R.C.), *Elsevier,* Amsterdam, pp. 131-209

Blundell, D.J. and B. Raynaud, Modeling lower crust reflections observed on BIRPS profiles. In. *Reflection Seismology: a global perspective,* (eds.: Barazangi, M. and L. Brown), *Geodynamics Series*, **13,** AGU, Washington, pp 287-296

Bowen, T.B., Marsh, J.S., Bowen, M.P. and H.V. Eales, 1986, Volcanic rocks of the Witwatersrand Triad, South Africa: Description, classification and geochemical stratigraphy. *Precambrian Res.*, **31,** pp. 297-324

Boyd, F.R., Gurney, J.J. and S.H. Richardson, 1985, Evidence for a 150-200km thick Archean lithosphere from diamond inclusion thermobarometry, *Nature*, **315,** pp. 387-389

Buck, S.G., 1980, Stromatolite and ooid deposits within the fluvial and lacustrine sediments of the Precambrian Ventersdorp Supergroup of South Africa. *Precambrian Res.*, **12,** pp. 311-330

Buick, I.S., Maas, R. and R. Gibson, 2001, Precise U-Pb titanite age constraints on the emplacement of the Bushveld Complex, South Africa, *Journal of the Geological Society, London*, **158,** pp.3-6

University of Cape Town

Burke, K., Kidd, W.S.F. and T.M. Kusky, 1986, Archean Foreland Basin Tectonics in the Witwatersrand, South Africa, *Tectonics,* **5** (3), pp. 439-456

Burov, E.B. and M. Diament, 1996, Isostasy, equivalent elastic thickness and rheology of continents and oceans, *Geology*, **24,** pp. 419-422

Burov, E.B. and M. Diament, 1995, The effective elastic thickness (Te) of continental lithosphere: What does it really mean?, *J. Geophys. Res.*, **100,** pp. 3905-3927

Button, A., 1986, The Transvaal sub-basin of the Transvaal Sequence. In. *Mineral Deposits of S. Africa. Vols. I and II.* (eds.: Anhaeusser, C.R., and S. Maske) *Geol. Soc. S. Afr.* pp. 811-817

Button, A., 1976, Transvaal and Hammersley Basins- Review of basin development and mineral deposits, *Minerals Sci. Engng*, **8,** (4) pp. 262-291

Button, A., 1973, A regional study of the stratigraphy and development of the Transvaal Basin in the eastern and northeastern Transvaal. Ph.D. thesis *(unpubl.) Univ. of the Witwatersrand*, South Africa

Carlson, R.W., Grover, T.L. de Wit, M.J. and J.J. Gurney, 1996, Program to study the crust and mantle of the Archean craton in Southern Africa. *EOS, Transactions, American Geophysical Union*, **77,** pp. 273-277

Cheney, E.S., Roering, C. and H. de la R. Winter, 1990, The Archean-Proterozoic boundary in the Kaapvaal province of southern Africa. *Precambrian Res.* **46,** pp. 329-340

Clendenin, C.W., 1989, Tectonic Influence on the Evolution of the Early Preterozoic Transvaal Sea, Southern Africa. Ph.D. Thesis *(unpubl.) Univ. of the Witwatersrand*, South Africa, 367 pp.

Clendenin, C.W., Charlesworth, E.G. and S. Maske, 1988, Tectonic style and mechanism of early Proterozoic successor basin development, southern Africa, *Tectonophysics*, **156,** pp. 275-291

Cornell, D.H., Armstrong, R.A. and F. Walraven, 1998, Geochronology of the Proterozoic Hartley Basalt Formation, South Africa: constraints on the Kheis tectogenesis and the Kaapvaal craton's earliest Wilson cycle. *Journal of African Earth Sciences*, **26,** pp. 5-27

Cornell, D.H., Schutte, S.S., and B.L. Eglington, 1996, The Ongeluk basaltic andesite formation in Griqualand West, South Africa: submarine alteration in a 2222 Ma Proterozoic sea, *Precambrian Research*, **79,** pp. 101-123

Cornell, D.H., 1987, Stratigraphy and petrography of the Hartley Basalt Formation, northern Cape Province, *S. Afr. J. Geol.*, **90,** pp. 7-24

University of Cape Town

Corner, B., 1998, A Geophysical perspective of the Kaapvaal Province, *Southern African Geophysical Review,* South African Geophysical Association, **2,** pp. 19-28

Coward, M.P. and R. Potgieter, 1983, Thrust zones and shear zones of the margin of the Namaqua and Kheis mobile belts, southern Africa, *Precambrian Research*, **21,** pp. 39-54

Courtillot, V., Jaupart, C., Manighetti, I., Tapponnier, P. and J. Besse, 1999, On causal links between flood basalts and continental breakup, *Earth and Planetary Science Letters*, **166,** pp. 177-195

Crockett, R.N. 1972, The Transvaal System in Botswana: its geotectonic and depositional environment and special problems. *Trans. Geol. Soc. S. Afr.* **75,** pp. 275-292

De Wit, M.J., Roering, C., Hart, R.J., Armstrong, R.A., Ronde, C.E.J., Green, R.W.E., Tredoux, M. and R.A. Hart, 1992, Formation of an Archean continent. *Nature*, **357,** pp. 553-562

Doucouré, C.M and M.J. de Wit, 2001, The Competent Lithosphere of the Kaapvaal Craton, TerraNova (submitted)

Doucouré, C.M., Mushayandebvu, M. F. and M.J. de Wit, 1996, Effective elastic thickness of the continental lithosphere in South Africa. *J. Geophys. Res.*, **101** B5, pp. 11,291-11,303

Duncan, R.A., Hooper, P.R., Rehacek, J., Marsh, J.S. and A.R. Duncan, 1997, The timing and duration of the Karoo igneous event, southern Gondwana. *Journal of Geophysical Research*, **102**, 127-138

Durrheim, R.J., Nicolaysen, L.O. and B. Corner, 1991, A deep seismic reflection profile across the Archean- Proterozoic Witwatersrand Basin, South Africa, *Continental Lithosphere: Deep Seismic Reflections*. Geodynamics, AGU, **22,** pp. 213-224

Durrheim, R.J., 1986, Recent reflection seismic developments in the Witwatersrand basin. In: **Baraganzi , M. and l. Brown** (Eds.) *Reflection Seismology: a global perspective*, pp. 77-83, Geodynamics Series, **13**, AGU, Washington

Eriksson, P.G., Van Der Merwe, R. and A.J. Bumby, 1998, The Palaeoproterozoic Woodlands Formation of eastern Botswana- northwestern South Africa: lithostratigraphy and relationship with Transvaal Basin inversion structures. *J. Afr. Earth. Sci.* **27,** 3/4 pp. 349-358

Eriksson, P.G., Schweitzer, J.K., Bosch, P.J.A., Schereiber, U.M., Van Deventer, J.L. and C.J. Hatton, 1993, The Transvaal Sequence: an overview, *Journal of African Earth Sciences*, **16,** ½, pp. 25-51

University of Cape Town

Eriksson, P.G., Schreiber, U.M., and M. van der Neut, 1991, A review of the sedimentology of the Early Proterozoic Pretoria Group, Transvaal Sequence, South Africa: implications for tectonic setting. *J. Afr. Earth. Sci.* **13,** pp. 107-119

Eriksson, P.G., Twist, D., Snyman, C.P. and L. Burger, 1990, The geochemistry of the Silverton Shale Formation, Transvaal Sequence. *S. Afr. J. Geol.* **93,** pp. 454-462

Eriksson, P.G. and C.W. Clendenin, 1990, A review of the Transvaal Sequence, South Africa, *J. Afr. E. Sci.,* **10,** pp. 101-116

Evans, D.A., Beukes, N.J. and J.L. Kirschvink, 1997, Low-latitude glaciation in the Palaeoproterozoic era. Nature **386,** pp. 262-266

Geological Map of South Africa, Transkei, Bophuthatswana, Venda and Ciskei and the Kingdoms of Lesotho and Swaziland. 1: 1 000 000, 1984, *Geol. Surv. of S. Afr.*

Geological Sheet of Bothaville/ Vredefort (2726B/ 2727A), 1962, *publ. by Geol. Surv. of S. Afr.*

Geological Sheet of West Rand (2626), 1986, *publ. by Geol. Surv. of S. Afr.*

Grobbelaar, W.S., Burger, M.A., Pretorius, A.L., Marais, W. and I.J.M. van Niekerk, Stratigraphic and structural setting of the Griqualand West and the Olifantshoek Sequences at Black Rock, Beeshoek and Rooinekke Mines, Griqualand West, South Africa, *Mineralium Deposita*, **30** (2), pp. 152-161

Grotzinger, J.P. and L. Royden, 1990, Elastic strength of the Slave craton at 1.9 Gyr and implications for the thermal evolution of the continents, *Nature,* **347,** (6288) pp. 64-66

Grotzinger, J.P., 1989, Facies and evolution of Precambrian carbonate depositional systems: emergence of the modern platform archetype. In *Controls on Carbonate Platform and Basin Development.* (eds.: Crevello, P.D., Wilson, J.L., Sarg, J.F. and J.F Reid) *Soc. Econ. Paleontol. Mineral., Spec. Publ.*, **44,** pp. 79-106

Gurney, J.J., 1990, The diamondiferous roots of our wandering continent, *S.Afr. J. Geol.*, **93,** pp. 423-437

Haddad, D. and A.B. Watts, 1999, Subsidence history, gravity anomalies, and flexure of the northeast Australian margin in Papua New Guinea, *Tectonics*, **18** (5), pp. 827-842

Haddon, I.G., 1999, Isopach Map of the Kalahari Group, *publ. by Council for Geoscience*

Halbich, I.W., Scheepers, R., Lamprecht, D., van Deventer, J.L. and J.J. De Cock, 1993, The Transvaal-Griqualand West banded iron formation: geology, genesis, iron exploitation. *J. Afr. Earth. Sci.* **16** 1/2, pp. 63-120

University of Cape Town

Hartley, R.W., Watts, A.B. and J.D. Fairhead, 1996, Isostasy of Africa, *Earth Planet. Sci. Lett.* **137**, pp. 1-18

Hatton, C.J., 1995, Mantle plume origin for the Bushveld and Ventersdorp magmatic provinces, *Journal of African Earth Sciences*, **21**, pp. 571-577

Henry, G., Clendenin, C.W., and E.G. CHarlesworth, 1990, Depositional facies of the Black Reef Quartzite Formation in the eastern Transvaal. *GeoCongress '90 (Cape Town, South Africa): Extended Abstracts*, pp. 230-233

Hinz, K. and W. Krause, 1982, The continental margin of Queen Maud Land, Antarctica: Seismic sequence, structural elements and geological development. *Geologisches Jahrbuch*, **E23**, pp. 17-41

Jahn, B.M., Bertrand-Sarfati, J., Morin, N., and J. Macé, 1990, Direct dating of stromatolitic carbonates from the Schmidtsdrif Formation (Transvaal Dolomite), South Africa, with implications on the age of the Ventersdorp Supergroup, *Geology* **18**, pp. 1211-1214

Jokat, W., Hubsher, C., Meyer, U., Oszho, L. Schore, T., Verstees, W. and Miller, 1996, The Continental Margin of East Antarctica between 10 W and 30 W, In (eds.) Storey, B.C *et al. Weddel Sea Tectonics and Gondwana break up.* Geol. Soc. [London] Special Publication **108**, pp. 129-141

Johnson, M.R. van Vurren, C.J., Hegenberger, W.F., Rey, R. and U. Shoko, 1996, Stratigraphy of the Karoo Supergroup in South Africa: an overview. *Journal of African Earth Sciences*, **23**, pp. 3-15

Key, R.M. 1983, The geology of the area around Gabarone and Lobatse, Kweneng, Kgatleng, Southern and South East Districts. *District Memoir Geol. Surv. Botswana* ***5***

Klein, C. and N.J. Beukes, 1989, Geochemistry and sedimentology of a facies transition from limestone to iron-formation deposition in the Early Proterozoic Transvaal Supergroup, South Africa. *Econ. Geol.*, **84**, pp. 1733-1774

Klemperer, S.L. and the BIRPS group, 1987, Reflectivity of the crystalline crust: hypothesis and tests, *Geophys. J. R. astr. Soc.*, **89**, pp. 217-222

Kominz, M.A. and G.C. Bond, 1986, Geophysical modelling of the thermal history of foreland basins, *Nature*, **320**, pp. 252-256

Kruse, S.E. and L.H. Royden, 1994, Bending and unbending of an elastic lithosphere: The Cenozoic history of the Appenine and Dinaride foredeep basins, *Tectonics*, **13** (2), pp. 278-302

Linton, P.L., McCarthy, T.S. and R.E. Myers, 1990, A Geochemical reappraisal of the stratigraphy of the Klipriviersberg Group in the type borehole LL1 in the Bothaville area. *S. Afr. J. Geol*, **93** (1), pp. 239-252

University of Cape Town

Martin, D. mcB., Clendenin, C.W., Krapez, B. and N.J. Mc Naughton, 1998, Tectonic and geochronology constraints on late Archaean and Palaeoproterozoic stratigraphic correlation within and between the Kaapvaal and Pilbara Cratons, *Journal of the Geological Society, Londo*n, **155**, pp.311-322

McIver, J.R., Cawthorn, R.G., and B.A. Wyatt, 1981, TheVentersdorp Supergroup- the youngest komatiitic sequence in South Africa. In **E.G. Nisbet and N.T. Arndt** (Eds.) *Komatiites.* Allen and Unwin, London, pp. 81-90

McKenzie, D.P., 1978, Some remarks on the development of sedimentary basins. *Earth and Planetary Sci. Lett.* **40,** pp. 25-32

McNutt, M.K., M. Diament and M.G. Kogan, 1988, Variations of elastic thickness at continental thrust belts, *J. Geophys. Res.*, **93,** pp. 8825-8838

Moen, H.F.G., 1999, The Kheis Tectonic Subprovince, southern Africa: A lithostratigraphic perspective, S. Afr. J. Geol., **102,** (1) pp. 27-42

Mooney, W.D. and T.M. Brocher, 1987, Coincident seismic reflection/refraction studies of the continental lithosphere: a global review, *Rev. of Geophys.* **25,** pp. 723-742

Moore, J.M., Tsikos, H. and S. Polteau, 2000, Deconstructing the Transvaal Supergroup, South Africa. Geocongress 2000: 27th Earth Science Congress of the GSSA (abstracts) J. Afr. Earth Sci. **31,** 1A

Myers, R.E., McCarthy, T.S. and I.G. Stanistreet, 1990a, A tectono-sedimentary reconstruction of the development and evolution of the Witwatersrand Basin, with particular emphasis on the Central Rand Group. *S. Afr. J. Geol*, **93,** (1) pp. 180-201

Myers, R.E., McCarthy, T.S., Bunyard, M., Cawthorn, M., Falatsa, T.M., Hewitt, T., Linton, P., Myers, J.M., Palmer, K.J. and R. Spencer, 1990b, Geochemical stratigraphy of the Klipriviersberg volcanic rocks. *S. Afr. J. Geol.* **93** (1), pp. 224-238

Nelson, D.R., Trendall, A.F., and W. Altermann, 1999, Chronological correlations between the Pilbara and Kaapvaal cratons, *Precambrian Research*, **97,** pp. 165-189

Palmer, K.J., Spencer, R.M., Hewitt, T. and T.S. McCarthy, 1986, Geochemistry of the Klipriviersberg lavas as a stratigraphic guide in the Witwatersrand Basin. *Abstr. Geocongress '86, Geol. Soc. S. Afr.*, pp. 171-174

Pollack, H.N., 1997, Thermal Characteristics of the Archaean, In. De Wit, M. and L.D. Ashwal (eds.), *Greenstone Belts*, Clarendon Press, Oxford, **3.1,** pp. 224-232

Pretorius, C.C., Steenkamp, W.H. and R.G. Smith, 1994, Developments in Data Acquisition, Processing, and Interpretation over Ten Years of Deep Vibroseismic Surveying in South Africa, *XVth CMMI Congress*, Johannesburg, SAIMM, **3,** 249-258

University of Cape Town

Pretorius, C.C., Jamison, A.A. and C. Irons, Seismic Exploration in the Witwatersrand Basin, Republic of South Africa, 1987, Exploration '87 Proceedings, *Geophysical Methods: Advances in the state of the art*, **22,** pp. 241-253

Reemst, P. and S. Cloetingh, 2000, Polyphase rift evolution of the Voring margin (mid-Norway): Constraints from forward tectonostratigraphic modeling, *Tectonics*, **19,** pp. 225-240

Reczko B.F.F., Eriksson, P.G. and C.P Snyman, 1992, Geochemistry of the shales interbedded in the Magaliesberg Formation, Pretoria Group, near Pretoria: palaeoenvironmental and diagenetic implications. *GeoCongress '92 (Bloemfontein, South Africa): Abstracts*, pp. 305-307

Robb, L.J., Davis, D.W. and S.L. Kamo, 1990, U-Pb ages on single detrital zircon grains from the Witwatersrand Basin, South Africa: constraints on the age of sedimentation and on the evolution of granites adjacent to the basin. *Journal of Geology*, **98,** pp. 311-328

Royden, L., 2000, Graduate class notes, MIT, unpublished.

Royden, L., 1988, Flexural Behavior of the Continental Lithosphere in Italy: Constraints Imposed by Gravity and Deflection Data, *Journal of Geophysical Research*, **93** (B7), pp. 7747-7766

Schlegel, G.C.J., 1988, Contribution to the metamorphic and structural evolution of the Kheis tectonic province, northern Cape. *S. Afr. J. Geol.* **92,** pp. 207-222

Schreiber, J.K. and P.G. Eriksson, 1992, The sedimentology of the post-Magaliesberg formations of the Pretoria Group, Transvaal Sequence, in the eastern Transvaal, *S. Afr. J. Geol.* **95** (1), pp. 1-16

Sharpe, M. R., Brits, R. and J.P. Engelbrecht, 1983, Rare earth and trace element evidence pertaining to the petrogenesis of 2.3 Ga old continental andesites and other volcanic rocks from the Transvaal Sequence, South Africa. *Res. Rep. Inst. Geol. Res. Bushveld Complex, Univ. Pretoria* **40**

Smith, R.H., Eriksson, P.G. and W.J. Botha, 1993, A review of stratigraphy and sedimentary environments of the Karoo-aged basins of Southern Africa. *Journal of African Earth Sciences*, **16**, 143-169

South African Committee for Stratigraphy (SACS), 1980, Stratigraphy of South Africa. Part 1. (ed.: L.E. Kent) Lithostratigraphy of the Republic of South Africa, South West Africa/ Namibia, and the republics of Bophuthatswana, Transkei and Venda.

Stettler, E.H, Prinsloo, J. and M.E. Hauger, 1998a, A Geophysical Transect between Avondale on the Kheis Tectonic Province and Keimoes on the Namaqua Metamorphic Province, South Africa, *Southern African Geophysical Review*, **2**, pp. 83-93

University of Cape Town

Stettler, E.H., Prinsloo, J., Hauger, M.E. and M.C. du Toit, 1998b, A Crustal Geophysical Model for the Kheis Tectonic Province, South Africa Based on Magnetotelluric, Reflection Seismic, Gravity and Magnetic Data Sets, *South African Geophysical Association*, **3**, pp. 54-68

Stewart, J. and A.B. Watts, 1997, Gravity anomalies and spatial variations of flexural rigidity at mountain ranges, *J. Geophys. Res.*, **102**, pp. 5327-5352

Stowe, C.W. 1986, Synthesis and interpretation of structures along the north-eastern trending boundary of the Namaqua tectonic province, South Africa, *Trans. Geol. Soc. S. Afr.* **89**, pp. 182-198

Sumner, D.Y. and S.A. Bowring, 1996, U-Pb geochronologic constraints on deposition of the Campbellrand Subgroup, Transvaal Supergroup, South Africa, *Precambrian Research*, **79**, pp. 25-35

Tankard, A. J., Jackson, M.P.A., Eriksson, K.A., Hobday, D.K., Hunter, D.R. and W.E.L. Minter, 1982, *Crustal Evolution of South Africa*, Springer-Verlag, New York, 523 pp.

Thomas, R.J., Von Veh, M.W. and S. McCourt, 1993, The tectonic evolution of southern Africa: an overview. *J. Afr. Earth Sci.* **16**, pp. 5-24

Truswell, J.F. and K.A. Eriksson, 1973, Stromatolitic associations and their palaeoenvironmental significance: a re-appraisal of a Lower Proterozoic locality from the northern Cape Province, South Africa. *Sediment. Geol.* **10**, pp. 1-23

Turner, B.R. Tectonostratigraphic development of the upper Karoo foreland basin: orogenic unloading versus thermally-induced Gondwana rifting, *Journal of African Earth Sciences*, **28** (1), 215-238

Van der Westhuizen, W.A., De Bruyn, H. and P.G. Meintjes, 1991, The Ventersdorp Supergroup: an overview. *J. Afr. Earth Sci.* **13**, pp. 83-105

Visser, J.N., 1969, 'n Sedimentologiese studie van die Serie Pretoria in Transvaal. Ph.D. thesis (unpubl.), University of the Orange Free State, Bloemfontein, South Africa.

Visser, J.N. 1971, The deposition of the Griquatown Glacial Member in the Transvaal Supergroup, *Trans. Geol. Soc. S. Afr.* **74**, pp.187-199

Walraven, F. and J. Martini, 1995, Zircon Pb-evaporation age determinations of the Oak Tree Formation, Chuniespoort Group, Transvaal Sequence: implications for Transvaal-Griqualand West basin correlations, *S. Afr. J. Geol*, **98** (1), pp. 58-67

Walraven, F., Smith, C.B. and F.J. Kruger, 1991, Age determinations of the Zoetlief Group- Ventersdorp Supergroup correlatives. *S. Afr. J. Geol.*, **94** pp. 220-227

Watts A.B., Lamb, S.H., Fairhead, J.D., and J.F. Dewey, 1995, Lithospheric flexure and bending of the Central Andes, *Earth Planet. Sci. Lett.*, **134**, pp. 9-21

University of Cape Town

Weder, E.E.W., 1994, Structure of the Area South of the Central Rand Gold Mines as Derived from Gravity and Vibroseis Surveys, *XVth CMM1 Congress*, Johannesberg. SAIMM, **3,** pp. 271-281

Winter, H. de la R., 1976, A lithostratigraphic classification of the Ventersdorp Succession. *Trans. Geol. Soc. S. Afr.,* **79,** 31-48

Yilmaz, O., 1987, Seismic Data Processing. In **S. Doherty** (Ed.) *Investigations in Geophysics: 2.* Society of Exploration Geophysicists, USA, pp. 43-263

Zegers, T.E., de Wit, M.J., Dann, J. and S.H. White, 1998, Vaalbara, Earth's oldest assembled continent? A combined structural, geochronological and paleomagnetic test, *Terra Nova*, **10,** pp. 250-259

Zoetemeijer, R., Desegaulx, P., Cloetingh, S., Roure, F. and I. Moretti, 1990, Lithospheric dynamics and tectonic-stratigraphic evolution of the Ebro Basin, *J. Geoph. Res.,* **95,** pp. 2701-2711

Zoetemeijer, R., Tomek, C. and S. Cloetingh, 1999, Flexural expression of European continental lithosphere under the western outer Carpathians, *Tectonics,* **18** (5), pp. 843-861

University of Cape Town

Appendix A : Data Acquisition and Processing

Before seismic reflection data may be interpreted it must be acquired and processed. The seismic reflection data interpreted in this study were acquired using the Vibroseis method by the *AngloGold Corp. Ltd*, between the years of 1985 and 1994. A list of recording equipment and acquisition parameters is included in table A-1.

Instruments Recording parameters	1983 reconnaissance	1993 reconnaissance	1993 detailed
Instruments			
Vibrators	4 * Failing BBV 27 000 lb	5 * Failing Y1100 27 000 lb	2 * Mertz M18 40 000 lb
Recording Instruments	SN338	SN368/I/O CS	SN368 CS2502
Number of Channels	96	120	120
Geophones	SM4 10 Hz	SM4 10Hz	Sensor 10 Hz
Vibrator QC System	-	Vigil/ Valid	Pelton Advance 2
Sweep Parameters			
Sweep Length	26 sec	24 sec	8 sec
Sweeps per VP	8	3	4
Frequencies	10-91 Hz up	10-61 Hz up	20-120 Hz up
Listening Period	6 secs	6 secs	6 secs
Sample Rate	4 msecs	2 msecs	2 msecs
Geometric Parameters			
Field Spread	End on 0-175-4925 m	Split Straddle 2975-25-X-25-2975	Split Straddle 743.75-6.25-X-6.25-743.75 m
Station Interval	50 m	50 m	12.5 m
VP Interval	50 m	25 m	12.5 m
Vib Pattern	150 m linear	50 m linear	12.5 m linear
Receiver Pattern	100 m	50 m	12.5 m
Fold of Cover	48	50	60

Table A-1: Acquisition parameters: 1983 to 1993 (from Pretorius *et al.*, 1994).

Parameters specific to several of the seismic profiles interpreted in this study are included in table A-2.

University of Cape Town

Line Number	Line names used in text	Acquisition starting date	Processing starting date	Datum	Number of Channels	Record Length	Sample Rate	Station Interval
OB-41	**OB**	19-02-85	02-03-85		96	24 s	4 ms	50 m
OB-74		01-10-85	21-10-85	1400 m	96	24 s	4 ms	50 m
KV-117		23-04-86	07-05-86	1400 m	96	24 s	4 ms	50 m
KV-119	**AG**	07-05-86	20-05-86	1400 m	96	24 s	4 ms	50 m
AG-130		20-08-86	28-08-86	1400 m	96	24 s	4 ms	50 m
YS-62	**YS**	02-07-85	16-08-85	1400 m	96	24 s	4 ms	50 m
RZ-254	**Rz**	15-08-88	10-09-88	1200 m	120	6 s	4 ms	50 m
KBF-03A	**KBF**	28-11-94			120	16 s	4 ms	50 m

Table A-2: Acquisition details for several of the seismic profiles interpreted in this study.

The data was processed to improve signal to noise ratio as follows:

1983/84 Processing Route	**1993 Processing Route**
DEMULTIPLEX (including gain removal, cross-correlation and minimum phase conversion)	DEMULIPLEX (including gain removal and minimum phase conversion)
EDIT/MUTE, FLOATING DATUM STATITICS AND SOURCE DOMAIN FK FILTER	
AMPLITUDE RECOVERY	AMPLITUDE RECOVERY (PROGRAMMED GAIN)
SOURCE DOMAIN DECONVOLUTION	
FILTER AND NORMALIZATION Removed because these processing steps had only limited effects in improving data	
RECEIVER SORT, DOMAIN FK FILTER AND DECONVOLUTION	
FILTER Removed because it gave little improvement in data	
NORMALIZATION AND SORT INTO SOURCE	
SOURCE DECONVOLUTION, FILTER AND NORMALIZATION RECEIVER SORT AND DECONVOLUTION FILTER AND EQUALIZATION Removed because these steps added significantly to the length and cost of processing but gave only marginal improvement in data	
	DIP MOVE-OUT Added to improve interpretations, especially in areas of steep dip
COMMON MID-POINT SORT, NMO/MUTE, DATUM STATICS AND RESIDUAL STATICS (surface constant)	
	RESIDUAL STATICS (COMMON MID-POINT (CONSISTENT)) Added to correct for effects of the weathering layer
STACK	
	OMEGA-X (random noise attenuation)
MIGRATION AND FILTER	
PRODUCTION RATE FOR 6 SEC TWT DATA-3 KM/DAY	PRODUCTION RATE FOR 6 SEC TWT DATA-12 KM/DAY

Table A-3: Seismic processing route (from Pretorius *et al.*, 1994).

University of Cape Town

For more technical details on seismic processing methods, the reader is referred to Yilmaz (1987).

University of Cape Town

Appendix B : Derivation of the Flexural Equation

$$D * (\partial^4 W / \partial x^4) = \text{all applied loads}$$

The following derivation has been adapted from Royden (2000).

Symbols in order used in derivation:

- P = load
- V = shear stress
- M = bending moment
- E_{xx} = strain in x direction
- σ_{xx} = stress in x direction
- E = Young's modulus
- V = Poisson's ratio
- W = flexure
- D = flexural rigidity

The flexed plate is treated as a thin elastic sheet involving the following assumptions. First, the plate behaves elastically. Secondly, stresses are oriented parallel to the plate edge (fibre stresses). Thirdly, a fairly low curvature is assumed (figure B-1, 2).

University of Cape Town

B-1. Balancing forces

Consider a load applied to an elastic plate in the **absence of a balancing force** (buoyancy) due to underlying material. Since there is no acceleration, all the forces and torques shown in figure B-2 must sum to zero. Thus by balancing the forces and torques the following equations are produced.

Balancing Forces:

$$dx\, P(x) + V(x) - V(x + dx) = 0 \qquad P(x) = \partial V / \partial x \ldots\ldots\ldots 1$$

(The spatial derivative of the vertical load)

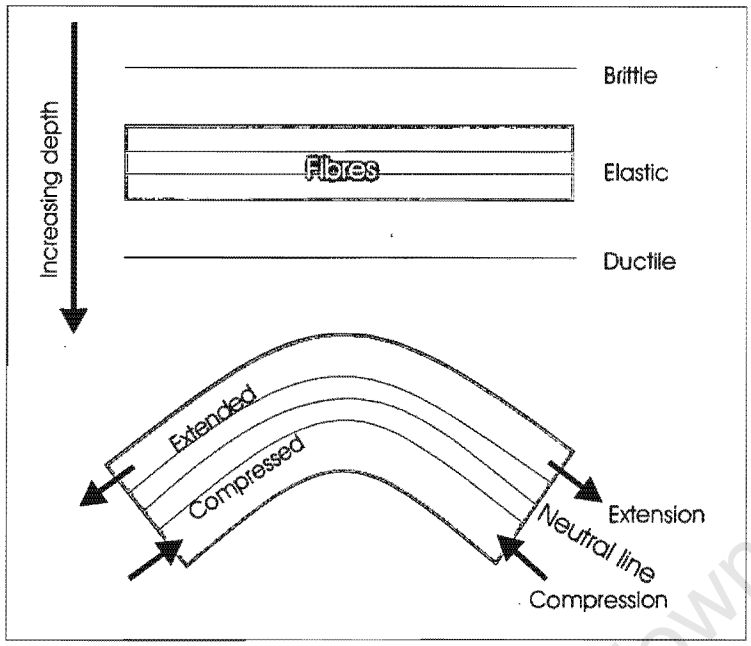

Figure B-1: Assumptions underlying the thin elastic sheet model: Elastic flexure of plate involves the extension and compression of 'fibres' oriented parallel to plate edge.

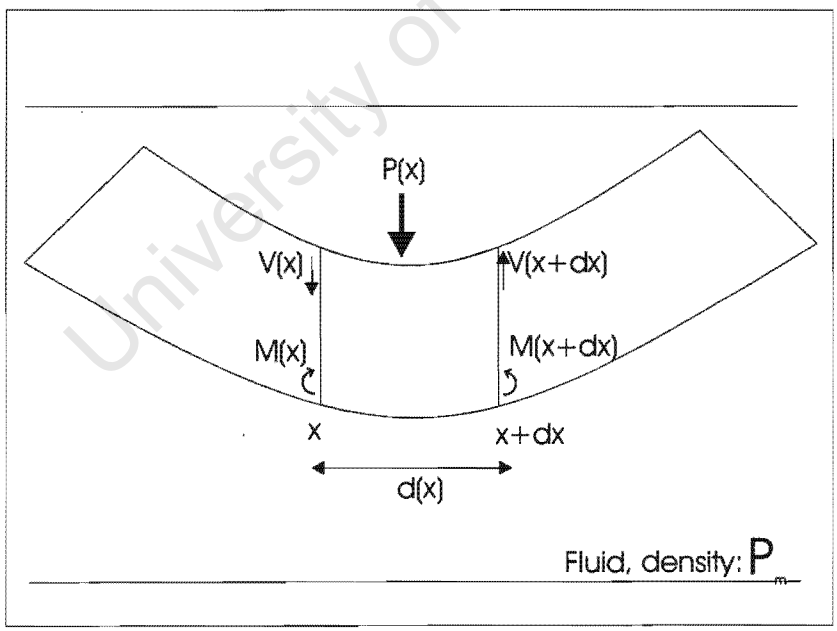

Figure B-2: Applied load, P(x) results in deflection, shear stress, V and bending moment, M.

University of Cape Town

Balancing Torques:

$M(x) - M(x + dx) - V(x)dx = 0 \qquad V = - \partial M / \partial x$

Thus: $P = - \partial^2 M / \partial x^2$ 2

Since the plate is regarded as elastic, stress and strain are linearly related as shown in equations 3 and 4.

(Strain in the X direction:

$E_{xx} = 1/E \, (\sigma_{xx} - \nu \, \sigma_{yy})$.....3

Strain in the Y direction:

$E_{yy} = 1/E \, (\sigma_{yy} - \nu \, \sigma_{xx})$.....4

ν= Poisson's Ratio

E= Young's Modulus

From the second assumption, that only fibre stresses are considered, there is no strain in the Y direction (Eyy = 0).

Thus: $\sigma_{yy} = \nu \, \sigma_{xx}$.....5

From 3 and 5:

Strain is layerly proportional to stress in the X direction.

$E_{xx} = \sigma_{xx} \, (1 - \nu^2) / E$.....6

University of Cape Town

B-2. Relating the load to the bending of the plate, M (figure 3)

The bending of the plate can be described in terms of a bending moment, M which is related to the fibre stresses, σ_{xx}. The neutral line at the centre of the plate is a line along which there is no extension or compression. Above this neutral line a compressional force, $\sigma_{xx}(y)$, acts. Below the neutral line, at position –y, the stress is extensional. The extensional and compressional stresses exert a torque around the neutral line.

$$\text{torque} = \sigma_{xx}\, y\, dx \quad \ldots\ldots\ldots\ldots\ldots\ldots\ldots\ldots\ldots\ldots\ldots\ldots\ldots\ldots\ldots\ldots 7$$

Or, in words: torque is equal to stress in the x direction multiplied by the derivative of the distance from the neutral line.

The total bending moment, M, is obtained by integrating all the torques acting on this element.

$$M = \int_{-h/2}^{h/2} \sigma_{xx}\, y\, dx \quad \ldots\ldots\ldots\ldots\ldots\ldots\ldots\ldots\ldots\ldots\ldots\ldots\ldots\ldots\ldots\ldots 8$$

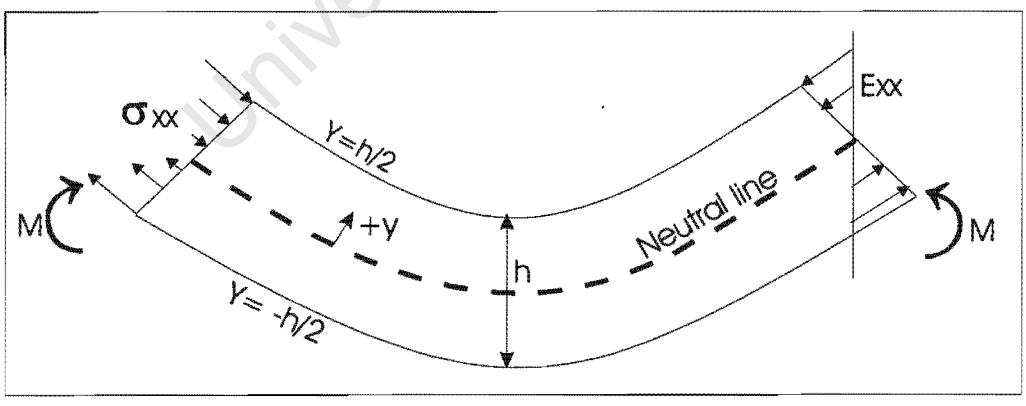

Figure B-3: Relating fibre stresses to the bending moment, M: The neutral line separates the zone of compression, +y, from the zone of extension, -y.

University of Cape Town

B-3. Relating the moment, M to the deflection, W (figure 4)

First, strain changes along a bending plate are considered. These are then related to changes in stress. As in the discussion of stress above, there is a neutral axis along which there is no change in length. Fibres at the top of the sheet are shortened and those at the bottom are lengthened. The change in strain is related to the deflection, W (figure 5).

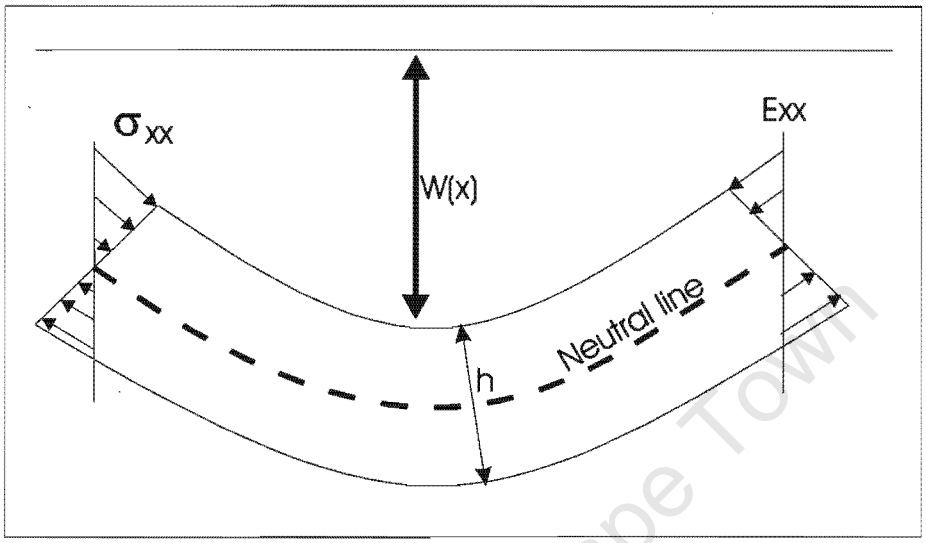

Figure B-4: Relation of strain, E to stress, J and subsequently to deflection, W.

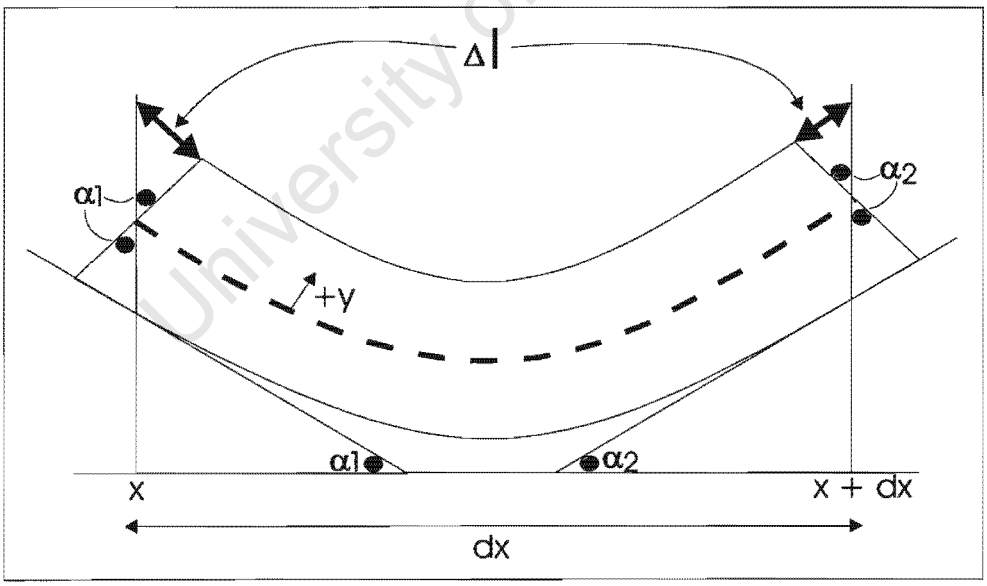

Figure B-5: Relation of change in length, delta I, to deflection, W(x).

University of Cape Town

Let: l be the length of the neutral line ($l \approx dx$)

y be the height above the neutral line

Δl be the change in l for $y \neq 0$

Then: $\Delta l\,(y) = - \alpha_1 y + \alpha_2 y$ 9

$\alpha_1 = - \partial W / \partial x \,|_x \qquad \alpha_2 = + \partial W / \partial x \,|_{x + dx}$

$E_{xx} = \Delta l / l$ (Strain = change in line length divided by original line length). 10

From 9 and 10:

$$E_{xx} = \Delta l / dx = (y / dx) * \{\partial W / \partial x \,|_x - \partial W / \partial x \,|_{x + dx}\}$$

$$E_{xx} = \Delta l / l = - y\,(\partial^2 W / \partial x^2) \text{ .....11}$$

Note: The above is only valid if curvature is small so that α_1 and α_2 are small.

Combining the equations 2, 6, 8 and 11 listed below:

$$P = - \partial^2 M / \partial x^2 \text{ .....2}$$

$$E_{xx} = \sigma_{xx} * ((1 - \nu^2) / E) \text{ .....6}$$

$$M = \int_{-h/2}^{h/2} \sigma_{xx}\, y\, dx \text{ .....8}$$

$$E_{xx} = - y\,(\partial^2 W / \partial x^2) \text{ .....11}$$

Substitution and integration results in the following steps:

$$M = \int_{-h/2}^{h/2} E_{xx} * (E \,/\, (1 - \nu^2))\, y\, dy$$

$$M = - \partial^2 W / \partial x^2\, (E \,/\, (1 - \nu^2)) * \int_{-h/2}^{h/2} y^2\, dy$$

University of Cape Town

$$M = -\partial^2 W / \partial x^2 [(E / (1 - \nu^2)) * h^3 / 12]$$

Note: $(E / (1 - \nu^2)) * h^3 / 12 = D$ = Flexural Rigidity with units of Nm.

Thus: $M = - D * (\partial^2 W / \partial x^2)$.....12

From 2: $\mathbf{P(x) = D * (\partial^4 W / \partial x^4)}$

B-4. Buoyancy Force (figure 5)

The final step involves the consideration of fluid beneath the elastic plate. A downward deflection of the plate, W(x), will result in an upwardly directed force of $W(x)\rho_m g$ acting on the base of the plate (ρ_m = density of underlying fluid). At increased depth the elastic plate will feel an increased fluid pressure.

Thus the force balance calculated at the beginning of this section has to include a 'buoyancy' term, $\rho_m g w(x)$, to accommodate the fluid pressure from below.

$$dx \{P(x) - \rho_m g w(x)\} - v(x) + v(x+dx) = 0$$

$$P(x) - \rho_m g w(x) = - \partial v / \partial x$$

$$\rightarrow P(x) - \rho_m g w(x) = - \partial^2 M / \partial x^2$$

$$\rightarrow P(x) - \rho_m g w(x) = D * (\partial^4 W / \partial x^4)$$

OR: $\mathbf{D * (\partial^4 W / \partial x^4) + \rho_m g w(x) = P(x)}$.....13

University of Cape Town

Similarly, if a load, with density = ρ_i is added to the top of the plate it provides an additional downward force of $\rho_i g w(x)$. Using the same method as above results in **the flexural equation.**

$$D * (\partial^4 W / \partial x^4) + (\rho_m - \rho_i) g w(x) = P(x)$$

$$\text{– (XIV) } D * (\partial^4 W / \partial x^4) = \text{all applied loads}$$

Or, in words: Flexural rigidity multiplied by the fourth derivative of flexure with respect to x is equal to the sum of all applied loads.

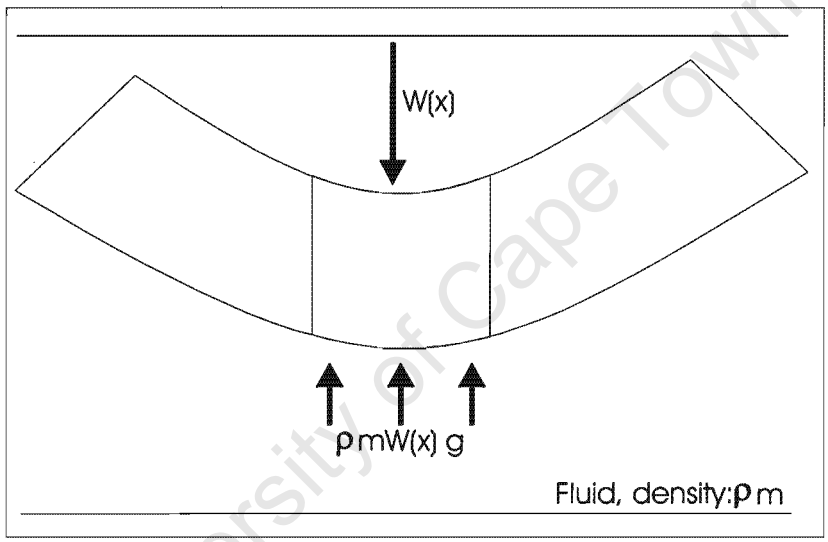

Figure B-6: Buoyancy force acts upwards in response to downward directed deflection.

University of Cape Town

Appendix C : Calculation of flexure (adapted from Royden (1988))

C-1. Observations

To calculate flexure, the deflection of a reflector that was horizontal in orientation prior to loading, was measured. In this way load related flexure is isolated. Both the Ventersdorp sediments and flood basalts and the Schmidtsdrif Subgroup show significant thickening towards the west, indicating that preferential subsidence, unrelated to later thrusting, occurred in the west during their deposition. The Campbellrand Subgroup however is uniform in thickness across the line and is proposed to have formed in a shallow marine platform setting. Thus the contact between the Schmidtsdrif and Campbellrand subgroup was chosen for the calculation, and regarded as initially horizontal.

The end of line KBF03A was taken conservatively at CDP 4800 to the east of the normal fault, F2. This allowed for an exclusion of deflection of strata that may have been caused by subsequent normal faulting. From this point eastward, the depth to the Campbellrand/ Schmidtsdrif contact was calculated every 7.5 km, using p-wave velocity estimates. East of CDP 2700, where the contact reaches the surface, its position prior to erosion was estimated by adding the average thickness of Schmidtsdrif Subgroup above its contact with the underlying granitic basement. East of CDP 1500, where granite outcrops, no estimate could be made.

The seismic line was extended to the east to incorporate the Ventersdorp Supergroup, Schmidtsdrif and Campbellrand Subgroups where they reappear on the eastern side of the flexural bulge. Two further data points were taken where the contact between the Campbellrand and Schmidtsdrif Subgroup outcrops (read from the geological map, figure C-1). The line was extended a further 100 km to the east with flexure calculated every 10 km.

University of Cape Town

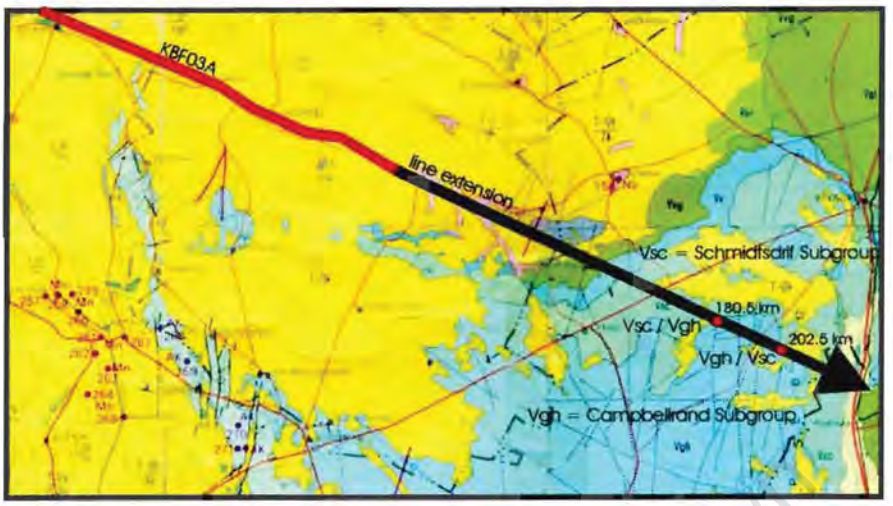

Figure C-1: Geological map including the extension of line KBF03A to two observation points (marked in red).

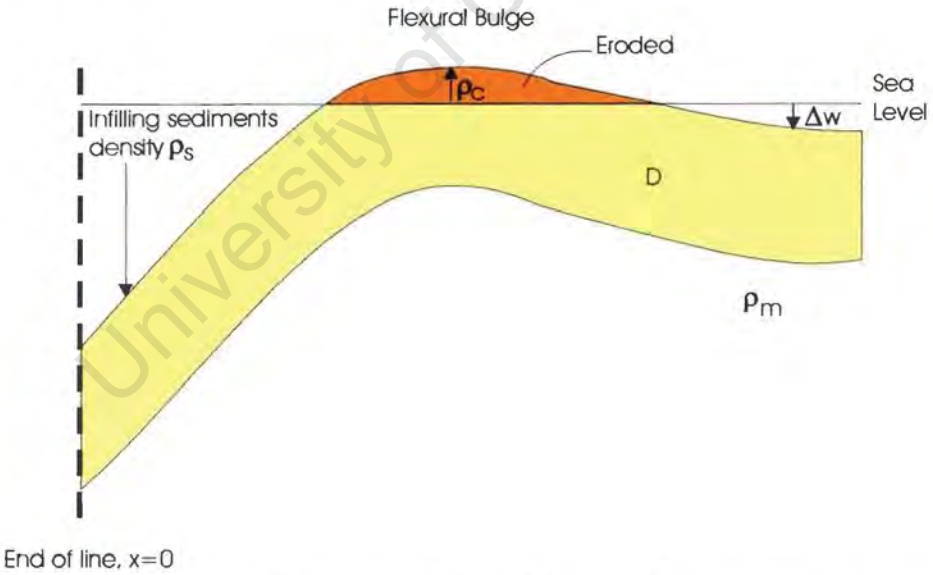

Figure C-2: Parameters involved in the calculation of flexure, ρm, s and c= density of the mantle, infilling sediments and crust respectively, D = flexural rigidity, ΔW= base level shift equivalent to initial water depth, ρc = ρs. Figure is a duplicate of figure 3.6, included to facilitate easier reading.

University of Cape Town

C-2. Calculations

Total flexure is the sum of flexure due to loading and a possible base level shift since deposition, equivalent to initial water depth. The latter is assumed to be uniform along the line. The schematic figure C-2 roughly shows the geometric set up and main parameters involved in the flexural problem.

The total load on the foreland is composed of a downward force produced by sediments both filling accommodation space created by flexure associated with thrusting and also that created due to the change in base level shift unrelated to thrusting. This downward force is balanced by upward directed buoyancy due to the fluid pressure of the mantle beneath the flexed plate. Thus the total load on the line is as follows:

$$Psg W + \rho sg \Delta W - \rho mg W - \rho mg \Delta W$$

$$\text{Or: } (Ps - \rho m)g(W + \Delta W)$$

From the derivation of the flexural equation (appendix B) we have:

$$D * (\partial^4 W / \partial x^4) = \text{all applied loads} = (Ps - \rho m)g(W + \Delta W)$$

Rearranging and substituting the solution to the flexural equation:

$$W = \text{observations} = [\rho m \Delta W / (\rho m - \rho s)] + [A\cos(x/\alpha) + B\sin(x/\alpha)] * e^{-x/\alpha}$$

In this equation there are four unknowns to be solved, ΔW, A, B and α (We can input estimates of ρm and ρs and x is the horizontal distance from line end). We assume a geologically plausible value of α and are left with three unknowns. Common values of α are given in table C-1.

University of Cape Town

		Te (km)	D (Nm)	α (km)
very weak eg. mid ocean ridge	Oceanic	1	$7.2 * 10^{21}$	8
		5	$9.0 * 10^{22}$	26
		10	$7.2 * 10^{23}$	45
		20	$5.8 * 10^{24}$	76
very strong eg. India/ Himalayas	Continental	30	$2.0 * 10^{25}$	102
		50	$9.0 * 10^{25}$	150
		80	$3.7 * 10^{26}$	214
		100	$7.2 * 10^{26}$	253

Table C-1: Typical values of flexural wavelength (α), flexural rigidity (D) and elastic thickness (Te) (Royden, 2000).

To calculate the variety of answers for ΔW, A and B for varying values of α and to minimise the difference between observed and calculated values,a root mean squares best fit is done:

$$\Sigma (W_{observed} - \Delta W)^2 = \text{a minimum}$$

In fuller form:

$$\Sigma ([W_{obs} - (\Delta W(\rho m / (\rho m - \rho s) + (A\cos(x/\alpha) + B\sin(x/\alpha) * e^{-x/\alpha})^2]) = \text{minimum}$$

To solve the above equation we take the derivative of ΔW, A and B and make equal to 0. The result is three new equations and three unknowns (α is estimated).

University of Cape Town

1) $0 = \mathbf{\Sigma W_{obs}} - \Delta W[(\boldsymbol{\rho m} / (\boldsymbol{\rho m} - \boldsymbol{\rho s}))*N] - A[\mathbf{\Sigma}\cos(x/\boldsymbol{\alpha})*e^{-x/\boldsymbol{\alpha}}]$

$- B[\mathbf{\Sigma}\sin(x/\boldsymbol{\alpha})* e^{-x/\boldsymbol{\alpha}}]$

N = number of observations
$F_1 = \Sigma W_{obs}$
$C_1 = (\rho m / (\rho m - \rho s))*N$
$A_1 = \Sigma\cos(x/\alpha)*e^{-x/\alpha}$
$B_1 = \Sigma\sin(x/\alpha)* e^{-x/\alpha}$

2) $0 = \mathbf{\Sigma}(W_{obs}(\cos(x/\boldsymbol{\alpha})*e^{-x/\boldsymbol{\alpha}}) -$

$\Delta W*(\boldsymbol{\rho m} / (\boldsymbol{\rho m} - \boldsymbol{\rho s}))[\mathbf{\Sigma}\cos(x/\boldsymbol{\alpha})*e^{-2x/\boldsymbol{\alpha}}] -$

$\mathbf{A}[\Sigma\cos^2(x/\alpha)*e^{-2x/\alpha}] - \mathbf{B}[\Sigma\cos(x/\alpha)\sin(x/\alpha)* e^{-2x/\alpha}]$

$F_2 = \Sigma(W_{obs}(\cos(x/\alpha)*e^{-x/\alpha})$
$C_2 = (\rho m / (\rho m - \rho s))[\Sigma\cos(x/\alpha)*e^{-2x/\alpha}]$
$A_2 = \Sigma\cos^2(x/\alpha)*e^{-2x/\alpha}$
$B_2 = \Sigma\cos(x/\alpha)\sin(x/\alpha)* e^{-2x/\alpha}$

3) $0 = \mathbf{\Sigma}(W_{obs}\sin(x/\boldsymbol{\alpha})* e^{-x/\boldsymbol{\alpha}}) -$

$\Delta W*(\boldsymbol{\rho m} / (\boldsymbol{\rho m} - \boldsymbol{\rho s}))\ [\sin(x/\boldsymbol{\alpha})* e^{-2x/\boldsymbol{\alpha}}] -$

$A[\mathbf{\Sigma}\cos(x/\boldsymbol{\alpha})\sin(x/\boldsymbol{\alpha})* e^{-2x/\boldsymbol{\alpha}}] - B[\sin^2(x/\boldsymbol{\alpha})* e^{-2x/\boldsymbol{\alpha}}]$

$F_3 = \Sigma(W_{obs}\sin(x/\alpha)* e^{-x/\alpha})$
$C_3 = (\rho m / (\rho m - \rho s))\ [\sin(x/\alpha)* e^{-2x/\alpha}]$
$A_3 = \Sigma\cos(x/\alpha)\sin(x/\alpha)* e^{-2x/\alpha}$
$B_3 = \sin^2(x/\alpha)* e^{-2x/\alpha}$

The above equations are solved simultaneously as follows:

$F_1 = \Delta WC_1 + AA_1 + BB_1$

$F_2 = \Delta WC_2 + AA_2 + BB_2$

$F_3 = \Delta WC_3 + AA_3 + BB_3$

University of Cape Town

$$F_1C_2 - F_2C_1 = A(A_1C_2) + B(B_1C_2) - A(C_1A_2) - B(C_1B_2)$$

$$\varsigma F_1C_2 - F_2C_1 = A(A_1C_2 - C_1A_2) + B(B_1C_2 - C_1B_2)$$

$$\varsigma F_3C_2 - F_2C_3 = A(A_3C_2 - C_2A_3) + B(B_3C_2 - C_3B_2)$$

$$Q_1 = F_1C_2 - F_2C_1$$
$$P_1 = A_1C_2 - C_1A_2$$
$$R_1 = B_1C_2 - C_1B_2$$
$$Q_2 = F_3C_2 - F_2C_3$$
$$P_2 = A_3C_2 - C_2A_3$$
$$R_2 = B_3C_2 - C_3B_2$$

$$Q_1 = P_1A + R_1B$$

$$Q_2 = P_2A + R_2B$$

$$\varsigma A = (Q_1R_2 - Q_2R_1) / (P_1R_2 - R_1P_2)$$

$$\varsigma B = (Q_1/R_1) - (P_1/R_1)*A$$

$$\varsigma \Delta W = F_1/C_1 - A*(A_1/C_1) - B(B_1/C_1)$$

The coefficients A, B and ΔW calculated above are then substituted into equation:

$$W = [\rho m \Delta W / (\rho m - \rho s)] + [A\cos(x/\alpha) + B\sin(x/\alpha)]*e^{-x/\alpha}$$

Thus, for each value of x and estimated flexural wavelength, α, a deflection, W, is calculated. A plot of these deflection values with increasing horizontal distance from line end is created for each chosen α (figure 3.5).

The flexural wavelength is linked to the elastic thickness in the following way. From the flexural wavelength it is possible to calculated the flexural rigidity, D:

$$\alpha = [4D / (\rho m - \rho s)*g]^{1/4}$$

Flexural rigidity, D, in turn gives elastic thickness, Te:

University of Cape Town

$$Te^3 = [12D (1- \nu^2)] / E$$

ν = Poisson's ratio

E = Young's modulus

$E / (1- \nu^2) = 8.7*10^{10}$ N/m^2

University of Cape Town

University of Cape Town

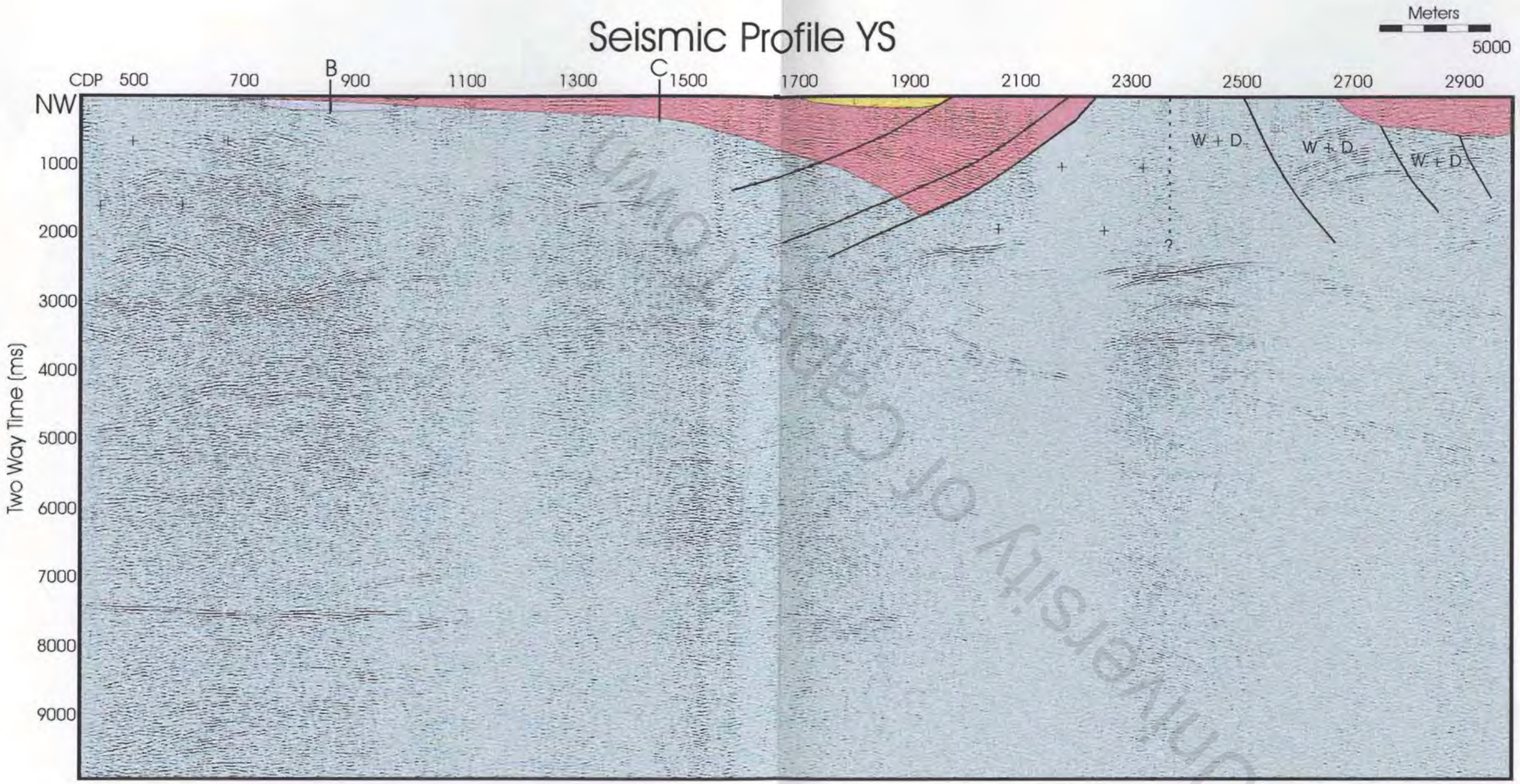

Figure 2.56: Stratigraphic and structural interpretation of seismic profile YS. Position of the boreholes marked with B and C.

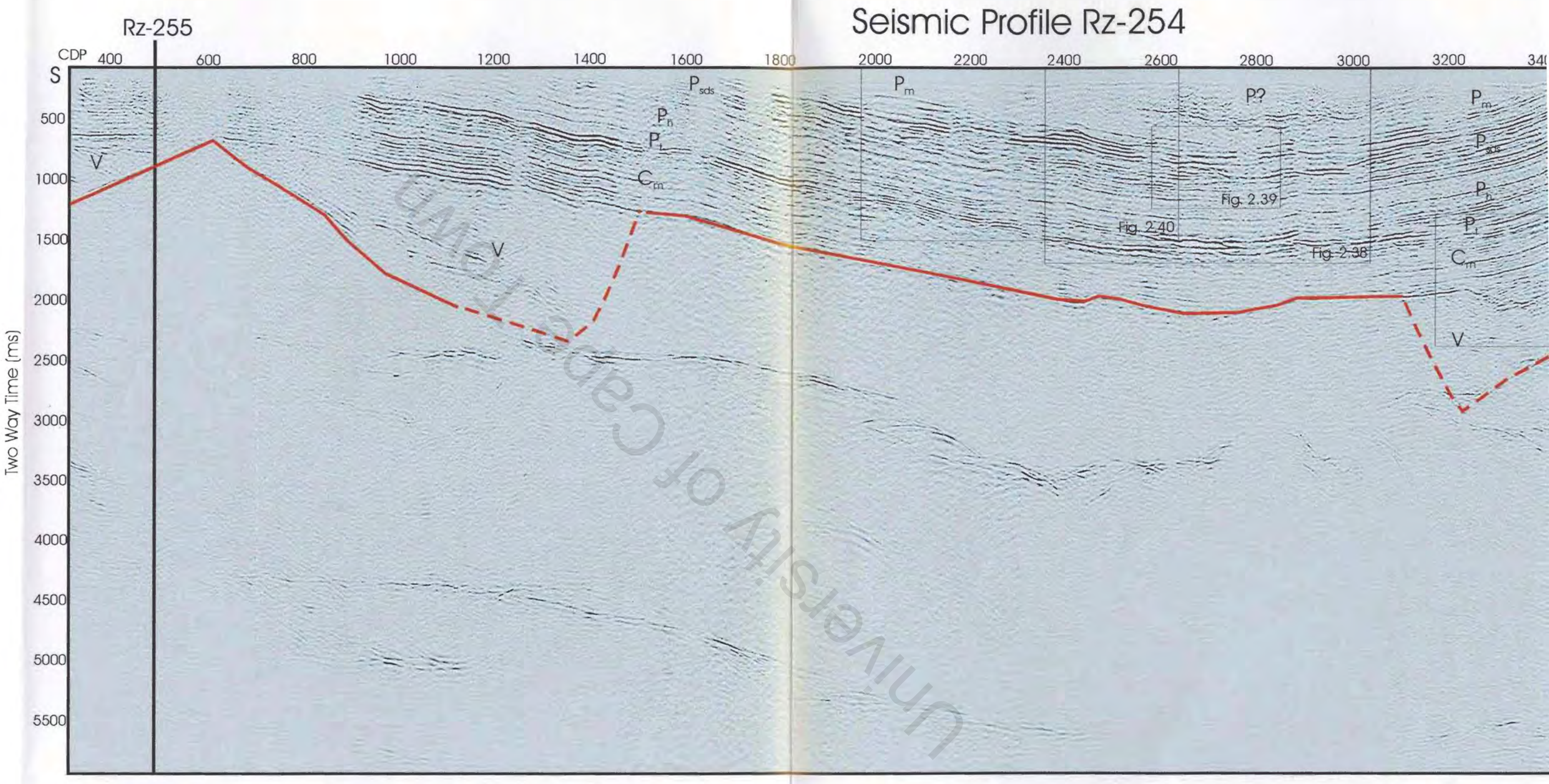

Figure 2.29: Processed, uninterpreted seismic profile Rz-254. Codes relate to the stratigraphic nomenclature given in section 2.3.2. Sediment/basement interface is marked with a red line. D
marked with a vertical black line. Box outlines show location of figures 2.37, 2.38, 2.39 and 2.40.

University of Cape Town

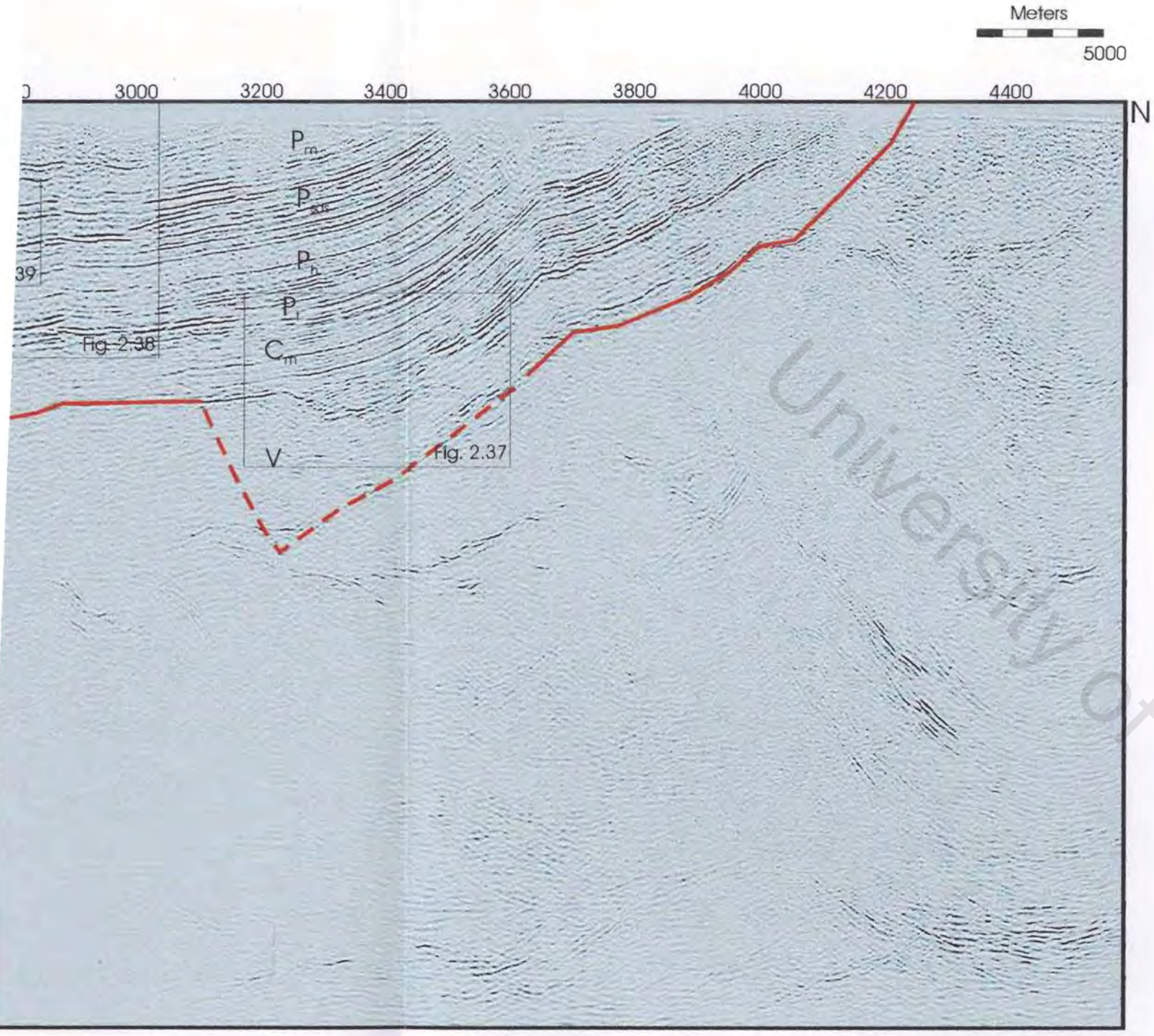

nt interface is marked with a red line. Dashed sections indicate uncertainty in its position Tie with Rz-255 is

University of Cape Town

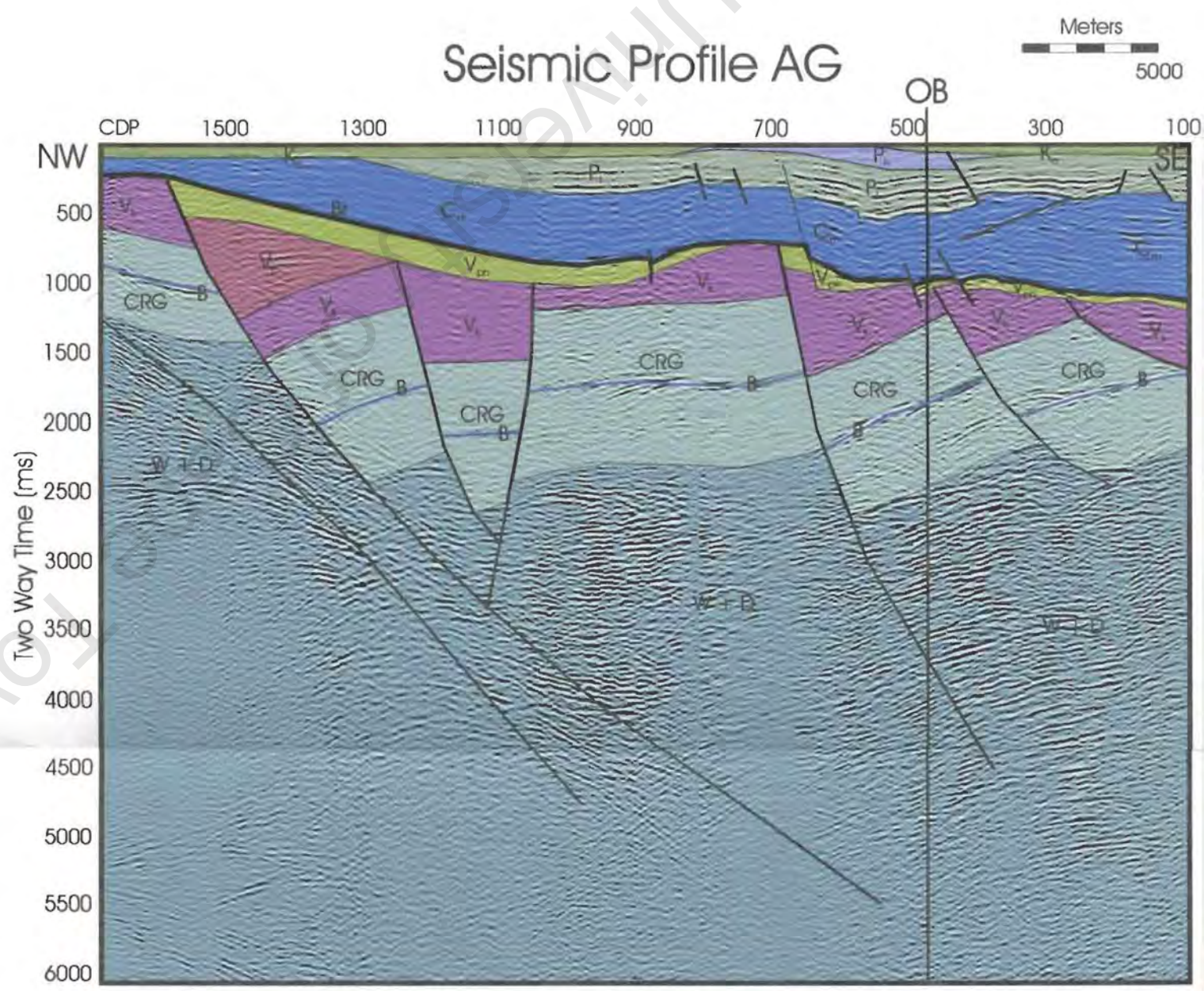

Figure 2.45: Stratigraphic and structural interpretation of seismic profile AG. Tie with seismic profile OB marked by vertical black line.

Seismic Profile OB-A and B

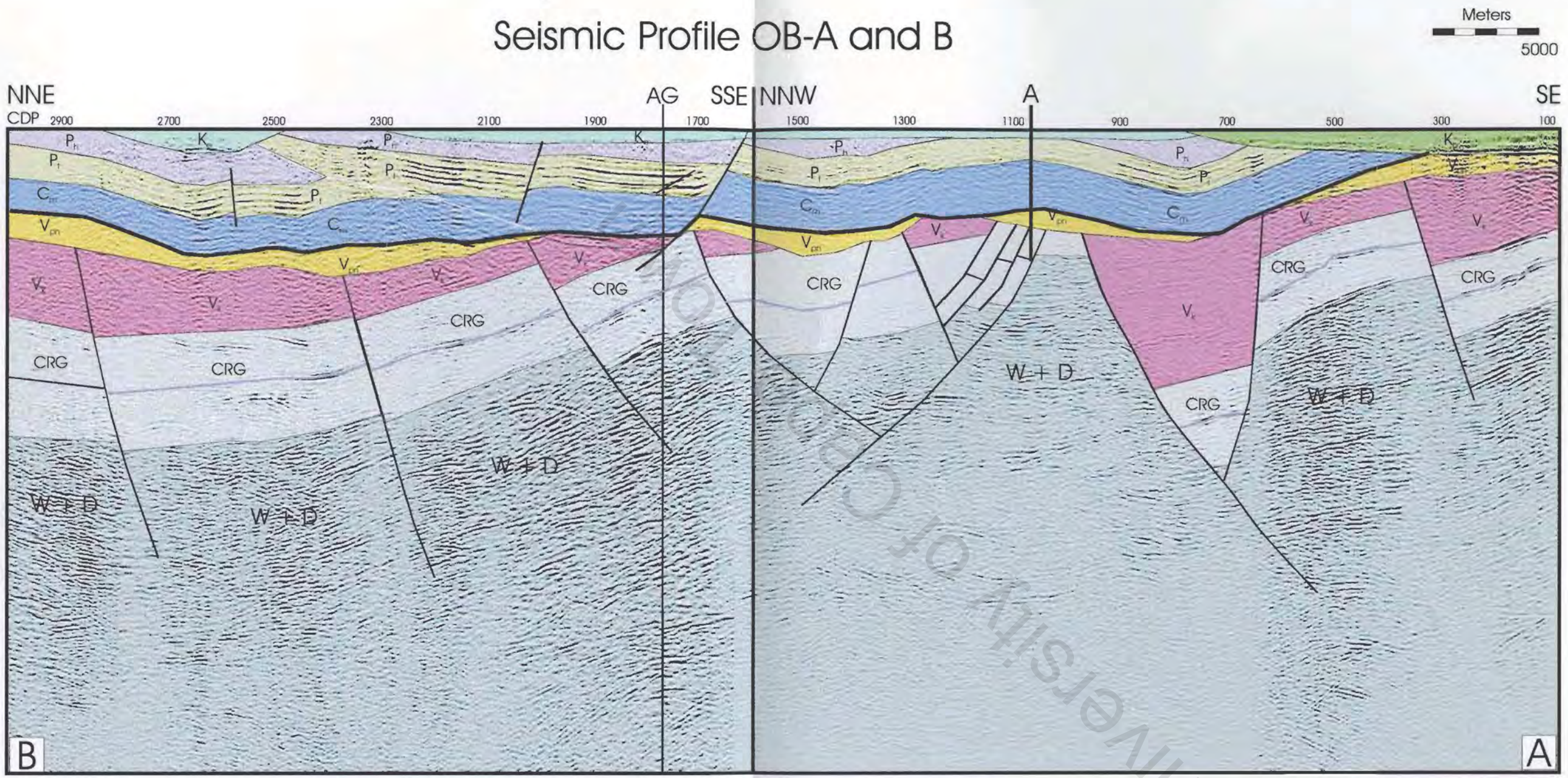

Figure 2.44: Stratigraphic and structural interpretation of seismic profile OB. Tie with seismic profile AG and location of borehole A are marked by vertical black lines.

Karoo
- Beaufort Group
- Ecca Group

Transvaal
- Hekpoort Formation
- Timeball Hill and Dwaalheuwel Formations
- Malmani Subgroup
- Black Reef Formation

Ventersdorp
- Pniel Sequence
- Platberg Group
- Klipriviersberg Group

Witwatersrand
- Central Rand Group — Booysens Formation
- W + D West Rand and Dominion Group

University of Pretoria

Seismic Profile OB-A and B

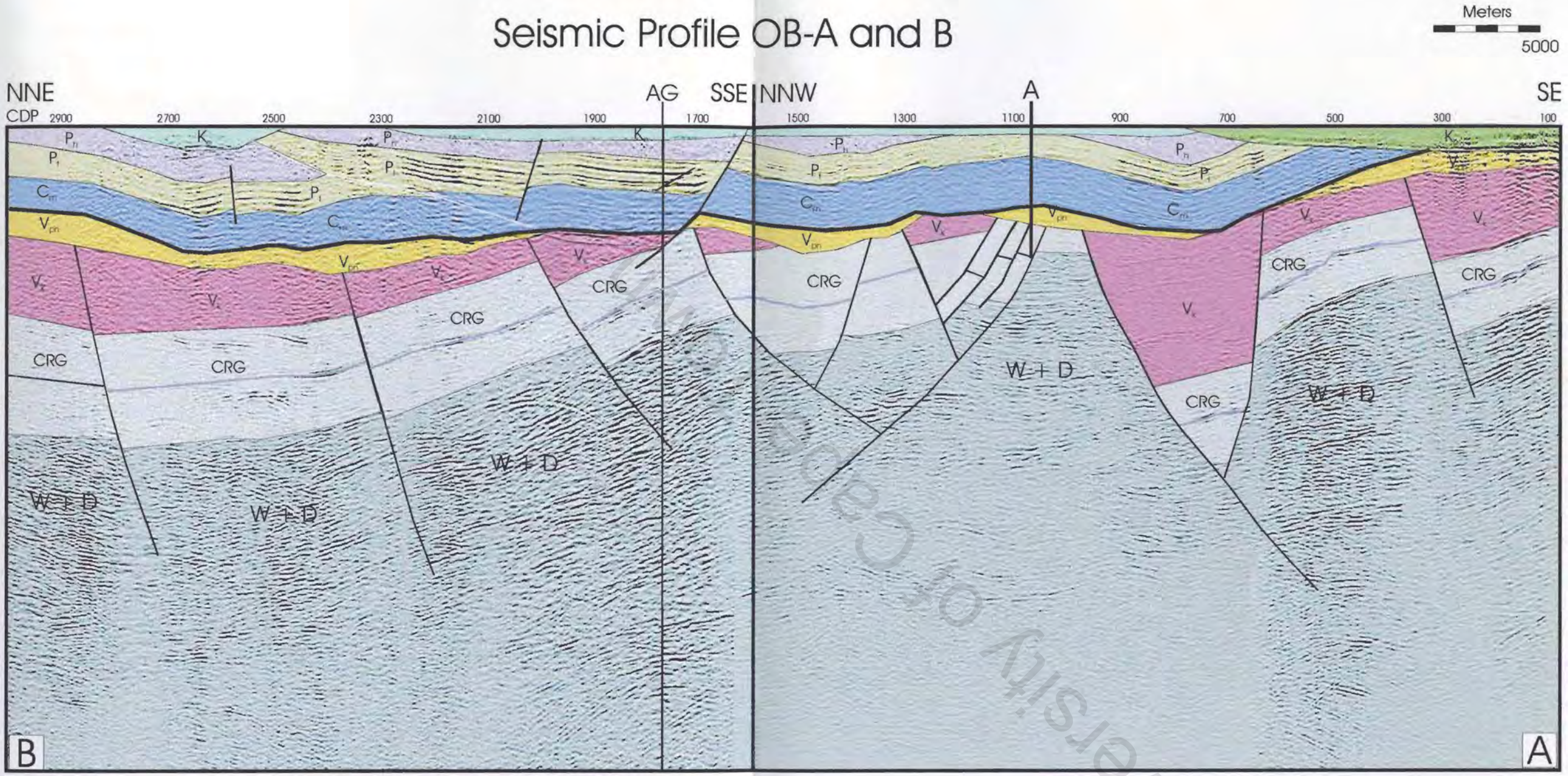

Figure 2.44: Stratigraphic and structural interpretation of seismic profile OB. Tie with seismic profile AG and location of borehole A are marked by vertical black lines.

Karoo
- Beaufort Group
- Ecca Group

Transvaal
- Hekpoort Formation
- Timeball Hill and Dwaalheuwel Formations
- Malmani Subgroup
- Black Reef Formation

Ventersdorp
- Pniel Sequence
- Platberg Group
- Klipriviersberg Group

Witwatersrand
- Central Rand Group — Booysens Formation
- W + D West Rand and Dominion Group

University of Pretoria

eismic Profile Rz-256

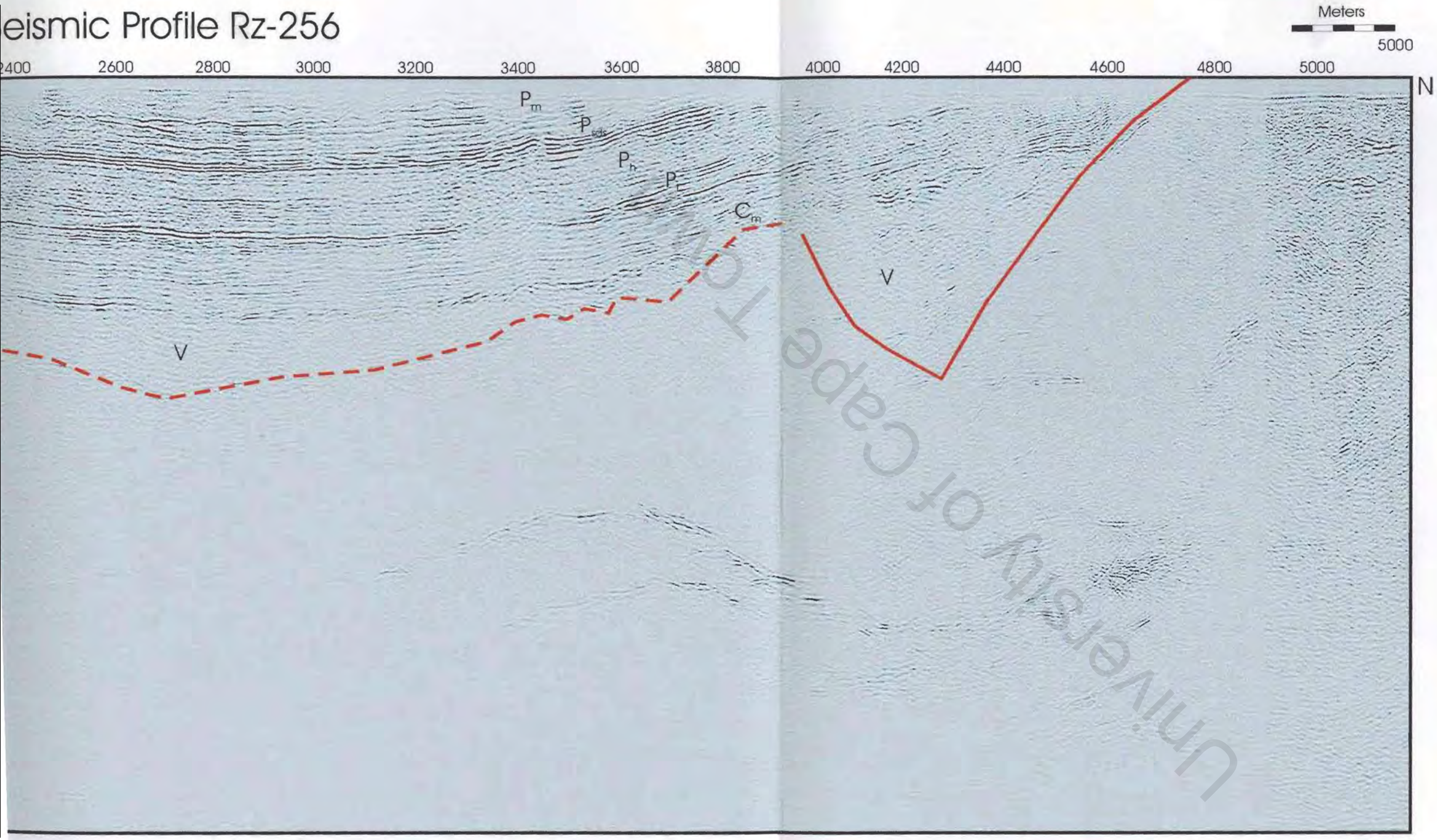

University of Cape Town

ction 2.3.2. Sediment/ basement interface marked in red. Where uncertainty in its position exists, the line is dashed. Tie with Rz-255 is marked with a vertical black line.

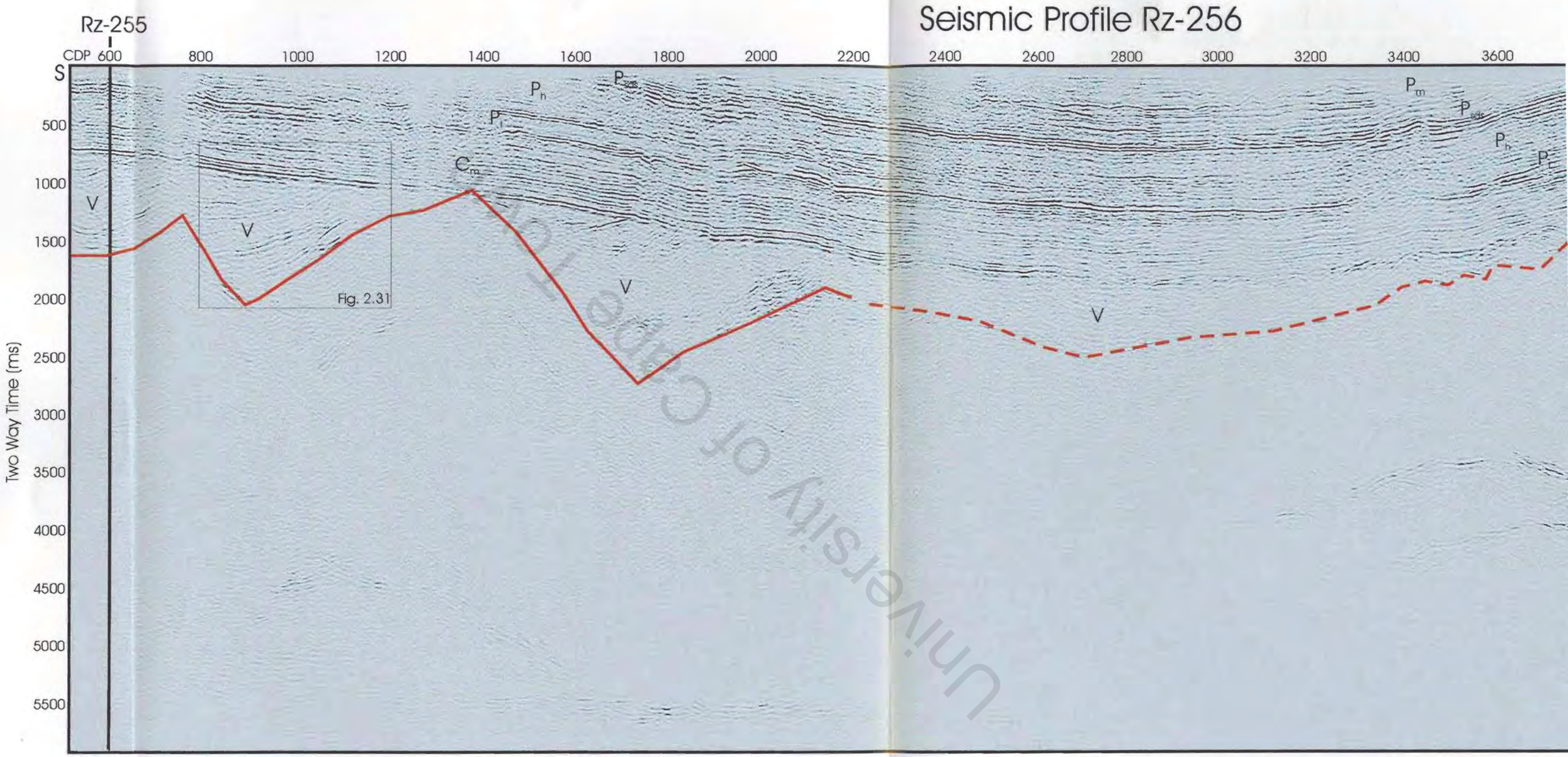

Figure 2.31: Processed uninterpreted seismic profile Rz-256. Codes relate to stratigraphic nomenclature given in section 2.3.2. Sediment/ basement interface marked in red. Where uncertainty in its
Box outline shows location of figure 2.36.

University of Cape Town

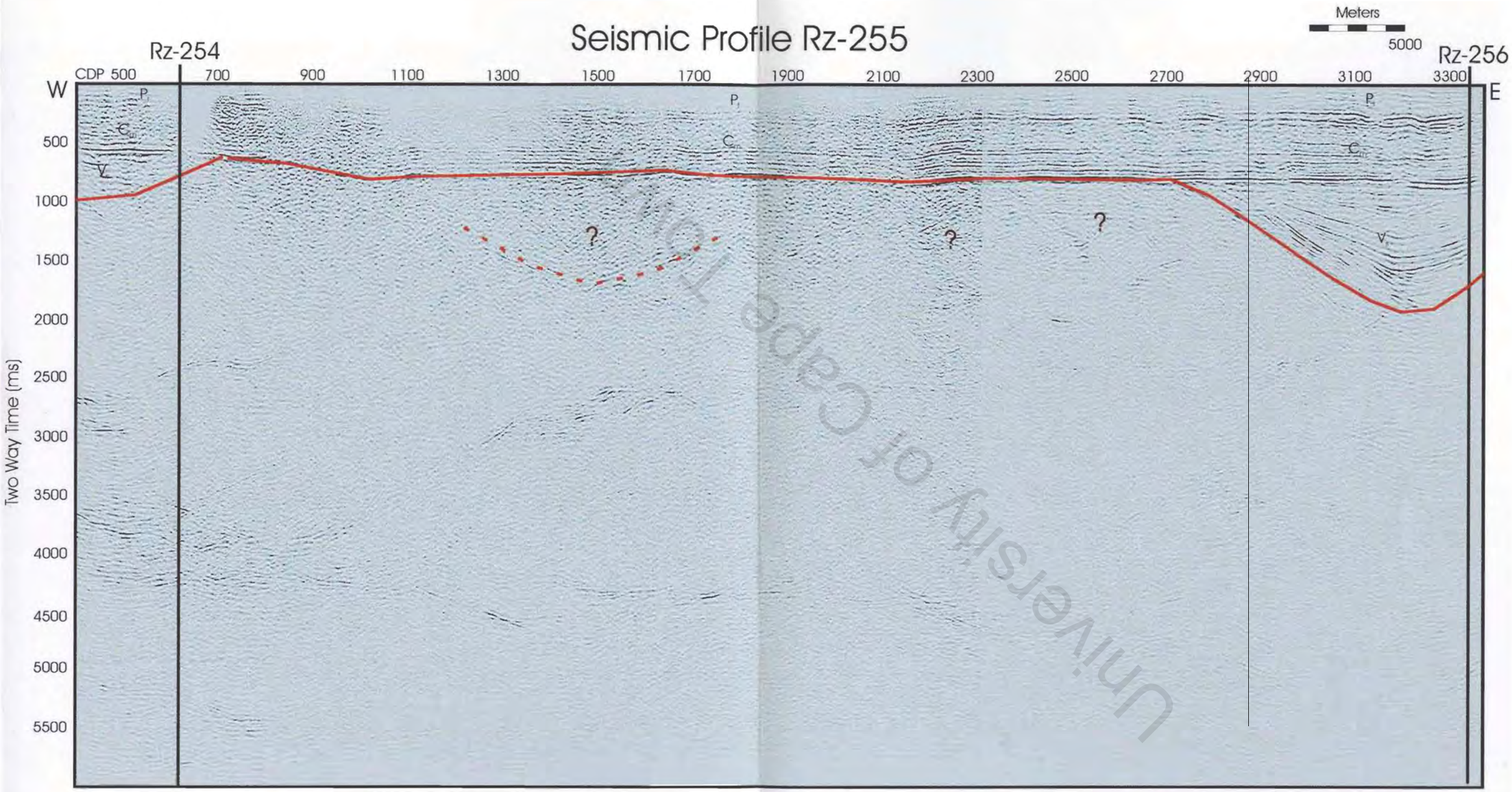

Figure 2.30: Processed, uninterpreted seismic profile Rz-255. Codes relate to the stratigraphic nomenclature given in section 2.3.2. Sediment/ basement interface is marked with a red line. Uncertainty in its position is shown by a dashed line, and '?'s.

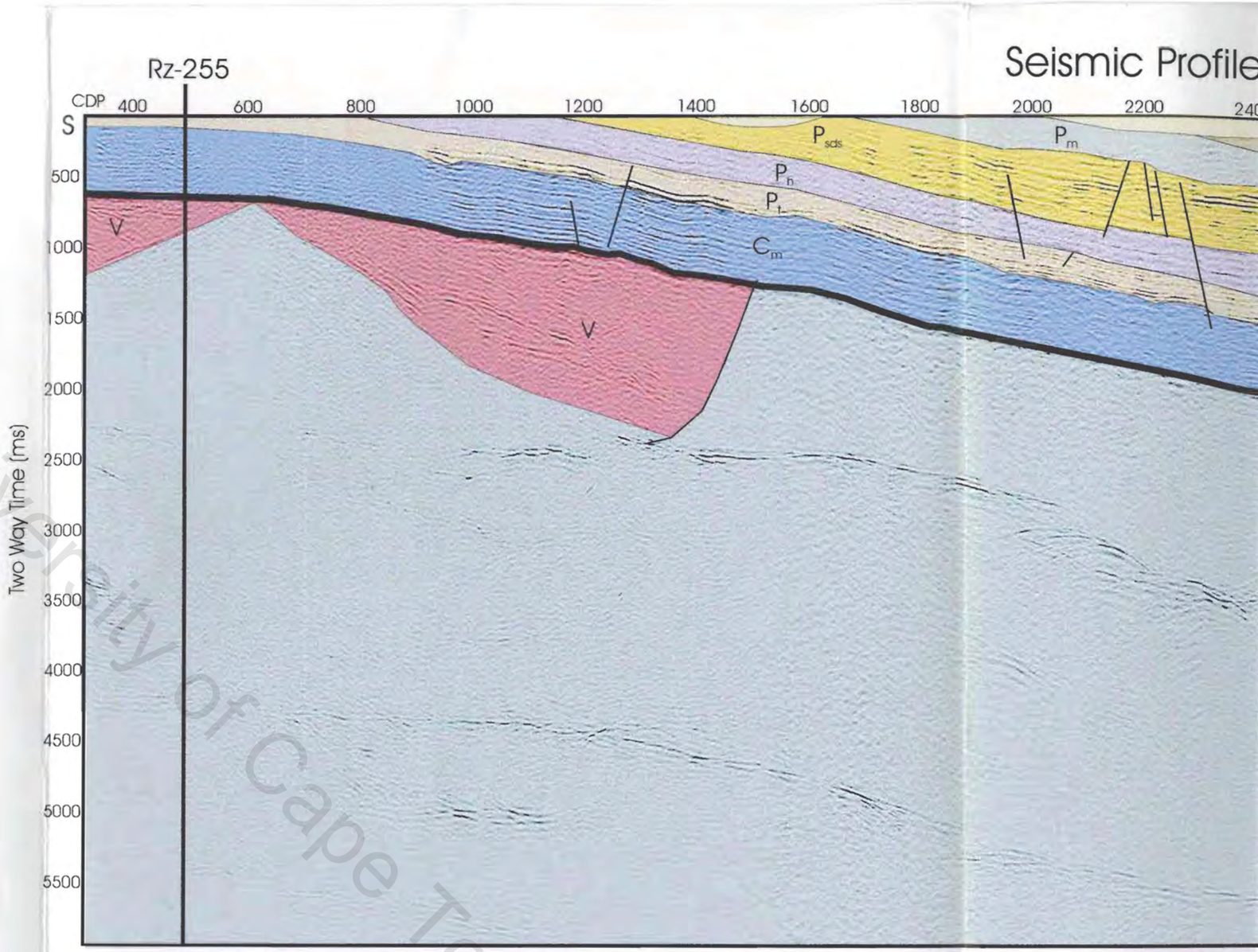

Figure 2.32: Stratigraphic and structural interpretation of seismic profile Rz-254. Tie with Rz-255 is marked with a vertical black line

University of Cape Town

Seismic Profile Rz-254

Meters
5000

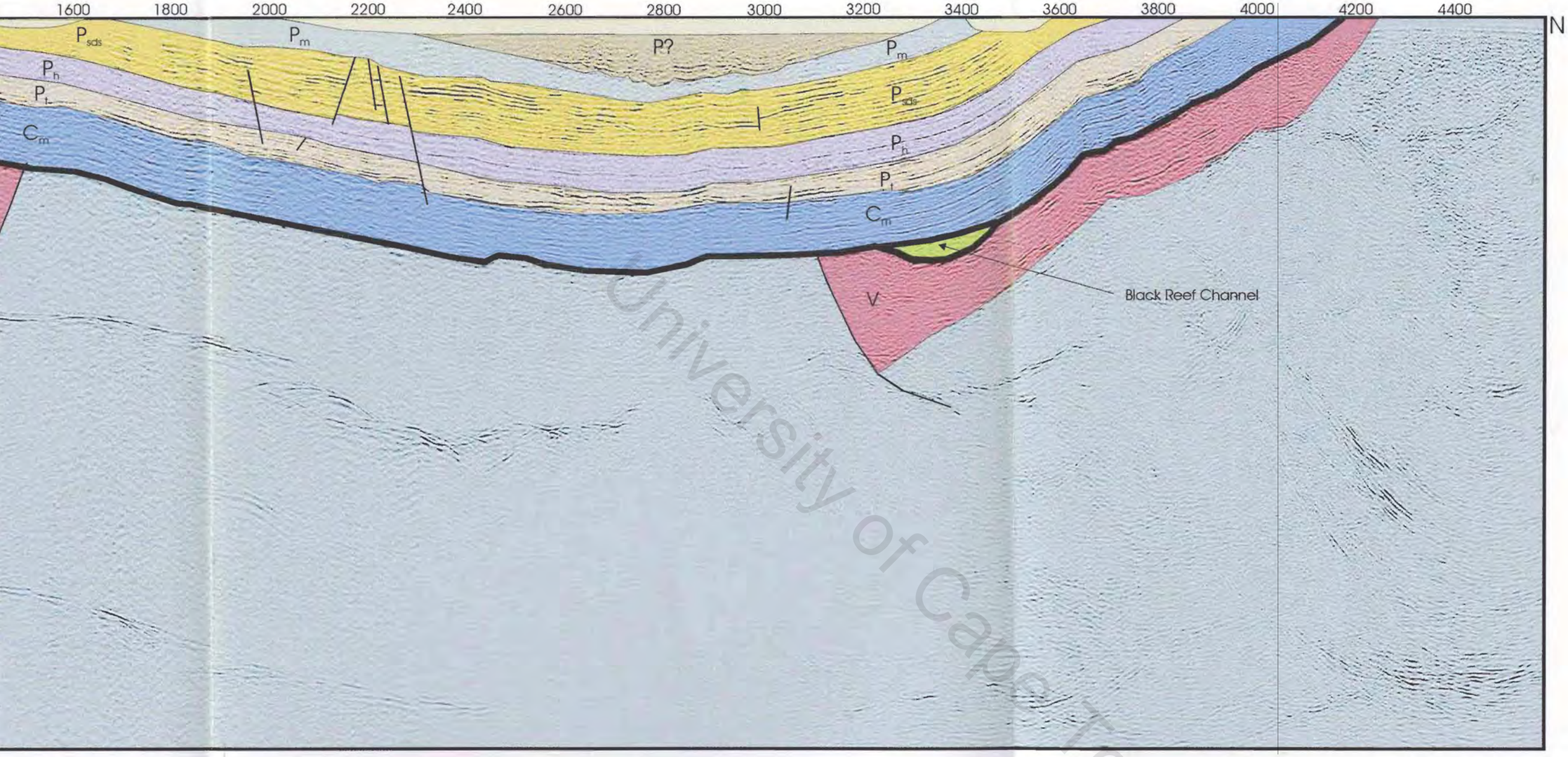

e Rz-254. Tie with Rz-255 is marked with a vertical black line.

- Quaternary cover
- P ?
- Magaliesberg Formation
- Strubenkop, Daspoort and Silverton Formations
- Hekpoort and Dwaalheuwel Formations
- Timeball Hill and Boshoek Formations

} Pretoria Group

- Malmani Subgroup } Chuniespoort Group
- Black Reef Formation
- Ventersdorp Supergroup

University of Cape Town

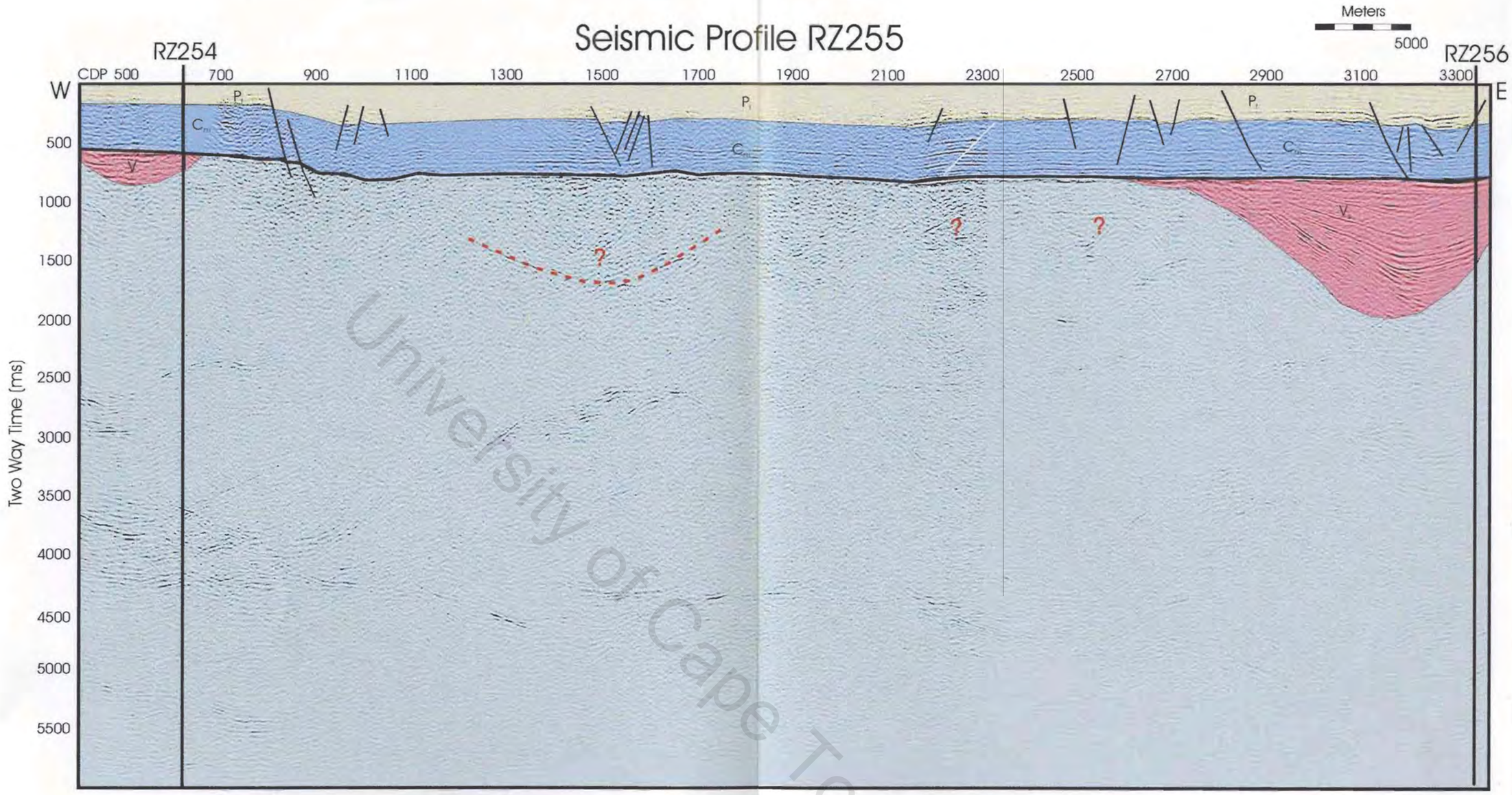

Figure 2.33: Stratigraphic and structural interpretation of seismic profile Rz-255. Ties with lines Rz-254 and 256 marked with vertical black lines. Normal faults are marked in black, reverse faults in white.

University of Cape Town

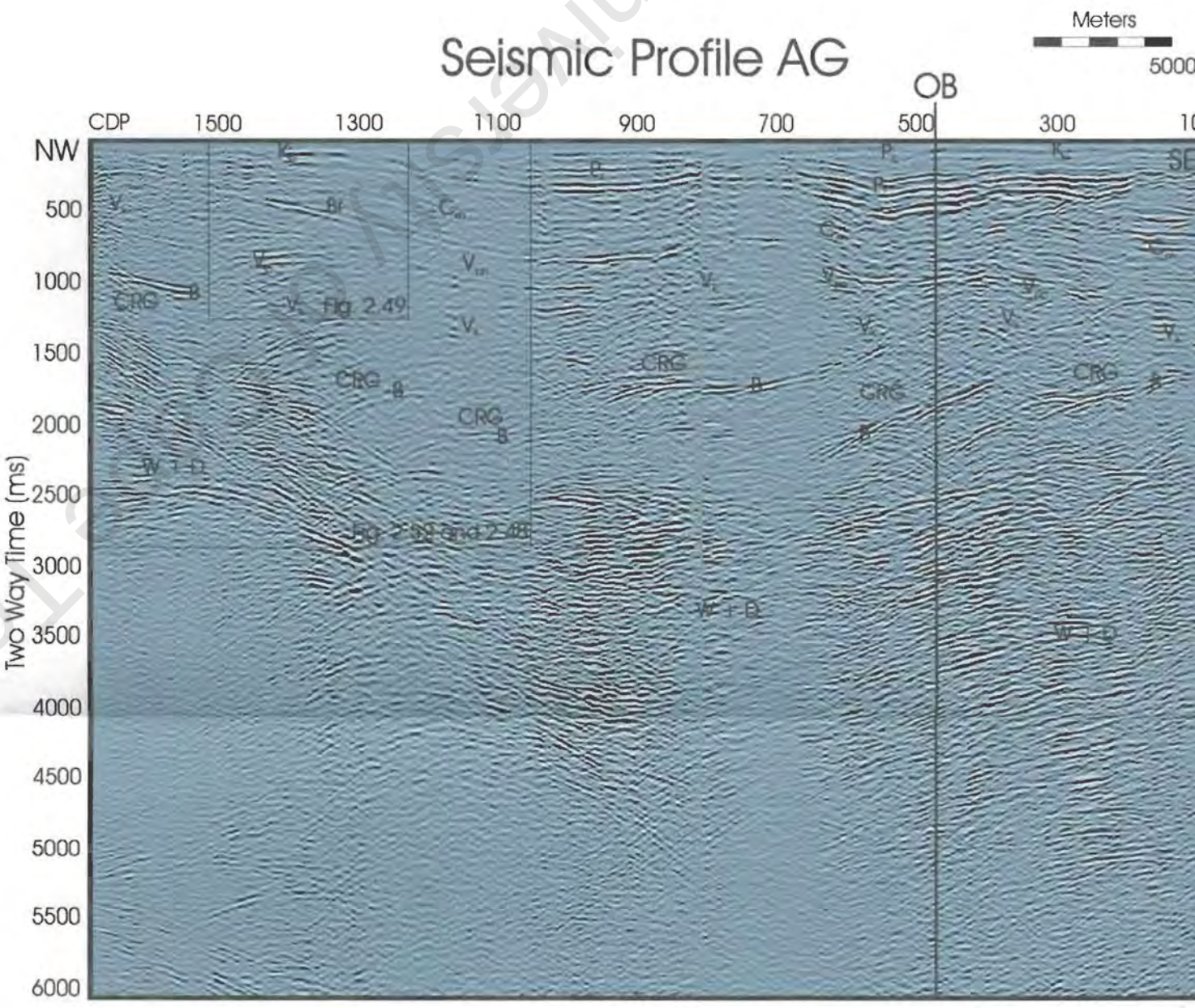

Figure 2.43: Processed, uninterpreted profile AG. Codes relate to stratigraphic nomenclature given in section 2.4.1.ii. Tie with line OB-A marked with vertical black line. Box outlines show location of figures 2.48, 2.49 and 2.52.

Seismic Profile Rz-256

Meters
5000

0 2000 2200 2400 2600 2800 3000 3200 3400 3600 3800 4000 4200 4400 4600 4800 5000

N

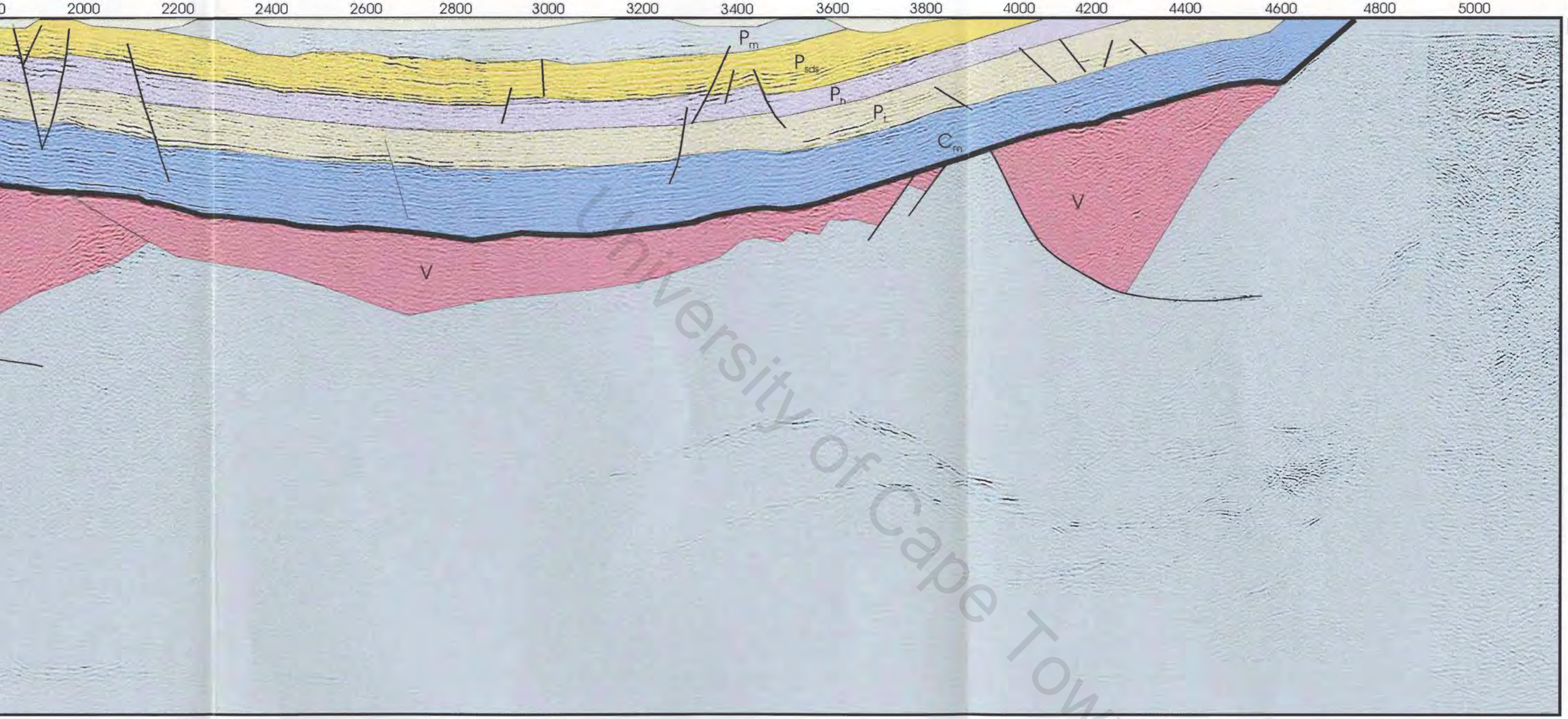

University of Cape Town

e with Rz-255 is marked with a vertical black line.

- Quaternary cover
- P ?
- Magaliesberg Formation
- Strubenkop, Daspoort and Silverton Formations
- Hekpoort and Dwaalheuwel Formations
- Timeball Hill and Boshoek Formations

} Pretoria Group

- Malmani Subgroup } Chuniespoort Group
- Black Reef Formation
- Ventersdorp Supergroup

01

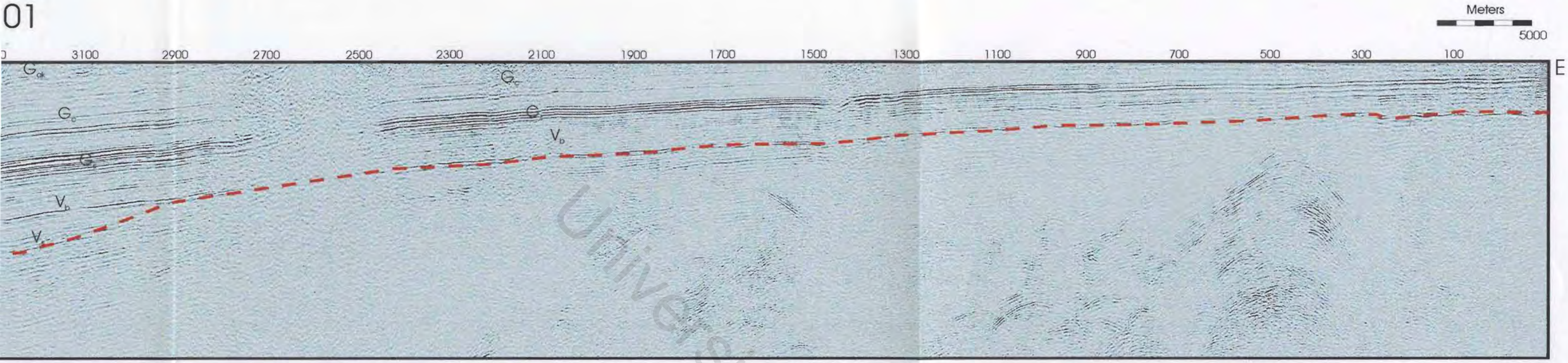

University of Cape Town

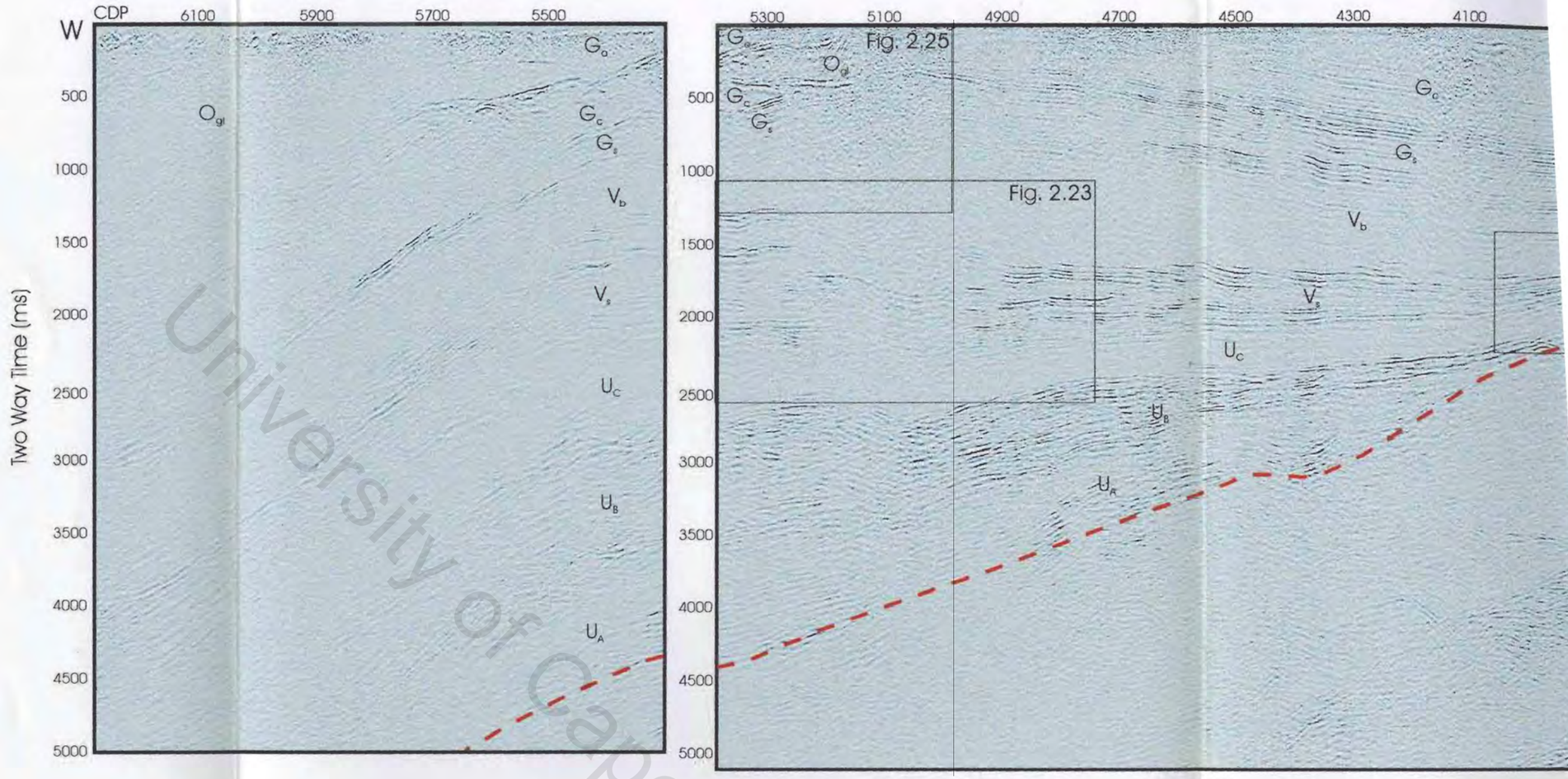

Figure 2.21: Processed, uninterpreted profile KBF01. Codes relate to the stratigraphic nomenclature given in section 2.2.2.ii. (page 2-31). The sediment/base red dashed line. Box outlines show location of figures 2.23, 2.24 and 2.25.

University of Cape Town

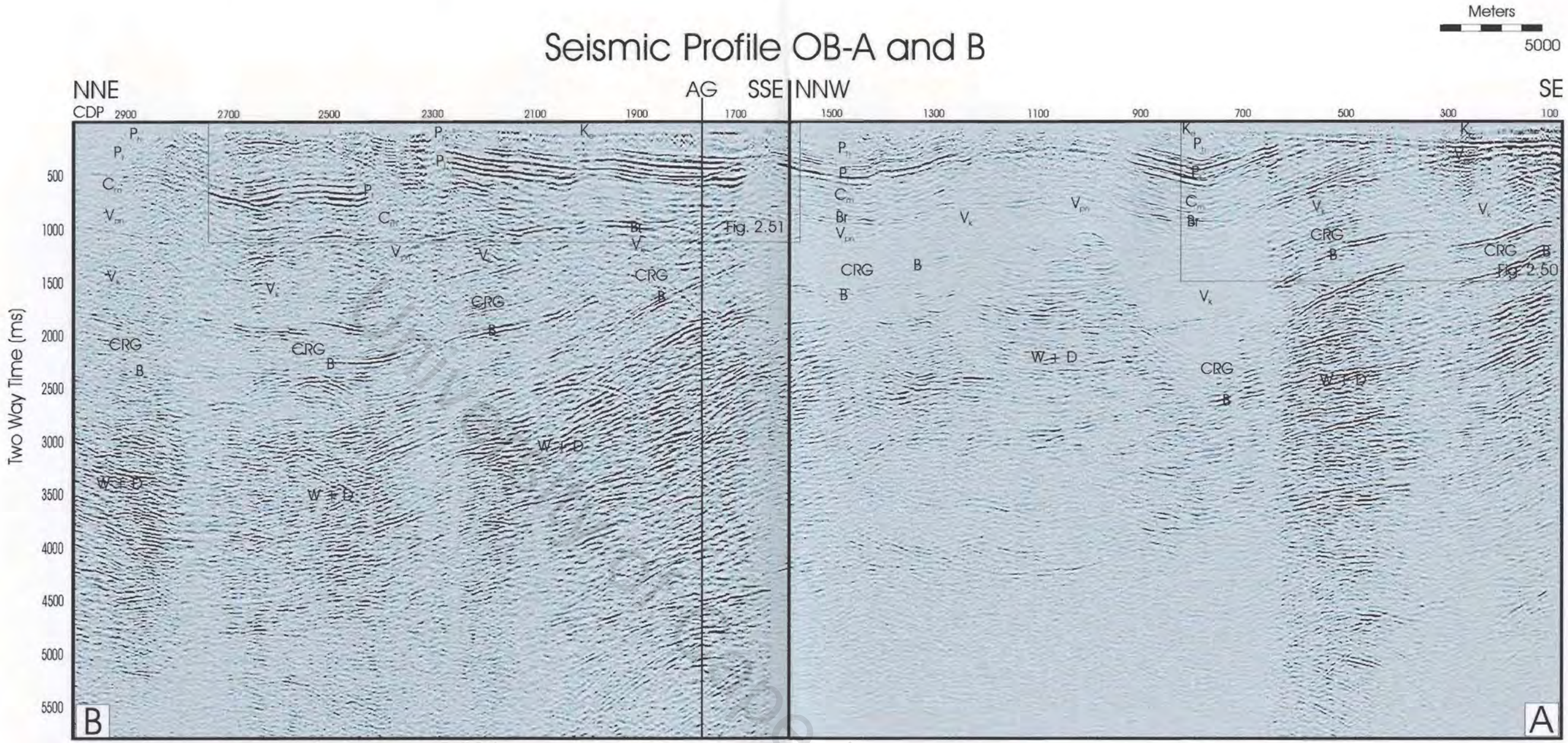

Figure 2.42: Processed, uninterpreted seismic profile OB. Codes relate to stratigraphic nomenclature given in section 2.4.1.ii. Tie with line AG marked with a vertical black line. Box outlines show location of figures 2.50 and 2.51.

University of Cape Town

Seismic Profile KBF03A

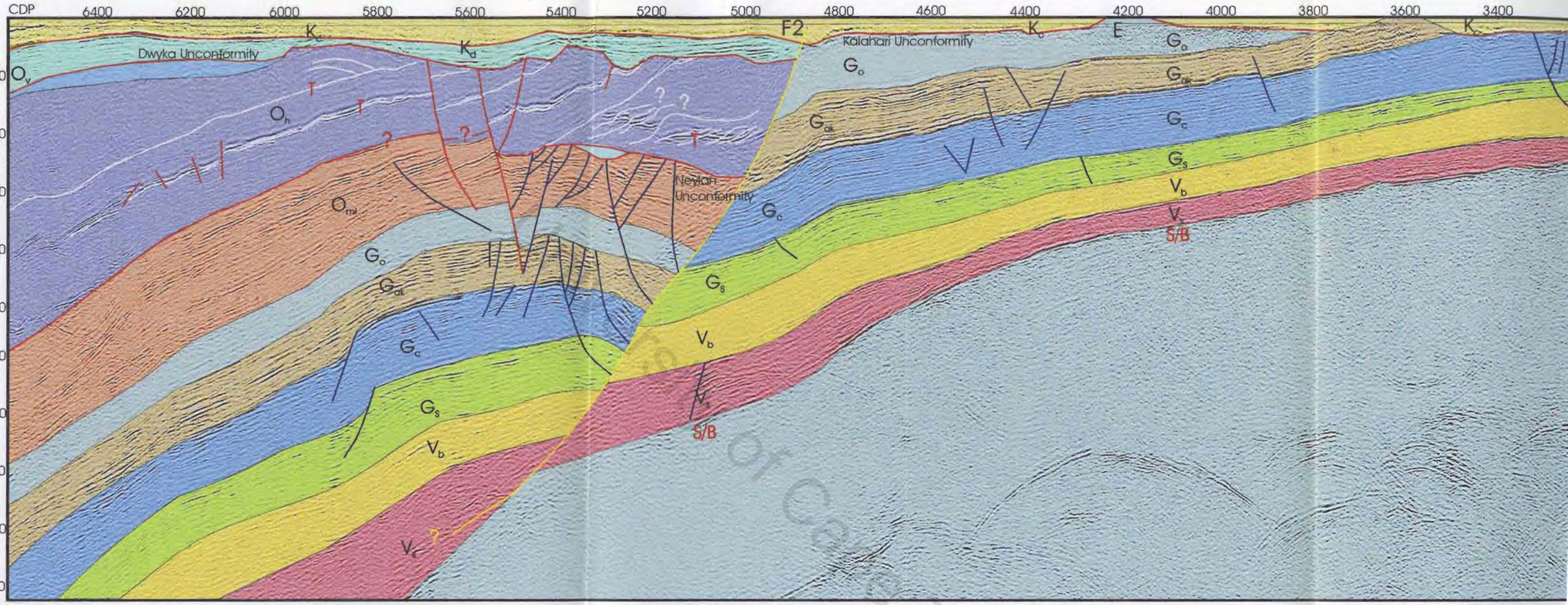

Figure 2.3: Stratigraphic and structural interpretation of profile KBF03A. Phases of faulting are distinguished by colours: the listric normal fault, F2, in yellow; normal faulting within the lower Olifantshoek Group, prior to the fo the Neylan Unconformity, F3 in blue; thrusting of the Hartley Formation, F4, in white and later normal faults which displace the thrusts (F5 in red).The Neylan, Dwyka and Kalahari unconformities are marked in red.

University of Cape Town

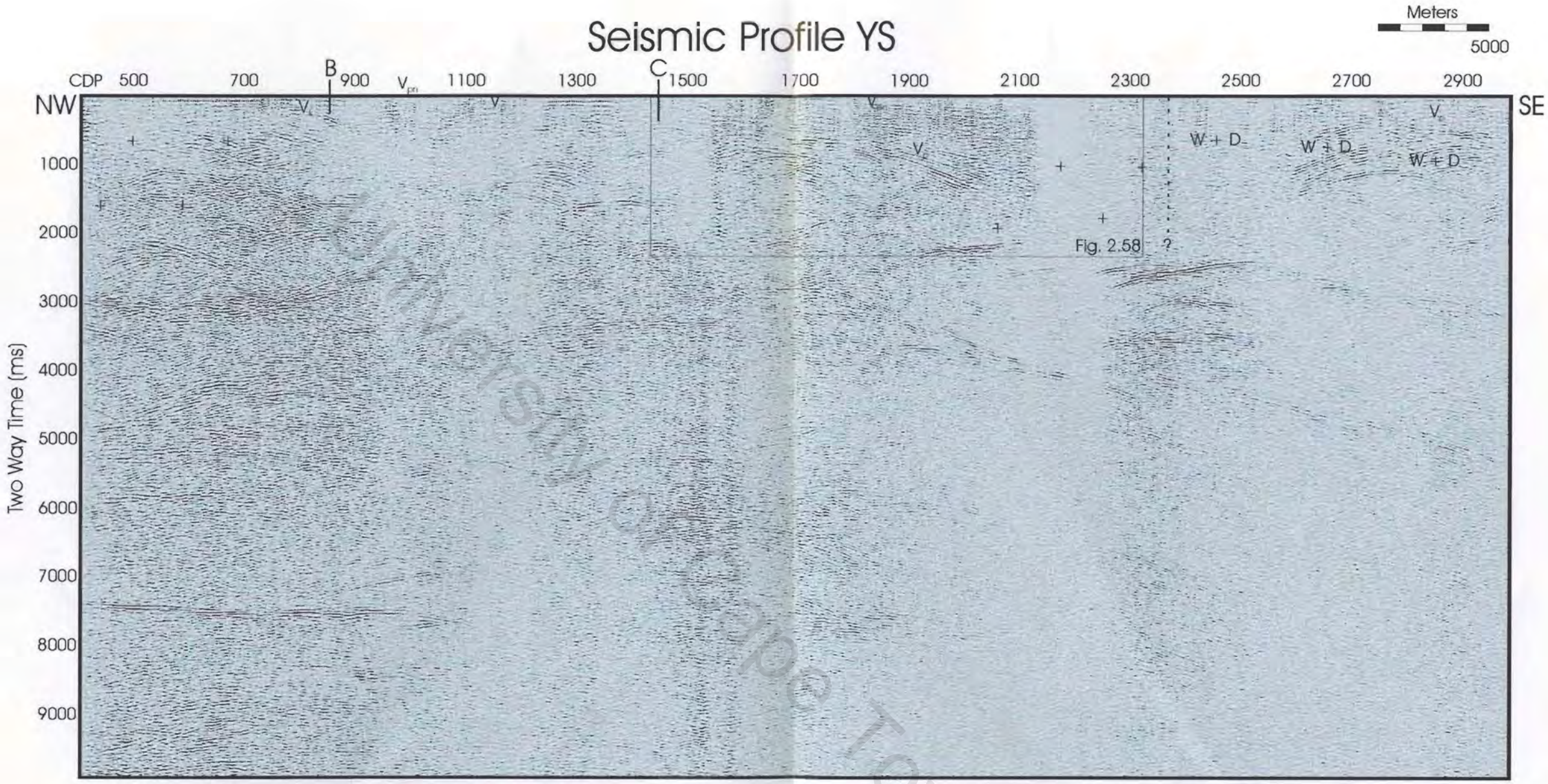

Figure 2.55: Processed, uninterpreted seismic profile YS. Codes relate to the stratigraphic nomenclature given in section 2.4.2.ii. Position of the boreholes marked with B and C. Box outline shows location of figure 2.58.

University of Cape Town

eismic Profile KBF03A

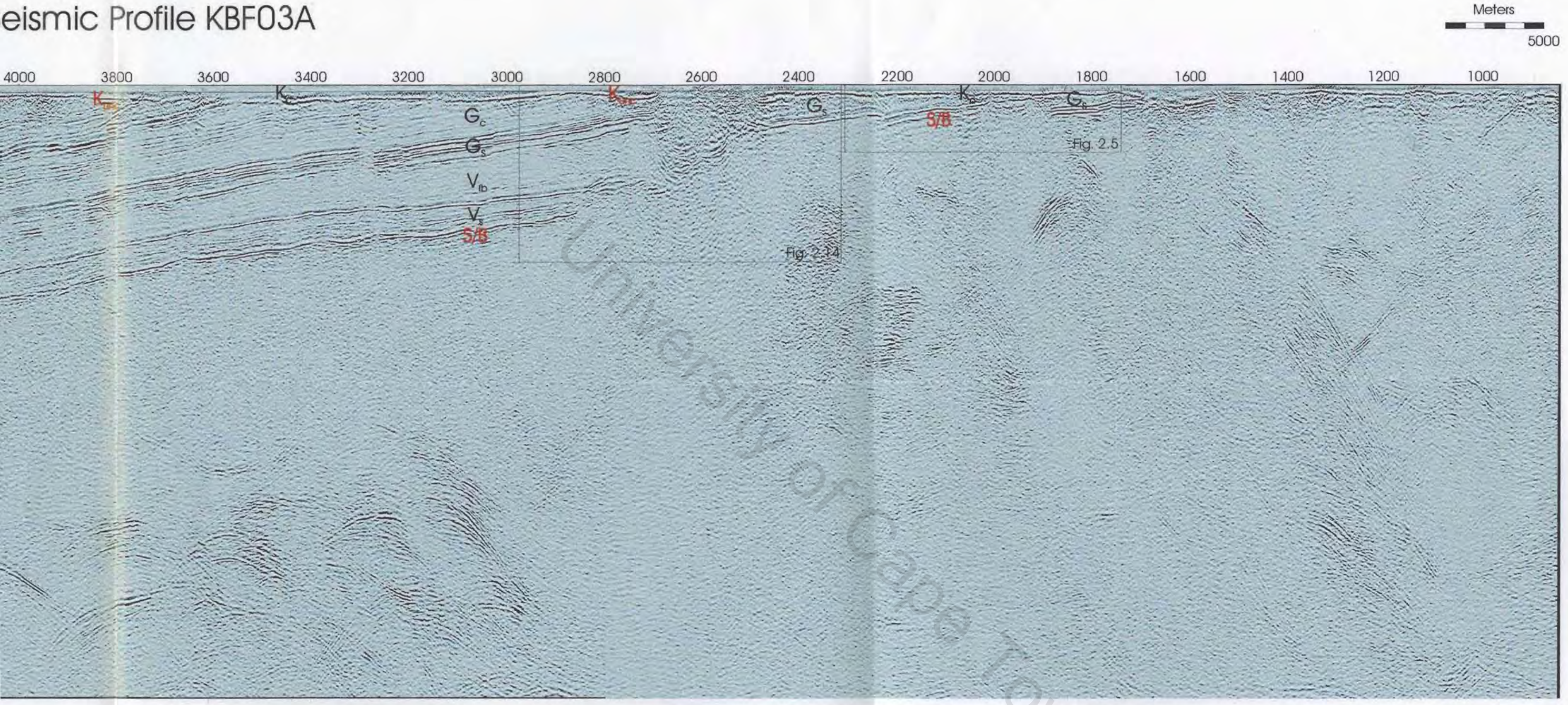

red, units in black. Box outlines show location of figures 2.4,.2.5, 2.6, 2.9, 2.10, 2.11, 2.12, 2.13 and 2.14.

Cannot be copied

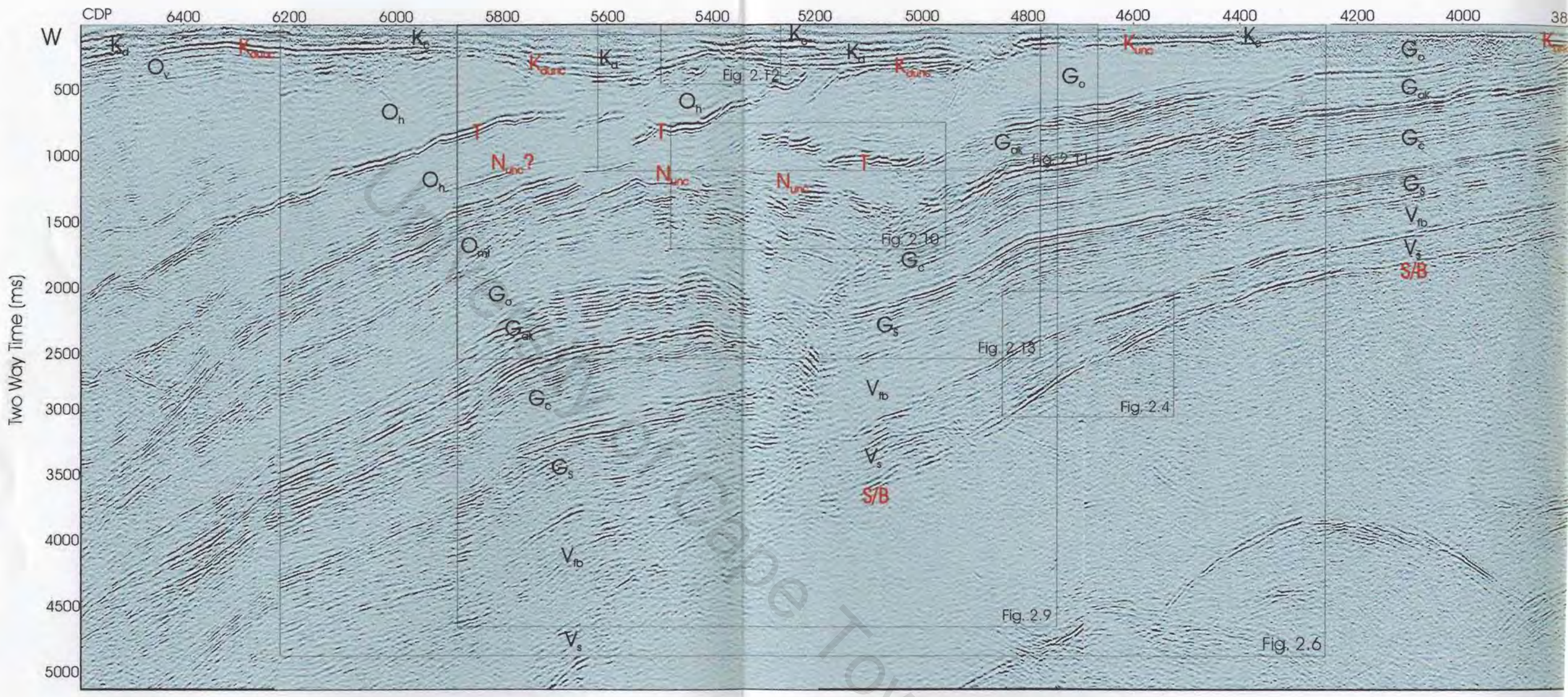

Figure 2.2: Processed, uninterpreted profile KBF03A. Codes relate to the stratigraphic nomenclature given in section 2.2.1.ii. (page 2-3). Marker reflectors are labelled in red, units in bl

University of Cape Town

Seismic Profile KBF01

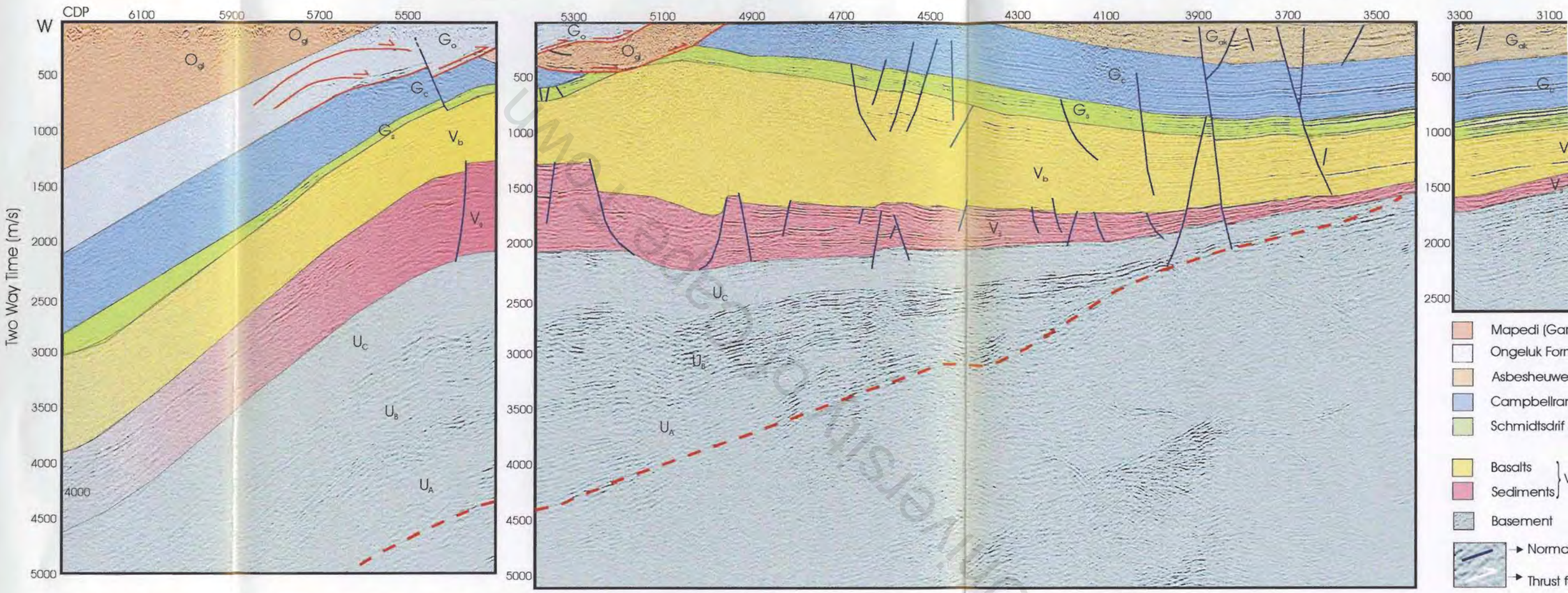

Figure 2.22: Stratigraphic and structural interpretation of seismic profile, KBF01. Normal faults are marked in blue and thrusting is shown by red arrows.

Unrestricted